Adaptive Multilevel Methods for Mortar Edge Element Methods in $\mathbb{R}^3$

Dissertation
zur Erlangung des akademischen Titels eines
Doktors der Naturwissenschaften
der Mathematisch Naturwissenschaftlichen Fakultät
der Universität Augsburg

vorgelegt von
Dipl. Phys. Werner Ernst Schabert

1. Gutachter: Prof. Dr. Ronald H.W. Hoppe
2. Gutachter: Prof. Dr. Kunibert G. Siebert
3. Gutachter: Prof. Dr. Jin-Fa Lee

Tag der mündlichen Prüfung: 9. Februar 2006

Abstract

This thesis is concerned with the application of adaptive mortar edge element methods to the numerical solution of the quasi-stationary limit of Maxwells equations, also known as the eddy current model, in three space dimensions. Although eddy current model is time-dependent, we restrict our analysis to time-independent problems that arise from a time discretization of the partial differential equations.

For the solution of these equations we consider the mortar approach, which relies on the macro-hybrid variational formulation of the problem with respect to a geometrically conforming, nonoverlapping decomposition of the computational domain (cf. [Hop99]). Based on independent, locally quasi-uniform and shape regular simplicial triangulation of the subdomains we use the lowest order curl-conforming edge elements of Nédélec's first family for the discretization of the problem. Due to nonmatching triangulations at the interfaces of adjacent subdomains, we have to impose weak continuity constraints on the tangential traces across the skeleton of the decomposition by means of appropriately chosen Lagrange multipliers.

The mortar edge element discretized problems give rise to indefinite algebraic saddle point problems. Since the saddle point problem behaves utterly different on the large kernel of the **curl**-operator, standard iterative solvers that do not take care of the the kernel fail in this case. We analyze this problem in great detail and develop a multilevel iterative solver featuring a hybrid smoother that is based on the smoother presented in [Hip98]. The key ingredient of the smoother is an additional defect correction on the subspace of irrotational vector fields. However, in order to guarantee convergence of the iterative scheme, we have to impose compatibility constraints on the triangulations at the interfaces.

To improve the accuracy of the computed solution while keeping the computational cost as small as possible, we put particular emphasis on mesh adaptivity. We present an a posteriori error estimator that combines elements of the error estimators given in [BHHW00, Woh99c] and relies on a Helmholtz decomposition of the error into an irrotational and weakly solenoidal part. We show that the error estimator is both efficient and reliable, provided certain assumptions are fulfilled.

Finally, we demonstrate the convergence properties of the multigrid scheme and the quality of the error estimator by solving several academic test problems that cover a wide range of physical applications.

Contents

List of Tables

List of Figures

Introduction

Schläft ein Lied in allen Dingen,
Die da träumen fort und fort,
Und die Welt hebt an zu singen,
Triffst du nur das Zauberwort.

Slumb'ring deep in everything
Dreams a song as yet unheard,
And the world begins to sing,
If you find the magic word.

Joseph Freiherr von Eichendorff,
Wünschelrute.

Although electromagnetic phenomena have been known since the time of the Greeks, it took a long time until scientist started to develop a theory for electromagnetism. Despite the fact that many scientists, e.g., Faraday and Ampère, contributed to this development, the modern theory of electromagnetism is accredited to one person — James Clerk Maxwell (1831-1879). In 1873 Maxwell published the textbook *A Treatise on Electricity and Magnetism*. In this work Maxwell combined previous experimental and theoretical results to formulate a set of coupled partial differential equations that were sufficient to describe all phenomena that had been known at that time. To honor his work, the equations presented in his work now bear his name and are known as Maxwell's equations.

Since Maxwell's equations describe a great range of different physical phenomena, ranging from stationary fields to wave propagation, it can be very difficult to solve these equations. However, in many situations we are able to make simplifying assumptions to obtain new models that are solvable more easily. One of these models is the eddy current model. It is derived from Maxwell's equations by neglecting the displacement currents. The name "eddy current" results from the fact that temporally changing magnetic fields induce electric currents that flow on closed paths.

Although the partial differential equations of the eddy current model are less complex, it is still difficult to find analytic solutions of these equations. Therefore, we have to use numerical methods to approximate the electric and magnetic fields. Despite the development of a vast array of numerical techniques for the compu-

tation of electromagnetic fields, the efficient solution of eddy current problems remains a challenging task.

For the solution of the algebraic equations arising from the finite element discretization of the partial differential equations, domain decomposition methods have aroused great interest in past decades. A particular domain decomposition approach is the mortar element method. The mortar method is based on a decomposition of the computational domain into nonoverlapping subdomains. It allows us to use independent individual triangulations, which are well adapted to the local behaviour of the electromagnetic field, for each subdomain. Moreover, it offers the possibility of parallelization, which can be used to accelerate the numerical solution process. Therefore, the main focus of this thesis is on the development of adaptive algorithms for the numerical solution of mortar edge element discretized three-dimensional eddy current problems.

The outline of this thesis is as follows: in Chapter 1 we will introduce Maxwell's equations together with suitable constitutive equations and boundary conditions. Additionally, we will present the most important simplified models. Chapter 2 will provide an elaborate introduction to the function spaces needed for the derivation of the variational formulation. Based on the Hilbert space $H^1(\Omega)$, we will introduce the Hilbert spaces $\mathbf{H}(\mathrm{div};\Omega)$ and $\mathbf{H}(\mathbf{curl};\Omega)$. Special attention will be paid to the trace space of $\mathbf{H}(\mathbf{curl};\Omega)$, which plays a central role in the construction of suitable Lagrange multipliers for the mortar element method.

Chapter 3 is dedicated to the model problem. First we will derive the variational formulation of the eddy current problem and prove the existence and uniqueness of a solution. In a second step we will employ an implicit timestepping scheme in order to discretize the problem in time. The resulting time-independent variational problem will serve as our model problem. The rest of this chapter is concerned with the macro-hybrid variational formulation of the model problem with respect to a geometrically conforming, nonoverlapping decomposition of the computational domain [Hop99].

In Chapter 4 we will consider the mortar approach based on individual discretizations of the subdomain problems by Nédélec's edge elements [Néd83]. Since this approach crucially depends on the choice of a suitable discrete Lagrange multiplier space, we will discuss its construction in great detail. At the end of this chapter we will prove an inf-sup condition for the associated discrete saddle point problem. Optimal a priori error estimates for the global discretization error [XH05] are presented in Chapter 5.

Chapter 6 deals with an efficient and reliable residual-type a posteriori error estimator. By decomposing the global discretization error into an irrotational and weakly solenoidal part, we will prove both the efficiency and reliability of the error estimator. An efficient multilevel iterative solver for the solution of the discrete saddle point problem will be developed and analyzed in Chapter 7.

We will show that a good smoother depends on the appropriate treatment of the nontrivial kernel of the **curl**-operator and discuss problems arising from this fact. As main result of this chapter, we will introduce a new hybrid smoother which consists of two steps. The first step performs preconditioned Richardson-type iterative sweeps on the fully edge element discretized problem. In the second step we apply similar iterative sweeps to a defect problem defined on the subspace of irrotational vector fields.

Chapter 8 addresses the performance of the multilevel iterative solver and the residual-type a posteriori error estimator for several academic test problems. In order to obtain these numerical results, the algorithms developed in Chapters 6 and 7 have been implemented using the software toolbox $\mathcal{UG}$ [BBL$^+$97]. Finally, in Chapter 9 we will summarize the results of the previous chapters and discuss limitations of the proposed methods together with possible remedies.

Acknowledgements

I would like to thank my supervisor Prof. Dr. Ronald H.W. Hoppe for giving me the opportunity to write this thesis. I appreciate his constant support as well as the numerous stimulating suggestions on the subject. Furthermore, I want to express my gratitude to Prof. Dr. Jozef Kačur and Christian Boltner for proofreading this thesis. I want to thank Stefan Krömer and Markus Lilli for valuable discussions related to the theoretical aspects of my work. But most of all I want to thank my family for their support and understanding during the years I have been working on my thesis.

Chapter 1

Physical Models of Electromagnetism

The following presentation of the physical background is only a summary of the theory that is important for the later work and follows standard textbooks on electromagnetism, such as [Gre91, Nol90]. It is by far not a complete treatment of the physics of electromagnetism. A much more detailed description can be found in the references given above.

Before we start with the introduction of the physical background, we want to say some words about notation. We will distinguish vectors from scalars by the use of bold typeface. In general, this convention does not carry over to operators. Unless stated otherwise, vectors will be three-dimensional and either elements of $\mathbb{R}^3$ or $\mathbb{C}^3$. For example, $\mathbf{x} \in \mathbb{R}^3$ denotes a vector with components x_1, x_2, and x_3, i.e. $\mathbf{x} = (x_1, x_2, x_3)^T$, where T denotes the transpose. For two vectors $\mathbf{a} \in \mathbb{C}^N$ and $\mathbf{b} \in \mathbb{C}^N$, we define the dot product on $\mathbb{C}^N$ by

$$\mathbf{a} \cdot \mathbf{b} = \sum_{j=1}^{N} a_j \, b_j \ .$$

Moreover, the vector product of two vectors $\mathbf{a} \in \mathbb{C}^3$ and $\mathbf{b} \in \mathbb{C}^3$ is given by

$$\mathbf{a} \wedge \mathbf{b} = (a_2 \, b_3 - a_3 \, b_2, a_3 \, b_1 - a_1 \, b_3, a_1 \, b_2 - a_2 \, b_1)^T \ .$$

A comprehensive list of the notation, used in this work, can be found at the end of the thesis.

1.1 Maxwell's Equations

The classical electromagnetic field is described by four vector-valued functions of position $\mathbf{x} \in \mathbb{R}^3$ and time t. These vector fields are the electric field intensity

E, the magnetic field intensity **H**, the electric displacement **D**, and the magnetic induction **B**. The vector functions **D** and **B** are also called the electric flux and the magnetic flux density, respectively. Since both **D** and **B** can be eliminated via suitable constitutive laws, they are less important than **E** and **H**. Therefore, **E** and **H** are the fundamental field vectors, and we will call them the electric and magnetic field, respectively.

An electromagnetic field can be created by resting charges and by currents, which are the directed flows of electric charge. The distribution of charge is given by a scalar function ρ, while currents are described by a vector-valued function **J**. Both are functions of position $\mathbf{x} \in \mathbb{R}^3$ and time t and are called the electric charge density and the electric current density, respectively. Table 1.1 summarizes these fields in terms of SI units.

Quantity	Units	Quantity	Units
Electric field intensity **E**	Vm^{-1}	Magnetic field intensity **H**	Am^{-1}
Electric displacement **D**	Cm^{-2}	Magnetic induction **B**	T
Electric current density **J**	Am^{-2}	Electric charge density ρ	Cm^{-3}

Table 1.1: Summary of the electromagnetic field quantities and their corresponding SI units.

These field variables and sources are connected by Maxwell's equations, which are two pairs of coupled partial differential equations that are given by

$$\text{Faraday's law} \qquad \frac{\partial \mathbf{B}}{\partial t} + \mathbf{curl}\,\mathbf{E} = 0 \ , \tag{1.1}$$

$$\text{Gauss's law} \qquad \operatorname{div}\mathbf{B} = 0 \ , \tag{1.2}$$

$$\text{Maxwell-Ampère's law} \qquad \frac{\partial \mathbf{D}}{\partial t} - \mathbf{curl}\,\mathbf{H} = -\mathbf{J} \ , \tag{1.3}$$

$$\text{Gauss's law} \qquad \operatorname{div}\mathbf{D} = \rho \ , \tag{1.4}$$

where $\mathbf{curl}\,\mathbf{u}$ and $\operatorname{div}\mathbf{u}$ are defined by

$$\mathbf{curl}\,\mathbf{u} = \nabla \wedge \mathbf{u} := \left(\frac{\partial u_3}{\partial x_2} - \frac{\partial u_2}{\partial x_3}, \frac{\partial u_1}{\partial x_3} - \frac{\partial u_3}{\partial x_1}, \frac{\partial u_2}{\partial x_1} - \frac{\partial u_1}{\partial x_2}\right)^T \ , \tag{1.5}$$

$$\operatorname{div}\mathbf{u} = \nabla \cdot \mathbf{u} := \sum_{i=1}^{3} \frac{\partial u_i}{\partial x_i} \ . \tag{1.6}$$

Faraday's law describes the effect of a changing magnetic flux **B** on the electric field **E**, while Ampère's circuital law states that the magnetic field **H** can be

created by a current $\mathbf{J}$. Maxwell modified this law to include the effects of a changing electric displacement field $\mathbf{D}$ on the magnetic field $\mathbf{H}$. The two Gaussian laws finally give the effect of the charge density ρ on the electric displacement and express the fact that the magnetic induction $\mathbf{B}$ is solenoidal.

The two Gaussian laws (1.2) and (1.4) are also consequences of equations (1.1) and (1.3), provided charge is conserved. This can be seen by taking the divergence of (1.1) and (1.3) and recalling that $\operatorname{div}(\mathbf{curl}\,\mathbf{A}) = 0$ for any vector-valued function $\mathbf{A}$. This gives

$$\operatorname{div}\frac{\partial \mathbf{B}}{\partial t} = 0 \quad \text{and} \quad \operatorname{div}\frac{\partial \mathbf{D}}{\partial t} = -\operatorname{div}\mathbf{J}\ . \tag{1.7}$$

If charge is conserved then ρ and $\mathbf{J}$ are connected by

$$\frac{\partial \rho}{\partial t} + \operatorname{div}\mathbf{J} = 0\ , \tag{1.8}$$

which gives

$$\frac{\partial}{\partial t}\operatorname{div}\mathbf{B} = \frac{\partial}{\partial t}\left(\operatorname{div}\mathbf{D} - \rho\right) = 0\ . \tag{1.9}$$

Equation (1.9) shows that equations (1.2) and (1.4) hold at all times if they hold at one time.

1.1.1 Constitutive Equations

Since equations (1.1)-(1.4) form a system of 7 independent scalar equations that involve 16 unknown scalar functions (one scalar function ρ and 15 scalar components of the vector fields $\mathbf{E}$, $\mathbf{H}$, $\mathbf{D}$, $\mathbf{B}$, and $\mathbf{J}$), the system is under-determined. Therefore, these equations must be augmented by constitutive equations.

Two of the constitutive equations relate the electric field $\mathbf{E}$ with the electric displacement $\mathbf{D}$ and the magnetic field $\mathbf{H}$ with the magnetic induction $\mathbf{B}$, i.e.

$$\mathbf{D} = \mathcal{D}(\mathbf{E}) \quad \text{and} \quad \mathbf{B} = \mathcal{B}(\mathbf{H})\ . \tag{1.10}$$

The functions $\mathcal{D}$ and $\mathcal{B}$ can be nonlinear, but in the following only the linear case is considered. Then these constitutive laws are given by

$$\mathbf{D} = \boldsymbol{\epsilon}\,\mathbf{E} \quad \text{and} \quad \mathbf{B} = \boldsymbol{\mu}\,\mathbf{H}\ , \tag{1.11}$$

where $\boldsymbol{\epsilon}$ and $\boldsymbol{\mu} \in \mathbb{R}^{3\times 3}$ are positive definite matrix-valued functions that can depend on position $\mathbf{x}$ and time t. There are two important simplifications of these two constitutive equations. In vacuum or free space (1.11) reduces to

$$\mathbf{D} = \epsilon_0\mathbf{E} \quad \text{and} \quad \mathbf{B} = \mu_0\mathbf{H}\ , \tag{1.12}$$

where ϵ_0 and μ_0 are called the electric permittivity and the magnetic permeability, respectively. In SI units they are given by

$$\begin{aligned} \epsilon_0 &= 4\pi \cdot 10^{-7}\ Hm^{-1} && \text{(henrys/meter)} \\ \mu_0 &\approx 8.854 \cdot 10^{-12}\ Fm^{-1} && \text{(farads/meter)}\ . \end{aligned}$$

Additionally, the speed of light in vacuum, denoted by c, is given by $c = 1/\sqrt{\epsilon_0 \mu_0}$. In inhomogeneous but isotropic materials $\boldsymbol{\epsilon}$ and $\boldsymbol{\mu}$ are given by positive, bounded scalar functions ϵ and μ, respectively. Then we have

$$\mathbf{D} = \epsilon \mathbf{E} \quad \text{and} \quad \mathbf{B} = \mu \mathbf{H}\ . \tag{1.13}$$

To solve the system of partial differential equations (1.1)-(1.4), one additional constitutive law is needed. In a conducting medium an electric field gives rise to electric currents. If the strength of the electric field is not too large, the relation between $\mathbf{E}$ and $\mathbf{J}$ can be expressed by means of Ohm's law that is given by

$$\mathbf{J} = \boldsymbol{\sigma} \mathbf{E} + \mathbf{J}_a\ , \tag{1.14}$$

where $\boldsymbol{\sigma}$ is called conductivity and $\mathbf{J}_a$ is a vector-valued function that describes an applied current density. In the general case, $\boldsymbol{\sigma}$ is a positive semi-definite matrix-valued function of position. However, we will only consider the case where the conductivity can be expressed as a nonnegative scalar function σ. Regions with positive σ are called conducting regions, while regions with $\sigma = 0$ are called insulators. Insulators with $\epsilon \neq \epsilon_0$ are called dielectrics and ϵ is called the dielectric constant. Finally, in air at low field strengths or in vacuum we have the case that $\sigma = 0$, $\epsilon = \epsilon_0$, and $\mu = \mu_0$.

1.1.2 Interface Conditions

In many cases ϵ or μ are discontinuous, e.g., at a conductor-air interface. Then equations (1.1)-(1.4) are not a complete classical description, since they are not valid at the interfaces between media where either ϵ or μ are discontinuous. At these interfaces the partial differential equations have to be replaced by suitable interface conditions.

Let us consider the case of two materials with different electric and magnetic properties. The materials are separated by a surface Γ with unit normal $\mathbf{n}$ pointing from region B to A (cf. Figure 1.1). If $\mathbf{E}_A$ and ϵ_A denote the limiting values of the electric field and the permittivity as Γ is approached from region A, and $\mathbf{E}_B$ and ϵ_B denote the corresponding values of region B then the interface conditions for the electric field are given by

$$\mathbf{n} \wedge (\mathbf{E}_A - \mathbf{E}_B) = 0\ , \tag{1.15}$$

$$\mathbf{n} \cdot (\epsilon_A \mathbf{E}_A - \epsilon_B \mathbf{E}_B) = \rho_S \quad \text{on } \Gamma\ , \tag{1.16}$$

where ρ_S is called the surface charge density. Taking equations (1.15) and (1.16), we see that the tangential component of the electric field is continuous at the surface Γ, while the normal component of $\mathbf{D} = \epsilon\mathbf{E}$ is discontinuous if surface charges are present.

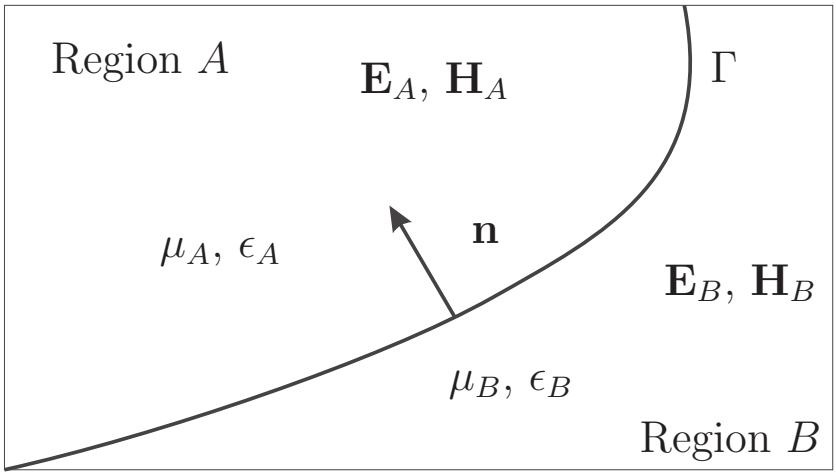

Figure 1.1: Geometry of the surface Γ separating two media with discontinuous permittivity and permeability.

For the magnetic field the interface conditions are just the other way round. Here we have

$$\mathbf{n} \wedge (\mathbf{H}_A - \mathbf{H}_B) = \mathbf{J}_S \ , \tag{1.17}$$

$$\mathbf{n} \cdot (\mu_A \mathbf{H}_A - \mu_B \mathbf{H}_B) = 0 \quad \text{on } \Gamma \ , \tag{1.18}$$

where $\mathbf{J}_S$ is called the surface current density and $\mu_{A,B}$ and $\mathbf{H}_{A,B}$ are defined as above. In this case the normal component of $\mathbf{B} = \mu\mathbf{H}$ is continuous, while the tangential component of $\mathbf{H}$ is discontinuous at the interface Γ if surface currents are present. However, in most instances the magnetic field has continuous tangential components.

Considering these interface conditions, any numerical scheme for the approximation of Maxwell's equations has to take into account that the tangential components of the electric and magnetic field are continuous, while the normal components jump at the discontinuities of the material.

1.1.3 Boundary Conditions

In order to find a solution of Maxwell's equations, we have to impose boundary conditions at the boundary of the domain we are considering. These conditions

are necessary to guarantee the uniqueness of the solution. Very often we are interested in the electromagnetic field in a bounded domain that is surrounded by different materials. Then the boundary conditions can be considered as special cases of the interface conditions.

A particularly important case occurs when parts of the boundary consist of a perfect conductor. Taking Ohm's law, we can see that if we require the current density $\mathbf{J}$ to be bounded inside the perfect conductor, the electric field $\mathbf{E}$ tends to 0 as σ tends to infinity. This suggests that the electric field vanishes inside a perfect conductor.

This effect is just a special case of the response of a perfect conductor to external fields. In general, a perfect conductor prevents electric and magnetic fields from entering the conductor. In order to achieve this, surface charges and currents are induced. Thus we get on the boundary

$$\mathbf{n} \wedge \mathbf{E} = 0 \ , \tag{1.19}$$

$$\mathbf{n} \cdot \mathbf{D} = \rho_S \ , \tag{1.20}$$

$$\mathbf{n} \cdot \mathbf{B} = 0 \ , \tag{1.21}$$

$$\mathbf{n} \wedge \mathbf{H} = \mathbf{J}_S \ , \tag{1.22}$$

which means that the electric field is orthogonal and the magnetic field is tangential to the boundary.

Equally important is the case when parts of the boundary are not perfect conductors, but allow the field to penetrate only a small distance into the material. Then a more appropriate boundary condition is the impedance or imperfectly conducting boundary condition which is given by

$$\mathbf{n} \wedge \mathbf{H} - \lambda \left(\mathbf{n} \wedge \mathbf{E} \right) \wedge \mathbf{n} = 0 \ , \tag{1.23}$$

where the impedance λ is a positive function of position which is defined on the boundary.

1.2 Simplified Electromagnetic Models

Maxwell's equations, as given in the last section, describe a great range of different physical phenomena, ranging from stationary fields to wave propagation. This behavior suggests that it might be unwise to use this general form for the computation of electromagnetic fields. Indeed, there are a variety of physical models arising from additional assumptions that allow substantial simplifications of the equations. In the following we present those simplified models that are encountered most frequently. They have in common that these additional assumptions concern the temporal variation of the fields.

1.2.1 Stationary Models: Electrostatics and Magnetostatics

The most obvious simplification is to assume that there is no variation in time of the electric and magnetic fields. In this case the close connections between the electric and the magnetic field, as given by equations (1.1) and (1.3), do not exist any more. In fact, the two fields can be treated independently. The equations for the electric field take the form

$$\begin{aligned} \mathbf{curl}\,\mathbf{E} &= 0 \quad , && (1.24)\\ \operatorname{div}\mathbf{D} &= \rho \quad , && (1.25)\\ \mathbf{D} &= \epsilon\mathbf{E} \ , && (1.26) \end{aligned}$$

with a static charge density ρ. Equations (1.24)-(1.26) are also called the electrostatic model. A consequence of equation (1.24) is the fact that on simply connected domains the electric field $\mathbf{E}$ can be expressed as the gradient of a scalar function φ, i.e $\mathbf{E} = -\,\mathbf{grad}\,\varphi$. Employing the remaining equations, we arrive at

$$-\operatorname{div}(\epsilon\,\mathbf{grad}\,\varphi) = \rho \ . \tag{1.27}$$

Equation (1.27) is called Poisson's equation and it admits a unique solution when provided with suitable boundary conditions. In a similar way we get the magnetostatic model that is given by

$$\begin{aligned} \mathbf{curl}\,\mathbf{H} &= \mathbf{J} \quad , && (1.28)\\ \operatorname{div}\mathbf{B} &= 0 \quad , && (1.29)\\ \mathbf{B} &= \mu\mathbf{H} \ , && (1.30) \end{aligned}$$

for a time-independent source current density $\mathbf{J}$. The vanishing divergence of the magnetic field implies the existence of a vector potential field $\mathbf{A}$ for $\mathbf{B}$, which means that $\mathbf{B} = \mathbf{curl}\,\mathbf{A}$. Using this fact, we arrive at the essential equation of magnetostatics

$$\mathbf{curl}\left(\mu^{-1}\,\mathbf{curl}\,\mathbf{A}\right) = \mathbf{J} \ . \tag{1.31}$$

Equations (1.27) and (1.31) show that in the static case Maxwell's equations boil down to elliptic boundary value problems corresponding to a minimization of energy (electrostatics) or energy dissipation (magnetostatics).

1.2.2 The Quasi-Static Model - The Eddy Current Case

In transient, slowly-varying applications, it is possible to neglect the Maxwellian displacement current $\partial_t\mathbf{D}$ [ABN00], which basically means that the wave propagation is ignored. This simplification yields a reasonable approximation if the

wavelength of the electric field is much greater than the size of the region of interest and if the conductivity is big enough. In this case we arrive at parabolic equations that are given by

$$\mathbf{curl}\,\mathbf{E} = -\frac{\partial \mathbf{B}}{\partial t} \quad , \tag{1.32}$$

$$\mathbf{curl}\,\mathbf{H} = \mathbf{J} \quad , \tag{1.33}$$

$$\mathrm{div}\,\mathbf{B} = 0 \quad , \tag{1.34}$$

$$\mathrm{div}\,\mathbf{D} = \rho \quad . \tag{1.35}$$

1.2.3 The Time-Harmonic Model

Another way to simplify the time-dependent Maxwell's equations is to perform a Fourier transform in time. In the general case, this would give an infinite number of equations for the frequencies $\omega \in (0, \infty)$. However, it is often enough to analyze the electromagnetic propagation at a single frequency. This is the case if the source currents and charges vary sinusoidally in time. Then the electric and magnetic fields are given by

$$\mathbf{E}(x,t) = \mathrm{Re}\left(\hat{\mathbf{E}}(x)\exp(-i\omega t)\right) \quad , \tag{1.36}$$

$$\mathbf{D}(x,t) = \mathrm{Re}\left(\hat{\mathbf{D}}(x)\exp(-i\omega t)\right) \quad , \tag{1.37}$$

$$\mathbf{H}(x,t) = \mathrm{Re}\left(\hat{\mathbf{H}}(x)\exp(-i\omega t)\right) \quad , \tag{1.38}$$

$$\mathbf{B}(x,t) = \mathrm{Re}\left(\hat{\mathbf{B}}(x)\exp(-i\omega t)\right) \quad , \tag{1.39}$$

$$\mathbf{J}(x,t) = \mathrm{Re}\left(\hat{\mathbf{J}}(x)\exp(-i\omega t)\right) \quad , \tag{1.40}$$

$$\rho(x,t) = \mathrm{Re}\left(\hat{\rho}(x)\exp(-i\omega t)\right) \quad , \tag{1.41}$$

where the amplitudes $\hat{\mathbf{E}}$, $\hat{\mathbf{D}}$, $\hat{\mathbf{H}}$, $\hat{\mathbf{B}}$, $\hat{\mathbf{J}}$, and $\hat{\rho}$ are complex. Electromagnetic fields of this form are called time-harmonic, and the resulting Maxwell's equations are named time-harmonic Maxwell's equations. Substituting relations (1.36)-(1.41) into (1.1)-(1.4) gives

$$-i\omega\hat{\mathbf{B}} + \mathbf{curl}\,\hat{\mathbf{E}} = 0 \quad , \tag{1.42}$$

$$\mathrm{div}\,\hat{\mathbf{D}} = \hat{\rho} \quad , \tag{1.43}$$

$$-i\omega\hat{\mathbf{D}} - \mathbf{curl}\,\hat{\mathbf{H}} = -\hat{\mathbf{J}} \quad , \tag{1.44}$$

$$\mathrm{div}\,\hat{\mathbf{B}} = 0 \quad . \tag{1.45}$$

Then the charge conservation and the constitutive equations have the form

$$i\omega\hat{\rho} = \operatorname{div}\hat{\mathbf{J}} \quad , \tag{1.46}$$

$$\hat{\mathbf{D}} = \epsilon\hat{\mathbf{E}} \quad , \tag{1.47}$$

$$\hat{\mathbf{B}} = \mu\hat{\mathbf{H}} \quad , \tag{1.48}$$

$$\hat{\mathbf{J}} = \sigma\hat{\mathbf{E}} + \hat{\mathbf{J}}_a \ . \tag{1.49}$$

Chapter 2

Sobolev and Vector Function Spaces

A powerful method for solving partial differential equations is to derive a variational formulation of the problem and look for a generalized solution in an appropriate Hilbert space. In the context of Maxwell's equations, these Hilbert spaces are built on Sobolev spaces for scalar and vector-valued functions. Therefore, the purpose of the first part of this chapter is to recall main results and notions for scalar Sobolev spaces. These results are quite standard and will be stated without proofs. Detailed proofs can be found in the excellent books [Ada78, GR79, Gri85].

In the second part of this chapter we generalize the concept of the classical Sobolev space and introduce two important spaces of vector-valued functions that are appropriate for analyzing Maxwell's equations. Although these spaces have been intensively studied in recent years, they are still a little less standard, so we shall give more details. In particular, their trace spaces will be analyzed in great detail, since they are essential for the variational formulation of the problem.

2.1 Standard Sobolev Spaces

Let $\Omega \subset \mathbb{R}^d$, $d = 1, 2, 3$, be a domain, i.e. an open and connected set. Its closure will be denoted by $\bar{\Omega}$ and we will refer to $\Gamma = \partial\Omega := \bar{\Omega} \setminus \Omega$ as its boundary. Since Ω is a subset of $\mathbb{R}^d$, we also have an exterior domain, which is defined by $\Omega_e := \mathbb{R}^d \setminus \bar{\Omega}$. A point in $\mathbb{R}^d$ is denoted by $\mathbf{x} = (x_1, ..., x_d)$.

A d-tuple $\alpha = (\alpha_1, ..., \alpha_d)$ consisting of nonnegative integers $\alpha_i \in \mathbb{N}_0$ is called a multi-index. Denoting by $\mathbf{x}^\alpha$ the monomial $x_1^{\alpha_1} \cdot ... \cdot x_d^{\alpha_d}$, which has degree $|\alpha| = \sum_{i=1}^d \alpha_i$, the partial derivatives $D^\alpha u$ of $u \in C^{|\alpha|}(\Omega)$ can be written as

$$D^\alpha u = \frac{\partial^{|\alpha|} u}{\partial x_1^{\alpha_1} \partial x_2^{\alpha_2} ... \partial x_d{}^{\alpha_d}} \ . \tag{2.1}$$

For $m \in \mathbb{N}_0$ we denote by $C^m(\Omega)$ the space of m times continuously differentiable functions u on Ω. In the following we abbreviate $C^0(\Omega) \equiv C(\Omega)$ and refer to $C_0^m(\Omega)$ as the set of functions $u \in C^m(\Omega)$ having compact support in Ω. Moreover, we define

$$C^\infty(\Omega) := \bigcap_{m=0}^{\infty} C^m(\Omega)$$

and denote by $C_0^\infty(\Omega)$ the subspace of functions $u \in C^\infty(\Omega)$ with compact support.

Since Ω is an open set, we cannot expect that an arbitrary element of $C^m(\Omega)$ is bounded. Considering this we define $C^m(\bar{\Omega})$ as the set of functions in $C^m(\Omega)$ which have uniformly continuous and bounded derivatives up to order m on $\bar{\Omega}$, i.e

$$C^m(\bar{\Omega}) := \left\{ u|_\Omega \mid u \in C_0^m(\mathbb{R}^d) \right\} \ .$$

$C^m(\bar{\Omega})$ is a Banach space with respect to the norm

$$\|u\|_{C^m(\bar{\Omega})} := \max_{0 \le |\alpha| \le m} \sup_{\mathbf{x} \in \Omega} |D^\alpha u(x)| \ . \tag{2.2}$$

For $1 \le p < \infty$ we denote by $L^p(\Omega)$ the linear space of measurable functions u on Ω satisfying

$$\int_\Omega |u(\mathbf{x})|^p \, dV < \infty \ . \tag{2.3}$$

$L^p(\Omega)$ is a Banach space with respect to the norm

$$\|u\|_{0,p,\Omega} := \left(\int_\Omega |u(\mathbf{x})|^p \, dV \right)^{1/p} \ . \tag{2.4}$$

The most important case is $p = 2$, which is the set of all square integrable functions. $L^2(\Omega)$ is a Hilbert space with respect to the inner product

$$(u, v)_{0,\Omega} := \int_\Omega uv \, dV \ . \tag{2.5}$$

A measurable function u on Ω is said to be essentially bounded on Ω if there exists a constant K such that $|u(\mathbf{x})| \le K$ almost everywhere on Ω. The infimum of such constants K is denoted by $ess\ \sup_{\mathbf{x} \in \Omega} |u(\mathbf{x})|$ and is called the essential supremum of u on Ω. Taking this notation, we can define the space $L^\infty(\Omega)$ as the vector space of all functions that are essentially bounded on Ω. This space is a Banach space with respect to the norm

$$\|u\|_\infty := ess \sup_{\mathbf{x} \in \Omega} |u(\mathbf{x})| \ . \tag{2.6}$$

For a given Hilbert space X we denote by X' its dual space, which consists of all bounded linear functionals on X. For $f \in X'$ the norm of f is given by

$$\|f\|_{X'} := \sup_{u \in X, u \neq 0} \frac{|f(u)|}{\|u\|_X} .$$

Moreover, we define the dual pairing $< \cdot, \cdot >_X$ by

$$< f, u >_X = f(u) \quad \forall u \in X,\ f \in X' .$$

The space of distributions, denoted by $(C_0^\infty(\Omega))'$, is the dual space of $C_0^\infty(\Omega)$ in the sense that a linear functional $T : C_0^\infty(\Omega) \to \mathbb{R}$ is an element of $(C_0^\infty(\Omega))'$ if for every compact set $K \subset \Omega$ there exist constants C and k such that

$$|T(\phi)| \leq C \sum_{|\alpha| \leq k} \sup_K |D^\alpha \phi| \quad \forall \phi \in C_0^\infty. \tag{2.7}$$

The elements of $(C_0^\infty(\Omega))'$ are called distributions, and we can identify each function $u \in L^1(\Omega)$ with a distribution $T(\cdot)$ by setting

$$T(\phi) = \int_\Omega u\, \phi \, dV \quad \forall \phi \in (C_0^\infty(\Omega)) .$$

Observing this property, we can generalize the classical concept of differentiability and introduce the weak derivative.

Definition 2.1 (Weak derivative)
A function $u \in L^1(\Omega)$ has a weak derivative, denoted by $v = D_w^\alpha u$, $\alpha \in \mathbb{N}_0^d$, if $v \in L^1(\Omega)$ and

$$\int_\Omega v\, \phi \, dV = (-1)^{|\alpha|} \int_\Omega u\, D^\alpha \phi \, dV \quad \forall \phi \in C_0^\infty(\Omega) . \tag{2.8}$$

The weak derivative of a function is unique. Moreover, for functions $u \in C^m\left(\bar{\Omega}\right)$ the weak and the standard (strong) derivatives agree given that $|\boldsymbol{\alpha}| \leq m$. After these preliminaries we are able to state the definition of the standard Sobolev spaces which are relevant for our analysis.

Definition 2.2 (Sobolev spaces $H^m(\Omega)$)
Let $\Omega \in \mathbb{R}^d$ be a domain, $m \in \mathbb{N}_0$. Then the Sobolev space $H^m(\Omega)$ is given by

$$H^m(\Omega) := \left\{ u \in L^2(\Omega) \mid\ D_w^\alpha u \in L^2(\Omega)\ ,\ |\alpha| \leq m \right\} . \tag{2.9}$$

$H^m(\Omega)$ is a Hilbert space endowed with the norm

$$\|u\|_{m,\Omega} := \left(\sum_{|\alpha| \leq m} \int_\Omega |D_w^\alpha u|^2 \, dV \right)^{1/2} \tag{2.10}$$

and the inner product

$$(u,v)_{m,\Omega} := \sum_{|\alpha|\le m} \int_\Omega D_w^\alpha u D_w^\alpha v \, dV \ . \tag{2.11}$$

Additionally, we denote the corresponding semi-norm by

$$|u|_{m,\Omega} := \left(\sum_{|\alpha|=m} \int_\Omega |D_w^\alpha u|^2 \, dV \right)^{1/2} \ . \tag{2.12}$$

The definition of the standard Sobolev space is not unique. As shown by Meyers and Serrin [MS64], the Sobolev space $H^m(\Omega)$ can be defined as the completion of the space

$$\{u \in C^m(\Omega) \mid \|u\|_{m,\Omega} < \infty\}$$

with respect to the $\|\cdot\|_{m,\Omega}$-norm.

Although this alternative characterization is useful, as it states that any function $u \in H^m(\Omega)$ can be approximated by smooth functions, it is not sufficient for the treatment of boundary value problems. On bounded domains the properties of Sobolev spaces depend on the smoothness or regularity of the boundary of the domain. In the framework of our analysis we will consider $(m,1)$-regular domains, especially Lipschitz polyhedral domains in $\mathbb{R}^3$.

Definition 2.3 (Lipschitz and $(m,1)$-regular domain)
The boundary $\partial\Omega$ of a bounded domain $\Omega \subset \mathbb{R}^d$ is called Lipschitz if there exist constants $\alpha > 0$ and $\beta > 0$, a finite number of local coordinate systems $(x_1^r, ..., x_d^r)$, $1 \le r \le R$, and local Lipschitz continuous functions a_r defined on

$$\mathcal{O}^r = \left\{ \hat{x}^r = (x_2^r, ..., x_d^r) \in \mathbb{R}^{d-1} \mid |x_i^r| \le \alpha \ , \ 2 \le i \le d \right\}$$

such that the following properties hold

- $\partial\Omega = \bigcup_{r=1}^R \{(x_1^r, \hat{x}^r) \mid x_1^r = a_r(\hat{x}_r) \ , \ \hat{x}^r \in \mathcal{O}^r\}$,
- $\{(x_1^r, \hat{x}^r) \mid a_r(\hat{x}^r) < x_1^r < a_r(\hat{x}^r) + \beta \ , \ \hat{x}^r \in \mathcal{O}^r\} \subset \Omega \ , \ 1 \le r \le R$,
- $\{(x_1^r, \hat{x}^r) \mid a_r(\hat{x}^r) - \beta < x_1^r < a_r(\hat{x}^r) \ , \ \hat{x}^r \in \mathcal{O}^r\} \subset \Omega_e \ , \ 1 \le r \le R$.

The domain Ω is said to be $(m,1)$-regular, for an integer $m \ge 1$, if the mappings a_r can be chosen m-times differentiable with Lipschitz-continuous partial derivatives of order m.

An important property of Lipschitz domains is the fact that $C^\infty(\bar{\Omega})$ is dense in $H^m(\Omega)$ with respect to the $\|\cdot\|_{m,\Omega}$-norm [Ada78]. This allows us to define the trace of functions $u \in H^m(\Omega)$. This is particulary important for boundary value

problems, since the solution has to satisfy boundary conditions, e.g., Dirichlet boundary conditions. Moreover, on Lipschitz domains Ω the space $H^m(\Omega)$ can be alternatively defined using Fourier transforms [Wlo82]. So far Sobolev spaces have been defined for nonnegative integers m. However, in order to be able to define trace spaces, the notion of a Sobolev space has to be extended to real values of m. Following [Gri85] we have:

Definition 2.4 (Sobolev spaces with real index)
Let $s \in \mathbb{R}_+$ and $m \in \mathbb{Z}_+$. Suppose $s = m + \sigma > 0$, where $\sigma \in \mathbb{R}$ and $0 < \sigma < 1$. Then the space $H^s(\Omega)$ is defined to be the space of functions $u \in (C_0^\infty)'$ such that $u \in H^m(\Omega)$ and

$$\int_\Omega \int_\Omega \frac{|D_w^\alpha u(\mathbf{x}) - D_w^\alpha u(\mathbf{y})|^2}{|\mathbf{x}-\mathbf{y}|^{d+2\sigma}}\, dV(\mathbf{x})\, dV(\mathbf{y}) < \infty \quad \forall\ |\alpha| = m\ . \tag{2.13}$$

$H^s(\Omega)$ is a Hilbert space with respect to the norm

$$\|u\|_{s,\Omega} := \left(\|u\|_{m,\Omega}^2 + \int_\Omega \int_\Omega \frac{|D_w^\alpha u(\mathbf{x}) - D_w^\alpha u(\mathbf{y})|^2}{|\mathbf{x}-\mathbf{y}|^{d+2\sigma}}\, dV(\mathbf{x})\, dV(\mathbf{y}) \right)^{1/2} . \tag{2.14}$$

Moreover, observing that $C_0^\infty(\Omega) \subset H^s(\Omega)$, $s > 0$, we denote by $H_0^s(\Omega)$, $s \geq 0$, the closure of $C_0^\infty(\Omega)$ with respect to the norm $\|\cdot\|_{s,\Omega}$. Finally, the Sobolev space $H^{-s}(\Omega)$ is defined as the dual space of $H_0^s(\Omega)$.

Observing Definition 2.3, for every $\mathbf{x} \in \Gamma$ there exists a neighborhood $\mathcal{O}$ of $\mathbf{x} \in \mathbb{R}^d$ and a Lipschitz continuous map $\varphi : \mathcal{O}' \subset \mathbb{R}^{d-1} \to \mathbb{R}$ such that

$$\Gamma \cap \mathcal{O} = \{ y = (\varphi(y'), y') \in \mathcal{O} \mid y' \in \mathcal{O}' \}\ . \tag{2.15}$$

Defining ϕ via $\phi(y) = (\varphi(y_2, ..., y_d), y_2, ..., y_d)$ then ϕ^{-1} exists and is Lipschitz continuous on $\phi(\mathcal{O}')$. This gives rise to the following definition [Gri85].

Definition 2.5 (Sobolev spaces on the boundary)
Let Ω be a $(m,1)$-regular domain with boundary Γ and Γ_0 an open subset of Γ. A distribution u on Γ_0 belongs to $H^s(\Gamma_0)$ for $|s| \leq m+1$ if the composition $u \circ \phi$ is contained in $H^s(\mathcal{O}' \cap \phi^{-1}(\Gamma_0 \cap \mathcal{O}))$ for all possible $\mathcal{O}$ and ϕ fulfilling the assumptions in Definition 2.3.

A norm on $H^s(\Gamma_0)$ is given by

$$\|u\|_{s,\Gamma_0} := \left(\sum_{j=1}^R \|u \circ \phi\|_{s,\mathcal{O}_j' \cap \phi_j^{-1}(\Gamma_0 \cap \mathcal{O}_j)} \right)^{1/2} , \tag{2.16}$$

where $(\mathcal{O}_j, \phi_j)_{j=1}^R$ is any atlas of Γ such that each pair $(\mathcal{O}_j, \phi_j)$ satisfies the assumptions of Definition 2.3. For $s \in [0,1)$ this definition is equivalent to

$$\|u\|_{s,\Gamma_0} = \left(\int_{\Gamma_0} |u|^2\, d\sigma + \int_{\Gamma_0} \int_{\Gamma_0} \frac{|u(\mathbf{x}) - u(\mathbf{y})|^2}{|\mathbf{x}-\mathbf{y}|^{d-1+2s}}\, d\sigma(\mathbf{x})\, d\sigma(\mathbf{y}) \right)^{1/2} . \tag{2.17}$$

For functions $u \in C^\infty(\bar{\Omega})$ the restriction of u to the boundary is well-defined. Thus it makes sense to define the trace operator γ_0 for such functions by

$$\gamma_0(u) := u|_{\partial\Omega} \ . \tag{2.18}$$

The extension of this operator to the Sobolev spaces $H^s(\Omega)$ is given by the following theorem [Gri85].

Theorem 2.6 (Trace theorem)
Let Ω be a $(m,1)$-regular domain. Then, if $1/2 < s \leq m+1$, the mapping γ_0, defined on $C^\infty(\bar{\Omega})$ by (2.18), has a unique continuous extension as a linear operator from $H^s(\Omega)$ onto $H^{s-1/2}(\partial\Omega)$. Moreover,

$$H_0^1(\Omega) := \left\{ u \in H^1(\Omega) \mid \gamma_0(u) = 0 \right\} \ . \tag{2.19}$$

For $\Gamma_0 \subset \Gamma$ we define

$$H_{\Gamma_0}^1(\Omega) := \left\{ u \in H^1(\Omega) \mid \gamma_0(u)|_{\Gamma_0} = 0 \right\} \ . \tag{2.20}$$

According to Definition 2.5, the trace space is well-defined if the boundary is sufficiently smooth. However, since we are mostly concerned with Lipschitz domains, this definition restricts the maximal order of the trace space to $s = 1$. Therefore, we define the space $H^{m+1/2}(\Gamma)$, $1 \leq m$, as the restriction of the space $H^{m+1}(\Omega)$ on the boundary Γ, i.e.

$$H^{m+1/2}(\Gamma) := \left\{ u|_\Gamma \mid u \in H^{m+1}(\Omega) \right\} \ . \tag{2.21}$$

$H^{m+1/2}(\Gamma)$ is a Hilbert space with respect to the norm

$$\|\varphi\|_{m+1/2,\Gamma} := \inf_{u \in H^{m+1}(\Omega), u|_\Gamma = \varphi} \|u\|_{m+1,\Omega} \ . \tag{2.22}$$

In the analysis of Maxwell's equations we have to consider the extension of functions $u \in H^s(\Sigma)$, $\Sigma \subset \Omega$ or $\Sigma \subset \Gamma$, to $H^s(\Omega)$ and $H^s(\Gamma)$, respectively. The trivial way to do this is to extend u by zero outside Σ. Of course, this extension is not well-defined for all functions in $u \in H^s(\Sigma)$. Denoting by $\tilde{u}$ this trivial extension of u, we define

$$\begin{aligned} H_{00}^s(\Sigma) &:= \{ u \in H^s(\Sigma) \mid \tilde{u} \in H^s(\Omega) \} \text{ and} \\ H_{00}^s(\Sigma) &:= \{ u \in H^s(\Sigma) \mid \tilde{u} \in H^s(\Gamma) \} \text{, respectively .} \end{aligned}$$

$H_{00}^s(\Sigma)$ is a Hilbert space with respect to the norm

$$\begin{aligned} \|u\|_{H_{00}^s(\Sigma)} &:= \|\tilde{u}\|_{s,\Omega} \text{ and} \\ \|u\|_{H_{00}^s(\Sigma)} &:= \|\tilde{u}\|_{s,\Gamma} \text{, respectively.} \end{aligned}$$

So far only scalar Sobolev spaces have been considered. However, for the treatment of electromagnetic problems vector-valued functions are needed. Regarding Maxwell's equations, especially functions with a well-defined curl or divergence are essential. The appropriate spaces will be introduced in the following sections.

2.2 The Space $\mathbf{H}(\mathrm{div};\Omega)$

In this section we consider the space of vector-valued functions with square-integrable divergence. The properties of this space will be stated without proofs and we refer the reader to [Gri85] for details.

Let $\Omega \subset \mathbb{R}^3$ be a Lipschitz domain and let $\Gamma := \partial\Omega$ be its boundary. Recalling that for functions $u \in C^1(\Omega)$ the gradient of u, denoted by $\mathbf{grad}\, u$, is defined by

$$\mathbf{grad}\, u := (\frac{\partial u}{\partial x_1}, \frac{\partial u}{\partial x_2}, \frac{\partial u}{\partial x_3})^T \ , \tag{2.23}$$

we proceed as in the previous section and define for a function $\mathbf{u} \in \mathbf{L}^2(\Omega)$ its weak divergence $\operatorname{div}\mathbf{u} \in (C_0^\infty)'$ by means of

$$< \operatorname{div}\mathbf{u}, \phi > = -\int_\Omega \mathbf{u} \cdot \mathbf{grad}\, \phi \, dV \quad \forall \phi \in C_0^\infty(\Omega) \ , \tag{2.24}$$

where $< \cdot, \cdot >$ denotes the dual pairing between $(C_0^\infty)'$ and C_0^∞. Then the space of functions with square-integrable divergence, denoted by $\mathbf{H}(\mathrm{div};\Omega)$, is defined as

$$\mathbf{H}(\mathrm{div};\Omega) := \left\{ \mathbf{u} \in \mathbf{L}^2(\Omega) \mid \operatorname{div}\mathbf{u} \in L^2(\Omega) \right\} \ . \tag{2.25}$$

Associated with this space is the norm

$$\|\mathbf{u}\|_{\mathrm{div},\Omega} := \left(\|\mathbf{u}\|_{2,\Omega}^2 + \|\operatorname{div}\mathbf{u}\|_{2,\Omega}^2 \right)^{1/2} \ .$$

$\mathbf{H}(\mathrm{div};\Omega)$ is a Hilbert space with respect to the inner product

$$(\mathbf{u}, \mathbf{v})_{\mathrm{div},\Omega} := (\mathbf{u}, \mathbf{v})_{0,\Omega} + (\operatorname{div}\mathbf{u}, \operatorname{div}\mathbf{v})_{0,\Omega} \ , \ \mathbf{u}, \mathbf{v} \in \mathbf{H}(\mathrm{div};\Omega) \ .$$

Taking this norm, we can define the space $\mathbf{H}_0(\mathrm{div};\Omega)$ as the closure of $(C_0^\infty(\Omega))^3$ with respect to the $\|\cdot\|_{\mathrm{div},\Omega}$-norm. Moreover, on Lipschitz domains the space $(C^\infty(\bar{\Omega}))^3$ is dense in $\mathbf{H}(\mathrm{div};\Omega)$. This property is very important for boundary value problems, since it enables us to define the trace of the space $\mathbf{H}(\mathrm{div};\Omega)$.

For a function $\mathbf{u} \in \left(C^\infty\left(\bar{\Omega}\right)\right)^3$ the normal trace operator γ_n is defined almost everywhere by

$$\gamma_n(\mathbf{u}) := \mathbf{u}|_\Gamma \cdot \mathbf{n} \ , \tag{2.26}$$

where $\mathbf{n}$ is the unit outward normal on Γ. By density arguments we can extend the normal trace operator γ_n to a continuous linear mapping, also denoted by γ_n, from $\mathbf{H}(\mathrm{div};\Omega)$ onto $H^{-1/2}(\Gamma)$ $(= (H^{1/2}(\Gamma))')$. Moreover, the following Green's theorem is valid for functions $\mathbf{u} \in \mathbf{H}(\mathrm{div};\Omega)$ and $\phi \in H^1(\Omega)$:

$$(\mathbf{u}, \mathbf{grad}\, \phi) + (\operatorname{div}\mathbf{u}, \phi) = < \mathbf{n} \cdot \mathbf{u}, \phi >_{1/2,\Gamma} \ , \tag{2.27}$$

where $< \cdot, \cdot >_{1/2,\Gamma}$ denotes the dual pairing between $H^{-1/2}(\Gamma)$ and $H^{1/2}(\Gamma)$. The continuity of γ_n implies that

$$\|\mathbf{n} \cdot \mathbf{u}\|_{H^{-1/2}(\Gamma)} \leq C \|\mathbf{u}\|_{\mathrm{div},\Omega} \ . \tag{2.28}$$

By means of γ_n, an alternative characterization of $\mathbf{H}_0(\mathrm{div};\Omega)$ is given by

$$\mathbf{H}_0(\mathrm{div};\Omega) = \{\mathbf{u} \in \mathbf{H}(\mathrm{div};\Omega) \mid \gamma_n(\mathbf{u}) = 0\} \ . \tag{2.29}$$

2.3 The Space $\mathbf{H}(\mathbf{curl};\Omega)$

The second important space for Maxwell's equations is related to the **curl**-operator. As in the previous section, we present the properties of this space without proofs and refer to [Gri85, Mon03] for details.

Let $\Omega \subset \mathbb{R}^3$ and let Γ denote its boundary. Following the steps of the last sections, we define the weak curl $\mathbf{curl}\,\mathbf{u} \in (C_0^\infty(\Omega)^3)'$ of a function $\mathbf{u} \in \mathbf{L}^2(\Omega)$ by means of

$$< \mathbf{curl}\,\mathbf{u}, \mathbf{v} > = \int_\Omega \mathbf{u} \cdot \mathbf{curl}\,\mathbf{v}\, dV \quad \forall \mathbf{v} \in (C_0^\infty(\Omega))^3 \ , \tag{2.30}$$

where $< \cdot, \cdot >$ denotes the dual pairing between $((C_0^\infty)^3)'$ and $(C_0^\infty)^3$. Then the space of vector-valued functions whose **curl** is an element of $\mathbf{L}^2(\Omega)$ is given by

$$\mathbf{H}(\mathbf{curl};\Omega) := \left\{\mathbf{u} \in \mathbf{L}^2(\Omega) \mid \mathbf{curl}\,\mathbf{u} \in \mathbf{L}^2(\Omega)\right\} \ . \tag{2.31}$$

$\mathbf{H}(\mathbf{curl};\Omega)$ is a Hilbert space with respect to the inner product

$$(\mathbf{u}, \mathbf{v})_{\mathbf{curl},\Omega} := (\mathbf{u}, \mathbf{v})_{0,\Omega} + (\mathbf{curl}\,\mathbf{u}, \mathbf{curl}\,\mathbf{v})_{0,\Omega} \ , \ \mathbf{u}, \mathbf{v} \in \mathbf{H}(\mathbf{curl};\Omega) \ . \tag{2.32}$$

The associated norm will be denoted by $\|\cdot\|_{\mathbf{curl},\Omega}$. Moreover, for $s \geq 0$ we define

$$\mathbf{H}^s(\mathbf{curl},\Omega) := \{\mathbf{u} \in \mathbf{H}^s(\Omega) \mid \mathbf{curl}\,\mathbf{u} \in \mathbf{H}^s(\Omega)\} \ , \tag{2.33}$$

$$\|\mathbf{u}\|_{s,\mathbf{curl},\Omega} := \left(\|\mathbf{u}\|_{s,\Omega}^2 + \|\,\mathbf{curl}\,\mathbf{u}\|_{s,\Omega}^2\right)^{1/2} \ . \tag{2.34}$$

The space $\mathbf{H}_0(\mathbf{curl};\Omega)$ is defined as the closure of $(C_0^\infty(\Omega))^3$ with respect to the $\|\cdot\|_{\mathbf{curl},\Omega}$-norm. If Ω is a Lipschitz domain, the space $\left(C^\infty\left(\bar{\Omega}\right)\right)^3$ is dense in $\mathbf{H}(\mathbf{curl};\Omega)$, which allows us to define the trace of $\mathbf{H}(\mathbf{curl};\Omega)$.

In contrast to the previous sections, the definition and characterization of the trace space is more complicated since it contains vector-valued functions. For the space $\mathbf{H}(\mathbf{curl};\Omega)$ two mappings play an important role: the tangential trace mapping γ_t and the tangential components trace mapping γ_T. For functions $\mathbf{u} \in \left(C^\infty\left(\bar{\Omega}\right)\right)^3$ these two mappings are defined by

$$\text{tangential trace} \quad : \quad \gamma_t(\mathbf{u}) := \mathbf{n} \wedge \mathbf{u}|_\Gamma \ , \tag{2.35}$$

$$\text{tangential components trace} : \quad \gamma_T(\mathbf{u}) := \mathbf{n} \wedge (\mathbf{u} \wedge \mathbf{n})\,|_\Gamma \ , \tag{2.36}$$

where $\mathbf{n}$ is the unit outward normal. We start the analysis by considering the trace of the space $\mathbf{H}^1(\Omega)$ with respect to the trace operators γ_T and γ_t. The ranges of these operators are given by

$$\begin{aligned}\mathbf{V}_{\gamma_T} &:= \gamma_T(\mathbf{H}^1(\Omega)) \ , \\ \mathbf{V}_{\gamma_t} &:= \gamma_t(\mathbf{H}^1(\Omega)) \ ,\end{aligned}$$

respectively. On smooth domains both spaces coincide with the space

$$\mathbf{TH}^{1/2}(\Gamma) := \{\mathbf{q} : \Gamma \to \mathbb{R}^3 \mid \mathbf{q} = (q_1, q_2, q_3)^T \in \mathbf{H}^{1/2}(\Gamma) \ , \ \mathbf{n} \cdot \mathbf{q} = 0\} \ , \tag{2.37}$$

which means that both trace operators are surjective mappings onto the space $\mathbf{TH}^{1/2}(\Gamma)$ [BCS02]. Since the boundary of the domain is smooth, the dual space of $\mathbf{TH}^{1/2}(\Gamma)$, denoted by $\mathbf{TH}^{-1/2}(\Gamma)$, can be defined according to

$$\mathbf{TH}^{-1/2}(\Gamma) := \{\mathbf{q} : \Gamma \to \mathbb{R}^3 \mid \mathbf{q} = (q_1, q_2, q_3)^T \in \mathbf{H}^{-1/2}(\Gamma) \ , \ \mathbf{n} \cdot \mathbf{q} = 0\} \ . \tag{2.38}$$

Moreover, for $\mathbf{u} \in \mathbf{H}(\mathbf{curl};\Omega)$ both traces $\gamma_t(\mathbf{u})$ and $\gamma_T(\mathbf{u})$ are an element of $\mathbf{TH}^{-1/2}(\Gamma)$. However, in the case of Lipschitz domains, the situation is completely different. As pointed out in [BCS02], the spaces $\mathbf{V}_{\gamma_T}$, $\mathbf{V}_{\gamma_t}$, and $\mathbf{TH}^{1/2}(\Gamma)$ do no longer coincide. Additionally, the definition of $\mathbf{TH}^{-1/2}(\Gamma)$ according to (2.38) does not make sense any more, since $\mathbf{n} \cdot \mathbf{q}$ is not defined for $\mathbf{q} \in \mathbf{H}^{-1/2}(\Gamma)$ in this case. Since the later part of this thesis will focus on the numerical solution of Maxwell's equations on polyhedral Lipschitz domains, we have to characterize the spaces $\mathbf{V}_{\gamma_T}$ and $\mathbf{V}_{\gamma_t}$ in more detail.

Let $\Omega \subset \mathbb{R}^3$ be a simply connected polyhedral domain with boundary Γ. We can split Γ into K open faces Γ_i, $1 \le i \le K$, such that $\Gamma = \bigcup_{i=1}^{K} \bar{\Gamma}_i$. Furthermore, let e_{ij} be the common edge of two adjacent faces Γ_i and Γ_j and let $\mathbf{n}$ denote the unit outward normal to Ω, which is defined almost everywhere. Let $\boldsymbol{\tau}_{ij}$ be a unit vector parallel to e_{ij}, $\mathbf{n}_i = \mathbf{n}|_{\Gamma_i}$, and $\boldsymbol{\tau}_i = \boldsymbol{\tau}_{ij} \wedge \mathbf{n}_i$. Then the couple $(\boldsymbol{\tau}_i, \boldsymbol{\tau}_{ij})$ forms an orthonormal basis of the plane generated by Γ_i, and $(\boldsymbol{\tau}_i, \boldsymbol{\tau}_{ij}, \mathbf{n}_i)$ is an orthonormal basis of $\mathbb{R}^3$. For elements $\mathbf{u} \in \mathbf{L}^2(\Gamma)$ we adopt the notation $\mathbf{u}_i = \mathbf{u}|_{\Gamma_i}$.

Since we are dealing with polyhedra, the definition of $\gamma_t(\mathbf{u})$ and $\gamma_T(\mathbf{u})$ has to be understood face by face:

$$\begin{aligned}\gamma_{t,j}(\mathbf{u}) &:= \mathbf{n}_j \wedge \mathbf{u}_j && \forall \mathbf{u} \in \left(C^\infty\left(\bar{\Omega}\right)\right)^3 \ , \\ \gamma_{T,j}(\mathbf{u}) &:= \mathbf{u}_j - (\mathbf{u}_j \cdot \mathbf{n}_j)\,\mathbf{n}_j && \forall \mathbf{u} \in \left(C^\infty\left(\bar{\Omega}\right)\right)^3 \ .\end{aligned}$$

This gives an equivalent definition of γ_t and γ_T:

$$\begin{aligned}\gamma_t(\mathbf{u})(x) &= \gamma_{t,j}(\mathbf{u})(x) \quad a.a.\ \mathbf{x} \in \Gamma_j \\ \gamma_T(\mathbf{u})(x) &= \gamma_{T,j}(\mathbf{u})(x) \quad a.a.\ \mathbf{x} \in \Gamma_j \ .\end{aligned}$$

Before we can extend these operators to $\mathbf{H}^1(\Omega)$ and $\mathbf{H}(\mathbf{curl};\Omega)$, we introduce two additional spaces which are defined by

$$\begin{aligned}\mathbf{L}_t^2(\Gamma) &:= \left\{\mathbf{u}\in\mathbf{L}^2(\Gamma) \mid \mathbf{u}\cdot\mathbf{n}|_\Gamma = 0\right\},\ <\cdot,\cdot>_T \text{ its scalar product}\\ \mathbf{H}_-^{1/2}(\Gamma) &:= \left\{\boldsymbol{\lambda}\in\mathbf{L}_t^2(\Gamma) \mid \boldsymbol{\lambda}_j\in\mathbf{H}^{1/2}(\Gamma_j)\ ,\ 1\le j\le K\right\}\ .\end{aligned}$$

Recalling that $\left(C^\infty\left(\bar\Omega\right)\right)^3$ is dense in $\mathbf{H}^1(\Omega)$, we immediately see that the mappings γ_t and γ_T can be extended to linear continuous mappings from $\mathbf{H}^1(\Omega)$ into $\mathbf{H}_-^{1/2}(\Gamma)$. However, the range of the mappings γ_t and γ_T is a proper subset of $\mathbf{H}_-^{1/2}(\Gamma)$. To characterize the images of these operators in more detail, we start with an alternative characterization of $H^{1/2}(\Gamma)$ [BC01a, Proposition 2.2].

Theorem 2.7 (Characterization of $H^{1/2}(\Gamma)$)
A function φ belongs to $H^{1/2}(\Gamma)$ if and only if $\varphi|_{\Gamma_i}\in H^{1/2}(\Gamma_i)$, $1\le i\le K$, and

$$\int_{\Gamma_i}\int_{\Gamma_j}\frac{|\varphi(\mathbf{x})-\varphi(\mathbf{y})|^2}{\|\mathbf{x}-\mathbf{y}\|^3}\,d\sigma(\mathbf{x})\,d\sigma(\mathbf{y})<\infty\quad\forall i\neq j\ s.t.\ \bar\Gamma_i\cap\bar\Gamma_j=e_{ij}\ . \tag{2.39}$$

Motivated by this theorem we introduce the equality on common edges and faces. Let $(\varphi_i,\varphi_j)\in H^{1/2}(\Gamma_i)\times H^{1/2}(\Gamma_j)$, $i\neq j$, and $e_{ij}=\bar\Gamma_i\cap\bar\Gamma_j\neq\emptyset$. Then we define the equality on e_{ij} by means of

$$\varphi_i =_{e_{ij}} \varphi_j \Leftrightarrow \int_{\Gamma_i}\int_{\Gamma_j}\frac{|\varphi(\mathbf{x})-\varphi(\mathbf{y})|^2}{\|\mathbf{x}-\mathbf{y}\|^3}\,d\sigma(\mathbf{x})\,d\sigma(\mathbf{y})<\infty\ . \tag{2.40}$$

Denoting by $\mathcal{I}_i$ the set of indices given by

$$\mathcal{I}_i := \left\{j\in 1,...,K \mid \bar\Gamma_i\cap\bar\Gamma_j=e_{ij}\neq\emptyset\right\}\ ,$$

we define the space $\mathbf{H}_\parallel^{1/2}(\Gamma)$ by

$$\mathbf{H}_\parallel^{1/2}(\Gamma) := \left\{\mathbf{u}\in\mathbf{H}_-^{1/2}(\Gamma) \mid \mathbf{u}_i\cdot\boldsymbol{\tau}_{ij} =_{e_{ij}} \mathbf{u}_j\cdot\boldsymbol{\tau}_{ij}\ ,\ 1\le i\le K\ ,\ \forall j\in\mathcal{I}_i\right\}\ . \tag{2.41}$$

$\mathbf{H}_\parallel^{1/2}(\Gamma)$ is a Hilbert space with respect to the norm

$$\|\mathbf{u}\|^2_{\parallel,1/2,\Gamma} := \sum_{i=1}^K\|\mathbf{u}_i\|^2_{1/2,\Gamma_i}+\sum_{i=1}^K\sum_{j\in\mathcal{I}_i}\int_{\Gamma_i}\int_{\Gamma_j}\frac{|\boldsymbol{\tau}_{ij}\cdot\mathbf{u}_i(\mathbf{x})-\boldsymbol{\tau}_{ij}\cdot\mathbf{u}_j(\mathbf{y})|^2}{\|\mathbf{x}-\mathbf{y}\|^3}\,d\sigma(\mathbf{x})\,d\sigma(\mathbf{y})\ .$$

In view of (2.41) we see that elements of $\mathbf{H}_\parallel^{1/2}(\Gamma)$ have some kind of continuity of their component parallel to $\boldsymbol{\tau}_{ij}$. Similarly, we can define a space consisting

of elements with a similar property for their components parallel to $\boldsymbol{\tau}_i$ and $\boldsymbol{\tau}_j$. Therefore, we introduce the space $\mathbf{H}_{\perp}^{1/2}(\Gamma)$ which is defined by

$$\mathbf{H}_{\perp}^{1/2}(\Gamma) := \left\{ \mathbf{u} \in \mathbf{H}_{-}^{1/2}(\Gamma) \mid \mathbf{u}_i \cdot \boldsymbol{\tau}_i =_{e_{ij}} \mathbf{u}_j \cdot \boldsymbol{\tau}_j \, , \, 1 \le i \le K \, , \, \forall j \in \mathcal{I}_i \right\} \, . \quad (2.42)$$

$\mathbf{H}_{\perp}^{1/2}(\Gamma)$ is a Hilbert space with respect to the norm

$$\|\mathbf{u}\|_{\perp,1/2,\Gamma}^2 := \sum_{i=1}^{K} \|\mathbf{u}_i\|_{1/2,\Gamma_i}^2 + \sum_{i=1}^{K} \sum_{j \in \mathcal{I}_i} \int_{\Gamma_i} \int_{\Gamma_j} \frac{|\boldsymbol{\tau}_i \cdot \mathbf{u}_i(\mathbf{x}) - \boldsymbol{\tau}_j \cdot \mathbf{u}_j(\mathbf{y})|^2}{\|\mathbf{x}-\mathbf{y}\|^3} \, d\sigma(\mathbf{x}) \, d\sigma(\mathbf{y}) \, .$$

Then the range of the trace operators γ_t and γ_T can be characterized by $\mathbf{H}_{\parallel}^{1/2}(\Gamma)$ and $\mathbf{H}_{\perp}^{1/2}(\Gamma)$ [BC01a, Proposition 2.7].

Theorem 2.8 (Range of the trace operators γ_t and γ_T part I)
The mappings

$$\gamma_T : \mathbf{H}^1(\Omega) \to \mathbf{H}_{\parallel}^{1/2}(\Gamma) \text{ and } \gamma_t : \mathbf{H}^1(\Omega) \to \mathbf{H}_{\perp}^{1/2}(\Gamma)$$

are linear, continuous, and surjective. Moreover, denoting by

$$\ker(\gamma_T) := \{\mathbf{u} \in \mathbf{H}^1(\Omega) \mid \mathbf{n} \wedge (\mathbf{u} \wedge \mathbf{n})|_\Gamma = 0\}$$
$$\text{and} \quad \ker(\gamma_t) := \{\mathbf{u} \in \mathbf{H}^1(\Omega) \mid \mathbf{n} \wedge \mathbf{u}|_\Gamma = 0\}$$

the kernels of the trace operators, the mappings

$$\gamma_T : \mathbf{H}^1(\Omega)/\ker(\gamma_T) \to \mathbf{H}_{\parallel}^{1/2}(\Gamma) \text{ and } \gamma_t : \mathbf{H}^1(\Omega)/\ker(\gamma_t) \to \mathbf{H}_{\perp}^{1/2}(\Gamma)$$

are linear, continuous, and bijective. Finally, there exist continuous lifting maps

$$\mathcal{R}_{\gamma_T} : \mathbf{H}_{\parallel}^{1/2}(\Gamma) \to \mathbf{H}^1(\Omega) \text{ and } \mathcal{R}_{\gamma_t} : \mathbf{H}_{\perp}^{1/2}(\Gamma) \to \mathbf{H}^1(\Omega) \, .$$

So far we have considered the trace mappings for functions $\mathbf{u} \in \mathbf{H}^1(\Omega)$. Before we can extend this operator to functions in $\mathbf{H}(\mathbf{curl};\Omega)$, we first have to introduce some tangential operators. We start with the definition of the tangential gradient operator, denoted by $\mathbf{grad}_\Gamma$. Since we deal with polyhedra, this operator is given facewise by

$$\mathbf{grad}_\Gamma \, u|_{\Gamma_i} := \mathbf{grad}_{\Gamma_j} \, u = \gamma_{T,i}(\mathbf{grad}\, u) = \gamma_T(\mathbf{grad}\, u)|_{\Gamma_i} \quad \forall u \in H^2(\Omega) \, . \quad (2.43)$$

In the same way, we can define the tangential curl operator $\mathbf{curl}_\Gamma$ by

$$\mathbf{curl}_\Gamma \, u := \gamma_t(\mathbf{grad}\, u) \, . \quad (2.44)$$

Let $\mathbf{H}_{\parallel}^{-1/2}(\Gamma)$ and $\mathbf{H}_{\perp}^{-1/2}(\Gamma)$ be the dual spaces of $\mathbf{H}_{\parallel}^{1/2}(\Gamma)$ and $\mathbf{H}_{\perp}^{1/2}(\Gamma)$ with $\mathbf{L}_t^2(\Gamma)$ as the pivot space, and let and $< \cdot, \cdot >_{\parallel,1/2,\Gamma}$ and $< \cdot, \cdot >_{\perp,1/2,\Gamma}$ be the dual pairings between $\mathbf{H}_{\parallel}^{-1/2}(\Gamma)$ and $\mathbf{H}_{\parallel}^{1/2}(\Gamma)$ and between $\mathbf{H}_{\perp}^{-1/2}(\Gamma)$ and $\mathbf{H}_{\perp}^{1/2}(\Gamma)$, respectively. Then the dual norms on $\mathbf{H}_{\parallel}^{-1/2}(\Gamma)$ and $\mathbf{H}_{\perp}^{-1/2}(\Gamma)$ are given by

$$\|\boldsymbol{\lambda}\|_{\parallel,-1/2,\Gamma} := \sup_{\mathbf{u}\in\mathbf{H}_{\parallel}^{1/2}(\Gamma)} \frac{< \boldsymbol{\lambda}, \mathbf{u} >_{\parallel,1/2,\Gamma}}{\|\mathbf{u}\|_{\parallel,1/2,\Gamma}} , \tag{2.45}$$

$$\|\boldsymbol{\lambda}\|_{\perp,-1/2,\Gamma} := \sup_{\mathbf{u}\in\mathbf{H}_{\perp}^{1/2}(\Gamma)} \frac{< \boldsymbol{\lambda}, \mathbf{u} >_{\perp,1/2,\Gamma}}{\|\mathbf{u}\|_{\perp,1/2,\Gamma}} . \tag{2.46}$$

The tangential divergence operator $\operatorname{div}_\Gamma : \mathbf{H}_{\parallel}^{-1/2}(\Gamma) \to H^{-3/2}(\Gamma)$ and the tangential curl operator $\operatorname{curl}_\Gamma : \mathbf{H}_{\perp}^{-1/2}(\Gamma) \to H^{-3/2}(\Gamma)$ are defined as the adjoint operators of $-\mathbf{grad}_\Gamma$ and $\mathbf{curl}_\Gamma$ according to

$$\begin{aligned} < \operatorname{div}_\Gamma \mathbf{q}, u >_{3/2,\Gamma} &= - < \mathbf{q}, \mathbf{grad}_\Gamma u >_{\parallel,1/2,\Gamma} \quad \forall u \in H^{3/2}(\Gamma),\ \mathbf{q} \in \mathbf{H}_{\parallel}^{-1/2}(\Gamma) , \\ < \operatorname{curl}_\Gamma \mathbf{q}, u >_{3/2,\Gamma} &= \quad < \mathbf{q}, \mathbf{curl}_\Gamma u >_{\perp,1/2,\Gamma} \quad \forall u \in H^{3/2}(\Gamma),\ \mathbf{q} \in \mathbf{H}_{\perp}^{-1/2}(\Gamma) , \end{aligned}$$

where $< \cdot, \cdot >_{3/2,\Gamma}$ denotes the dual pairing between $H^{3/2}(\Gamma)$ and $H^{-3/2}(\Gamma)$. Introducing the Hilbert spaces

$$\mathbf{H}_{\parallel}^{-1/2}(\operatorname{div}_\Gamma, \Gamma) := \left\{ \boldsymbol{\lambda} \in \mathbf{H}_{\parallel}^{-1/2}(\Gamma) \mid \operatorname{div}_\Gamma \boldsymbol{\lambda} \in H^{-1/2}(\Gamma) \right\} , \tag{2.47}$$

$$\mathbf{H}_{\perp}^{-1/2}(\operatorname{curl}_\Gamma, \Gamma) := \left\{ \boldsymbol{\lambda} \in \mathbf{H}_{\perp}^{-1/2}(\Gamma) \mid \operatorname{curl}_\Gamma \boldsymbol{\lambda} \in H^{-1/2}(\Gamma) \right\} , \tag{2.48}$$

which are equipped with the norms

$$\|\boldsymbol{\lambda}\|^2_{\mathbf{H}_{\parallel}^{-1/2}(\operatorname{div}_\Gamma,\Gamma)} := \|\boldsymbol{\lambda}\|^2_{\parallel,-1/2,\Gamma} + \|\operatorname{div}_\Gamma \boldsymbol{\lambda}\|^2_{-1/2,\Gamma} , \tag{2.49}$$

$$\|\boldsymbol{\lambda}\|^2_{\mathbf{H}_{\perp}^{-1/2}(\operatorname{curl}_\Gamma,\Gamma)} := \|\boldsymbol{\lambda}\|^2_{\perp,-1/2,\Gamma} + \|\operatorname{div}_\Gamma \boldsymbol{\lambda}\|^2_{-1/2,\Gamma} , \tag{2.50}$$

the trace spaces of $\mathbf{H}(\mathbf{curl};\Omega)$ are characterized by the following theorem [BCS02, Theorem 4.1].

Theorem 2.9 (Range of the trace operators γ_t and γ_T part II)
The mappings

$$\begin{aligned} \gamma_t :\ & \mathbf{H}(\mathbf{curl};\Omega) \to \mathbf{H}_{\parallel}^{-1/2}(\operatorname{div}_\Gamma, \Gamma) \\ \textit{and} \quad \gamma_T :\ & \mathbf{H}(\mathbf{curl};\Omega) \to \mathbf{H}_{\perp}^{-1/2}(\operatorname{curl}_\Gamma, \Gamma) \end{aligned}$$

are linear, continuous, and surjective.

Regarding the tangential trace mapping γ_t, an alternative definition of $\mathbf{H}_0(\mathbf{curl};\Omega)$ is given by

$$\mathbf{H}_0(\mathbf{curl};\Omega) = \{\mathbf{u} \in \mathbf{H}(\mathbf{curl};\Omega) \mid \gamma_t(\mathbf{u}) = 0\} \ . \tag{2.51}$$

For $\Gamma_0 \subset \Gamma$ we define

$$\mathbf{H}_{\Gamma_0}(\mathbf{curl},\Omega) := \{\mathbf{u} \in \mathbf{H}(\mathbf{curl};\Omega) \mid \gamma_t(\mathbf{u})|_{\Gamma_0} = 0\} \ . \tag{2.52}$$

In the next chapter we will derive the variational formulation of Maxwell's equations. To be able to do this, we need the following integration by parts formula [BC01a].

Theorem 2.10 (Stokes' theorem)
Let $\mathbf{u}$, $\mathbf{v} \in (C^1(\bar{\Omega}))^3$. *Then*

$$\int_\Omega (\mathbf{curl}\,\mathbf{v}\cdot\mathbf{u} - \mathbf{v}\cdot\mathbf{curl}\,\mathbf{u})\,dV = \int_\Gamma \gamma_t(\mathbf{v})\cdot\mathbf{u}\,d\sigma \ . \tag{2.53}$$

Moreover, for $\mathbf{u} \in \mathbf{H}(\mathbf{curl};\Omega)$ *and* $\mathbf{v} \in \mathbf{H}^1(\Omega)$ *we have*

$$\int_\Omega (\mathbf{curl}\,\mathbf{v}\cdot\mathbf{u} - \mathbf{v}\cdot\mathbf{curl}\,\mathbf{u})\,dV = <\gamma_t(\mathbf{u}),\mathbf{v}>_{1/2,\Gamma} \ , \tag{2.54}$$

$$\int_\Omega (\mathbf{curl}\,\mathbf{v}\cdot\mathbf{u} - \mathbf{v}\cdot\mathbf{curl}\,\mathbf{u})\,dV = <\gamma_t(\mathbf{u}),\gamma_T(\mathbf{v})>_{\|,1/2,\Gamma} \ . \tag{2.55}$$

Finally, for $\mathbf{u}$, $\mathbf{v} \in \mathbf{H}(\mathbf{curl};\Omega)$ *we have*

$$\int_\Omega (\mathbf{curl}\,\mathbf{v}\cdot\mathbf{u} - \mathbf{v}\cdot\mathbf{curl}\,\mathbf{u})\,dV = <\gamma_t(\mathbf{u}),\gamma_T(\mathbf{v})>_t \ . \tag{2.56}$$

Note that equation (2.56) expresses the fact that $\mathbf{H}_\|^{1/2}(\Gamma)$ is the dual space of $\mathbf{H}_\perp^{1/2}(\Gamma)$ with respect to the pivot space $\mathbf{L}_t^2(\Gamma)$ [BC01b]. Based on Stokes' theorem we can give one further characterization of $\mathbf{H}_0(\mathbf{curl};\Omega)$.
Let $\Omega_i \subset \Omega$, $1 \le i \le N$, be a nonoverlapping decomposition of Ω such that

$$\bar{\Omega} = \bigcup_{i=1}^N \bar{\Omega}_i \ , \ \Omega_i \cap \Omega_j = \emptyset, i \neq j \ ,$$

and define

$$\mathbf{X} := \{\mathbf{u} \in \mathbf{L}^2(\Omega) \mid \mathbf{u}|_{\Omega_i} \in \mathbf{H}(\mathbf{curl},\Omega_i) \ , \ (\mathbf{u}\wedge\mathbf{n})|_{\Gamma\cap\partial\Omega_i} = 0 \ , \ 1 \le i \le N\} \ .$$

Then we have

$$\mathbf{H}_0(\mathbf{curl};\Omega) = \{\mathbf{u} \in \mathbf{X} \mid \sum_{i=1}^N <\mathbf{n}\wedge\mathbf{u}_i, \boldsymbol{\varphi}>_{1/2,\partial\Omega_i} = 0 \quad \forall \boldsymbol{\varphi} \in \mathbf{H}^1(\Omega)\} \ , \tag{2.57}$$

where $\mathbf{u}_i := \mathbf{u}|_{\Omega_i}$.

2.4 Scalar and Vector Potentials

In the treatment of electromagnetic problems the decomposition of a given vector-valued function into scalar and vector potentials is an essential tool for analyzing Maxwell's equations. To simplify the presentation, we only consider simply connected Lipschitz domains in $\mathbb{R}^3$ with a connected boundary. A more detailed analysis for a larger class of Lipschitz domains can be found in [ABDG98].

Recalling the definitions of $H^1(\Omega)$, $\mathbf{H}(\mathbf{curl};\Omega)$, and $\mathbf{H}(\mathrm{div};\Omega)$, one clearly sees that $\mathbf{curl}(\mathbf{grad}\, p) = 0$, $p \in H^1(\Omega)$, and $\mathrm{div}(\mathbf{curl}\,\mathbf{u}) = 0$, $\mathbf{u} \in \mathbf{H}(\mathbf{curl};\Omega)$. This can be summarized in the following de Rham diagram:

$$H^1(\Omega)/\mathbb{R} \xrightarrow{\mathbf{grad}} \mathbf{H}(\mathbf{curl};\Omega) \xrightarrow{\mathbf{curl}} \mathbf{H}(\mathrm{div};\Omega) \xrightarrow{\mathrm{div}} L^2(\Omega). \tag{2.58}$$

A similar result, regarding boundary conditions, is

$$H^1_0(\Omega) \xrightarrow{\mathbf{grad}} \mathbf{H}_0(\mathbf{curl};\Omega) \xrightarrow{\mathbf{curl}} \mathbf{H}_0(\mathrm{div};\Omega) \xrightarrow{\mathrm{div}} L^2(\Omega)/\mathbb{R}. \tag{2.59}$$

A characterization of these diagrams is given by the following theorem [Mon03].

Theorem 2.11 (Properties of the de Rham diagram)
The diagrams (2.58) *and* (2.59) *have the property that the range of one operator is contained in the kernel of the one following it in the sequence. If* Ω *is a simply connected Lipschitz domain with connected boundary then the ranges are the kernels.*

Observing Theorem 2.11, we have the following characterization of functions in the kernel of the curl and divergence operators [ABDG98, Mon03].

Theorem 2.12 (Existence of scalar and vector potentials)
If $\mathbf{u} \in \mathbf{H}_0(\mathbf{curl};\Omega)$ *is such that* $\mathbf{curl}\,\mathbf{u} = 0$ *in* Ω *then there exists a unique scalar potential* $p \in H^1_0(\Omega)$ *such that*

$$\mathbf{u} = \mathbf{grad}\, p\ . \tag{2.60}$$

If $\mathbf{w} \in \mathbf{H}_0(\mathrm{div};\Omega)$ *is such that* $\mathrm{div}\,\mathbf{w} = 0$ *in* Ω *then there exists a vector potential* $\mathbf{A} \in \mathbf{H}_0(\mathbf{curl};\Omega)$ *such that*

$$\mathbf{w} = \mathbf{curl}\,\mathbf{A}\ . \tag{2.61}$$

The vector potential is unique if we additionally require that $\mathrm{div}\,\mathbf{A} = 0$ *in* Ω *and* $\int_{\partial\Omega} \mathbf{n}\cdot\mathbf{A}\, d\sigma = 0$. *Moreover, every* $\mathbf{u} \in \mathbf{L}^2(\Omega)$ *has the Helmholtz decomposition*

$$\mathbf{u} = \mathbf{grad}\, p + \mathbf{curl}\,\mathbf{A} \tag{2.62}$$

for unique $p \in H^1_0(\Omega)$ *and*

$$\mathbf{A} \in \{\mathbf{w} \in \mathbf{H}(\mathbf{curl};\Omega) \mid \mathrm{div}\,\mathbf{w} = 0 \text{ in } \Omega\ ,\ \mathbf{n}\cdot\mathbf{w} = 0 \text{ on } \partial\Omega\}\ .$$

The Helmholtz decomposition in (2.62) is also called Hodge decomposition. Since the kernel of the **curl**-operator is a closed subspace of $\mathbf{H}_0(\mathbf{curl};\Omega)$, we can decompose $\mathbf{H}_0(\mathbf{curl};\Omega)$ into a direct sum of the kernel and its complement as given by

$$\mathbf{H}_0(\mathbf{curl};\Omega) = \mathbf{grad}\, H_0^1(\Omega) \oplus \mathbf{X}_0 \ ,$$

where

$$\mathbf{X}_0 = \{\mathbf{w} \in \mathbf{H}_0(\mathbf{curl};\Omega) \mid (\mathbf{w}, \mathbf{grad}\, p)_{0,\Omega} = 0 \quad \forall p \in H_0^1(\Omega)\} \ .$$

According to [Mon03, Remark 4.6], a function $\mathbf{w} \in \mathbf{X}_0$ is characterized by

$$\operatorname{div} \mathbf{w} = 0 \ ,$$
$$\int_\Omega \mathbf{n} \cdot \mathbf{w}\, d\sigma = 0 \ .$$

If Ω is convex, $\mathbf{X}_0$ is continuously embedded in $\mathbf{H}^1(\Omega)$ [ABDG98, Theorem 2.17], while on an arbitrary Lipschitz domain the space $\mathbf{X}_0$ is embedded in $\mathbf{H}^{1/2}(\Omega)$ [ABDG98, Cos90].

2.5 Time-Dependent Function Spaces

So far we considered spaces that only depend on the spatial variable $\mathbf{x}$. However, recalling that Maxwell's equations involve time derivatives, we have to consider time-dependent function spaces as well. To address this we introduce the space $L^p(a,b;\mathbf{B})$.

Definition 2.13 (The space $L^p(a,b;\mathbf{B})$)
Let $1 \le p < \infty$ and $(\mathbf{B}, \|\cdot\|)$ be a Banach space. Then the space $L^p(a,b;\mathbf{B})$ is given by

$$L^p(a,b;\mathbf{B}) := \left\{ u : [a,b] \to \mathbf{B} \mid \ u \text{ is Bochner measurable, } \int_a^b \|u\|^p \, dt < \infty \right\} \ .$$

For the definition of the Bochner measure we refer to [Wlo82, Ada78]. As in the previous sections, we can define a weak time derivative according to

Definition 2.14 (Weak time derivative)
Let $(\mathbf{X}, (\cdot,\cdot))$ be a separable Hilbert space and $0 < T < \infty$ and $u \in L^1(0,T;\mathbf{X})$. Then the function $q \in L^1(0,T;\mathbf{X}')$ is called the weak time derivative of u if

$$\int_0^T \partial_t \varphi(t)(u(t), v)\, dt = -\int_0^T \varphi(t) \ < q(t), v >_{\mathbf{X}'} \ dt \quad \forall \varphi \in C^\infty(0,T) \ , \ v \in \mathbf{X} \ ,$$

where the integrals are Bochner integrals and $(\cdot,\cdot)$ denotes the inner product of $\mathbf{X}$ and $< \cdot, \cdot >_{\mathbf{X}'}$ the dual pairing between $\mathbf{X}$ and $\mathbf{X}'$.

In the following we denote the weak time derivative of u by $\dot{u}$. Combining the previous definitions, we define $W(0,T,\mathbf{X})$ by:

Definition 2.15 (The Space $W(0,T,\mathbf{X})$)
Let $\Omega \subset \mathbb{R}^d$ be a bounded domain, $\mathbf{X}$ a separable Hilbert space and $0 < T < \infty$. Then the space $W(0,T,\mathbf{X})$ is given by

$$W(0,T;\mathbf{X}) := \{u \in L^2(0,T;\mathbf{X}) \mid \dot{u} \in L^2(0,T;\mathbf{X}')\} \ .$$

Chapter 3

Variational Theory for the Eddy Current Model

For the solution of Maxwell's equations we generally have to rely on numerical methods, like finite difference, finite volume, or finite element methods. The latter are based on variational or weak formulations of boundary value problems. Thus we first have to establish a reliable variational formulation of the eddy current model before we can proceed and discretize the resulting equations.

3.1 Derivation of the Model Problem

In Section 1.2.2 we showed that the eddy current model arises from Maxwell's equations as a magnetostatic approximation by neglecting the displacement current. There are many different formulations of this model focusing, for example, on the magnetic field $\mathbf{H} = \mathbf{H}(\mathbf{x}, t)$ or the magnetic vector potential $\mathbf{A} = \mathbf{A}(\mathbf{x}, t)$ as primary unknown. However, in the following we choose the approach that eliminates the magnetic field $\mathbf{H}$ from equations (1.32)-(1.35) and retains $\mathbf{E} = \mathbf{E}(\mathbf{x}, t)$ as unknown. Moreover, we assume that the coefficients are time-independent.

Following this approach, we end up with a degenerate parabolic initial-boundary value problem given by

$$\sigma \partial_t \mathbf{E} + \mathbf{curl}(\chi \, \mathbf{curl}\, \mathbf{E}) = -\partial_t \mathbf{J}_a \ , \quad \text{in } \Omega \times [0, T] \ , \tag{3.1}$$

$$\mathbf{E} \wedge \mathbf{n} = \quad 0 \quad , \quad \text{on } \Gamma \times [0, T] \ , \tag{3.2}$$

$$\mathbf{E}(\mathbf{x}, 0) = \quad \mathbf{E}_0 \quad , \quad \text{in } \Omega \times \{0\} \ , \tag{3.3}$$

where $\chi = \mu^{-1}$. For physical reasons we have to require that $\operatorname{div} \mathbf{J}_a(\cdot, t) = 0$ in Ω for all times. The label degenerate is due to the fact that there is a crisp distinction between insulating regions ($\sigma = 0$) and conducting regions ($\sigma > 0$). To simplify the theory, we will take for granted that $\sigma \geq \underline{\sigma} > 0$.

To derive the variational formulation of the parabolic initial-boundary value problem, we multiply (3.1) with test functions $\mathbf{v} \in \mathbf{H}_0(\mathbf{curl};\Omega)$ and apply Stokes' theorem. Then the weak form of (3.1) yields the following variational problem: Find $\mathbf{E} \in W(0,T,\mathbf{H}_0(\mathbf{curl};\Omega))$ such that

$$< \sigma\dot{\mathbf{E}}, \mathbf{v} >_{curl} + (\chi\,\mathbf{curl}\,\mathbf{E}, \mathbf{curl}\,\mathbf{v})_{0,\Omega} = -(\partial_t \mathbf{J}_a, \mathbf{v})_{0,\Omega} \quad \forall \mathbf{v} \in \mathbf{H}_0(\mathbf{curl};\Omega) \tag{3.4}$$

$$\mathbf{E}(0) = \mathbf{E}_0 \in \mathbf{L}^2(\Omega)\ , \tag{3.5}$$

where $\partial_t \mathbf{J}_a \in L^2(0,T,\mathbf{L}^2(\Omega))$ and $< \cdot,\cdot >_{curl}$ denotes the dual pairing between $\mathbf{H}_0(\mathbf{curl};\Omega)$ and $\mathbf{H}_0(\mathbf{curl};\Omega)'$. Setting $\tilde{a}(\mathbf{E},\mathbf{v}) := (\chi\,\mathbf{curl}\,\mathbf{E}, \mathbf{curl}\,\mathbf{v})_{0,\Omega}$, the existence and uniqueness of a solution of (3.4) is given by the following theorem.

Theorem 3.1 (Existence and uniqueness)
Let σ, $\chi \in L^\infty(\Omega)$ such that $0 < \underline{\sigma} \le \sigma \le \bar{\sigma}$ and $0 < \underline{\chi} \le \chi \le \bar{\chi}$. Additionally, let $\partial_t \mathbf{J}_a \in L^2(0,T,\mathbf{L}^2(\Omega))$ and $\mathbf{E}_0 \in \mathbf{L}^2(\Omega)$. Then there exists a unique solution $\mathbf{E} \in W(0,T,\mathbf{H}_0(\mathbf{curl};\Omega))$ such that

$$< \sigma\dot{\mathbf{E}}, \mathbf{v} >_{curl} + \tilde{a}(\mathbf{E},\mathbf{v}) = -(\partial_t \mathbf{J}_a, \mathbf{v})_{0,\Omega} \quad \forall \mathbf{v} \in \mathbf{H}_0(\mathbf{curl};\Omega)$$

$$\mathbf{E}(0) = \mathbf{E}_0 \in \mathbf{L}^2(\Omega)\ .$$

Proof:
Note that $\mathbf{H}_0(\mathbf{curl};\Omega)$ is a separable and reflexive Hilbert space that is dense in $\mathbf{L}^2(\Omega)$. The bilinear form $\tilde{a}(\cdot,\cdot)$ fulfills the Gårding inequality

$$\begin{aligned}
\tilde{a}(\mathbf{u},\mathbf{u}) + \underline{\chi}(\mathbf{u},\mathbf{u})_{0,\Omega} &= (\chi\,\mathbf{curl}\,\mathbf{u}, \mathbf{curl}\,\mathbf{u})_{0,\Omega} + \underline{\chi}(\mathbf{u},\mathbf{u})_{0,\Omega} \\
&\ge \underline{\chi}(\mathbf{curl}\,\mathbf{u}, \mathbf{curl}\,\mathbf{u})_{0,\Omega} + \underline{\chi}(\mathbf{u},\mathbf{u})_{0,\Omega} \\
&= \underline{\chi}\|\mathbf{u}\|^2_{\mathbf{curl},\Omega}
\end{aligned}$$

and is bounded

$$\begin{aligned}
|\tilde{a}(\mathbf{u},\mathbf{v})| &= \left(\int_\Omega \chi\,\mathbf{curl}\,\mathbf{u}\,\mathbf{curl}\,\mathbf{v}\,dV\right)^{1/2} \\
&\le \bar{\chi}\left(\int_\Omega \mathbf{curl}\,\mathbf{u}\,\mathbf{curl}\,\mathbf{u}\,dV\right)^{1/2}\left(\int_\Omega \mathbf{curl}\,\mathbf{v}\,\mathbf{curl}\,\mathbf{v}\,dV\right)^{1/2} \\
&\le \bar{\chi}\|\mathbf{u}\|_{\mathbf{curl},\Omega}\cdot\|\mathbf{v}\|_{\mathbf{curl},\Omega}\ .
\end{aligned}$$

Then the existence of a unique solution is a consequence of Theorem 24.A in [Zei90]. A more general proof considering nonlinear eddy current equations can be found in [BLS04].

•

In general, a solution of (3.4) in closed form is not available. Therefore, we have to resort to numerical methods to approximate the solution. Since (3.4) involves

both temporal and spacial variables, there are several approaches to discretize (3.4). For our analysis we first choose a semi-discretization in time. To do this we divide the interval $I = [0, T]$ into n subintervals by using nodal points

$$0 = t_0 < t_1 < ... < t_n = T \ . \tag{3.6}$$

The corresponding timestep is given by $\tau_i = t_i - t_{i-1}$, $1 \leq i \leq n$. Resulting from these subintervals, we obtain a sequence of functions $\mathbf{E}^{(i)} \in \mathbf{H}_0(\mathbf{curl}; \Omega)$ that approximate the exact solution $\mathbf{E}(t, \mathbf{x})$ at $t = t_i$. To finish the discretization, we replace $\dot{\mathbf{E}}$ by means of suitable difference quotients. Following these steps, we end up with variational equations for the unknowns $\mathbf{E}^{(i)}$.

In general, we also have to use numerical methods to approximate $\mathbf{E}^{(i)}$. Then the stability of the resulting fully discrete scheme critically depends on the choice of the difference quotients in the timestepping scheme. Since (3.4) is a stiff problem, the timestepping scheme has to be L-stable [DB94]. In order to simplify the presentation, we choose the implicit Euler scheme, which reads as follows:

Find $\mathbf{E}^{(i)} \in \mathbf{H}_0(\mathbf{curl}; \Omega)$, $1 \leq i \leq n$, satisfying

$$\frac{1}{\tau_i}(\sigma(\mathbf{E}^{(i)} - \mathbf{E}^{(i-1)}), \mathbf{v})_{0,\Omega} + \tilde{a}(\mathbf{E}^{(i)}, \mathbf{v}) = -(\partial_t \mathbf{J}_a(t_i), \mathbf{v})_{0,\Omega} \, \forall \mathbf{v} \in \mathbf{H}_0(\mathbf{curl}; \Omega) \, , \tag{3.7}$$

where $\mathbf{E}^{(0)} = \mathbf{E}_0$.

This means that in each timestep we have to solve a time-independent equation given by

$$a_\Omega^{(i)}(\mathbf{E}^{(i)}, \mathbf{v}) = f^{(i)}(\mathbf{v}) \quad \forall \mathbf{v} \in \mathbf{H}_0(\mathbf{curl}; \Omega) \ , \tag{3.8}$$

where the bilinear form $a_\Omega^{(i)}(\cdot, \cdot) : \mathbf{H}_0(\mathbf{curl}; \Omega) \times \mathbf{H}_0(\mathbf{curl}; \Omega) \to \mathbb{R}$ and the functional $f^{(i)}(\cdot) : \mathbf{H}_0(\mathbf{curl}; \Omega) \to \mathbb{R}$ are given by

$$a_\Omega^{(i)}(\mathbf{u}, \mathbf{v}) := (\beta_i \, \mathbf{u}, \mathbf{v})_{0,\Omega} + \tilde{a}(\mathbf{u}, \mathbf{v}) \ , \tag{3.9}$$

$$f^{(i)}(\mathbf{v}) := -(\partial_t \mathbf{J}_a(t_i), \mathbf{v})_{0,\Omega} + (\beta_i \mathbf{E}^{(i-1)}, \mathbf{v})_{0,\Omega} \ , \tag{3.10}$$

with $\beta_i = \frac{\sigma}{\tau_i}$.

If we assume that σ, $\chi \in L^\infty(\Omega)$ and $0 < \underline{\sigma} \leq \sigma \leq \bar{\sigma}$ then the existence and uniqueness of a solution $\mathbf{E}^{(i)} \in \mathbf{H}_0(\mathbf{curl}; \Omega)$ for equation (3.8) is given by the Lax-Milgram theorem [Bra92], since $a_\Omega(\cdot, \cdot)$ is bounded and coercive and both $\partial_t \mathbf{J}_a(t_i)$ and $\mathbf{E}^{(i-1)}$ are elements of $\mathbf{L}^2(\Omega)$.

If we apply the discretization mentioned above, we see that the originally time-dependent problem reduces to a time-independent one of the form:

Find $\mathbf{u} \in \mathbf{H}_0(\mathbf{curl}; \Omega)$ such that

$$a_\Omega(\mathbf{u}, \mathbf{v}) = f(\mathbf{v}) \quad \forall \mathbf{v} \in \mathbf{H}_0(\mathbf{curl}; \Omega) \ , \tag{3.11}$$

where $a_\Omega(\mathbf{u}, \mathbf{v})$ and $f(\mathbf{v})$ are given by

$$a_\Omega(\mathbf{u}, \mathbf{v}) := (\beta\, \mathbf{u}, \mathbf{v})_{0,\Omega} + (\chi\, \mathbf{curl}\, \mathbf{u}, \mathbf{curl}\, \mathbf{v})_{0,\Omega} \ ,$$
$$f(\mathbf{v}) := (\mathbf{f}, \mathbf{v})_{0,\Omega} \ , \ \mathbf{f} \in \mathbf{L}^2(\Omega) \ .$$

Note that we still assume $\operatorname{div} \mathbf{f} = 0$.

3.2 Macro-Hybrid Variational Formulation

Since equation (3.11) plays a central role for the solution of eddy current problems, the rest of this thesis will focus on solving this equation. In general, we cannot expect to find a solution of (3.11) but have to use numerical methods to approximate the solution. In recent years several efficient solvers for the algebraic equations arising from the discretization of (3.11) have been developed. Among the most powerful solvers, domain decomposition methods have aroused great interest in the last decades. The basic idea of these methods is to split the problem formulated on Ω into a sequence of smaller problems that are solvable more easily [SBG96, QV99].

A special approach in this class of methods are the mortar finite element methods. These methods use a nonoverlapping decomposition of Ω and allow individual triangulations on each subdomain. Therefore, complicated geometries or moving structures [FMRW04] can be modelled as unions of relatively simple subdomains with locally constructed grids. Moreover, local features of the problem such as corner singularities or discontinuously varying coefficients can be resolved by locally well adapted meshes [Hop02, HIM00]. In all cases achieving conformity of the grid would result in a large number of elements or a remeshing at every timestep. However, this flexibility stands in contrast to the conformity requirements among subdomains for the solution.

Originally, mortar finite element methods have been introduced by Bernadi, Maday, and Patera [BMP93, BMP94]. Subsequently, this approach has been extended to a variety of problems. Especially the analysis and implementation of problems related to Maxwell's equations have been done in [BMR99, BBM01, BBM02, Hop99, XH05, LVL05]. In the following we will introduce the mortar approach developed in [Hop99, XH05].

For mortar methods the trace space of $\mathbf{H}(\mathbf{curl}; \Omega)$ is of great importance. As mentioned in Section 2.3, the definition of this space depends on the regularity of the boundary. In the sequel we will consider domains Ω that are simply connected Lipschitz polyhedra with connected boundary. Motivated by (2.57) we start by decomposing Ω into N open sets. Let $\Omega_i \subseteq \Omega$, $1 \leq i \leq N$, be a nonoverlapping,

polyhedral partition of Ω with

$$\bar{\Omega} = \bigcup_{i=1}^{N} \bar{\Omega}_i \ , \ \Omega_i \cap \Omega_j = \emptyset \ , \ 1 \leq j \leq N \ , \ i \neq j \ . \tag{3.12}$$

Additionally, we assume that the decomposition is geometrically conforming in the sense that the intersection of two subdomains is either a common face, edge or vertex of the subdomains (see Figure 3.1).

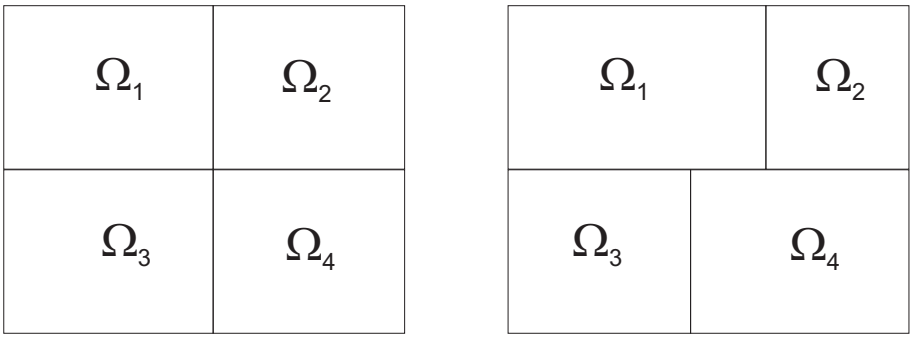

Figure 3.1: Geometric decomposition of the domain. On the left the decomposition is geometrically conforming, while the decomposition is nonconforming on the right.

Let $\bar{\Gamma}_{ij} := \partial\Omega_i \cap \partial\Omega_j$, $1 \leq i, j \leq N$, be the possibly empty intersection of the two subdomains Ω_i and Ω_j and denote by Γ_{ij} the interior of $\bar{\Gamma}_{ij}$ with respect to $\partial\Omega_i$. For every interface γ_k, $1 \leq k \leq M$, $\gamma_k \neq \emptyset$, there exists a unique couple $(i(k), j(k))$ such that $\gamma_k = \Gamma_{i(k),j(k)} = \Gamma_{j(k),i(k)}$. Then the skeleton S of the decomposition (3.12) is defined according to

$$S \ := \ \bigcup_{k=1}^{M} \bar{\gamma}_k \ , \ \gamma_k \cap \gamma_l = \emptyset \ , \ 1 \leq l \leq M \ , \ k \neq l \ . \tag{3.13}$$

As mentioned above, we have two adjacent subdomains at each interface γ_k. Without preference, we choose one of the subdomains to be the mortar or master domain $\Omega_{m(k)}$, while the other subdomain will be called nonmortar or slave domain $\Omega_{s(k)}$ (see Figure 3.2). To simplify the presentation, we will drop k and write Ω_m and Ω_s for the master and slave domain if it is clear from the context which interface is meant. Additionally, we set $\varrho_k := \partial\Omega_{m(k)} \cap \gamma_k$, and $\delta_k := \partial\Omega_{s(k)} \cap \gamma_k$. Using this definition, we can define for each interface γ_k the unit outer normal $\mathbf{n}_{i(k),j(k)}$ as the normal to the interface γ_k pointing from $\Omega_{i(k)}$ towards $\Omega_{j(k)}$ and we set $\mathbf{n}_k := \mathbf{n}_{s(k),m(k)}$.

The variational formulation of the model problem, given in (3.11), is not convenient for the mortar method, since we want to deal independently with each

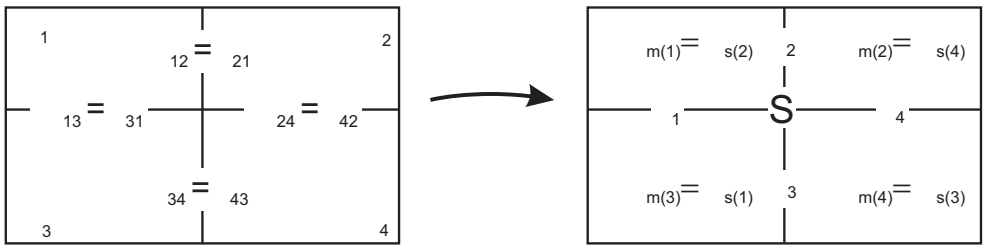

Figure 3.2: Choosing mortar and nonmortar sides at the interfaces. Each subdomain can be both master and slave domain.

subdomain. Therefore, it is more reasonable to use a different space of test functions than $\mathbf{H}_0(\mathbf{curl};\Omega)$. Let $\mathbf{n}$ denote the unit outward normal to $\partial\Omega$ and $\Gamma_i := \partial\Omega_i \cap \partial\Omega$, $1 \leq i \leq N$. Considering the decomposition (3.12), a natural choice for the new test space would be given by the product space

$$\mathbf{X} = \left\{\mathbf{q} \in \mathbf{L}^2(\Omega) \mid \mathbf{q}|_{\Omega_i} \in \mathbf{H}_{\Gamma_i}(\mathbf{curl}, \Omega_i)\right\} \tag{3.14}$$

equipped with the broken norm

$$\|\mathbf{q}\|_{\mathbf{X}} := \left(\sum_{i=1}^{N} \|\mathbf{q}\|^2_{\mathbf{H}(\mathbf{curl},\Omega_i)}\right)^{1/2} . \tag{3.15}$$

However, for the variational formulation we have to consider a subspace of $\mathbf{X}$. Recall that for $\Gamma_{ij} \subset S$, the space $\mathbf{TH}^{1/2}(\Gamma_{ij})$ is given by

$$\mathbf{TH}^{1/2}(\Gamma_{ij}) = \{\mathbf{q} \in \mathbf{H}^{1/2}(\Gamma_{ij}) \mid \mathbf{n}\cdot\mathbf{q}|_{\Gamma_{ij}} = 0\} .$$

Moreover, denoting by $\mathbf{TH}^{1/2}_{00}(\Gamma_{ij})$ the space of those elements $\mathbf{q} \in \mathbf{TH}^{1/2}(\Gamma_{ij})$ whose trivial extension $\tilde{\mathbf{q}}$ by zero to all of $\partial\Omega_i$ belongs to $\mathbf{TH}^{1/2}(\partial\Omega_i)$, i.e.

$$\mathbf{TH}^{1/2}_{00}(\Gamma_{ij}) = \left\{\mathbf{q} \in \mathbf{TH}^{1/2}(\Gamma_{ij}) \mid \tilde{\mathbf{q}} \in \mathbf{TH}^{1/2}(\partial\Omega_i)\right\} , \tag{3.16}$$

we consider the space

$$\mathbf{V} := \left\{\mathbf{q} \in \mathbf{X} \,|\, [\mathbf{n}\wedge\mathbf{q}]|_{\Gamma_{ij}} \in \mathbf{TH}^{1/2}_{00}(\Gamma_{ij}) \quad \forall\, \Gamma_{ij} \subset S\right\} , \tag{3.17}$$

where $[\mathbf{n}\wedge\mathbf{q}]|_{\Gamma_{ij}}$ denotes the jump of the tangential trace across the interface Γ_{ij} given by

$$[\mathbf{n}\wedge\mathbf{q}]|_{\Gamma_{ij}} := \mathbf{n}_{ij}\wedge\mathbf{q}|_{\Gamma_{ij}\cap\partial\Omega_i} - \mathbf{n}_{ij}\wedge\mathbf{q}|_{\Gamma_{ij}\cap\partial\Omega_j} . \tag{3.18}$$

$\mathbf{V}$ is a Hilbert space provided with the norm

$$\|\mathbf{q}\|_{\mathbf{V}} := \left(\|\mathbf{q}\|^2_{\mathbf{X}} + \|[\mathbf{n}\wedge\mathbf{q}]\|^2_{1/2,S}\right)^{1/2} , \tag{3.19}$$

where

$$\|[\mathbf{n}\wedge\mathbf{q}]\|_{1/2,S} := \left(\sum_{\Gamma_{ij}\subset S} \|[\mathbf{n}\wedge\mathbf{q}]|_{\Gamma_{ij}}\|^2_{\mathbf{H}^{1/2}_{00}(\Gamma_{ij})}\right)^{1/2} . \tag{3.20}$$

Note that $\mathbf{TH}^{1/2}_{00}(\Gamma_{ij})$ is a subspace of $\mathbf{H}^{-1/2}_{\|}(\mathrm{div}_\Gamma, \partial\Omega_i)$.

Since we are looking for a solution of problem (3.11), we have to assure that a solution $\mathbf{u}\in\mathbf{V}$ is an element of $\mathbf{H}_0(\mathbf{curl};\Omega)$. To achieve this we impose a weak continuity constraint on the tangential trace across S by using suitable Lagrange multipliers. Since $[\mathbf{n}\wedge\mathbf{q}]|_{\Gamma_{ij}}$ is contained in $\mathbf{TH}^{1/2}_{00}(\Gamma_{ij})$, a natural candidate for the Lagrange multiplier space is given by

$$\mathbf{M}(S) := \prod_{\Gamma_{ij}\subset S} \mathbf{TH}^{-1/2}(\Gamma_{ij}) , \tag{3.21}$$

where $\mathbf{TH}^{-1/2}(\Gamma_{ij})$ denotes the dual space of $\mathbf{TH}^{1/2}_{00}(\Gamma_{ij})$. We equip this space with the norm

$$\|\boldsymbol{\mu}\|_{\mathbf{M}(S)} := \left(\sum_{\Gamma_{ij}\subset S} \|\boldsymbol{\mu}|_{\Gamma_{ij}}\|^2_{-1/2,\Gamma_{ij}}\right)^{1/2} . \tag{3.22}$$

After these definitions we have to adjust (3.11) to the new setting. We replace $a_\Omega(\cdot,\cdot)$ with the sum of bilinear forms associated with the subdomain problems. Thus we define the bilinear form $a(\cdot,\cdot):\mathbf{V}\times\mathbf{V}\to\mathbb{R}$ according to

$$a(\mathbf{u},\mathbf{q}) := \sum_{i=1}^N a_{\Omega_i}(\mathbf{u}|_{\Omega_i},\mathbf{q}|_{\Omega_i}) = \sum_{i=1}^N \int_{\Omega_i} \chi\,\mathbf{curl}\,\mathbf{u}\cdot\mathbf{curl}\,\mathbf{q} + \beta\,\mathbf{u}\cdot\mathbf{q}\,dV . \tag{3.23}$$

To enforce the weak continuity constraint, we further introduce the bilinear form $b(\cdot,\cdot):\mathbf{V}\times\mathbf{M}(S)\to\mathbb{R}$ which is given by

$$b(\mathbf{q},\boldsymbol{\mu}) := <[\mathbf{n}\wedge\mathbf{q}]|_S,\boldsymbol{\mu}>_{1/2,S} , \tag{3.24}$$

with $<\cdot,\cdot>_{1/2,S} := \sum_{k=1}^M <\cdot,\cdot>_{1/2,\gamma_k}$. Associated with $b(\cdot,\cdot)$ is the linear operator $B:\mathbf{V}\to\mathbf{M}(S)' = \prod_{\Gamma_{ij}\subset S}\mathbf{TH}^{1/2}_{00}(\Gamma_{ij})$ according to

$$<B\mathbf{q},\boldsymbol{\mu}>_{1/2,S} = b(\mathbf{q},\boldsymbol{\mu}) \quad \forall\boldsymbol{\mu}\in\mathbf{M}(S) . \tag{3.25}$$

Obviously, $\mathrm{Ker}\,B\subset\mathbf{H}_0(\mathbf{curl};\Omega)$. Thus the appropriate macro-variational formulation of (3.11) is given by:

Find $(\mathbf{u},\boldsymbol{\lambda})\in\mathbf{V}\times\mathbf{M}(S)$ such that

$$\begin{aligned} a(\mathbf{u},\mathbf{q}) + b(\mathbf{q},\boldsymbol{\lambda}) &= f(\mathbf{q}) \quad \forall\mathbf{q}\in\mathbf{V} , \\ b(\mathbf{u},\boldsymbol{\mu}) &= 0 \quad \forall\boldsymbol{\mu}\in\mathbf{M}(S) . \end{aligned} \tag{3.26}$$

The existence and uniqueness of a solution to the saddle point problem (3.26) is given by the following theorem [Hop99, Theorem 3.2].

Theorem 3.2 (Existence and uniqueness)
The bilinear form $a(\cdot,\cdot)$ is Ker B-elliptic and the bilinear form $b(\cdot,\cdot)$ satisfies the Babuska-Brezzi condition

$$\inf_{\boldsymbol{\mu}\in\mathbf{M}(S)} \sup_{\mathbf{q}\in\mathbf{V}} \frac{b(\mathbf{q},\boldsymbol{\mu})}{\|\mathbf{q}\|_V \|\boldsymbol{\mu}\|_{M(S)}} \geq \alpha > 0 \ . \tag{3.27}$$

Proof:
Since $\|\mathbf{q}\|_{\mathbf{V}} = \|\mathbf{q}\|_{\mathbf{curl},\Omega}$ for a function $\mathbf{q} \in \text{Ker } B \subset \mathbf{H}_0(\mathbf{curl};\Omega)$, the ellipticity of $a(\cdot,\cdot)$ follows from the ellipticity of $a_{\Omega_i}(\cdot,\cdot)$. We have

$$\begin{aligned} a(\mathbf{u},\mathbf{u}) &= \sum_{i=1}^{N} a_{\Omega_i}(\mathbf{u}|_{\Omega_i},\mathbf{u}|_{\Omega_i}) \geq \sum_{i=1}^{N} c_i \|\mathbf{u}|_{\Omega_i}\|^2_{\mathbf{H}(\mathbf{curl},\Omega_i)} \\ &\geq c\|\mathbf{u}\|^2_{\mathbf{curl},\Omega} = c\|\mathbf{u}\|^2_{\mathbf{V}} \ , \end{aligned} \tag{3.28}$$

which proves that $a(\cdot,\cdot)$ is Ker B-elliptic.
For the proof of the Babuska-Brezzi condition we consider an arbitrary $\boldsymbol{\mu} \in \mathbf{M}(S)$. For $\Gamma_{ij} \subset S$ we can surely find $\mathbf{p}_{ij} \in \mathbf{TH}^{1/2}_{00}(\Gamma_{ij})$ such that

$$\|\mathbf{p}_{ij}\|_{\mathbf{H}^{1/2}_{00}(\Gamma_{ij})} = 1 \text{ and } \ < \mathbf{p}_{ij}, \boldsymbol{\mu} >_{1/2,\Gamma_{ij}} \geq \frac{1}{2}\|\boldsymbol{\mu}|_{\Gamma_{ij}}\|_{-1/2,\Gamma_{ij}} \ . \tag{3.29}$$

We set $\mathbf{p}^{(j)}_{\partial\Omega_i} := \tilde{\mathbf{p}}_{ij} \in \mathbf{TH}^{1/2}_{00}(\partial\Omega_i)$ and determine $\mathbf{p}^{(j)}_{\Omega_i} \in \mathbf{H}(\mathbf{curl},\Omega_i)$ such that $\mathbf{n} \wedge \mathbf{p}^{(j)}_{\Omega_i}|_{\partial\Omega_i} = \mathbf{p}^{(j)}_{\partial\Omega_i}$ and

$$\|\mathbf{p}^{(j)}_{\Omega_i}\|_{\mathbf{H}(\mathbf{curl},\Omega_i)} \leq C\|\mathbf{p}^{(j)}_{\partial\Omega_i}\|_{1/2,\Gamma_{ij}} \leq C_1\|\mathbf{p}^{(j)}_{\partial\Omega_i}\|_{\mathbf{H}^{1/2}_{00}(\Gamma_{ij})} = C_1 \ . \tag{3.30}$$

Finally, if we define $\mathbf{p} \in \mathbf{V}$ by $\mathbf{p}|_{\Omega_i} = \sum_{\Gamma_{ij}\subset\partial\Omega_i} \mathbf{p}^{(j)}_{\Omega_i}$ we end up with the inequality

$$\begin{aligned} \sup_{\mathbf{q}\in\mathbf{V}} \frac{b(\mathbf{q},\boldsymbol{\mu})}{\|\mathbf{q}\|_{\mathbf{V}}} \geq \frac{b(\mathbf{p},\boldsymbol{\mu})}{\|\mathbf{p}\|_{\mathbf{V}}} &\geq C_2 b(\mathbf{p},\boldsymbol{\mu}) = C_2 \sum_{\Gamma_{ij}\subset S} < \mathbf{p}_{ij} + \mathbf{p}_{ji}, \boldsymbol{\mu}|_{\Gamma_{ij}} >_{1/2,\Gamma_{ij}} \\ &\geq C_2 \sum_{\Gamma_{ij}\subset S} \|\boldsymbol{\mu}|_{\Gamma_{ij}}\|_{-1/2,\Gamma_{ij}} \geq C_2\|\boldsymbol{\mu}\|_{\mathbf{M}(S)} \ , \end{aligned}$$

which asserts the Babuska-Brezzi condition. Then the existence of a unique solution is a classical result of the theory of saddle point problems (cf. [BF91]).

•

Chapter 4

The Mortar Edge Element Approximation

As mentioned in the previous chapter, we cannot expect to find an analytic solution of the saddle point problem (3.26). Thus one has to rely on numerical methods to approximate the solution. In order to compute this approximation, we have to replace the continuous problem by a discrete formulation, which results in a system of linear equations. Before we can state the discrete formulation we have to equip the domain Ω with a triangulation. Based on this mesh we introduce finite element spaces that will replace $\mathbf{V}$ and $\mathbf{M}(S)$. Finally, at the end of this chapter, we will formulate the discrete problem and show that it has a unique solution.

4.1 Geometrical Setting

Starting from the nonoverlapping, geometrically conforming decomposition of Ω (3.12), we use individual simplicial triangulations $\mathcal{T}_i$ for each subdomain Ω_i, $1 \leq i \leq N$. At the interface γ_k, $1 \leq k \leq M$, these triangulations induce two independent simplicial triangulations $\mathcal{T}_{\delta_k}$ and $\mathcal{T}_{\varrho_k}$ inherited from the triangulations $\mathcal{T}_{s(k)}$ and $\mathcal{T}_{m(k)}$ of the slave and master domain, respectively. Since the individual triangulations are independent of each other, we cannot expect $\mathcal{T}_{\delta_k}$ and $\mathcal{T}_{\varrho_k}$ to match on γ_k (see fig. 4.1).

For $T \in \mathcal{T}_i$, $1 \leq i \leq N$, and $T \in \mathcal{T}_{\delta_k}$ respectively $T \in \mathcal{T}_{\varrho_k}$, $1 \leq k \leq M$, we denote by $h(T)$ the diameter and by $\rho(T)$ the radius of the largest ball respectively circle that can be inscribed to T. For each subdomain Ω_i we assume that the triangulation $\mathcal{T}_i$ is shape regular in the sense that $h(T)/\rho(T) \leq \sigma_i$ uniformly for all $T \in \mathcal{T}_i$ and locally quasi-uniform in the sense that there exist constants $\bar{\tau}_i > \underline{\tau}_i > 0$ such that

$$0 < \underline{\tau}_i \, h(T') \leq h(T) \leq \bar{\tau}_i \, h(T') \quad \forall T,\ T' \in \mathcal{T}_i,\ \bar{T} \cap \bar{T}' \neq \emptyset \ .$$

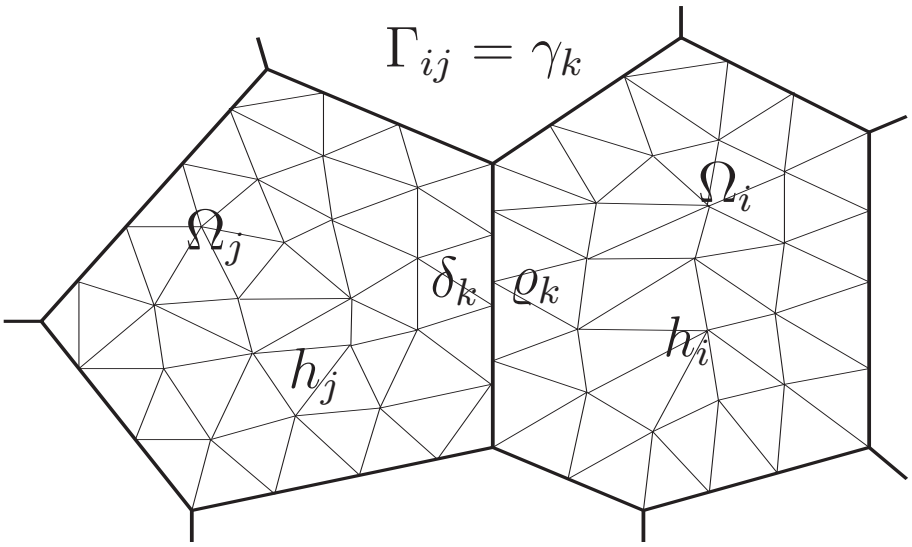

Figure 4.1: Situation at the interface between two subdomains. The individual triangulations are independent and do in general not match.

These properties are inherited by the triangulations $\mathcal{T}_{\delta_k}$ and $\mathcal{T}_{\varrho_k}$ on the interfaces γ_k. Defining global mesh sizes h_{δ_k}, h_{ϱ_k}, and h_i according to

$$\begin{aligned} h_i &:= \max\{\operatorname{diam} T \mid T \in \mathcal{T}_i\} \ , \\ h_{\delta_k} &:= \max\{\operatorname{diam} T \mid T \in \mathcal{T}_{\delta_k}\} \ , \\ h_{\varrho_k} &:= \max\{\operatorname{diam} T \mid T \in \mathcal{T}_{\varrho_k}\} \ , \end{aligned}$$

we assume that the granularities of the triangulations $\mathcal{T}_{\delta_k}$ and $\mathcal{T}_{\varrho_k}$ are such that there exist constants $0 < \underline{\kappa}_{\gamma_k} \leq \bar{\kappa}_{\gamma_k}$ independent of h_{δ_k} and h_{ϱ_k} satisfying

$$\underline{\kappa}_{\gamma_k} h_{\varrho_k} \leq h_{\delta_k} \leq \bar{\kappa}_{\gamma_k} h_{\varrho_k} \ . \tag{4.1}$$

Moreover, for $\Sigma_i \subset \bar{\Omega}_i$ we define $\mathcal{F}_h(\Sigma_i)$ and $\mathcal{E}_h(\Sigma_i)$ as the sets of faces respectively edges of $\mathcal{T}_i$ in Σ_i. Analogously, for $\Sigma_{\delta_k} \subset \delta_k$, $\delta_k \subset S$, and $\Sigma_{\varrho_k} \subset \gamma_{\varrho_k}$, $\gamma_{\varrho_k} \subset S$, we denote by $\mathcal{E}_h(\Sigma_{\delta_k})$ and $\mathcal{E}_h(\Sigma_{\varrho_k})$ the set of edges of $\mathcal{T}_{\delta_k}$ and $\mathcal{T}_{\varrho_k}$ in Σ_{δ_k} and Σ_{ϱ_k}, respectively.

After these assumptions on the triangulations of the subdomains we are now able to define the discrete counterparts of the spaces $\mathbf{V}$ and $\mathbf{M}(S)$.

4.2 Nédélec's Lowest Order Curl Conforming Elements

Recalling from (3.17) that $\mathbf{V} \subset \mathbf{X}$ and that $\mathbf{X}$ is given by the product of the spaces

$$\mathbf{H}_{\Gamma_i}(\mathbf{curl}; \Omega_i) := \{\mathbf{q} \in \mathbf{H}(\mathbf{curl}; \Omega_i) \mid \mathbf{n} \wedge \mathbf{q}|_{\Gamma_i} = 0\} \ , \ 1 \leq i \leq N \ ,$$

it is obvious that we have to use a good finite element approximation of the space $\mathbf{H}_{\Gamma_i}(\mathbf{curl}; \Omega_i)$. The obvious choice of using vector continuous piecewise linear elements has several disadvantages.

Since we required that $\operatorname{div} \mathbf{f} = 0$, a constant coefficient function β results in a solution of (3.11) which is an element of the space $\mathbf{H}_0(\mathbf{curl}; \Omega) \cap \mathbf{H}(\operatorname{div}; \Omega)$. If the domain has reentrant corners, the space $\mathbf{H}^1(\Omega) \cap \mathbf{H}_0(\mathbf{curl}; \Omega)$ is a closed subspace of this space. However, since vector continuous elements are $\mathbf{H}^1(\Omega)$-conforming, it is possible to compute finite element solutions that do not converge to the solution of Maxwell's equations [Mon03, CD00]. Furthermore, when dealing with problems involving discontinuous coefficients (e.g., modelling different media), we cannot expect that the normal component of the solution is continuous at the interface between different media. This is in contrast to the continuity of vector continuous finite elements.

To avoid these problems, we will use Nédélec's curl-conforming edge elements of the first family as described in [Néd83]. A mortar approach based on the second family is described in [BBM01, BBM02].

For a tetrahedron $T \in \mathcal{T}_i$ the lowest order Nédélec element of the first family, denoted by $\mathbf{Nd}_1(T)$, is given by

$$\mathbf{Nd}_1(T) := \{\mathbf{q} := \mathbf{a} + \mathbf{b} \wedge \mathbf{x} \mid \ \mathbf{a}, \mathbf{b} \in \mathbb{R}^3 \ , \ \mathbf{x} \in T\} \ .$$

The degrees of freedom of this element are given by the zero order moments of the tangential components with respect to the edges $E \in \mathcal{E}_h(T)$

$$\ell_E^n(\mathbf{q}_h) := \int_E t_E \cdot \mathbf{q}_h \, d\sigma \ , \ E \in \mathcal{E}_h(T) \ , \tag{4.2}$$

where t_E stands for the tangential unit vector on E. Since the degrees of freedom are associated with the edges of the mesh, Nédélec elements are also termed *edge elements*. Moreover, the lowest order edge elements are termed Whitney elements, since they have been first used by Whitney [Whi57], although Whitney discovered these elements in a different context.

Then the edge element space $\mathbf{Nd}_1(\Omega_i; \mathcal{T}_i)$ is given by

$$\mathbf{Nd}_1(\Omega_i; \mathcal{T}_i) := \{\mathbf{q}_h \in \mathbf{H}(\mathbf{curl}; \Omega_i) \mid \mathbf{q}_h|_T \in \mathbf{Nd}_1(T) \ , \ T \in \mathcal{T}_i\} \ . \tag{4.3}$$

Moreover, we denote by $\mathbf{Nd}_{1,\Gamma_i}(\Omega_i;\mathcal{T}_i)$ the subspace of $\mathbf{Nd}_1(\Omega_i;\mathcal{T}_i)$ with vanishing tangential trace on Γ_i. From the definition of $\mathbf{Nd}_1(T)$ it is easy to see that on each tetrahedron $T \in \mathcal{T}_i$ a function $\mathbf{q}_h \in \mathbf{Nd}_1(T)$ is divergence free. However, this does not imply that a function $\mathbf{q}_h \in \mathbf{Nd}_1(\Omega_i;\mathcal{T}_i)$ is globally divergence free. Additionally, according to (4.2) only the tangential component of $\mathbf{q}_h$ is continuous at the faces of the triangulation.

Using the degrees of freedom (4.2), we can define an interpolant for $\mathbf{Nd}_1(\Omega_i;\mathcal{T}_i)$. Unfortunately, since the degrees of freedom involve integrals along edges, they are not defined for a general function in $\mathbf{H}(\mathbf{curl};\Omega_i)$ [ABDG98, Mon03]. Assuming that $\mathbf{u}$ has the necessary smoothness, the standard interpolation operator associated with the subdomain Ω_i, denoted by Π_h^i, is defined according to

$$\sum_{E\in\mathcal{E}_h(\Omega_i)} \ell_E^n(\Pi_h^i\mathbf{u}-\mathbf{u}) = 0\ . \tag{4.4}$$

If we choose basis functions $\mathbf{q}_{E_i}$ for $\mathbf{Nd}_1(\Omega_i;\mathcal{T}_i)$ that are associated with the edges $E_i \in \mathcal{E}_h(\Omega_i)$ such that $\ell_{E_i}^n(\mathbf{q}_{E_j}) = \delta_{ij}$, the interpolant is given by

$$\Pi_h^i\mathbf{u} := \sum_{E\in\mathcal{E}_h(\Omega_i)} \ell_E^n(\mathbf{u})\,\mathbf{q}_E\ . \tag{4.5}$$

An approximation property of the interpolation operator is given by the following lemma [XH05, Lemma 4.4].

Lemma 4.1 (Approximation properties of the interpolation operator) *Let $\Pi_h^i : \mathbf{H}^1(\mathbf{curl};\Omega_i) \to \mathbf{Nd}_1(\Omega_i;\mathcal{T}_i)$ be the standard interpolation operator associated with subdomain Ω_i. Then, for $K \in \mathcal{T}_i$ and $T \in \partial K$, the following holds*

$$(i) \qquad \|\mathbf{n_T}\cdot(\mathbf{curl}\,\Pi_h^i\mathbf{u}-\mathbf{curl}\,\mathbf{u})\|_{0,T} \le Ch_K^{\frac{1}{2}}\|\mathbf{curl}\,\mathbf{u}\|_{1,K}\ ,$$

$$(ii) \qquad \|\Pi_h^i\mathbf{u}-\mathbf{u}\|_{0,T} \le Ch_K^{\frac{1}{2}}\|\mathbf{u}\|_{1,\mathbf{curl},K}\ .$$

Further approximation properties of the interpolant can be found in [Mon03, Néd83]. An important norm equivalence for $\mathbf{Nd}_1(\Omega_i;\mathcal{T}_i)$ is given by the following Lemma [XH05, Lemma 4.2].

Lemma 4.2 (Norm equivalences for $\mathbf{Nd}_1(\Omega_i;\mathcal{T}_i)$) *For any $\mathbf{q}_h \in \mathbf{Nd}_1(\Omega_i;\mathcal{T}_i)$, the following norm equivalences hold*

$$ch_i^3 \sum_{T\in\mathcal{F}_h(\bar\Omega_i)} |(\mathbf{n}_T\cdot\mathbf{curl}\,\mathbf{q}_h)|_T|^2 \le \|\mathbf{curl}\,\mathbf{q}_h\|_{0,\Omega_i}^2 \le Ch_i^3 \sum_{T\in\mathcal{F}_h(\bar\Omega_i)} |(\mathbf{n}_T\cdot\mathbf{curl}\,\mathbf{q}_h)|_T|^2\ ,$$

$$\text{and}\quad ch_i^3 \sum_{E\in\mathcal{E}_h(\bar\Omega_i)} |(\mathbf{t}_E\cdot\mathbf{q}_h)(\mathbf{x}_E^M)|^2 \le \|\mathbf{q}_h\|_{0,\Omega_i}^2 \le Ch_i^3 \sum_{E\in\mathcal{E}_h(\bar\Omega_i)} |(\mathbf{t}_E\cdot\mathbf{q}_h)(\mathbf{x}_E^M)|^2\ ,$$

where $\mathbf{n}_T$ denotes the exterior unit normal vector with respect to $T \in \mathcal{F}_h(\bar\Omega_i)$, and $\mathbf{x}_E^M$ is the midpoint of the edge E.

An advantageous property of edge elements is the existence of discrete potentials. For a simply connected domain Ω and for Γ_D being a simply connected part of the boundary $\partial\Omega$ we have

$$\mathbf{Nd}_{1,\Gamma_D}(\Omega;\mathcal{T}_\Omega) \cap \mathcal{N}^0(\mathbf{curl},\Omega) = \mathbf{grad}\, S_{1,\Gamma_D}(\mathcal{T}_\Omega) \ , \tag{4.6}$$

where $\mathcal{N}^0(\mathbf{curl},\Omega) = \{\mathbf{q} \in \mathbf{H}(\mathbf{curl};\Omega) \mid \mathbf{curl}\,\mathbf{q} = 0\}$ and $S_{1,\Gamma_D}(\mathcal{T}_\Omega) \subset H^1_{\Gamma_D}(\Omega)$ denotes the Lagrangian finite element space of piecewise linear functions vanishing on Γ_D.

Based on the finite element spaces $\mathbf{Nd}_1(\Omega_i;\mathcal{T}_i)$ we discretize the function space $\mathbf{V}$ by the product space

$$\mathbf{V}_h := \{\mathbf{q}_h \in \mathbf{L}^2(\Omega) \mid \mathbf{q}_h|_{\Omega_i} \in \mathbf{Nd}_{1,\Gamma_i}(\Omega_i;\mathcal{T}_i) \ , \ 1 \le i \le N\} \ , \tag{4.7}$$

$$\|\mathbf{q}_h\|_{\mathbf{V}_h} := (\|\mathbf{q}_h\|^2_{\mathbf{X}} + \|[\mathbf{n}\wedge\mathbf{q}_h]|_S\|^2_{+\frac{1}{2},h,S})^{1/2} \ , \tag{4.8}$$

where $\|\cdot\|_{+\frac{1}{2},h,S}$ is given by

$$\|[\mathbf{n}\wedge\mathbf{q}_h]|_S\|_{+\frac{1}{2},h,S} := \left(\sum_{\gamma_k\subset S} \|[\mathbf{n}\wedge\mathbf{q}_h]|_{\delta_k}\|^2_{+\frac{1}{2},h,\delta_k}\right)^{1/2}$$

and $\|\cdot\|_{+\frac{1}{2},h,\delta_k}$ denotes the mesh-dependent norm

$$\|[\mathbf{n}\wedge\mathbf{q}_h]|_{\delta_k}\|_{+\frac{1}{2},h,\delta_k} := h_{\delta_k}^{-1/2}\|[\mathbf{n}\wedge\mathbf{q}_h]|_{\delta_k}\|_{0,\delta_k} \ .$$

The discrete potential space of $\mathbf{V}_h$ is given by

$$V_h := \{\ v_h \in L^2(\Omega) \mid v_h|_{\Omega_i} \in S_{1,\Gamma_i}(\Omega_i;\mathcal{T}_i) \ , \ 1 \le i \le N\} \ .$$

4.3 The Lagrange Multiplier Space

Observing (2.57), we see that the space $\mathbf{V}_h$ is not contained in $\mathbf{H}_0(\mathbf{curl};\Omega)$ due to the nonconformity arising on the interfaces γ_k. Neither the tangential trace $\mathbf{q}_h\wedge\mathbf{n}$ nor the tangential components trace $\mathbf{n}\wedge(\mathbf{q}_h\wedge\mathbf{n})$ can be expected to be continuous at the interfaces between adjacent subdomains. In order to keep the error, caused by this nonconformity, bounded, we have to impose weak continuity constraints for the tangential trace across the interfaces. This will be realized by means of appropriately chosen Lagrangian multipliers.

As seen in the last section, the trace of the space $\mathbf{Nd}_1(\Omega_i;\mathcal{T}_i)$ will be important for the development of a mortar finite element method. Considering (4.3), it is easy to see that $\gamma_t(\mathbf{q}_h)|_{\delta_k}$ is an element of the lowest order Raviart-Thomas finite element space. For a triangle $T \in \mathcal{T}_{\delta_k}$ the lowest order Raviart-Thomas divergence conforming finite element (cf. [BF91]) is given by

$$\mathbf{RT}_0(T) := \{\mathbf{q} = \mathbf{a} + b\mathbf{x} \ \mid \ \mathbf{a} \in \mathbb{R}^2, \ b \in \mathbb{R} \ , \ \mathbf{x} \in T\} \ . \tag{4.9}$$

Any $\mathbf{q}_h \in \mathbf{RT}_0(T)$ is uniquely defined by the degrees of freedom

$$\ell_E^r(\mathbf{q}_h) := \int_E \mathbf{n}_E \cdot \mathbf{q}_h \, d\sigma \ , \ E \in \mathcal{E}_h(T) \ , \tag{4.10}$$

where $\mathbf{n}_E$ stands for the exterior unit normal vector with respect to E. Then the Raviart-Thomas space $\mathbf{RT}_0(\delta_k; \mathcal{T}_{\delta_k})$ is given by

$$\mathbf{RT}_0(\delta_k; \mathcal{T}_{\delta_k}) := \{\mathbf{q}_h \in \mathbf{H}(\mathrm{div}; \delta_k) \ \mid \ \mathbf{q}_h|_T \in \mathbf{RT}_0(T) \ , \ T \in \mathcal{T}_{\delta_k}\} \ . \tag{4.11}$$

Additionally, the space $\mathbf{RT}_{0,0}(\delta_k; \mathcal{T}_{\delta_k}) \subset \mathbf{RT}_0(\delta_k; \mathcal{T}_{\delta_k})$ denotes the subspace of vector fields with vanishing normal components along the boundary $\partial\delta_k$. A consequence of the definition of $\mathbf{RT}_0(T)$ is that any function $\mathbf{q}_h \in \mathbf{RT}_0(T)$ is irrotational, i.e. $\mathrm{curl}_\tau \, \mathbf{q}_h = 0$. As in the case of the edge elements, this does not imply that a function $\mathbf{q}_h \in \mathbf{RT}_0(\delta_k; \mathcal{T}_{\delta_k})$ is globally irrotational. An important norm equivalence for functions in $\mathbf{RT}_0(\delta_k; \mathcal{T}_{\delta_k})$ is given by [XH05, Lemma 4.2].

Lemma 4.3 (Norm equivalences for $\mathbf{RT}_0(\delta_k; \mathcal{T}_{\delta_k})$)
For any $\delta_k \subset S$ and any $\mathbf{q}_h \in \mathbf{RT}_0(\delta_k; \mathcal{T}_{\delta_k})$, we have

$$ch_{\delta_k}^2 \sum_{T \in \mathcal{T}_{\delta_k}} |(\mathrm{div}_\tau \, \mathbf{q}_h)|_T|^2 \leq \| \mathrm{div}_\tau \, \mathbf{q}_h \|_{0,\delta_k}^2 \leq Ch_{\delta_k}^2 \sum_{T \in \mathcal{T}_{\delta_k}} |(\mathrm{div}_\tau \, \mathbf{q}_h)|_T|^2 \ ,$$

and

$$ch_{\delta_k}^2 \sum_{E \in \mathcal{E}_h(\bar{\delta}_k)} |(\mathbf{n}_E \cdot \mathbf{q}_h)(\mathbf{x}_E^M)|^2 \leq \|\mathbf{q}_h\|_{0,\delta_k}^2 \leq Ch_{\delta_k}^2 \sum_{E \in \mathcal{E}_h(\bar{\delta}_k)} |(\mathbf{n}_E \cdot \mathbf{q}_h)(\mathbf{x}_E^M)|^2 \ .$$

where $\mathbf{n}_E$ denotes the exterior unit normal vector with respect to $E \in \mathcal{E}_h(\bar{\delta}_k)$, and $\mathbf{x}_E^M$ is the midpoint of the edge E.

A consequence of the geometric decomposition (3.12) is that at each interface $\gamma_k \subset S$, $1 \leq k \leq M$, there are two sides: the master side ϱ_k and the slave side δ_k. Although ϱ_k and δ_k occupy the same geometric space, they are not equivalent since they inherit different nonmatching triangulations from the master domain $\Omega_{m(k)}$ and from the slave domain $\Omega_{s(k)}$, respectively. For the construction of the Lagrange multiplier space on γ_k we choose the slave side for the discretization. Recalling that $\mathcal{T}_{\delta_k}$ denotes the triangulation of γ_k inherited from the triangulation of the slave domain $\Omega_{s(k)}$, we define the multiplier space $\mathbf{M}_h(S)$ according to

$$\mathbf{M}_h(S) \ := \ \prod_{k=1}^{M} \mathbf{M}_h(\delta_k) \ , \tag{4.12}$$

with $\mathbf{M}_h(\delta_k)$ chosen such that

$$\mathbf{M}_h(\delta_k) \subset \mathbf{RT}_0(\delta_k; \mathcal{T}_{\delta_k}) \ , \tag{4.13}$$

$$\dim \mathbf{M}_h(\delta_k) \ = \ \dim \mathbf{RT}_{0,0}(\delta_k; \mathcal{T}_{\delta_k}) \ . \tag{4.14}$$

Additionally, we equip the Lagrange multiplier space $\mathbf{M}_h(S)$ with the mesh-dependent norm

$$\|\boldsymbol{\mu}_h\|_{\mathbf{M}_h(S)} := \left(\sum_{k=1}^{M} \|\boldsymbol{\mu}_h|_{\delta_k}\|^2_{-1/2,h,\delta_k} \right)^{1/2} , \tag{4.15}$$

where

$$\|\boldsymbol{\mu}_h|_{\delta_k}\|_{-1/2,h,\delta_k} := h_{\delta_k}^{1/2} \|\boldsymbol{\mu}_h|_{\delta_k}\|_{0,\delta_k} . \tag{4.16}$$

To obtain good approximation properties, we have to require that $\mathbf{M}_h(\delta_k)$ contains constant vectors. To achieve this we have to modify the basis fields of $\mathbf{RT}_{0,0}(\delta_k; \mathcal{T}_{\delta_k})$ in order to comply with conditions (4.13) and (4.14). Denoting by $\mathbf{q}_E$ the basis field associated with an edge $E \in \mathcal{E}_h(\bar{\delta}_k)$ according to

$$\ell^r_{E'}(\mathbf{q}_E) = \int_{E'} \mathbf{n}_{E'} \cdot \mathbf{q}_E \, d\sigma = h_{\delta_k} \delta_{E,E'} \ , \ E' \in \mathcal{E}_h(\bar{\delta}_k) \ , \tag{4.17}$$

we construct $\mathbf{M}_h(\delta_k)$ by an extension of the basis field $\mathbf{q}_E \in \mathbf{RT}_{0,0}(\delta_k; \mathcal{T}_{\delta_k})$ with respect to those edges $E \in \mathcal{E}_h(\delta_k)$ that have at least one neighboring edge on the boundary $\partial\delta_k$.

Before we proceed with the construction of the Lagrangian multiplier space, we have to introduce some additional notations. Given an interior edge $E \in \mathcal{E}_h(\delta_k)$, we denote by

$$\mathcal{E}_h^{\partial\delta_k}(E) \ := \ \{E' \in \mathcal{E}_h(\partial\delta_k) \mid E' \subset \mathit{supp}\ \mathbf{q}_E\} \ ,$$

the set of the neighboring edges on $\partial\delta_k$. Likewise, we define for a boundary edge $E \in \mathcal{E}_h(\partial\delta_k)$ the set of neighboring edges in the interior of δ_k by

$$\mathcal{E}_h^{\delta_k}(E) := \{E' \in \mathcal{E}_h(\delta_k) \mid E' \subset \mathit{supp}\ \mathbf{q}_E\} \ .$$

Finally, we define

$$\mathcal{E}_h^{\delta_k}(\partial\delta_k) := \bigcup_{E' \in \mathcal{E}_h(\partial\delta_k)} \mathcal{E}_h^{\delta_k}(E')$$

as the set of interior edges with a neighboring edge on $\partial\delta_k$.

At the boundary $\partial\delta_k$ a triangle $T \in \mathcal{T}_{\delta_k}$ shares either one or two edges with $\partial\delta_k$ (cf. Fig. 4.2). Let us first consider the case that the triangle T shares one edge with the boundary. Given a constant vector-valued function $\mathbf{C} \in \mathbb{R}^2$, we have

$$\mathbf{C}|_T = \sum_{i=1}^{3} h_{\delta_k}^{-1} \ell^r_{E_i}(\mathbf{C}) \, \mathbf{q}_{E_i} \ , \ E_i \in \mathcal{E}_h(T) \ . \tag{4.18}$$

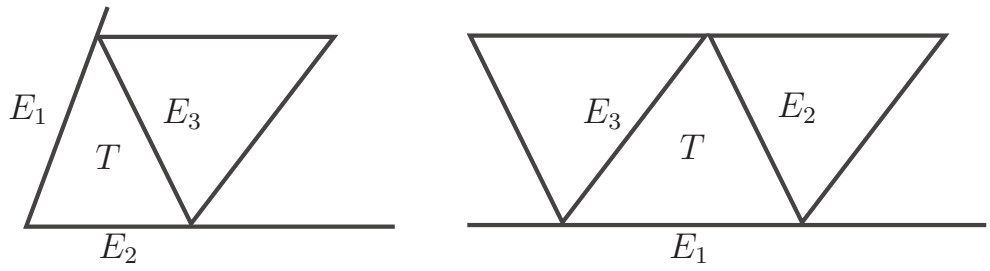

Figure 4.2: Situation at the boundary of the interface δ_k. A triangle $T \in \mathcal{T}_{\delta_k}$ shares either one (right) or two edges (left) with $\partial\delta_k$.

Recalling that $\ell^r_{E_i}(\mathbf{C}) = \int_{E_i} \mathbf{n}_{E_i} \cdot \mathbf{C}\, d\sigma$ and $\sum_{i=1}^{3} |E_i| \mathbf{n}_{E_i} = 0$, where $\mathbf{n}_{E_i}$ and $|E_i|$ denote the unit outer normal to E_i and the length of E_i, respectively, we have

$$\begin{aligned}
\mathbf{C}|_T &= \sum_{i=1}^{3} h_{\delta_k}^{-1} \ell^r_{E_i}(\mathbf{C})\, \mathbf{q}_{E_i} = \sum_{i=1}^{3} h_{\delta_k}^{-1} |E_i| (\mathbf{n}_{E_i} \cdot \mathbf{C})\, \mathbf{q}_{E_i} \qquad (4.19)\\
&= h_{\delta_k}^{-1} \left[-(|E_2|(\mathbf{n}_{E_2} \cdot \mathbf{C}) + |E_3|(\mathbf{n}_{E_3} \cdot \mathbf{C}))\, \mathbf{q}_{E_1} + \right.\\
&\quad \left. + |E_2|(\mathbf{n}_{E_2} \cdot \mathbf{C}) \mathbf{q}_{E_2} + |E_3|(\mathbf{n}_{E_3} \cdot \mathbf{C})\, \mathbf{q}_{E_3} \right]\\
&= h_{\delta_k}^{-1} \left[|E_2|(\mathbf{n}_{E_2} \cdot \mathbf{C})(\mathbf{q}_{E_2} - \mathbf{q}_{E_1}) + |E_3|(\mathbf{n}_{E_3} \cdot \mathbf{C})(\mathbf{q}_{E_3} - \mathbf{q}_{E_1}) \right]\\
&= h_{\delta_k}^{-1} \left(\ell^r_{E_2}(\mathbf{q}_{E_2} - \mathbf{q}_{E_1}) + \ell^r_{E_3}(\mathbf{q}_{E_3} - \mathbf{q}_{E_1}) \right) \ .
\end{aligned}$$

If we define new basis functions $\boldsymbol{\eta}_{E_2} := \mathbf{q}_{E_2} - \mathbf{q}_{E_1}$ and $\boldsymbol{\eta}_{E_3} := \mathbf{q}_{E_3} - \mathbf{q}_{E_1}$, we are able to reproduce constant vector fields on T under the restrictions of equations (4.13) and (4.14).

Now, let us consider a triangle T that shares two edges with the boundary of δ_k. Here the situation is very different. Since $\mathbf{C}$ has two degrees of freedom on T, its components c_1 and $c_2 \in \mathbb{R}$, we need at least two basis functions on T to reproduce $\mathbf{C}$. However, since we have to obey conditions (4.13) and (4.14), a modification of $\mathbf{q}_{E_3}$ is not enough. Therefore, we are forced to modify basis functions whose support does not contain T in order to be able to reproduce $\mathbf{C}$ on T. Let E^1, $E^2 \in \mathcal{E}_h(\delta_k)$ be such that $\mathbf{n}_{E_1} = \alpha_{11}\mathbf{n}_{E^1} + \alpha_{12}\mathbf{n}_{E^2}$ and $\mathbf{n}_{E_2} = \alpha_{21}\mathbf{n}_{E^1} + \alpha_{22}\mathbf{n}_{E^2}$. If we define new basis functions $\boldsymbol{\eta}_i$, $i \in \{1, 2\}$, according to

$$\boldsymbol{\eta}_i := \mathbf{q}_{E^i} + \sum_{j=1}^{2} \beta_{ij}\, \mathbf{q}_{E_j} \ , \qquad (4.20)$$

$$\beta_{ij} := \frac{\alpha_{ji}|E_j|}{|E^i|} \ , \qquad (4.21)$$

we have

$$
\begin{aligned}
h_{\delta_k}^{-1}(\ell^r_{E_3}(\mathbf{C})\,\mathbf{q}_{E_3} + \sum_{i=1}^{2} \ell^r_{E^i}(\mathbf{C})\,\boldsymbol{\eta}_i|_T) = \qquad & (4.22)\\
= h_{\delta_k}^{-1}(\ell^r_{E_3}(\mathbf{C})\,\mathbf{q}_{E_3} + \sum_{i,j=1}^{2} \ell^r_{E^i}(\mathbf{C})\,\beta_{ij}\,\mathbf{q}_{E_j}) \\
= h_{\delta_k}^{-1}(\ell^r_{E_3}(\mathbf{C})\,\mathbf{q}_{E_3} + \sum_{i,j=1}^{2} |E^i|\,(\mathbf{n}_{E^i}\cdot\mathbf{C})\,\frac{\alpha_{ji}|E_j|}{|E^i|}\,\mathbf{q}_{E_j}) \\
= h_{\delta_k}^{-1}(\ell^r_{E_3}(\mathbf{C})\,\mathbf{q}_{E_3} + \sum_{j=1}^{2} (\alpha_{j1}\mathbf{n}_{E^1}\cdot\mathbf{C} + \alpha_{j2}\mathbf{n}_{E^2}\cdot\mathbf{C})|E_j|\,\mathbf{q}_{E_j}) \\
= h_{\delta_k}^{-1}(\ell^r_{E_3}(\mathbf{C})\,\mathbf{q}_{E_3} + \sum_{j=1}^{2} (\mathbf{n}_{E_j}\cdot\mathbf{C})|E_j|\,\mathbf{q}_{E_j}) \\
= h_{\delta_k}^{-1}(\ell^r_{E_3}(\mathbf{C})\,\mathbf{q}_{E_3} + \sum_{j=1}^{2} \ell^r_{E_j}(\mathbf{C})\,\mathbf{q}_{E_j}) = \mathbf{C}\ .
\end{aligned}
$$

As it can be seen from the above calculations, the situation of triangles sharing two edges with $\partial\delta_k$ does not cause any essential difficulties, but is much more complicated. In order to avoid related technical difficulties, we will restrict ourselves to the case of triangles that share at most one edge with the boundary. Then we define the basis field $\tilde{\mathbf{q}}_E$, $E \in \mathcal{E}_h(\delta_k)$, according to

$$
\tilde{\mathbf{q}}_E = \begin{cases} \mathbf{q}_E, & E \in \mathcal{E}_h(\delta_k)\backslash\mathcal{E}_h^{\delta_k}(\partial\delta_k) \\ \boldsymbol{\eta}_E, & E \in \mathcal{E}_h^{\delta_k}(\partial\delta_k) \end{cases}\ . \tag{4.23}
$$

Using these modified basis fields, we define the Lagrange multiplier space as

$$
\mathbf{M}_h(\delta_k) := \text{span}\,\{\tilde{\mathbf{q}}_E \mid E \in \mathcal{E}_h(\delta_k)\}\ . \tag{4.24}
$$

According to the construction of $\mathbf{M}_h(\delta_k)$, it contains all constant two-dimensional vector fields on δ_k. Moreover, the tangential trace of $\mathbf{grad}\,S_1(\mathcal{T}_{\Omega_{s(k)}})$ is a subspace of $\mathbf{M}_h(\delta_k)$.

As in the case of edge elements, we want to interpolate functions $\mathbf{q}$ using an interpolation operator based on the degrees of freedom (4.17). Since the degrees of freedom have to be well-defined, we have to require that $\mathbf{q}$ is sufficiently smooth. So, assume $\mathbf{q}$ to be smooth enough (e.g., $\mathbf{q} \in \mathbf{H}^{1/2+\delta}(\delta_k)$, $\delta > 0$ [Mon03]). Then the global interpolation operator associated with the space $\mathbf{M_h}(\delta_k)$ is given by

$$
\mathbf{I}_h\mathbf{q} = \sum_{E\in\mathcal{E}_h(\delta_k)} \ell^r_E(\mathbf{q})\tilde{\mathbf{q}}_E\ .
$$

An important property of the global interpolation operator is given by the following lemma.

Lemma 4.4 (Properties of the interpolation operator)
Let $\mathbf{q} \in (H^1(\gamma_k))^2$. *Then we have*

$$\|(\mathbf{I} - \mathbf{I}_h)\,\mathbf{q}\|_{0,\gamma_k} \leq \; Ch_{\delta_k}|\mathbf{q}|_{1,\delta_k} \; . \tag{4.25}$$

Moreover, if $\mathbf{q}_h \in \mathbf{RT}_0(\delta_k;\mathcal{T}_{\delta_k})$ *or* $\mathbf{q}_h \in \mathbf{RT}_0(\delta_k;\mathcal{T}_{\varrho_k})$ *we have*

$$\|(\mathbf{I} - \mathbf{I}_h)(\mathbf{q}_h)\|_{0,\gamma_k} \leq Ch_{\delta_k}\|\operatorname{div}_\tau \mathbf{q}_h\|_{0,\gamma_k} \; , \; 1 \leq m \leq M \; . \tag{4.26}$$

Proof:
The proof of (4.25) is quite straightforward. Observing that $\mathbf{I}_h$ preservers constant vectors $\mathbf{C} \in \mathbb{R}^2$, we obtain by applying the standard Bramble-Hilbert lemma and scaling arguments

$$\begin{aligned}\|(\mathbf{I} - \mathbf{I}_h)\,\mathbf{q}\|^2_{0,\gamma_k} &= \sum_{T\in\mathcal{T}_{\delta_k}} \|(\mathbf{I} - \mathbf{I}_h)\,\mathbf{q}\|^2_{0,T} \leq \\ &\leq Ch^2_{\delta_k} \sum_{T\in\mathcal{T}_{\delta_k}} |\mathbf{q}|^2_{1,T} = Ch^2_{\delta_k}|\mathbf{q}|^2_{1,\delta_k} \; .\end{aligned}$$

Taking roots on both sides of the inequality gives (4.25).

The proof of (4.26) is more involving. Since $\mathbf{q}_h$ is a piecewise polynomial function with continuous normal components across the edges of the triangulations, the global interpolation operator $\mathbf{I}_h$ is well-defined for $\mathbf{q}_h$. Although an arbitrary function $\mathbf{q}_h \in \mathbf{RT}_0(\delta_k;\mathcal{T}_{\delta_k})$ or $\mathbf{q}_h \in \mathbf{RT}_0(\delta_k;\mathcal{T}_{\varrho_k})$ is not an element of $(H^1(\gamma_k))^2$, its restriction to a triangle T of $\mathcal{T}_{\delta_k}$ or $\mathcal{T}_{\varrho_k}$ is a polynomial and thus $\mathbf{q}_h|_T \in (H^1(T))^2$.

However, since $\mathbf{q}_h \in \mathbf{RT}_0(\delta_k;\mathcal{T}_{\varrho_k})$ and $\mathbf{I}_h\mathbf{q}_h$ are defined on different, in general nonmatching triangulations, we have to introduce a third mesh $\mathcal{T}_{\gamma_k}$ in such a way that given triangles $T \in \mathcal{T}_{\gamma_k}$, $T_1 \in \mathcal{T}_{\delta_k}$, and $T_2 \in \mathcal{T}_{\varrho_k}$ with $T \cap T_1 \neq \emptyset$ and $T \cap T_2 \neq \emptyset$ we have

$$T \cap T_1 = T \quad , \quad T \cap T_2 = T \; . \tag{4.27}$$

Now, if we restrict a function $\mathbf{q}_h \in \mathbf{RT}_0(\delta_k;\mathcal{T}_{\delta_k})$ or $\mathbf{q}_h \in \mathbf{RT}_0(\delta_k;\mathcal{T}_{\varrho_k})$ to a triangle $T \in \mathcal{T}_{\gamma_k}$, we have that $\mathbf{q}_h|_T \in (H^1(T))^2$.

Since $\mathbf{I}_h$ preserves constant tangential components, we get by a standard Bramble-Hilbert and scaling argument:

$$\begin{aligned}\|(\mathbf{I} - \mathbf{I}_h)(\mathbf{q}_h)\|_{0,T} \leq Ch_T \mid \mathbf{q}_h|_{1,T} &= Ch_T(\|\operatorname{div}_\tau \mathbf{q}_h\|^2_{0,T} + \|\operatorname{curl}_\tau \mathbf{q}_h\|^2_{0,T})^{1/2} = \\ &= Ch_T\|\operatorname{div}_\tau \mathbf{q}_h\|_{0,T} \; .\end{aligned}$$

Therefore, we get

$$\begin{aligned}\|(\mathbf{Id}-\mathbf{I}_h)(\mathbf{q}_h)\|^2_{0,\gamma_k} &= \sum_{T\in\mathcal{T}_{\gamma_k}} \|(\mathbf{Id}-\mathbf{I}_h)(\mathbf{q}_h)\|^2_{0,T} \leq \sum_{T\in\mathcal{T}_{\gamma_k}} Ch_T^2 \|\operatorname{div}_\tau \mathbf{q}_h\|^2_{0,T} \\ &\leq \sum_{T\in\mathcal{T}_{\gamma_k}} Ch_{\delta_k}^2 \|\operatorname{div}_\tau \mathbf{q}_h\|^2_{0,T} = Ch_{\delta_k}^2 \|\operatorname{div}_\tau \mathbf{q}_h\|^2_{0,\gamma_k} \ .\end{aligned}$$

Then equation (4.26) follows by taking roots on both sides of the inequality. •

4.4 Discrete Saddle Point Problem

After the introduction of the relevant finite element space we are able to formulate the mortar edge element approximation of (3.11):
Find $(\mathbf{u}_h, \boldsymbol{\lambda}_h) \in \mathbf{V}_h \times \mathbf{M}_h(S)$ such that

$$\begin{aligned} a_h(\mathbf{u}_h,\mathbf{q}_h) + b_h(\mathbf{q}_h,\boldsymbol{\lambda}_h) &= \ell(\mathbf{q}_h) \quad \forall\, \mathbf{q}_h \in \mathbf{V}_h \ , \\ b_h(\mathbf{u}_h,\boldsymbol{\mu}_h) &= 0 \qquad \forall\, \boldsymbol{\mu}_h \in \mathbf{M}_h(S) \ , \end{aligned} \tag{4.28}$$

where the bilinear form $a_h(\cdot,\cdot) : \mathbf{V}_h \times \mathbf{V}_h \to \mathbb{R}$ is the restriction of $a(\cdot,\cdot)$ to $\mathbf{V}_h \times \mathbf{V}_h$ and $b_h(\cdot,\cdot) : \mathbf{V}_h \times \mathbf{M}_h(S) \to \mathbb{R}$ is given by

$$b_h(\mathbf{q}_h,\boldsymbol{\mu}_h) := \sum_{\gamma_k\in S} ([\mathbf{q}_h \wedge \mathbf{n}]|_{\gamma_k}, \boldsymbol{\mu}_h)_{0,\delta_k} \ .$$

Associated with $b_h(\cdot,\cdot)$ is the operator $B_h : \mathbf{V}_h \to \mathbf{M}_h(S)'$ according to

$$b_h(\mathbf{q}_h,\boldsymbol{\mu}_h) := < B_h\mathbf{q}_h, \boldsymbol{\mu}_h >_{\frac{1}{2},h,S} \ , \tag{4.29}$$

where

$$< \cdot,\cdot >_{\frac{1}{2},h,S} := \sum_{k=1}^{M} < \cdot,\cdot >_{\frac{1}{2},h,\delta_k} \tag{4.30}$$

and $< \cdot,\cdot >_{\frac{1}{2},h,\delta_k}$ denotes the dual pairing between $\mathbf{M}_h(\delta_k)'$ and $\mathbf{M}_h(\delta_k)$.
In order to show the existence and uniqueness of a solution of (4.28), we have to prove the discrete counterpart of Theorem 3.2. According to the proof of this theorem, we have to verify the uniform ellipticity of $a_h(\cdot,\cdot)$ on Ker B_h. Additionally, we have to prove a discrete inf-sup condition (LBB-condition) for the saddle point problem (4.28). Following the approaches in [BD98, Hop99], we will first concentrate on the proof of the discrete inf-sup condition. To do this we start with the following auxiliary inf-sup conditions.

Lemma 4.5 (Auxiliary inf-sup conditions)
The following inf-sup conditions hold true

$$\inf_{\boldsymbol{\mu}_h \in \mathbf{M}_h(\delta_k)} \sup_{\mathbf{q}_h \in \mathbf{RT}_{0,0}(\delta_k;\mathcal{T}_{\delta_k})} \frac{(\mathbf{q}_h, \boldsymbol{\mu}_h)_{0,\delta_k}}{\|\mathbf{q}_h\|_{0,\delta_k} \, \|\boldsymbol{\mu}_h\|_{0,\delta_k}} \geq C > 0 \ , \tag{4.31}$$

and

$$\inf_{\mathbf{q}_h \in \mathbf{RT}_0(\delta_k;\mathcal{T}_{\delta_k})} \sup_{\boldsymbol{\mu}_h \in \mathbf{M}_h(\delta_k)} \frac{(\mathbf{q}_h, \boldsymbol{\mu}_h)_{0,\delta_k}}{\|\mathbf{q}_h\|_{0,\delta_k} \, \|\boldsymbol{\mu}_h\|_{0,\delta_k}} \geq C > 0 \ . \tag{4.32}$$

Proof:
In order to prove (4.31), we choose an arbitrary function $\mathbf{q}_h \in \mathbf{RT}_{0,0}$ and determine $\boldsymbol{\mu}_h \in \mathbf{M_h}(\delta_k)$ by specifying its degrees of freedom according to

$$\ell_E^r(\boldsymbol{\mu}_h) = \ell_E^r(\mathbf{q}_h) \ , \ E \in \mathcal{E}_h(\delta_k) \ .$$

If $K \in \mathcal{T}_{\delta_k}$ shares no edge with $\partial\delta_k$, we have

$$\begin{aligned} \|\mathbf{q}_h\|_{0,K} &= \|\boldsymbol{\mu}_h\|_{0,K} \ , \\ (\mathbf{q}_h, \boldsymbol{\mu}_h)_{0,K} &= \|\mathbf{q}_h\|_{0,K}^2 \ . \end{aligned}$$

Now, let $K \in \mathcal{T}_{\delta_k}$ share one edge with $\partial\delta_k$ and let $\mathbf{F}_K(\hat{x}) = \mathbf{B}_K\hat{x} + \mathbf{b}_K$, $\hat{\mathbf{x}} \in \hat{K}$, be the affine transformation mapping the reference element $\hat{K}$ onto K such that $\mathbf{F}(\hat{E}_i) = E_i$, $1 \leq i \leq 3$. Moreover, we assume that $E_2 \in \partial\delta_k$ (cf. Figure 4.3).

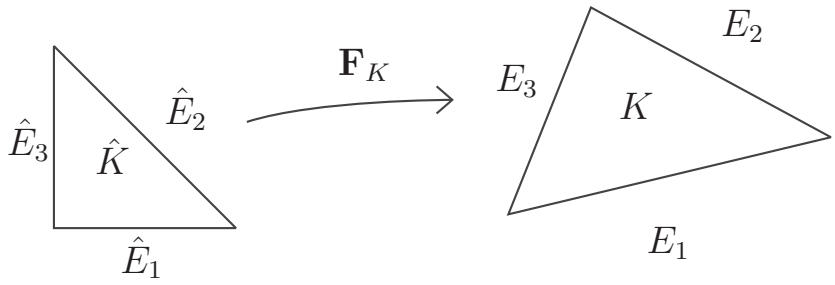

Figure 4.3: Affine transformation from the reference triangle $\hat{K}$ to K.

Setting $\hat{\mathbf{q}}_h = \frac{1}{\det \mathbf{B}_K^{-1}} \mathbf{B}_K^{-1}\mathbf{q}_h$ and $\hat{\boldsymbol{\mu}}_h = \frac{1}{\det \mathbf{B}_K^{-1}} \mathbf{B}_K^{-1}\boldsymbol{\mu}_h$, we have

$$(\hat{\mathbf{q}}_h, \hat{\boldsymbol{\mu}}_h)_{0,\hat{K}} = \frac{1}{|\det \mathbf{B}_K^{-1}|} \int_K \mathbf{B}_K^{-1}\mathbf{q}_h \cdot \mathbf{B}_K^{-1}\boldsymbol{\mu}_h \, dV \leq \frac{\|\mathbf{B}_K^{-1}\|^2}{|\det \mathbf{B}_K^{-1}|} (\mathbf{q}_h, \boldsymbol{\mu}_h)_{0,K} \ . \tag{4.33}$$

Observing the definition of the basis functions of $\mathbf{M}_h(S)$ and the properties of

$\mathbf{F}_K$, it is easy to see that $\bar{\mathbf{q}}_h$ and $\bar{\boldsymbol{\mu}}_h$ are given by

$$\hat{\mathbf{q}}_h = -\begin{pmatrix} a \\ b \end{pmatrix} + (a+b) \cdot \begin{pmatrix} \hat{x} \\ \hat{y} \end{pmatrix} \ ,$$

$$\hat{\boldsymbol{\mu}}_h = -\begin{pmatrix} a \\ b \end{pmatrix} \ ,$$

where a, $b \in \mathbb{R}$. It is easy to check that

$$\begin{aligned} \|\hat{\boldsymbol{\mu}}_h\|^2_{0,\hat{K}} &= \frac{1}{2}\,(a^2+b^2) \ , \\ \|\hat{\mathbf{q}}_h\|^2_{0,\hat{K}} &= \frac{1}{2}\,(a^2+b^2) - \frac{1}{6}\,(a+b)^2 \ , \\ (\hat{\mathbf{q}}_h, \hat{\boldsymbol{\mu}}_h)_{0,\hat{K}} &= \frac{1}{2}\,(a^2+b^2) - \frac{1}{6}\,(a+b)^2 \ , \\ \|\hat{\boldsymbol{\mu}}_h\|_{0,\hat{K}} &\leq \sqrt{6} \cdot \|\bar{\mathbf{q}}_h\|_{0,\hat{K}} \ . \end{aligned}$$

A consequence of these results is that

$$(\hat{\mathbf{q}}_h, \hat{\boldsymbol{\mu}}_h)_{0,\hat{K}} \ \geq C \|\hat{\mathbf{q}}_h\|_{0,\hat{K}} \, \|\hat{\boldsymbol{\mu}}_h\|_{0,\hat{K}} \ . \tag{4.34}$$

To finish the proof, we use the backward transformation to get

$$\|\mathbf{q}_h\|^2_{0,K} \leq \frac{\|\mathbf{B}_K\|^2}{|\det \ \mathbf{B}_K|} \, \|\hat{\mathbf{q}}_h\|^2_{0,\hat{K}} \ , \tag{4.35}$$

$$\|\boldsymbol{\mu}_h\|^2_{0,K} \leq \frac{\|\mathbf{B}_K\|^2}{|\det \ \mathbf{B}_K|} \, \|\hat{\boldsymbol{\mu}}_h\|^2_{0,\hat{K}} \ . \tag{4.36}$$

Taking into account that $\mathcal{T}_{\delta_k}$ is a regular triangulation, we have

$$\|\mathbf{B}_K^{-1}\| \, \|\mathbf{B}_K\| \leq C_1 \ , \ |\det \ \mathbf{B}_K| = \frac{\text{meas } (K)}{\text{meas } (\hat{K})} \leq C_2 \ . \tag{4.37}$$

Combining (4.33), (4.34), (4.35), (4.36), and (4.37) yields

$$(\mathbf{q}_h, \boldsymbol{\mu}_h)_{0,K} \ \geq C \|\mathbf{q}_h\|_{0,K} \, \|\boldsymbol{\mu}_h\|_{0,K} \ . \tag{4.38}$$

Summing over all triangles $K \in \mathcal{T}_{\delta_k}$ gives the assertion of (4.31). We can prove (4.32) in the same way if we define $\mathbf{q}_h \in \mathbf{RT}_{0,0}(\delta_k; \mathcal{T}_{\delta_k})$ according to

$$\ell^r_E(\mathbf{q}_h) = \ell^r_E(\boldsymbol{\mu}_h) \ , \ E \in \mathcal{E}_h(\delta_k) \ ,$$

where $\boldsymbol{\mu}_h \in \mathbf{M}_h(S)$ is chosen arbitrarily.

•

The second key ingredient of the proof of the discrete inf-sup condition is an appropriate discrete extension of functions $\boldsymbol{\lambda}_h \in \mathbf{RT}_{0,0}(\delta_k; \mathcal{T}_{\delta_k})$ to the interior of $\Omega_{s(k)}$. A good extension operator can be defined in the following way:

Definition 4.6 (Discrete extension operator)
The discrete extension operator $\mathbf{E}_h^{\delta_k} : \mathbf{RT}_{0,0}(\delta_k; \mathcal{T}_{\delta_k}) \rightarrow \mathbf{Nd}_1(\Omega_{s(k)}; \mathcal{T}_{s(k)})$ *is defined according to*

$$(\mathbf{E}_h^{\delta_k} \boldsymbol{\lambda}_h) \wedge \mathbf{n} = \boldsymbol{\lambda}_h \text{ on } \delta_k \ , \ \boldsymbol{\lambda}_h \in \mathbf{RT}_{0,0}(\delta_k; \mathcal{T}_{\delta_k}) \ ,$$

where all degrees of the freedom not located on δ_k *are set equal to zero.*

Using Lemmas 4.2 and 4.3, we can derive the following estimate [XH05, Lemma 4.3].

Lemma 4.7 (Properties of $\mathbf{E}_h^{\delta_k}$)
For $\boldsymbol{\lambda}_h \in \mathbf{RT}_{0,0}(\delta_k; \mathcal{T}_{\delta_k})$ *there holds*

$$\|\mathbf{E}_h^{\delta_k} \boldsymbol{\lambda}_h\|_{\mathbf{curl},\Omega_{s(k)}} \leq C \ h_{\delta_k}^{\frac{1}{2}} \ \|\boldsymbol{\lambda}_h\|_{\mathrm{div}_\tau,\delta_k} \ ,$$

where $\|\mathbf{v}\|_{\mathrm{div}_\tau,\delta_k} := (\|\mathbf{v}\|_{0,\delta_k}^2 + \|\operatorname{div}_\tau \mathbf{v}\|_{0,\delta_k}^2)^{\frac{1}{2}}$, $\mathbf{v} \in \mathbf{RT}_{0,0}(\delta_k; \mathcal{T}_{\delta_k})$.

Proof:
According to the definition of the extension operator $E_h^{\delta_k}$ and by Lemma 4.2 we get

$$\begin{aligned}
\|\mathbf{curl}(\mathbf{E}_h^{\delta_k} \boldsymbol{\lambda}_h)\|_{0,\Omega_{s(k)}}^2 &\leq C \ h_{s(k)}^3 \sum_{T \in \mathcal{T}_{\delta_k}} |\mathbf{n}_T \cdot \mathbf{curl}(\mathbf{E}_h^{\delta_k} \boldsymbol{\lambda}_h))|_T|^2 \\
&= C h_{s(k)}^3 \sum_{T \in \mathcal{T}_{\delta_k}} |\operatorname{div}_\tau(\mathbf{E}_h^{\delta_k} \boldsymbol{\lambda}_h \wedge \mathbf{n})|_T|^2 \\
&= C \ h_{s(k)}^3 \sum_{T \in \mathcal{T}_{\delta_k}} |\operatorname{div}_\tau(\boldsymbol{\lambda}_h)|_T|^2 \\
&\leq C \ h_{s(k)} \|\operatorname{div}_\tau(\boldsymbol{\lambda}_h)\|_{0,\delta_k}^2 \ .
\end{aligned}$$

Additionally, using Lemma 4.3, we have

$$\begin{aligned}
\|\mathbf{E}_h^{\delta_k} \boldsymbol{\lambda}_h\|_{0,\Omega_{s(k)}}^2 &\leq C h_{s(k)}^3 \sum_{E \in \mathcal{E}_h(\bar{\Omega}_{s(k)})} |(\mathbf{t}_E \cdot \mathbf{E}_h^{\delta_k} \boldsymbol{\lambda}_h)(\mathbf{x}_E^M)|^2 \\
&= C h_{s(k)}^3 \sum_{E \in \mathcal{E}_h(\bar{\Omega}_{s(k)})} |\mathbf{n}_E \cdot (\mathbf{E}_h^{\delta_k} \boldsymbol{\lambda}_h \wedge \mathbf{n})(\mathbf{x}_E^M)|^2 \\
&= C h_{s(k)}^3 \sum_{E \in \mathcal{E}_h(\delta_k)} |(\mathbf{n}_E \cdot \boldsymbol{\lambda}_h)(\mathbf{x}_E^M)|^2 \\
&\leq h_{s(k)} \|\boldsymbol{\lambda}_h\|_{0,\delta_k}^2 .
\end{aligned}$$

Adding both inequalities gives Lemma 4.7.

•

The results of Lemmas 4.5 and 4.7 enable us to prove the LBB-condition for the bilinear form $b_h(\cdot,\cdot)$ (cf. [XH05, Lemma 5.1]).

Lemma 4.8 (Discrete LBB-condition for $b_h(\cdot,\cdot)$)
The bilinear form $b_h(\cdot,\cdot) : \mathbf{V}_h \times \mathbf{M}_h \to \mathbf{R}$ satisfies a discrete inf-sup condition (LBB-condition) uniformly in h_i, i.e. there exists a constant $c > 0$ independent of the mesh sizes h_i, $1 \le i \le N$, such that

$$\sup_{\mathbf{q}_h \in \mathbf{V}_h} \frac{b_h(\mathbf{q}_h, \boldsymbol{\mu}_h)}{\|\mathbf{q}_h\|_{\mathbf{V}_h}} \ge c\|\boldsymbol{\mu}_h\|_{\mathbf{M}_h} \ .$$

Proof:
Given $\boldsymbol{\mu}_h \in \mathbf{M}_h(\delta_k)$ we define $\mathbf{p}_h^m \in \mathbf{RT}_{0,0}(\delta_k; \mathcal{T}_{\delta_k})$ by fixing the normal fluxes at the interior edges of δ_k, i.e.

$$\ell_E^r(\mathbf{p}_h^m) = \ell_E^r(\boldsymbol{\mu}_h) \ , \ E \in \mathcal{E}_h(\delta_k) \ .$$

Let $\mathbf{q}_h^m \in \mathbf{Nd}_1(\Omega_{s(k)}; \mathcal{T}_{s(k)})$ be the trivial extension of $\mathbf{p}_h^m$ given by $\mathbf{q}_h^m = \mathbf{E}_h^{\delta_k} \mathbf{p}_h^m$. Then we have $[\mathbf{q}_h^m \wedge \mathbf{n}] = \mathbf{p}_h^m$ and, according to Lemma 4.7, we have

$$\begin{aligned}
\|\mathbf{q}_h^m\|_{\mathbf{curl},\Omega_{s(k)}} &\le C \ h_{s(k)}^{\frac{1}{2}} \|\mathbf{p}_h^m\|_{\mathrm{div}_\tau,\delta_k} \\
&\le C h_{s(k)}^{-\frac{1}{2}} \|\mathbf{p}_h^m\|_{0,\delta_k} \\
&= C \ h_{s(k)}^{-\frac{1}{2}} \|[\mathbf{q}_h^m \wedge \mathbf{n}]|_{\delta_k}\|_{0,\delta_k} \ .
\end{aligned}$$

Using this inequality and Lemma 4.5, we obtain

$$\begin{aligned}
(\boldsymbol{\mu}_h, [\mathbf{q}_h^m \wedge \mathbf{n}]|_{\delta_k})_{0,\delta_k} &\ge C\|\boldsymbol{\mu}_h\|_{0,\delta_k} \|[\mathbf{q}_h^m \wedge \mathbf{n}]|_{\delta_k}\|_{0,\delta_k} \\
&\ge C h_{s(k)}^{\frac{1}{2}} \|\boldsymbol{\mu}_h\|_{0,\delta_k} \|\mathbf{q}_h^m\|_{\mathbf{curl},\Omega_{s(k)}} \\
&= C\|\boldsymbol{\mu}_h\|_{-\frac{1}{2},h,\delta_k} \ \|\mathbf{q}_h^m\|_{\mathbf{curl},\Omega_{s(k)}} \ .
\end{aligned}$$

On the other hand,

$$\begin{aligned}
(\boldsymbol{\mu}_h, [\mathbf{q}_h^m \wedge \mathbf{n}]|_{\delta_k})_{0,\delta_k} &\ge C\|\boldsymbol{\mu}_h\|_{0,\delta_k} \|[\mathbf{n} \wedge \mathbf{q}_h^m]|_{\delta_k}\|_{0,\delta_k} \\
&= C h_{s(k)}^{\frac{1}{2}} \|\boldsymbol{\mu}_h\|_{0,\delta_k} h_{s(k)}^{-\frac{1}{2}} \|[\mathbf{q}_h^m \wedge \mathbf{n}]|_{\delta_k}\|_{0,\delta_k} \\
&= C\|\mu_h\|_{-\frac{1}{2},h,\delta_k} \|[\mathbf{q}_h^m \wedge \mathbf{n}]|_{\delta_k}\|_{+\frac{1}{2},h,\delta_k} \ .
\end{aligned}$$

Finally, adding the above inequalities and summing over all $\delta_k \subset S$ gives the assertion.

•

In order to finish the proof of the existence and uniqueness of a solution of (4.28), it remains to be shown that the bilinear form $a_h(\cdot,\cdot)$ is uniformly elliptic in h on $\mathrm{Ker}\ B_h := \{\mathbf{q}_h \in \mathbf{V}_h \mid b_h(\mathbf{q}_h, \boldsymbol{\mu}_h) = 0 \quad \forall \boldsymbol{\mu}_h \in \mathbf{M}_h(S)\}$. The proof of this property is given in the following theorem [Hop99, Theorem 3.2].

Theorem 4.9 (Ker B_h ellipticity of the bilinear form $a_h(\cdot,\cdot)$)
The bilinear form $a_h(\cdot,\cdot) : \mathbf{V}_h \times \mathbf{V}_h \to I\!R$ is uniformly elliptic on Ker B_h, i.e. there exists a constant $\gamma > 0$ such that for all h

$$a_h(\mathbf{q}_h, \mathbf{q}_h) \geq \gamma \|\mathbf{q}_h\|^2_{\mathbf{V}_h} \quad \forall\, \mathbf{q}_h \in Ker\ B_h\ .$$

Proof:
According to the assumptions on χ and σ, we have

$$a_h(\mathbf{q_h}, \mathbf{q_h}) \geq \min(\underline{\sigma}, \underline{\chi}) \|\mathbf{q}_h\|^2_{\mathbf{X}}\ .$$

In contrast to the proof of Theorem 3.2, the space $\mathbf{V}_h$ is not a subspace of $\mathbf{H}_0(\mathbf{curl}; \Omega)$. This means that $\|\mathbf{q}_h\|^2_{\mathbf{X}} \neq \|\mathbf{q}_h\|^2_{\mathbf{V}_h}$. Recalling the definition of $\|\mathbf{q}_h\|_{\mathbf{V}_h}$, we have to show that for $\mathbf{q}_h \in$ Ker B_h

$$\|[\mathbf{n} \wedge \mathbf{q}_h]|_{\gamma_k}\|_{+\frac{1}{2},h,\gamma_k} \leq C(\|\mathbf{q}_h\|^2_{curl,\Omega_{s(k)}} + \|\mathbf{q}_h\|^2_{curl,\Omega_{m(k)}})^{1/2} \quad \forall \gamma_k \subset S\ .$$

Let P_h be the L^2-projection onto the multiplier space $\mathbf{M}_h(\delta_k)$ and let I_h and I_T, $T \in \mathcal{T}_{\delta_k}$, be the global respectively local interpolation operators which interpolate the zero order moments of the normal components with respect to the edges $E \in \mathcal{E}_h(\delta_k)$ and $E \in \mathcal{E}_h(T)$, $T \in \mathcal{T}_{\delta_k}$, respectively.
Since $\mathbf{q_h} \in \mathrm{Ker}\, B_h$ it follows that

$$\|P_h([\mathbf{n} \wedge \mathbf{q}_h]|_{\gamma_k})\|^2_{0,\gamma_k} = ([\mathbf{n} \wedge \mathbf{q}_h]|_{\gamma_k}, P_h([\mathbf{n} \wedge \mathbf{q}_h]|_{\gamma_k}))_{0,\gamma_k} = 0\ .$$

Hence, using Lemma 4.4, we obtain

$$\begin{aligned}\|[\mathbf{n} \wedge \mathbf{q}_h]|_{\gamma_k}\|_{0,\gamma_k} &= \|(Id - P_h)([\mathbf{n} \wedge \mathbf{q}_h]|_{\gamma_k})\|_{0,\gamma_k} \leq \\ &\leq \|(Id - I_h)([\mathbf{n} \wedge \mathbf{q}_h]|_{\gamma_k})\|_{0,\gamma_k} \leq C h_{\delta_k} \|\operatorname{div}_\tau [\mathbf{n} \wedge \mathbf{q}_h]|_{\gamma_k}\|_{0,\gamma_k}\ .\end{aligned}$$

Observing that $\operatorname{div}_\tau(\mathbf{n} \wedge \mathbf{q}|_T) = -\operatorname{curl}_\tau(\mathbf{q}|_T)$, Lemma 4.2 and (4.1) yield

$$\begin{aligned}\|[\mathbf{n} \wedge \mathbf{q}_h]|_{\gamma_k}\|^2_{0,\gamma_k} \leq& \\ &\leq C(h^2_{\delta_k} \|\operatorname{div}_\tau(\mathbf{n} \wedge \mathbf{q}_h|_{\gamma_k})\|^2_{0,\gamma_k} + \bar{\kappa}^2_{\gamma_k} h^2_{\varrho_k} \|\operatorname{div}_\tau(\mathbf{n} \wedge \mathbf{q}_h|_{\varrho_k})\|^2_{0,\varrho_k}) \\ &\leq C h^4_{\delta_k} \sum_{T \in \mathcal{T}_{\delta_k}} |\operatorname{div}_\tau(\mathbf{n} \wedge \mathbf{q}_h|_T)|^2 + C\bar{\kappa}^2_{\gamma_k} h^4_{\varrho_k} \sum_{T \in \mathcal{T}_{\varrho_k}} |\operatorname{div}_\tau(\mathbf{n} \wedge \mathbf{q}_h|_T)|^2 \\ &= C h^4_{\delta_k} \sum_{T \in \mathcal{T}_{\delta_k}} |\operatorname{curl}_\tau(\mathbf{q}_h|_T)|^2 + C\bar{\kappa}^2_{\gamma_k} h^4_{\varrho_k} \sum_{T \in \mathcal{T}_{\varrho_k}} |\operatorname{curl}_\tau(\mathbf{q}_h|_T)|^2 \\ &\leq C h_{\delta_k} h^3_{\delta_k} \sum_{F \in \mathcal{F}_h(\bar{\Omega}_{s(k)})} |\ \mathbf{n}_F \cdot \mathbf{curl}\, \mathbf{q}_h\ |^2_F + \\ &\quad + C\bar{\kappa}^2_{\gamma_k} h_{\varrho_k} h^3_{\varrho_k} \sum_{F \in \mathcal{F}_h(\bar{\Omega}_{m(k)})} |\ \mathbf{n}_F \cdot \mathbf{curl}\, \mathbf{q}_h\ |^2_F \\ &\leq C h_{\delta_k} \|\mathbf{curl}\, \mathbf{q}_h\|^2_{0,\Omega_{s(k)}} + C\bar{\kappa}^2_{\gamma_k} h_{\varrho_k} \|\mathbf{curl}\, \mathbf{q}_h\|^2_{0,\Omega_{m(k)}} \\ &\leq C h_{\delta_k} (\|\mathbf{curl}\, \mathbf{q}_h\|^2_{0,\Omega_{s(k)}} + \|\mathbf{curl}\, \mathbf{q}_h\|^2_{0,\Omega_{m(k)}})\ .\end{aligned}$$

Finally, multiplying by $h_{\delta_k}^{-1}$ results in

$$\begin{aligned}\|[\mathbf{n}\wedge\mathbf{q}_h]|_{\delta_k}\|^2_{+\frac{1}{2},h,\gamma_k} &= h_{\delta_k}^{-1}\|[\mathbf{n}\wedge\mathbf{q}_h]|_{\delta_k}\|^2_{0,\delta_k}\\ &\le C(\|\,\mathbf{curl}\,\mathbf{q}_h\|^2_{0,\Omega_{s(k)}}+\|\,\mathbf{curl}\,\mathbf{q}_h\|^2_{0,\Omega_{m(k)}})\\ &\le C(\|\mathbf{q}_h\|^2_{curl,\Omega_{s(k)}}+\|\mathbf{q}_h\|^2_{curl,\Omega_{m(k)}})\ .\end{aligned}$$

•

Lemma 4.8 and Theorem 4.9 imply that the mortar edge element approximation (4.28) has a unique solution $(\mathbf{u}_h,\boldsymbol{\lambda}_h)\in\mathbf{V}_h\times\mathbf{M}_h(S)$.

Chapter 5

A Priori Error Estimates

In Chapters 3 and 4 we showed that both the continuous and discrete problem have a unique solution. However, there are two important questions that have to be answered. Since we want to find an approximation of the continuous solution, the first question is if $\mathbf{u}_h$, the solution of the discrete problem, converges to $\mathbf{u}$, the solution of the continuous problem, for decreasing mesh size h. As mentioned in Section 4.2, the answer to this question strongly depends on the choice of our finite element space. Moreover, if the answer to the first question is yes, we would like to know how fast this convergence is, i.e. how the approximation error $\mathbf{u}-\mathbf{u}_h$ depends on the mesh size h.

In this chapter we will answer these questions. The results of this chapter are from [XH05]. For the sake of completeness, we will give all proofs of the results.

5.1 Formulation of the Problem Using the Constrained Space

In Chapter 4 we formulated the variational problem using the unconstrained space $\mathbf{V}_h$ and introduced the Lagrange multiplier space $\mathbf{M}_h$ to weakly enforce consistency requirements. This approach resulted in an indefinite saddle point problem. However, for the analysis of the convergence it is more convenient to formulate the problem using a constrained space which leads to a symmetric positive definite system.

In order to reformulate the problem, we first have to introduce the L^2-projection $Q_h^{\delta_k} : (L^2(\gamma_k))^2 \to \mathbf{M}_h(\delta_k)$ which is defined by

$$(Q_h^{\delta_k}\mathbf{q}, \mathbf{w})_{0,\gamma_k} = (\mathbf{q}, \mathbf{w})_{0,\gamma_k} \quad \forall \mathbf{w} \in \mathbf{M}_h(\delta_k) \ . \tag{5.1}$$

The stability of the L^2-projection is given by the following lemma [XH05, Lemma 3.1].

Lemma 5.1 (Approximation property of $Q_h^{\delta_k}$)
Let $Q_h^{\delta_k}$ be given by (5.1)*. Then there holds*

$$\|\mathbf{q} - Q_h^{\delta_k}\mathbf{q}\|_{0,\gamma_m} \leq C\ h_{\delta_k}^{\frac{1}{2}}\ |\mathbf{q}|_{\frac{1}{2},\delta_k}\ ,\ \mathbf{q} \in (H^{\frac{1}{2}}(\delta_k))^2\ . \tag{5.2}$$

Proof:
Let $\mathbf{I}_h$ denote the global interpolation operator associated with the space $\mathbf{M}_h(\delta_k)$ as defined in Section 4.3. Recalling Lemma 4.4 and observing that $Q_h^{\delta_k}$ is a projector, we have

$$\|(\mathbf{I} - Q_h^{\delta_k})\,\mathbf{q}\|_{0,\gamma_k} \leq \|(\mathbf{I} - \mathbf{I}_h)\,\mathbf{q}\|_{0,\gamma_k} \leq Ch_{\delta_k}|\mathbf{q}|_{1,\delta_k}\ ,\ \mathbf{q} \in (H^1(\delta_k))^2\ ,$$

and

$$\|(\mathbf{I} - Q_h^{\delta_k})\,\mathbf{q}\|_{0,\gamma_k} \leq 2\|\mathbf{q}\|_{0,\delta_k}\ .$$

Then the assertion of (5.2) follows from a standard interpolation of the preceding inequalities.

•

Using the projector $Q_h^{\delta_k}$, we introduce the constrained mortar edge element space

$$\tilde{\mathbf{V}}_h := \{\mathbf{q}_h \in \mathbf{V}_h \mid Q_h^{\delta_k}(\mathbf{q}_h \wedge \mathbf{n}|_{\varrho_k}) = Q_h^{\delta_k}(\mathbf{q}_h \wedge \mathbf{n}|_{\delta_k})\ ,\ 1 \leq k \leq M\}\ . \tag{5.3}$$

Then the mortar finite element approximation of (3.11) is given by:
Find $\mathbf{u}_h \in \tilde{\mathbf{V}}_h$ such that

$$a_h(\mathbf{u}_h, \mathbf{q}_h) = l(\mathbf{q}_h) \quad \forall \mathbf{q}_h \in \tilde{\mathbf{V}}_h\ . \tag{5.4}$$

Note that the solution of (5.4) is identical to the first component of the solution of (4.28). Since $\tilde{\mathbf{V}}_h$ is not contained in $\mathbf{H}(\mathbf{curl};\Omega)$, the basis for the error estimate is given by the well-known lemma of Strang (cf., e.g., [Cia78]).

Lemma 5.2 (Strang's Lemma)
Let $\mathbf{u}$ and $\mathbf{u}_h$ be the solutions of the equations (3.11) *and* (5.4)*, respectively. Then the discretization error is given by*

$$\begin{aligned}\|\mathbf{u} - \mathbf{u}_h\|_{a_h} &\leq C\left(\inf_{\mathbf{v}_h \in \tilde{\mathbf{V}}_h} \|\mathbf{u} - \mathbf{v}_h\|_{a_h} + \sup_{\mathbf{q}_h \in \tilde{\mathbf{V}}_h \setminus \{0\}} \frac{|a_h(\mathbf{u}, \mathbf{q}_h) - l(\mathbf{q}_h)|}{\|\mathbf{q}_h\|_{a_h}}\right) \\ &:= C(E_a + E_c)\ ,\end{aligned}$$

where $\|\cdot\|_{a_h} = a_h(\cdot,\cdot)^{\frac{1}{2}}$ denotes the energy norm.

Lemma 5.2 shows that the error consists of two terms. The first term E_a, usually referred to as the approximation error, describes how well a function $\mathbf{u}$ can be approximated by the finite element space $\tilde{\mathbf{V}}_h$. The second term E_c, the consistency error, is due to the fact that our finite element space is not contained in $\mathbf{H}(\mathbf{curl};\Omega)$. In the following we will first deal with the consistency error.

5.2 Consistency Error

According to Lemma 5.2, the consistency error is defined by the difference of volume integrals. However, from the previous analysis we would expect that the consistency error should be given by interface integrals. Although this sounds like a contradiction, this is not the case.
If $\mathbf{u} \in \mathbf{H}^1(\mathbf{curl}; \Omega)$ and $\chi \in C^1(\bar{\Omega})$, applying Stokes' theorem yields

$$\sum_{i=1}^{N} \left(\int_{\Omega_i} \mathbf{curl}(\chi\, \mathbf{curl}\, \mathbf{u}) \cdot \mathbf{q}_h \, dV - \int_{\Omega_i} \chi\, \mathbf{curl}\, \mathbf{u} \cdot \mathbf{curl}\, \mathbf{q}_h \, dV \right) = \tag{5.5}$$

$$= \sum_{i=1}^{N} (\mathbf{n} \wedge (\chi\, \mathbf{curl}\, \mathbf{u} \wedge \mathbf{n}), \mathbf{q}_h \wedge \mathbf{n})_{0,\partial\Omega_i} = \sum_{k=1}^{M} (\mathbf{n} \wedge (\chi\, \mathbf{curl}\, \mathbf{u} \wedge \mathbf{n}), [\mathbf{q}_h \wedge \mathbf{n}]|_{\gamma_k})_{0,\gamma_k} \ .$$

Note that in this case

$$\int_{\Omega_i} \mathbf{curl}(\chi\, \mathbf{curl}\, \mathbf{u}) \cdot \mathbf{q}_h \, dV = \int_{\Omega_i} \mathbf{f} \cdot \mathbf{q}_h \, dV \ .$$

Therefore, the consistency error can also be defined by

$$E_c = \sup_{\mathbf{q}_h \in \tilde{\mathbf{V}}_h \setminus \{0\}} \sum_{k=1}^{M} \frac{|(\mathbf{n} \wedge (\chi\, \mathbf{curl}\, \mathbf{u} \wedge \mathbf{n}), [\mathbf{q}_h \wedge \mathbf{n}]|_{\gamma_k})_{0,\gamma_k}|}{\|\mathbf{q}_h\|_{a_h}} \ .$$

From the above equality it is now clear that the consistency error arises at the interfaces. An estimate of the consistency error is given by the following theorem [XH05, Theorem 4.1].

Theorem 5.3 (Consistency error)
Assume $\mathbf{u} \in \mathbf{H}^1(\mathbf{curl}; \Omega)$. *Then the consistency error can be estimated as follows*

$$E_c \leq C \left(\sum_{j=1}^{N} h_j^2 \ \| \mathbf{curl}\, \mathbf{u}\|_{1,\Omega_j}^2 \right)^{\frac{1}{2}} \ .$$

Proof:
Considering the definition of $\tilde{\mathbf{V}}_h$, we obtain using Lemma 5.1 and the trace inequality for $\mathbf{H}^1(\Omega_{s(k)})$

$$\begin{aligned}
&|(\mathbf{n} \wedge (\chi\, \mathbf{curl}\, \mathbf{u} \wedge \mathbf{n}), [\mathbf{q}_h \wedge \mathbf{n}]|_{\gamma_k})_{0,\gamma_k}| \\
&\quad = |(\mathbf{n} \wedge (\chi\, \mathbf{curl}\, \mathbf{u} \wedge \mathbf{n}) - Q_h^{\delta_k}(\mathbf{n} \wedge (\chi\, \mathbf{curl}\, \mathbf{u} \wedge \mathbf{n})), [\mathbf{q}_h \wedge \mathbf{n}]|_{\gamma_k})_{0,\gamma_k}| \\
&\quad \leq \|\mathbf{n} \wedge (\chi\, \mathbf{curl}\, \mathbf{u} \wedge \mathbf{n}) - Q_h^{\delta_k}(\mathbf{n} \wedge (\chi\, \mathbf{curl}\, \mathbf{u} \wedge \mathbf{n}))\|_{0,\gamma_k} \|[\mathbf{q}_h \wedge \mathbf{n}]|_{\gamma_k}\|_{0,\gamma_k} \\
&\quad \leq C h_{\delta_k}^{\frac{1}{2}} \, |\mathbf{n} \wedge (\chi\, \mathbf{curl}\, \mathbf{u} \wedge \mathbf{n})|_{\frac{1}{2},\delta_k} \|[\mathbf{q}_h \wedge \mathbf{n}]|_{\gamma_k}\|_{0,\gamma_k} \\
&\quad \leq C h_{s(k)}^{\frac{1}{2}} \, \| \mathbf{curl}\, \mathbf{u}\|_{1,\Omega_{s(k)}} \|[\mathbf{q}_h \wedge \mathbf{n}]|_{\gamma_k}\|_{0,\gamma_k} \ .
\end{aligned}$$

On the other hand, Theorem 4.9 yields for $\mathbf{q}_h \in \tilde{\mathbf{V}}_h$

$$\|[\mathbf{q}_h \wedge \mathbf{n}]|_{\gamma_k}\|_{0,\gamma_k} \leq C h_{\delta_k}^{\frac{1}{2}} \left(\|\operatorname{\mathbf{curl}} \mathbf{q}_h\|_{0,\Omega_{s(k)}} + \|\operatorname{\mathbf{curl}} \mathbf{q}_h\|_{0,\Omega_{m(k)}} \right) . \tag{5.6}$$

Combining the preceding inequalities, we derive

$$\begin{aligned} |E_c| &\leq \big[\sum_{j=1}^{N} C h_j \|\operatorname{\mathbf{curl}} \mathbf{u}\|_{1,\Omega_j} (\|\operatorname{\mathbf{curl}} \mathbf{q}_h\|_{0,\Omega_i} + \|\operatorname{\mathbf{curl}} \mathbf{q}_h\|_{0,\Omega_j}) \big] / \|\mathbf{q}_h\|_{a_h} \\ &\leq C \ \big[\|\operatorname{\mathbf{curl}} \mathbf{q}_h\|_{0,\Omega} (\sum_{j=1}^{N} h_j^2 \|\operatorname{\mathbf{curl}} \mathbf{u}\|_{1,\Omega_j}^2)^{\frac{1}{2}} \big] / \|\mathbf{q}_h\|_{a_h} \\ &\leq C \ \big(\sum_{j=1}^{N} h_j^2 \ \|\operatorname{\mathbf{curl}} \mathbf{u}\|_{1,\Omega_j}^2 \big)^{\frac{1}{2}} . \end{aligned}$$

•

5.3 Approximation Error

The estimation of the approximation error E_a is more involving. The main difficulty is caused by the fact that we have to find the infimum of the space $\tilde{\mathbf{V}}_h$ and not the infimum of $\mathbf{V}_h$. This means that we cannot use standard approximation properties of the space $\mathbf{V}_h$, since we have to pay attention to the mortar constraint. To address this problem, we introduce a special projection operator $\pi_h^{\delta_k} : (L^2(\gamma_k))^2 \to \mathbf{RT}_{0,0}(\delta_k; \mathcal{T}_{\delta_k})$ which is defined according to

$$\int_{\delta_k} \pi_h^{\delta_k}(\mathbf{p}) \cdot \boldsymbol{\mu}_h \, dV = \int_{\delta_k} \mathbf{p} \cdot \boldsymbol{\mu}_h \, dV \quad \forall \, \boldsymbol{\mu}_h \in \mathbf{M}_h(\delta_k) . \tag{5.7}$$

The stability of $\pi_h^{\delta_k}$ is given by the following lemma [XH05, Corollary 4.7].

Lemma 5.4 (Stability of $\pi_h^{\delta_k}$)
Let $\pi_h^{\delta_k}$ be given by (5.7)*. Then there holds*

$$\|\pi_h^{\delta_k}(\mathbf{p})\|_{0,\delta_k} \ \leq \ C \ \|\mathbf{p}\|_{0,\gamma_k} \ , \ \mathbf{p} \in (L^2(\gamma_k))^2 .$$

Proof:
On basis of Lemma 4.5 we have

$$\begin{aligned} \|\pi_h^{\delta_k}(\mathbf{p})\|_{0,\delta_k} &\leq C \sup_{\mu_h \in \mathbf{M}_h(\delta_k)} \frac{(\pi_h^{\delta_k}(\mathbf{p}), \boldsymbol{\mu}_h)_{0,\delta_k}}{\|\boldsymbol{\mu}_h\|_{0,\delta_k}} = C \sup_{\boldsymbol{\mu}_h \in \mathbf{M}_h(\delta_k)} \frac{(\mathbf{p}, \boldsymbol{\mu}_h)_{0,\delta_k}}{\|\boldsymbol{\mu}_h\|_{0,\delta_k}} \\ &\leq C \ \|\mathbf{p}\|_{0,\gamma_k} . \end{aligned}$$

•

Based on Lemma 4.5 we can derive a further property of the projector $\pi_h^{\delta_k}$ (cf. [XH05, Lemma 4.8]).

Lemma 5.5
Let $\Pi_h : \mathbf{H}^1(\mathbf{curl};\Omega)\cap\mathbf{H}_0(\mathbf{curl};\Omega) \to \mathbf{V}_h$ be the standard interpolation operator. Then we have

$$\|\operatorname{div}_\tau \pi_h^{\delta_k}[\Pi_h\mathbf{u}\wedge\mathbf{n}]|_{\gamma_k}\|_{0,\gamma_k} \le C\|\operatorname{div}_\tau[\Pi_h\mathbf{u}\wedge\mathbf{n}]|_{\gamma_k}\|_{0,\gamma_k} \ .$$

Proof:
Let $P_h^{\delta_k}$ be the standard $\mathbf{RT}_0(\delta_k;\mathcal{T}_{\delta_k})$-interpolation operator, given in Section 4.3. Since $P_h^{\delta_k}|_T$, $T\in\mathcal{T}_{\delta_k}$, preserves constant tangential traces, we follow the steps of the proof of Lemma 4.4 and obtain

$$\begin{aligned}\|(I-P_h^{\delta_k})[\Pi_h\mathbf{u}\wedge\mathbf{n}]|_{\gamma_k}\|_{0,\gamma_k}^2 &\le Ch_{\delta_k}^2 \sum_{T\in\mathcal{T}_{\delta_k}} \sum_{T'\cap T\neq\emptyset,\ T'\in\mathcal{T}_{\varrho_k}} |[\Pi_h\mathbf{u}\wedge\mathbf{n}]_T|_{1,T'\cap T}^2\\ &= Ch_{\delta_k}^2 \sum_{T\in\mathcal{T}_{\delta_k}} \|\operatorname{div}_\tau[\Pi_h\mathbf{u}\wedge\mathbf{n}]_T\|_{0,T}^2\\ &= C\ h_{\delta_k}^2\ \|\operatorname{div}_\tau[\Pi_h\mathbf{u}\wedge\mathbf{n}]|_{\gamma_k}\|_{0,\gamma_k}^2 \ .\end{aligned}$$

Taking roots we get

$$\|(I-P_h^{\delta_k})[\Pi_h\mathbf{u}\wedge\mathbf{n}]|_{\gamma_k}\|_{0,\gamma_k} \le Ch_{\delta_k}\|\operatorname{div}_\tau[\Pi_h\mathbf{u}\wedge\mathbf{n}]|_{\gamma_k}\|_{0,\gamma_k} \ . \tag{5.8}$$

Observing that

$$\operatorname{div}_\tau P_h^{\delta_k}[\Pi_h\mathbf{u}\wedge\mathbf{n}]|_{\gamma_k} = W_h^{\delta_k}\operatorname{div}_\tau[\Pi_h\mathbf{u}\wedge\mathbf{n}]|_{\gamma_k} \ ,$$

where $W_h^{\delta_k}$ is the L^2-projection onto the elementwise constants, we have

$$\|\operatorname{div}_\tau P_h^{\delta_k}[\Pi_h\mathbf{u}\wedge\mathbf{n}]|_{\gamma_k}\|_{0,\gamma_k} \le C\|\operatorname{div}_\tau[\Pi_h\mathbf{u}\wedge\mathbf{n}]|_{\gamma_k}\|_{0,\gamma_k} \ . \tag{5.9}$$

Since $(\pi_h^{\delta_k}-P_h^{\delta_k})[\Pi_h\mathbf{u}\wedge\mathbf{n}]|_{\gamma_k} \in \mathbf{RT}_0(\delta_k;\mathcal{T}_{\delta_k})$ we obtain by applying Lemma 4.5 and (5.8)

$$\begin{aligned}\|(\pi_h^{\delta_k}-P_h^{\delta_k})[\Pi_h\mathbf{u}\wedge\mathbf{n}]|_{\gamma_k}\|_{0,\gamma_k} &\le C \sup_{\boldsymbol{\mu}\in\mathbf{M}_h(\delta_k)} \frac{((\pi_h^{\delta_k}-P_h^{\delta_k})[\Pi_h\mathbf{u}\wedge\mathbf{n}]|_{\gamma_k},\boldsymbol{\mu})}{\|\boldsymbol{\mu}\|_{0,\delta_k}}\\ &= C \sup_{\boldsymbol{\mu}\in\mathbf{M}_h(\delta_k)} \frac{((I-P_h^{\delta_k})[\Pi_h\mathbf{u}\wedge\mathbf{n}]|_{\gamma_k},\boldsymbol{\mu})}{\|\boldsymbol{\mu}\|_{0,\delta_k}}\\ &\le C\ h_{\delta_k}\ \|\operatorname{div}_\tau[\Pi_h\mathbf{u}\wedge\mathbf{n}]|_{\gamma_k}\|_{0,\gamma_k} \ .\end{aligned} \tag{5.10}$$

Combining (5.9) and (5.10), we get

$$\begin{aligned}&\|\operatorname{div}_\tau \pi_h^{\delta_k}[\Pi_h\mathbf{u}\wedge\mathbf{n}]|_{\gamma_k}\|_{0,\gamma_k} \le\\ &\quad\le \|\operatorname{div}_\tau(\pi_h^{\delta_k}-P_h^{\delta_k})[\Pi_h\mathbf{u}\wedge\mathbf{n}]|_{\gamma_k}\|_{0,\gamma_k} + \|\operatorname{div}_\tau P_h^{\delta_k}[\Pi_h\mathbf{u}\wedge\mathbf{n}]|_{\gamma_k}\|_{0,\gamma_k}\\ &\quad\le Ch_{\delta_k}^{-1}\|(\pi_h^{\delta_k}-P_h^{\delta_k})[\Pi_h\mathbf{u}\wedge\mathbf{n}]|_{\gamma_k}\|_{0,\gamma_k} + \|\operatorname{div}_\tau[\Pi_h\mathbf{u}\wedge\mathbf{n}]|_{\gamma_k}\|_{0,\gamma_k}\\ &\quad\le C\|\operatorname{div}_\tau[\Pi_h\mathbf{u}\wedge\mathbf{n}]|_{\gamma_k}\|_{0,\gamma_k} \ .\end{aligned}$$

•

Combining these auxiliary results, we can estimate the discretization error of the mortar edge element method (cf. [XH05, Theorem 4.2]).

Theorem 5.6 (Approximation error)
For any $\mathbf{u} \in \mathbf{H}^1(\mathbf{curl};\Omega)$ *there exists a function* $\mathbf{q}_h \in \tilde{\mathbf{V}}_h$ *such that*

$$\|\mathbf{u}-\mathbf{q}_h\|_{\mathbf{curl},h} \leq C\left(\sum_{j=1}^{N} h_j^2 \,\|\mathbf{u}\|^2_{1,\mathbf{curl},\Omega_j}\right)^{\frac{1}{2}} ,$$

where $\|\cdot\|_{\mathbf{curl},h} := (\sum_{j=1}^{N} \|\cdot\|^2_{\mathbf{curl},\Omega_j})^{\frac{1}{2}}$.

Proof:
Given $\mathbf{u} \in \mathbf{H}^1(\mathbf{curl};\Omega)$ we define $\mathbf{q}_h$ as follows

$$\mathbf{q}_h = \Pi_h\mathbf{u} - \sum_{k=1}^{M} E_h^{\delta_k}\left\{\pi_h^{\delta_k}[(\Pi_h^j\mathbf{u}\wedge\mathbf{n})|_{\delta_k} - (\Pi_h^i\mathbf{u}\wedge\mathbf{n})|_{\varrho_k}]\right\} .$$

From the definition of $\mathbf{q}_h$ it can easily be seen that $\mathbf{q}_h \in \tilde{\mathbf{V}}_h$. Applying Lemmas 4.7, 5.4, and 5.5, we get for each $\delta_k \in S$

$$\begin{aligned}
&\|E_h^{\delta_k}(\pi_h^{\delta_k}((\Pi_h^j\mathbf{u}\wedge\mathbf{n})|_{\delta_k} - (\Pi_h^i\mathbf{u}\wedge\mathbf{n})|_{\varrho_k}))\|_{\mathbf{curl},\Omega_j} \qquad (5.11)\\
&\quad\leq Ch_{\delta_k}^{\frac{1}{2}}\,\|\operatorname{div}_\tau\left(\pi_h^{\delta_k}((\Pi_h^j\mathbf{u}\wedge\mathbf{n})|_{\delta_k} - (\Pi_h^i\mathbf{u}\wedge\mathbf{n})|_{\varrho_k})\right)\|_{0,\gamma_k}\\
&\qquad + \;C\;h_{\delta_k}^{\frac{1}{2}}\,\|\pi_h^{\delta_k}\big((\Pi_h^j\mathbf{u}\wedge\mathbf{n})|_{\delta_k} - (\Pi_h^i\mathbf{u}\wedge\mathbf{n})|_{\varrho_k}\big)\|_{0,\gamma_k}\\
&\quad\leq\; C\;h_{\delta_k}^{\frac{1}{2}}\,\|\operatorname{div}_\tau\left((\Pi_h^j\mathbf{u}\wedge\mathbf{n})|_{\delta_k} - (\Pi_h^i\mathbf{u}\wedge\mathbf{n})|_{\varrho_k}\right)\|_{0,\gamma_k}\\
&\qquad + C\;h_{\delta_k}^{\frac{1}{2}}\,\|(\Pi_h^j\mathbf{u}\wedge\mathbf{n})|_{\delta_k} - (\Pi_h^i\mathbf{u}\wedge\mathbf{n})|_{\varrho_k}\|_{0,\gamma_k}\\
&\quad:=\; I_1 \;+\; I_2\;.
\end{aligned}$$

To estimate the first term I_1, we apply Lemma 4.1 and obtain

$$\begin{aligned}
I_1 &= Ch_{\delta_k}^{\frac{1}{2}}\|\operatorname{curl}_\tau((\mathbf{n}\wedge(\Pi_h^j\mathbf{u}\wedge\mathbf{n}))|_{\delta_k}) - \operatorname{curl}_\tau((\mathbf{n}\wedge(\Pi_h^i\mathbf{u}\wedge\mathbf{n}))|_{\varrho_k})\|_{0,\gamma_k} \qquad (5.12)\\
&\leq Ch_{\delta_k}^{\frac{1}{2}}(\|\operatorname{curl}_\tau\left((\mathbf{n}\wedge(\Pi_h^j\mathbf{u}\wedge\mathbf{n}))|_{\delta_k}\right) - (\mathbf{n}\wedge(\mathbf{u}\wedge\mathbf{n}))|_{\delta_k}\big)\|_{0,\gamma_k}\\
&\quad + \|\operatorname{curl}_\tau\left(\mathbf{n}\wedge(\Pi_h^i\mathbf{u}\wedge\mathbf{n}))|_{\varrho_k}\right) - (\mathbf{n}\wedge(\mathbf{u}\wedge\mathbf{n}))|_{\varrho_k}\big)\|_{0,\gamma_k})\\
&\leq Ch_{\delta_k}^{\frac{1}{2}}\big(\sum_{T\in\mathcal{T}(\delta_k)}(\|\mathbf{n}_T\cdot(\mathbf{curl}\,\Pi_h^j\mathbf{u} - \mathbf{curl}\,\mathbf{u})|_T\|^2_{0,T}\big)^{\frac{1}{2}}\\
&\quad + \big(\sum_{T\in\mathcal{T}(\varrho_k)}(\|\mathbf{n}_T\cdot(\mathbf{curl}\,\Pi_h^i\mathbf{u} - \mathbf{curl}\,\mathbf{u})|_T\|^2_{0,T})^{\frac{1}{2}}\big)\\
&\leq C\;h_{s(k)}^{\frac{1}{2}}\;\big(h_{s(k)}^{\frac{1}{2}}\|\,\mathbf{curl}\,\mathbf{u}\|_{1,\Omega_j} + h_{m(k)}^{\frac{1}{2}}\|\,\mathbf{curl}\,\mathbf{u}\|_{1,\Omega_i}\big)\;.
\end{aligned}$$

For the second term I_2 we obtain

$$\begin{aligned} I_2 &\leq C h_{\delta_k}^{\frac{1}{2}} \big(\|(\Pi_h^j \mathbf{u} \wedge \mathbf{n})|_{\delta_k} - (\mathbf{u} \wedge \mathbf{n})|_{\delta_k}\|_{0,\gamma_k} + \|(\Pi_h^i \mathbf{u} \wedge \mathbf{n})|_{\varrho_k} - (\mathbf{u} \wedge \mathbf{n})|_{\varrho_k}\|_{0,\gamma_k} \big) \\ &\leq C h_{s(k)}^{\frac{1}{2}} \big(h_{s(k)}^{\frac{1}{2}} \|\mathbf{u}\|_{1,\mathbf{curl},\Omega_j} + h_{m(k)}^{\frac{1}{2}} \|\mathbf{u}\|_{1,\mathbf{curl},\Omega_i} \big) \ . \end{aligned} \tag{5.13}$$

In view of the standard approximation property

$$\|\mathbf{u} - \Pi_h \mathbf{u}\|_{\mathbf{curl},h} \leq C \left(\sum_{j=1}^{N} h_j^2 \|\mathbf{u}\|_{1,\mathbf{curl},\Omega_j}^2 \right)^{\frac{1}{2}}$$

using (5.11), (5.12), and (5.13) results in

$$\begin{aligned} \|\mathbf{u} - \mathbf{q}_h\|_{\mathbf{curl},h}^2 \leq C \big(& \|\mathbf{u} - \Pi_h \mathbf{u}\|_{\mathbf{curl},h}^2 + \\ & + \sum_{k=1}^{M} \|E_h^{\delta_k}(\pi_h^{\delta_k}((\Pi_h^j \mathbf{u} \wedge \mathbf{n})|_{\delta_k} - (\Pi_h^i \mathbf{u} \wedge \mathbf{n})))\|_{\mathbf{curl},\Omega_j}^2 \big) \\ \leq \ & C \ \sum_{j=1}^{N} h_j^2 \ \|\mathbf{u}\|_{1,\mathbf{curl},\Omega_j}^2 \ . \end{aligned}$$

•

Combining the results of Theorems 5.3 and 5.6, we finally derive the estimate for the approximation error [XH05, Theorem 4.3].

Theorem 5.7 (Error of the solution $\mathbf{u}_h$)
Let $\mathbf{u} \in \mathbf{H}^1(\mathbf{curl};\Omega)$ and $\mathbf{u}_h \in \tilde{\mathbf{V}}_h$ be the solutions of the equations (3.11) *and* (5.4)*, respectively. Then the discretization error is bounded by*

$$\|\mathbf{u} - \mathbf{u}_h\|_{a_h} \leq C \left(\sum_{j=1}^{N} h_j^2 \|\mathbf{u}\|_{1,\mathbf{curl},\Omega_j}^2 \right)^{\frac{1}{2}} .$$

5.4 Error of the Lagrange Multiplier

In the previous section we proved the convergence of the discrete solution $\mathbf{u}_h$ of (5.4). However, since we are concerned with the discrete saddle point problem (4.28), we have to consider the discrete Lagrange multiplier $\boldsymbol{\lambda}_h$ as well. Since $\boldsymbol{\lambda}_h$ approximates the flux $\boldsymbol{\lambda}$, $\boldsymbol{\lambda}|_{\gamma_k} := \mathbf{n} \wedge (\chi \, \mathbf{curl}\, \mathbf{u} \wedge \mathbf{n})|_{\gamma_k}$, we have to require that $\boldsymbol{\lambda}_h$ converges to $\boldsymbol{\lambda}$ as h tends to zero. The proof of this convergence is given by the following theorem [XH05, Theorem 5.2].

Theorem 5.8 (Error of the Lagrange multiplier $\boldsymbol{\lambda}_h$)
Let $\mathbf{u} \in \mathbf{H}^1(\mathbf{curl};\Omega)$ and $(\mathbf{u}_h, \boldsymbol{\lambda}_h) \in \mathbf{V}_h \times \mathbf{M}_h(S)$ be the solutions of (3.11) and (4.28), respectively. Then the error, related to the Lagrange multiplier, is bounded by

$$\|\boldsymbol{\lambda} - \boldsymbol{\lambda}_h\|_{-\frac{1}{2},h,S} \leq C \left(\sum_{j=1}^{N} h_j^2 \|\mathbf{u}\|^2_{1,\mathbf{curl},\Omega_j} \right)^{\frac{1}{2}} .$$

Proof:
Applying similar arguments as in [BF91] for mixed finite element methods and [Woh99b] for the saddle point method for mortar element methods and observing the inf-sup condition developed in Lemma 4.8, we obtain

$$\|\boldsymbol{\lambda} - \boldsymbol{\lambda}_h\|_{-\frac{1}{2},h,S} \leq C(\|\mathbf{u} - \mathbf{u}_h\|_{a_h} + \inf_{\boldsymbol{\mu}_h \in \mathbf{M}_h} \|\boldsymbol{\lambda} - \boldsymbol{\mu}_h\|_{-\frac{1}{2},h,S}) .$$

In Theorem 5.7 we already showed that

$$\|\mathbf{u} - \mathbf{u}_h\|_{a_h} \leq C \left(\sum_{j=1}^{N]} h_j^2 \, \|\mathbf{u}\|^2_{1,\mathbf{curl},\Omega_j} \right)^{\frac{1}{2}} . \tag{5.14}$$

To obtain an upper bound for the second term, we apply Lemma 5.1 and get

$$\begin{aligned} \inf_{\mu_h \in \mathbf{M}_h(\delta_k)} \|\boldsymbol{\lambda} - \boldsymbol{\mu}_h\|_{-\frac{1}{2},h,\delta_k} &= h_{\delta_k}^{\frac{1}{2}} \inf_{\boldsymbol{\mu}_h \in \mathbf{M}_h(\delta_k)} \|\boldsymbol{\lambda} - \boldsymbol{\mu}_h\|_{0,\delta_k} \\ &\leq C h_j \, \|\mathbf{n} \wedge (\chi \ \mathbf{curl}\, \mathbf{u} \wedge \mathbf{n})\|_{\frac{1}{2},\delta_k} \\ &\leq C h_j \, \|\, \mathbf{curl}\, \mathbf{u}\|_{1,\Omega_j} . \end{aligned}$$

Summing over all δ_k gives

$$\inf_{\mu_h \in \mathbf{M}_h} \|\boldsymbol{\lambda} - \boldsymbol{\mu}_h\|_{-\frac{1}{2},h,S} \leq C \left(\sum_{j=1}^{N} h_j^2 \, \|\, \mathbf{curl}\, \mathbf{u}\|^2_{1,\Omega_j} \right)^{\frac{1}{2}} . \tag{5.15}$$

Finally, combining the estimates of (5.14) and (5.15) yields the assertion.

•

Chapter 6

Residual-type A Posteriori Error Estimator

In the last chapter we showed that the solution of mortar finite element approximation $\mathbf{u}_h$ converges to the solution $\mathbf{u}$ of our model problem as the mesh size h tends to zero. Although this result is quite encouraging, since it states that for decreasing h we get better approximations of $\mathbf{u}$, it is not helpful, since we have to decrease the mesh size globally. However, every refinement of the mesh is connected with an increase of the number of unknowns and thus results in a higher computational cost. From this point of view it is clear that we want to avoid global refinement, if possible, but want to use local refinement to keep the computational cost as small as possible. Therefore, an important part of any successful computational method is the development of efficient and reliable a posteriori error estimators and adaptive refinement strategies.

In the context of standard conforming methods the concepts of error estimation are based on the pioneering work due to Babuska and Rheinboldt [BR78a, BR78b], which has been further developed by others [AO00, BW85, EJ88, ZZ87]. For further references we refer to [Ver96]. In the context of error estimators for $P1$ mortar finite element methods we mention [Woh99a, Woh99b, Woh99c]. Residual based a posteriori error estimators for eddy current equations were introduced in [BHHW00, BDH$^+$99] and extended in [Sch]. Error estimators for time harmonic Maxwell's equations have been considered in [Mon98, Mon03]. For hierarchical error estimators we refer to [BHW00]. However, as far as mortar finite element approximations based on Nédélec curl-conforming elements are concerned not that much work has been done yet.

In this section, we will introduce a residual-type a posteriori error estimator η for the mortar edge element approximation of the eddy current problem with respect to the broken energy norm $\|\mathbf{v}\|_{a_h}^2 := a_h(\mathbf{v}, \mathbf{v})$. In order to develop the error estimator, we will combine elements of [BHHW00] and [Woh99c] and prove its efficiency and reliability under certain assumptions.

The key ingredient for the construction of the error estimator is a direct splitting of the function space $\mathbf{V}$ according to

$$\mathbf{V} = \mathbf{V}^0 \oplus \mathbf{V}^\perp \ , \tag{6.1}$$

where $\mathbf{V}^0$ stand for the subspace of subdomainwise irrotational vector fields with vanishing tangential trace on the skeleton, i.e.

$$\mathbf{V}^0 := \{\mathbf{q} \in \mathbf{V} \mid \mathbf{curl}\, \mathbf{q}|_{\Omega_i} = 0 \ , \ \gamma_t(\mathbf{q})|_S = 0 \ , \ 1 \leq i \leq N\} \ , \tag{6.2}$$

and $\mathbf{V}^\perp$ refers to its orthogonal complement

$$\mathbf{V}^\perp := \{\mathbf{q} \in \mathbf{V} \mid (\beta \mathbf{q}|_{\Omega_i}, \mathbf{q}^0|_{\Omega_i})_{0,\Omega_i} = 0 \ , \ 1 \leq i \leq N \quad \forall \mathbf{q}^0 \in \mathbf{V}^0\} \ . \tag{6.3}$$

Note that for $\mathbf{q} \in \mathbf{V}^0$ there exists on each subdomain a function $\varphi \in H_0^1(\Omega_i)$ such that $\mathbf{q}|_{\Omega_i} = \mathbf{grad}\, \varphi$. Evidently, the decomposition (6.1) is also orthogonal with respect to the scalar product induced by the bilinear form $a_h(\cdot, \cdot)$. Unfortunately, mere existence of such a decomposition is not enough for the construction of the error estimator. The reliability and the efficiency of the error estimator hinge on the following assumption (cf. [BHHW00, Mon03] for similar assumptions).

Assumption 1
Let $\mathbf{u}$ *and* $\mathbf{u}_h$ *be the solutions of equations* (3.11) *and* (5.4)*, respectively. We assume that for the error* $\mathbf{e_u} := \mathbf{u} - \mathbf{u}_h \in \mathbf{V}$ *a splitting* $\mathbf{e_u} = \mathbf{e_u^0} + \mathbf{e_u^\perp}$, $\mathbf{e_u^0} \in \mathbf{V}^0$, $\mathbf{e_u^\perp} \in \mathbf{V}^\perp$*, can be found such that* $\mathbf{e_u^\perp}|_{\Omega_i} \in \mathbf{H}^1(\Omega_i) \cap \mathbf{H}_{\Gamma_i}(\mathbf{curl}, \Omega_i)$ *and*

$$|\mathbf{e_q^\perp}|_{1,\Omega_i} \leq C(\Omega_i) \| \mathbf{curl}\, \mathbf{e_u^\perp}\|_{0,\Omega_i} \quad \forall\, \mathbf{q} \in \mathbf{V}^\perp \ .$$

We have to make this assumption, since in the derivation of the error estimator we have to approximate $\mathbf{e_u}$ by a discrete function $\mathbf{e}_{\mathbf{u},h}$. Since $\mathbf{e_u}$ is not regular enough, we cannot use the standard interpolation operator for edge elements but have to rely on quasi-interpolation operators. As mentioned in [Mon03], there is currently no such operator that is defined on the whole space $\mathbf{V}$. However, for $\mathbf{V}^0$ there are several quasi-interpolation operators that give good approximations of $\mathbf{e_u^0}$, while for $\mathbf{e_u^\perp}$ we need this assumption at the moment to define a good interpolant for $\mathbf{e_u^\perp}$. If better quasi-interpolation operators were available, we might be able to get rid of this assumption.

Moreover, defining the weighted norm $\| \cdot \|_L$ on the skeleton given by

$$\|\mathbf{v}\|_L := \left(\sum_{k=1}^{M} \sum_{F \in \mathcal{F}_h(\delta_k)} \frac{h_F}{\chi_T} \|\mathbf{v}\|_{0,F}^2 \right)^{1/2} \ ,$$

which is an equivalent norm to $\| \cdot \|_{-\frac{1}{2},h,S}$, we make the following saturation assumption:

Assumption 2
Let $\mathbf{u} \in \prod_{i=1}^{N} \mathbf{H}^1(\mathbf{curl}, \Omega_i)$ *and let the jump of* $\mathbf{n} \wedge (\mathbf{curl}\, \mathbf{u} \wedge \mathbf{n})$ *vanish on the skeleton. Then we assume*

$$\inf_{\boldsymbol{\mu}_h \in \mathbf{M}_h} \|\boldsymbol{\lambda} - \boldsymbol{\mu}_h\|_L \leq C_h \|\mathbf{e}_\mathbf{u}\|_{a_h} \ , \ C_h > 0 \ , \tag{6.4}$$

with $C_h < C_0 < \infty$ *for* $h \to 0$ *and* $\boldsymbol{\lambda}|_{\gamma_k} := \mathbf{n}_k \wedge (\mathbf{curl}\, \mathbf{u} \wedge \mathbf{n}_k)$, $1 \leq k \leq M$.

In the last section we showed that $\|\mathbf{e}_\mathbf{u}\|_{a_h}$ and $\inf_{\mu_h \in \mathbf{M}_h} \|\lambda - \mu_h\|_{-\frac{1}{2},h,S}$ are of order $\mathcal{O}(h)$. If we assume that $\mathbf{u}$ has higher regularity than in the previous chapter, say $\mathbf{u} \in \prod_{i=1}^{N} \mathbf{H}^2(\mathbf{curl}, \Omega_i)$, we have that $\inf_{\mu_h \in \mathbf{M}_h} \|\lambda - \mu_h\|_L$ is at least of order $\mathcal{O}(h^{3/2})$, which to some extend justifies Assumption 2. We refer to [Woh99c, WY05] for similar assumptions.

A consequence of Assumption 2 is that $\|\boldsymbol{\lambda} - \boldsymbol{\lambda}_h\|_L \leq C \|\mathbf{e}_u\|_{a_h}$. Moreover, we assume that χ and β are piecewise constant functions and that the triangulation is fine enough to resolve the jumps of the coefficients, i.e. we assume that the jump occurs at the faces of the elements.

From a physical or mathematical point of view, the contributions of the error estimator are straightforward. If the coefficients are continuous and no surface charges or currents are present, we expect both the normal component of the electric field and the tangential component of the magnetic field to be continuous. Globally, we cannot expect the discrete solution $\mathbf{u}_h$ to fulfill the strong formulation of our problem. However, locally on each element T the discrete solution is smooth and thus we expect it to fulfill the strong formulation. From this point of view, it is easy to understand that the error estimate involves element and face residuals and is given by

$$\begin{aligned} \eta^2 := \sum_{i=1}^{N} \Big[\sum_{T \in \mathcal{T}_i} \sum_{\nu=1}^{2} (\eta_T^{(\nu)})^2 + \sum_{F \in \mathcal{F}_h^{int}(\Omega_i)} \Big((\eta_F^{(1)})^2 + (\eta_F^{(2)})^2 \Big) \Big] + \\ + \sum_{k=1}^{M} \Big[\sum_{F \in \mathcal{F}_h(\delta_k)} \Big((\eta_F^{(3)})^2 + (\eta_F^{(4)})^2 \Big) + \sum_{F \in \mathcal{F}_h(\varrho_k)} (\eta_F^{(5)})^2 \Big] \ , \end{aligned} \tag{6.5}$$

where the element residuals $\eta_T^{(\nu)}$, $1 \leq \nu \leq 2$, are given by

$$\eta_T^{(1)} := \min\{\frac{h_T}{\sqrt{\chi_T}}, \frac{1}{\sqrt{\beta_T}_T}\} \|\mathbf{f}_h - \mathbf{curl}(\chi_T\, \mathbf{curl}\, \mathbf{u}_h) - \beta_T\ \mathbf{u}_h\|_{0,T} \ , \tag{6.6}$$

$$\eta_T^{(2)} := \frac{h_T}{\sqrt{\beta_T}} \| \operatorname{div}(\beta_T\, \mathbf{u}_h)\|_{0,T} \ . \tag{6.7}$$

Here $\mathbf{f}_h$ is the integral mean of $\mathbf{f}$ on $T \in \mathcal{T}_i$, $1 \leq i \leq N$, and χ_T and β_T denote the restrictions of χ and σ to the element T, respectively. The face residuals $\eta_F^{(\nu)}$, $1 \leq \nu \leq 5$, are given by

$$\eta_F^{(1)} := \sqrt{\frac{h_F}{\chi_a}} \|[\mathbf{n} \wedge (\chi_T \, \mathbf{curl}\, \mathbf{u}_h \wedge \mathbf{n})]|_F\|_{0,F} \ , \ F \in \mathcal{F}_h^{int}(\Omega_i) \ , \tag{6.8}$$

$$\eta_F^{(2)} := \sqrt{\frac{h_F}{\beta_a}} \|[\mathbf{n} \cdot (\beta_T \mathbf{u}_h)]|_F\|_{0,F} \ , \ F \in \mathcal{F}_h^{int}(\Omega_i) \ , \tag{6.9}$$

$$\eta_F^{(3)} := \sqrt{\frac{h_F}{\chi_T}} \|\boldsymbol{\lambda}_h - \{\mathbf{n} \wedge (\chi_T \, \mathbf{curl}\, \mathbf{u}_h \wedge \mathbf{n})\}\|_{0,F} \ , \ F \in \mathcal{F}_h(\delta_k) \ , \tag{6.10}$$

$$\eta_F^{(4)} := \sqrt{\frac{\chi_T}{h_F}} \|[\mathbf{u}_h \wedge \mathbf{n}]|_F\|_{0,F} \ , \ F \in \mathcal{F}_h(\delta_k) \ , \tag{6.11}$$

$$\eta_F^{(5)} := \sqrt{\frac{h_F}{\chi_T}} \|\boldsymbol{\lambda}_h - \{\mathbf{n} \wedge (\chi_T \, \mathbf{curl}\, \mathbf{u}_h \wedge \mathbf{n})\}\|_{0,F} \ , \ F \in \mathcal{F}_h(\varrho_k) \ , \tag{6.12}$$

where $\chi_a := 0.5 \cdot (\chi_{T_{in}} + \chi_{T_{out}})$, $\beta_a := 0.5 \cdot (\beta_{T_{in}} + \beta_{T_{out}})$, and T_{out}, $T_{in} \in \mathcal{T}_h$ are two adjacent elements of the face F. Furthermore, the error estimation involves the data oscillations

$$\mathrm{osc}_1^2 := \sum_{i=1}^{N} \sum_{T \in \mathcal{T}_i} \mathrm{osc}_T^2 \quad , \quad osc_T := \frac{h_T}{\sqrt{\chi_T}} \, \|\mathbf{f} - \mathbf{f}_h\|_{0,T} \ . \tag{6.13}$$

The data oscillations osc_T, $T \in \mathcal{T}_i$, $1 \leq i \leq N$, are of higher order if the right hand side $\mathbf{f}$ is sufficiently smooth. After these preliminaries we are able to state the following a posteriori estimate for the error $\mathbf{e_u}$ measured in the broken energy norm.

Theorem 6.1 (Efficiency and reliability of the error estimator)
There exist positive constants Γ_ν and γ_ν, $1 \leq \nu \leq 2$, depending only on the shape regularity of the triangulations $\mathcal{T}_i$, $1 \leq i \leq N$, such that

$$\gamma_1 \eta^2 - \gamma_2 osc^2 \leq \|\mathbf{e_u}\|_{a_h}^2 \leq \Gamma_1 \eta^2 + \Gamma_2 \ osc^2 \ . \tag{6.14}$$

The proof of this theorem will be done in two steps. First we will prove the second inequality in (6.14), which shows that the error estimator is reliable. Afterwards we show that the error estimator is efficient, i.e. the first inequality is valid.

6.1 Reliability of the Error Estimator

Without loss of generality, we assume in the following that $\frac{h_T}{\sqrt{\chi_T}} = \min\{\frac{h_T}{\sqrt{\chi_T}}, \frac{1}{\sqrt{\beta_T}}\}$. According to Assumption 2, it can easily be seen that the error $\mathbf{e_u}$ satisfies the continuous variational problem

$$a_h(\mathbf{e_u}, \mathbf{v}) = r(\mathbf{v}) \ , \ \mathbf{v} \in \mathbf{V} \ , \tag{6.15}$$

where the residual $r(\cdot)$ is given by $r(\mathbf{v}) := (f, \mathbf{v})_{0,\Omega} - b_h(\mathbf{v}, \lambda) - a_h(\mathbf{u}_h, \mathbf{v})$. Following [Woh99c] and using the decomposition $\mathbf{e_u} = \mathbf{e_u^0} + \mathbf{e_u^\perp}$, we have

$$a_h(\mathbf{e_u}, \mathbf{e_u}) = a_h(\mathbf{e_u}, \mathbf{e_u^0}) + a_h(\mathbf{e_u}, \mathbf{e_u^\perp}) \tag{6.16}$$

with

$$a_h(\mathbf{e_u^0}, \mathbf{e_u^0}) = a_h(\mathbf{e_u}, \mathbf{e_u^0}) = (f, \mathbf{e_u^0})_{0,\Omega} - a_h(\mathbf{u}_h^0, \mathbf{e_u^0}) =: r_1(\mathbf{e_u^0}) \ , \tag{6.17}$$

$$a_h(\mathbf{e_u^\perp}, \mathbf{e_u^\perp}) = a_h(\mathbf{e_u}, \mathbf{e_u^\perp}) = (f, \mathbf{e_u^\perp})_{0,\Omega} - b_h(\mathbf{e_u^\perp}, \lambda) - a_h(\mathbf{u}_h, \mathbf{e_u^\perp}) =: r_2(\mathbf{e_u^\perp}) \ . \tag{6.18}$$

We will first consider $r_1(\mathbf{e_u^0})$. Recalling that $\mathbf{e_u^0} = \mathbf{grad}\,\varphi$, $\varphi \in V$, and using the Galerkin orthogonality $r_1(\mathbf{grad}\,\psi_h) = 0$, $\psi_h \in V_h$, we obtain by integration by parts

$$\begin{aligned} r_1(\mathbf{e_u^0}) &= r_1(\mathbf{grad}(\varphi - \psi_h)) = \qquad (6.19)\\ &= \sum_{i=1}^{N} \Big(\sum_{T\in\mathcal{T}_i} \int_T \operatorname{div}(\beta_T \mathbf{u}_h) \cdot (\varphi - \psi_h)\, dV + \sum_{F\in\mathcal{F}_h^{int}(\Omega_i)} \int_F [\beta_T \mathbf{u}_h]|_F (\varphi - \psi_h)\, d\sigma \Big) \\ &\le \sum_{i=1}^{N} \Big(\sum_{T\in\mathcal{T}_i} \Big| \int_T \operatorname{div}(\beta_T \mathbf{u}_h) \cdot (\varphi - \psi_h)\, dV \Big| + \sum_{F\in\mathcal{F}_h^{int}(\Omega_i)} \Big| \int_F [\beta_T \mathbf{u}_h]|_F (\varphi - \psi_h)\, d\sigma \Big| \Big) \ . \end{aligned}$$

Equation (6.19) shows that an upper bound for $r_1(\mathbf{e_u^0})$ strongly depends on the choice of ψ_h. For the construction of ψ_h we use the Scott-Zhang interpolation operator

$$P_{S,h}^{(i)} : H_0^1(\Omega_i) \to S_{1,0}(\Omega_i; \mathcal{T}_i) \ , \tag{6.20}$$

which has the following properties (cf. [SZ90]):

Lemma 6.2 (Properties of the Scott-Zhang interpolation operator) *For $T \in \mathcal{T}_i$ and $F \in \mathcal{F}_h(\Omega_i)$ let $\tilde{D}_T$ and $\tilde{D}_E$ be given by*

$$\begin{aligned} \tilde{D}_T &:= \bigcup \{T' \in \mathcal{T}_i \mid \mathcal{N}_h(T') \cap \mathcal{N}_h(T) \neq \emptyset\} \ , \\ \tilde{D}_F &:= \bigcup \{T' \in \mathcal{T}_i \mid \mathcal{N}_h(T') \cap \mathcal{N}_h(F) \neq \emptyset\} \ , \end{aligned}$$

where $\mathcal{N}_h(T)$ and $\mathcal{N}_h(F)$ denote the set of nodes of T and F, respectively. Then there exists a constant $C > 0$ only depending on the shape regularity of $\mathcal{T}_i$, such that for $v \in H_0^1(\Omega_i)$ the operator $P_{S,h}^{(i)}$ satisfies

$$\begin{aligned} \|P_{S,h}^{(i)} v\|_{0,T} &\le C \|v\|_{0,\tilde{D}_T} \ , \\ \|\,\mathbf{grad}\; P_{S,h}^{(i)} v\|_{0,T} &\le C \|\,\mathbf{grad}\, v\|_{0,\tilde{D}_T} \ , \\ \|v - P_{S,h}^{(i)} v\|_{0,T} &\le C h_T \|\,\mathbf{grad}\, v\|_{0,\tilde{D}_T} \ , \\ \|v - P_{S,h}^{(i)} v\|_{0,F} &\le C h_F^{1/2} \ \|\,\mathbf{grad}\, v\|_{0,\tilde{D}_F} \ . \end{aligned}$$

Setting $\psi_h|_{\Omega_i} = P^{(i)}_{S,h}\varphi|_{\Omega_i}$ we obtain for the integrals in (6.19)

$$|\int_T \operatorname{div}(\beta_T \mathbf{u}_h)\,(\varphi-\psi_h)\,dV| \le C\frac{h_T}{\sqrt{\beta_T}}\|\operatorname{div}(\beta_T\mathbf{u}_h)\|_{0,T}\,\|\sqrt{\beta_T}\,\mathbf{grad}\,\varphi\|_{0,\tilde{D}_T}\ ,$$
$$|\int_F [\mathbf{n}\cdot\beta_T\mathbf{u}_h]|_F\,(\varphi-\psi_h)\,d\sigma| \le C\sqrt{\frac{h_F}{\beta_a}}\|[\mathbf{n}\cdot\beta_T\mathbf{u}_h]\|_{0,F}\|\sqrt{\beta_T}\,\mathbf{grad}\,\varphi\|_{0,\tilde{D}_F}\ .$$

Summing over all elements and faces and observing that $\|\mathbf{e}^0_{\mathbf{u}}\|_{a_h} = \|\sqrt{\sigma}\,\mathbf{grad}\,\varphi\|_{0,\Omega}$, we have

$$\|\mathbf{e}^0_{\mathbf{u}}\|_{a_h} \le C\left(\sum_{i=1}^N\Big(\sum_{T\in\mathcal{T}_i}(\eta_T^{(2)})^2 + \sum_{F\in\mathcal{F}_h^{int}(\Omega_i)}(\eta_F^{(2)})^2\Big)\right)^{1/2}\ . \tag{6.21}$$

Proving an upper bound for $r_2(\mathbf{e}^\perp_{\mathbf{u}})$ is more involving and hinges on Assumptions 1 and 2. Since $\mathbf{V}_h$ is not a subspace of $\mathbf{V}$, we cannot use the Galerkin orthogonality in this case, but have

$$a_h(\mathbf{u}_h,\mathbf{v}_h) + b_h(\mathbf{v}_h,\boldsymbol{\lambda}_h) = (\mathbf{f},\mathbf{v}_h)_{0,\Omega} \quad \forall \mathbf{v}_h\in\mathbf{V}_h\ , \tag{6.22}$$

and therefore

$$\begin{aligned} a_h(\mathbf{e}^\perp_{\mathbf{u}},\mathbf{e}^\perp_{\mathbf{u}}) &= r_2(\mathbf{e}^\perp_{\mathbf{u}}) + b_h(\mathbf{v}_h,\boldsymbol{\lambda}_h) - a_h(\mathbf{e}_{\mathbf{u}},\mathbf{v}_h) - (\mathbf{f},\mathbf{v}_h)_{0,\Omega} \qquad (6.23)\\ &= \sum_{i=1}^N\sum_{T\in\mathcal{T}_i}\Big[\int_T(\mathbf{f}-\mathbf{f}_h)\,\mathbf{z}\,dV + \int_T(\mathbf{f}_h - \mathbf{curl}(\chi_T\,\mathbf{curl}\,\mathbf{u}_h) - \beta_T\mathbf{u}_h)\,\mathbf{z}\,dV\Big]\\ &\quad + \sum_{i=1}^N\sum_{F\in\mathcal{F}_h^{int}(\Omega_i)}\int_F[\mathbf{n}\wedge(\chi_T\,\mathbf{curl}\,\mathbf{u}_h\wedge\mathbf{n})]|_F\,\mathbf{z}\wedge\mathbf{n}\,d\sigma\\ &\quad - \sum_{k=1}^M\sum_{F\in\mathcal{F}_h(\delta_k)}\int_F(\boldsymbol{\lambda}_h - \{\mathbf{n}\wedge(\chi_T\,\mathbf{curl}\,\mathbf{u}_h\wedge\mathbf{n})\})\,\mathbf{z}\wedge\mathbf{n}\,d\sigma\\ &\quad - \sum_{k=1}^M\sum_{F\in\mathcal{F}_h(\varrho_k)}\int_F(\boldsymbol{\lambda}_h - \{\mathbf{n}\wedge(\chi_T\,\mathbf{curl}\,\mathbf{u}_h\wedge\mathbf{n})\})\,\mathbf{z}\wedge\mathbf{n}\,d\sigma\\ &\quad + b_h(\mathbf{e}^\perp_{\mathbf{u}},\boldsymbol{\lambda}_h-\boldsymbol{\lambda})\ , \end{aligned}$$

where $\mathbf{z} := \mathbf{e}^\perp_{\mathbf{u}} - \mathbf{v}_h$. From equation (6.23) it is clear that upper bounds for $\|\mathbf{e}^\perp_{\mathbf{u}}\|_{a_h}$ crucially depend on the choice of $\mathbf{q}_h$. As mentioned before, standard interpolation as defined in Chapter 4 cannot be used, since degrees of freedom located on edges cannot be extended to continuous functionals on $\mathbf{H}^1(\Omega_i)$.

To circumvent this problem, one has to resort to quasi-interpolation operators or averaging operators to determine $\mathbf{q}_h$. However, for functions in $\mathbf{H}(\mathbf{curl};\Omega)$ a good quasi-interpolation operator (like the Clément interpolator in the case of $H^1(\Omega)$)

defined on the whole space $\mathbf{H}(\mathbf{curl};\Omega)$ is currently not available. In [Sch01, Sch] a quasi-interpolation operator for Lipschitz domains was introduced that can be viewed as an analogue of the Clément interpolator. However, its properties make it difficult to apply it in (6.23). Based on Assumption 1 we use the vector-valued quasi-interpolation operator

$$\mathbf{P}^{(i)}_{\mathbf{Nd},\mathbf{h}} : \mathbf{H^1}(\Omega_i) \cap \mathbf{H}_{0,\Gamma_i}(\mathbf{curl};\Omega_i) \to \mathbf{Nd}_{1,\Gamma_i}(\Omega_i;\mathcal{T}_i) \ , \tag{6.24}$$

that was introduced in [BHHW00]. The stability and approximation properties of $\mathbf{P}^{(i)}_{\mathbf{Nd},\mathbf{h}}$ are given by the following lemma [BHHW00, Lemma 5.1].

Lemma 6.3 (Stability and approximation properties of $\mathbf{P}^{(i)}_{\mathbf{Nd},\mathbf{h}}$)
For $T \in \mathcal{T}_i$, $F \in \mathcal{F}_h(\Omega_i)$, and $E \in \mathcal{E}_h(\Omega_i)$ let D_T, D_F, and D_E be given by

$$\begin{aligned} D_E &:= \bigcup \{T \in \mathcal{T}_i \mid E \in \mathcal{E}_h(T)\} \ , \\ D_F &:= \bigcup \{D_E \mid E \in \mathcal{E}_h(F)\} \ , \\ D_T &:= \bigcup \{D_E \mid E \in \mathcal{E}_h(T)\} \ . \end{aligned}$$

Then there exists a constant $C > 0$, only depending on the shape regularity of $\mathcal{T}_i$, such that for $\mathbf{q} \in \mathbf{H}^1(\Omega_i)$ the operator $\mathbf{P}^{(i)}_{\mathbf{Nd},\mathbf{h}}$ satisfies

$$\begin{aligned} \|\mathbf{P}^{(i)}_{\mathbf{Nd},\mathbf{h}}\mathbf{q}\|_{0,T} &\le C\,\|\mathbf{q}\|_{1,D_T} \ , \\ \|\,\mathbf{curl}\,\mathbf{P}^{(i)}_{\mathbf{Nd},\mathbf{h}}\mathbf{q}\|_{0,T} &\le C\,|\mathbf{q}|_{1,D_F} \ , \\ \|\mathbf{q} - \mathbf{P}^{(i)}_{\mathbf{Nd},\mathbf{h}}\mathbf{q}\|_{0,T} &\le C\,h_T|\mathbf{q}|_{1,D_T} \ , \\ \|\mathbf{q} \ - \ \mathbf{P}^{(i)}_{\mathbf{Nd},\mathbf{h}}\mathbf{q}\|_{0,F} &\le C\,h_F^{1/2}|\mathbf{q}|_{1,D_F} \ . \end{aligned}$$

Choosing $\mathbf{v}_h|_{\Omega_i} = \mathbf{P}^{(i)}_{\mathbf{Nd},\mathbf{h}}\mathbf{e}^{\perp}_{\mathbf{u}}|_{\Omega_i}$ we get the following estimates for the volume integrals on the right hand side of (6.23)

$$|\int_T (\mathbf{f} - \mathbf{f}_h)\,\mathbf{z}\,d\sigma| \le C\frac{h_T}{\sqrt{\chi_T}}\,\|(\mathbf{f} - \mathbf{f}_h)\|_{0,T}\ \|\sqrt{\chi_T}\,\mathbf{e}^{\perp}_{\mathbf{u}}\|_{1,D_T} \ , \tag{6.25}$$

$$\begin{aligned} |\int_T (\mathbf{f}_h - \mathbf{curl}(\chi_T\,\mathbf{curl}\,\mathbf{u}_h) - \beta_T\mathbf{u}_h)\,\mathbf{z}\,d\sigma| \le \\ \le C\frac{h_T}{\sqrt{\chi_T}}\|\mathbf{f}_h - \mathbf{curl}(\chi_T\,\mathbf{curl}\,\mathbf{u}_h) - \beta_T\mathbf{u}_h\|_{0,T}\ \|\sqrt{\chi_T}\,\mathbf{e}^{\perp}_{\mathbf{u}}\|_{1,D_T} \ . \end{aligned} \tag{6.26}$$

For the face integrals on the right hand side in (6.23) we obtain

$$|\int_F [\mathbf{n}\wedge(\chi_T\,\mathbf{curl}\,\mathbf{u}_h\wedge\mathbf{n})]|_F\,\mathbf{z}\wedge\mathbf{n}\,d\sigma| \leq \tag{6.27}$$
$$\leq C\sqrt{\frac{h_F}{\chi_a}}\|[\mathbf{n}\wedge(\chi_T\,\mathbf{curl}\,\mathbf{u}_h\wedge\mathbf{n})]|_F\|_{0,F}\|\sqrt{\chi_T}\,\mathbf{e}_{\mathbf{u}}^{\perp}\|_{1,D_F}\ ,$$
$$|\int_F \{\boldsymbol{\lambda}_h-\{\mathbf{n}\wedge(\chi_T\,\mathbf{curl}\,\mathbf{u}_h\wedge\mathbf{n})\}\,\mathbf{z}\wedge\mathbf{n}\,d\sigma| \leq \tag{6.28}$$
$$\leq C\sqrt{\frac{h_F}{\chi_T}}\|\boldsymbol{\lambda}_h-\mathbf{n}\wedge(\chi_T\,\mathbf{curl}\,\mathbf{u}_h\wedge\mathbf{n})\|_{0,F}\|\sqrt{\chi_T}\,\mathbf{e}_{\mathbf{u}}^{\perp}\|_{1,D_F}\ .$$

Using Assumption 2, we obtain for the last term on the right hand side in (6.23)

$$\begin{aligned} b_h(\mathbf{e}_{\mathbf{u}}^{\perp},\boldsymbol{\lambda}_h-\boldsymbol{\lambda}) &\leq \sum_{k=1}^{M}\sum_{F\in\mathcal{F}_h(\delta_k)}\|\boldsymbol{\lambda}_h-\boldsymbol{\lambda}\|_{0,F}\,\|[\mathbf{e}_{\mathbf{u}}^{\perp}\wedge\mathbf{n}]|_F\|_{0,F}\\ &= \sum_{k=1}^{M}\sum_{F\in\mathcal{F}_h(\delta_k)}\sqrt{\frac{h_F}{\chi_T}}\|\boldsymbol{\lambda}_h-\boldsymbol{\lambda}\|_{0,F}\,\sqrt{\frac{\chi_T}{h_F}}\|[\mathbf{e}_{\mathbf{u}}^{\perp}\wedge\mathbf{n}]|_F\|_{0,F}\\ &\leq \|\boldsymbol{\lambda}_h-\boldsymbol{\lambda}\|_L\,\|[\mathbf{e}_{\mathbf{u}}^{\perp}\wedge\mathbf{n}]|_S\|_{L^{-1}} \leq C\|\mathbf{e}_{\mathbf{u}}\|_{a_h}\|[\mathbf{e}_{\mathbf{u}}^{\perp}\wedge\mathbf{n}]|_S\|_{L^{-1}}\ , \end{aligned}$$

where $\|[\mathbf{e}_{\mathbf{u}}^{\perp}\wedge\mathbf{n}]|_S\|_{L^{-1}}^2 := \sum_{k=1}^{M}\sum_{F\in\mathcal{F}_h(\delta_k)}\frac{\chi_T}{h_F}\|[\mathbf{e}_{\mathbf{u}}^{\perp}\wedge\mathbf{n}]|_F\|_{0,F}^2$. Using Assumption 1 to switch from $\mathbf{H}^1$-norms back to the relevant energy norm and summing over all elements gives

$$\|\mathbf{e}_{\mathbf{u}}^{\perp}\|_{a_h}^2 \leq C\left(\sum_{i=1}^{N}\Big(\sum_{T\in\mathcal{T}_i}((\eta_T^{(1)})^2+osc_T^2)+\sum_{F\in\mathcal{F}_h^{int}(\Omega_i)}(\eta_F^{(1)})^2\Big)+\right. \tag{6.29}$$
$$\left.+\sum_{k=1}^{M}\Big(\sum_{F\in\mathcal{F}_h(\delta_k)}\Big((\eta_F^{(3)})^2+(\eta_F^{(4)})^2\Big)+\sum_{F\in\mathcal{F}_h(\varrho_k)}(\eta_F^{(5)})^2\Big)+\right)^{1/2}\|\mathbf{e}_{\mathbf{u}}\|_{a_h}\ .$$

Finally, combining (6.21) and (6.29) gives the assertion of the second inequality in Theorem 6.1.

6.2 Local Efficiency of the Error Estimator

To establish the lower bound for η, as given by (6.5), we use local bubble functions. For $T\in\mathcal{T}_i$, $1\leq i\leq N$, and $F\in\mathcal{F}_h(\Omega_i)$ we define element bubble functions

κ_T and face bubble functions κ_F according to

$$\kappa_T := \prod_{\nu=1}^{4} \lambda_\nu^{(T)} \quad , \quad \kappa_F := \prod_{\nu=1}^{3} \lambda_\nu^{(F)} \ ,$$

where $\lambda_\nu^{(T)}, 1 \le \nu \le 4$, and $\lambda_\nu^{(F)}$, $1 \le \nu \le 3$, are the barycentric coordinates associated with the vertices $p_\nu^{(T)}$, $1 \le \nu \le 4$, of T and $p_\nu^{(F)}$, $1 \le \nu \le 3$, of F. For $p_h \in P_k(T)$, $k \in \mathbb{N}_0$, and $q_h \in P_k(F)$, $k \in \mathbb{N}_0$, the following norm equivalences hold

$$\|\kappa_T^{1/2} p_h\|_{0,T} \le \|p_h\|_{0,T} \le C \|\kappa_T^{1/2} p_h\|_{0,T} \ , \tag{6.30}$$

$$\|\kappa_F^{1/2} q_h\|_{0,F} \le \|q_h\|_{0,F} \le C \|\kappa_F^{1/2} q_h\|_{0,F} \ . \tag{6.31}$$

Moreover, we will frequently use the following inverse inequalities for polynomials

$$\|\operatorname{\mathbf{grad}} p_h\|_{0,T} \le h_T^{-1} \|p_h\|_{0,T} \ , \ p_h \in P_k(T) \ , \ k \in \mathbb{N}_0 \ , \tag{6.32}$$

$$\|\operatorname{\mathbf{curl}} \mathbf{p}_h\|_{0,T} \le h_T^{-1} \|\mathbf{p}_h\|_{0,T} \ , \ \mathbf{p}_h \in \mathbf{P}_k(T) \ , \ k \in \mathbb{N}_0 \ , \tag{6.33}$$

$$\|\operatorname{div}_\Gamma \mathbf{q}_h\|_{0,F} \le h_F^{-1} \|\mathbf{q}_h\|_{0,F} \ , \ \mathbf{q}_h \in \mathbf{P}_k(F) \ , \ k \in \mathbb{N}_0 \ . \tag{6.34}$$

To prove the first inequality in Theorem 6.1, we will consider the local contributions of η separately. We start by proving an upper bound for the volume residuals.

Lemma 6.4 (Upper bound for the volume residuals)
Let $T \in \mathcal{T}_i$, $1 \le i \le N$. Then upper bounds for $\eta_T^{(1)}$ and $\eta_T^{(2)}$ are given by

$$\eta_T^{(1)} \le C \left(\|\mathbf{e_u}\|_{a_h,T} + osc_T \right) \ , \tag{6.35}$$

$$\eta_T^{(2)} \le C \, \|\mathbf{e_u}\|_{a_h,T} \ . \tag{6.36}$$

Proof:

We start with the proof of (6.35) and set $\mathbf{g}_h := \mathbf{f}_h - \mathbf{curl}(\chi_T \operatorname{\mathbf{curl}} \mathbf{u}_h) - \beta_T \mathbf{u}_h$. Applying the norm equivalence (6.30), we get

$$\frac{\chi_T}{h_T^2} \, (\eta_T^{(1)})^2 = \|\mathbf{f}_h - \mathbf{curl}(\chi_T \operatorname{\mathbf{curl}} \mathbf{u}_h) - \beta_T \mathbf{u}_h\|_{0,T}^2 \le \tag{6.37}$$

$$\le C \int_T (\mathbf{f}_h - \mathbf{curl}(\chi_T \operatorname{\mathbf{curl}} \mathbf{u}_h) - \beta_T \mathbf{u}_h) \cdot (\kappa_T \mathbf{g}_h) \, dV =$$

$$= C \Big[\int_T (\mathbf{f}_h - \mathbf{f}) \cdot (\kappa_T \mathbf{g}_h) \, dV + \int_T (\mathbf{f} - \mathbf{curl}(\chi_T \operatorname{\mathbf{curl}} \mathbf{u}_h) - \beta_T \mathbf{u}_h) \cdot (\kappa_T \mathbf{g}_h) \, dV \Big] \ .$$

Taking into account that $(\kappa_T \mathbf{g}_h)|_{\partial T} = 0$, we obtain using Stokes' theorem

$$\int_T \mathbf{curl}(\chi_T \operatorname{\mathbf{curl}} \mathbf{u}_h) \cdot (\kappa_T \mathbf{g}_h) \, dV = \int_T \chi_T \operatorname{\mathbf{curl}} \mathbf{u}_h \cdot \mathbf{curl}(\kappa_T \mathbf{g}_h) \, dV \ .$$

On the other hand, the solution $\mathbf{u}$ satisfies

$$\int_T \mathbf{f} \cdot (\kappa_T \mathbf{g}_h)\, dV = \int_T \Big[\chi_T\, \mathbf{curl}\, \mathbf{u} \cdot \mathbf{curl}(\kappa_T \mathbf{g}_h) + \beta_T \mathbf{u} \cdot (\kappa_T \mathbf{g}_h)\Big]\, dV\ . \tag{6.38}$$

Moreover, using the inverse inequality (6.33), we have

$$\begin{aligned} \|\mathbf{g}_h\|^2_{a_h,T} &= \chi \|\, \mathbf{curl}\, \mathbf{g}_h\|^2_{0,T} + \beta_T \|\mathbf{g}_h\|^2_{0,T} \\ &\le C \left(\frac{\chi}{h_T^2} \|\mathbf{g}_h\|^2_{0,T} + \beta_T \|\mathbf{g}_h\|^2_{0,T} \right) \le C \frac{1}{h_T^2} \|\sqrt{\chi}\mathbf{g}_h\|^2_{0,T}\ . \end{aligned} \tag{6.39}$$

Combining equations (6.30),(6.38), and (6.39) yields

$$\begin{aligned} \|\mathbf{g}_h\|^2_{0,T} = \|\mathbf{f}_h - \mathbf{curl}(\chi_T\, \mathbf{curl}\, \mathbf{u}_h) - \beta_T \mathbf{u}_h\|^2_{0,T} \le\ & C \Big[\int_T (\mathbf{f}_h - \mathbf{f}) \cdot (\kappa_T \mathbf{g}_h)\, dV + \\ & + \int_T \left(\chi_T\, \mathbf{curl}\, \mathbf{e_u} \cdot \mathbf{curl}(\kappa_T\ \mathbf{g}_h) + \beta_T \mathbf{e_u} \cdot (\kappa_T\ \mathbf{g}_h)\right)\, dV \Big] \\ \le C \left(\|\frac{1}{\sqrt{\chi_T}}\ (\mathbf{f} - \mathbf{f}_h)\|_{0,T}\, \|\sqrt{\chi_T}\mathbf{g}_h\|_{0,T} + \|\mathbf{e_u}\|_{a_h,T}\, \|\mathbf{g}_h\|_{a_h,T} \right) \\ \le C \left(\|\frac{1}{\sqrt{\chi_T}}\ (\mathbf{f} - \mathbf{f}_h)\|_{0,T} + \frac{1}{h_T}\, \|\mathbf{e_u}\|_{a_h,T} \right) \|\sqrt{\chi_T}\mathbf{g}_h\|_{0,T}\ . \end{aligned}$$

Finally, observing equation (6.37), the volume residual $\eta_T^{(1)}$ is bounded from above by

$$\eta_T^{(1)} \le C\, (\|\mathbf{e_u}\|_{a_h,T} + \mathrm{osc}_T)\ .$$

Likewise, in order to verify (6.36), we set $g_h := \mathrm{div}(\beta_T \mathbf{u}_h)$. Green's formula together with (6.30) yields

$$\begin{aligned} \frac{\beta_T}{h_T^2}\ (\eta_T^{(2)})^2 = \|\, \mathrm{div}\, \beta_T \mathbf{u}_h\|^2_{0,T} \le \\ \le C \int_T \mathrm{div}(\beta_T \mathbf{u}_h)(\kappa_T g_h)\, dV = -\, C \int_T \beta_T \mathbf{u}_h \cdot \mathbf{grad}(\kappa_T g_h)\, dV\ . \end{aligned} \tag{6.40}$$

Recalling that $\mathrm{div}\, \mathbf{f} = 0$, we obtain for the solution $\mathbf{u}$

$$\int_T \beta_T \mathbf{u} \cdot \mathbf{grad}(\kappa_T g_h)\, dV = \int_T \mathbf{f} \cdot \mathbf{grad}(\kappa_T g_h)\, dV = -\int_T \mathrm{div}\, \mathbf{f} \cdot \kappa_T g_h\, dV = 0\ .$$

Combining the equations above, we get

$$\begin{aligned} \|\, \mathrm{div}\, \beta_T \mathbf{u}_h\|^2_{0,T} \le C \int_T \beta_T \mathbf{e_u} \cdot \mathbf{grad}(\kappa_T g_h)\, dV \le \\ \le C \|\sqrt{\beta_T}\mathbf{e_u}\|_{0,T} \|\sqrt{\beta_T}\, \mathbf{grad}(\kappa_T g_h)\|_{0,T} \le C h_T^{-1} \|\sqrt{\beta_T} g_h\|_{0,T} \|\sqrt{\beta_T}\mathbf{e_u}\|_{0,T}\ . \end{aligned} \tag{6.41}$$

Inserting (6.41) into (6.40) gives

$$\eta_T^{(2)} \leq C\|\mathbf{e_u}\|_{a_h,T} \ ,$$

which proves (6.36).

•

In the second step we prove an upper bound for the face residuals in the interior of Ω_i.

Lemma 6.5 (Upper bound for the face residuals $\eta_F^{(1)}$ and $\eta_F^{(2)}$)
For $F \in \mathcal{F}_h^{int}(\Omega_i)$, $1 \leq i \leq N$, such that $F = \bar{T}_1 \cap \bar{T}_2$ for some $T_\nu \in \mathcal{T}_i$, $1 \leq \nu \leq 2$, let $\eta_F^{(1)}$ and $\eta_F^{(5)}$ be given by (6.8) and (6.9), respectively. Then the face residuals $\eta_F^{(1)}$ and $\eta_F^{(5)}$ are bounded from above by

$$\eta_F^{(1)} \leq C \sum_{\nu=1}^{2} \left(\|\mathbf{e_u}\|_{a_h,T_\nu} + \eta_{T_\nu}^{(1)} + osc_{T_\nu} \right) , \tag{6.42}$$

$$\eta_F^{(2)} \leq C \sum_{\nu=1}^{2} \left(\|\mathbf{e_u}\|_{a_h,T_\nu} + \eta_{T_\nu}^{(2)} \right) . \tag{6.43}$$

Proof:
In order to prove (6.42), we set $\mathbf{g}_h := [\mathbf{n} \wedge \chi_T \, \mathbf{curl}\, \mathbf{u}_h]|_F$ and define a continuous piecewise polynomial function $\tilde{\mathbf{g}}_h$ on $T_1 \cup T_2$ such that

$$\tilde{\mathbf{g}}_h \wedge \mathbf{n}|_F = \mathbf{g}_h \quad \text{and} \quad \|\tilde{\mathbf{g}}_h\|_{0,T_\nu} \leq C h_{T_\nu}^{1/2} \|\mathbf{g}_h\|_{0,F} \quad , \quad 1 \leq \nu \leq 2 \ .$$

Using (6.31), we obtain

$$\begin{aligned} \frac{\chi_a}{h_F}(\eta_F^{(1)})^2 = \|[\mathbf{n} \wedge (\chi_T \, \mathbf{curl}\, \mathbf{u}_h \wedge \mathbf{n})]|_F\|_{0,F}^2 \leq \\ \leq C \int_F [\mathbf{n} \wedge (\chi_T \ \ \mathbf{curl} \ \ \mathbf{u}_h \wedge \mathbf{n})]|_F \cdot (\kappa_F \tilde{\mathbf{g}}_h \wedge \mathbf{n}) \, d\sigma \ . \end{aligned} \tag{6.44}$$

Applying Stokes' theorem, we can rewrite the term on the right hand side of (6.44) according to

$$\begin{aligned} &\int_F [\mathbf{n} \wedge (\chi_T \, \mathbf{curl}\, \mathbf{u}_h \wedge \mathbf{n})]|_F \cdot (\kappa_F \tilde{\mathbf{g}}_h \wedge \mathbf{n}) \, d\sigma = \\ &= \sum_{\nu=1}^{2} \int_{T_\nu} \chi_T \, \mathbf{curl}\, \mathbf{u}_h \cdot \mathbf{curl}(\kappa_F \tilde{\mathbf{g}}_h) \, dV - \sum_{\nu=1}^{2} \int_{T_\nu} \mathbf{curl}(\chi_T \, \mathbf{curl}\, \mathbf{u}_h) \cdot (\kappa_F \tilde{\mathbf{g}}_h) \, dV \ . \end{aligned}$$

Observing that $\mathbf{u}$ satisfies

$$\sum_{\nu=1}^{2}\int\limits_{T_\nu}\left[\chi_T\,\mathbf{curl}\,\mathbf{u}\cdot\mathbf{curl}(\kappa_F\tilde{\mathbf{g}}_h)+\beta_T\mathbf{u}\cdot(\kappa_F\tilde{\mathbf{g}}_h)\right]dV=\sum_{\nu=1}^{2}\int\limits_{T_\nu}\mathbf{f}\cdot(\kappa_F\tilde{\mathbf{g}}_h)\,dV$$

and that $\kappa_F\tilde{\mathbf{g}}_h$ is bounded by $\|\kappa_F\tilde{\mathbf{g}}_h\|_{a_h,T_\nu}\le C\frac{1}{h_T}\,\|\sqrt{\chi}\kappa_F\tilde{\mathbf{g}}_h\|_{0,T}$, we get

$$\begin{aligned}\|[\mathbf{n}\wedge(\chi_T\ \ \mathbf{curl}\ \ \mathbf{u}_h\wedge\mathbf{n})]|_F\|_{0,F}^2\le C\Big[&\sum_{\nu=1}^{2}\int\limits_{T_\nu}(\mathbf{f}-\mathbf{f}_h)\cdot(\kappa_F\tilde{\mathbf{g}}_h)\,dV+\\&+\int\limits_{T_\nu}(\mathbf{f}_h-\mathbf{curl}(\chi_T\,\mathbf{curl}\,\mathbf{u}_h)-\beta_T\mathbf{u}_h)\cdot(\kappa_F\tilde{\mathbf{g}}_h)\,dV-\\&-\int\limits_{T_\nu}\big(\chi_T\,\mathbf{curl}\,\mathbf{e}_\mathbf{u}\cdot\mathbf{curl}(\kappa_F\tilde{\mathbf{g}}_h)+\beta_T\mathbf{e}_\mathbf{u}\cdot(\kappa_F\tilde{\mathbf{g}}_h)\big)\,dV\Big]\le\\\le C\|\sqrt{\chi_a}\mathbf{g}_h\|_{0,F}\sum_{\nu=1}^{2}\Big[&\sqrt{\frac{h_{T_\nu}}{\chi_T}}\big(\|\mathbf{f}-\mathbf{f}_h\|_{0,T_\nu}+\\&+\|\mathbf{f}_h-\mathbf{curl}(\chi_T\,\mathbf{curl}\,\mathbf{u}_h)-\beta_T\mathbf{u}_h\|_{0,T_\nu}\big)+h_{T_\nu}^{-1/2}\ \|\mathbf{e}_\mathbf{u}\|_{a_h,T_\nu}\Big]\ .\end{aligned}$$

Finally, in view of the shape regularity of the triangulations $\mathcal{T}_i$, $1\le i\le N$, we arrive at

$$\eta_F^{(1)}\le C\sum_{\nu=1}^{2}(\|\mathbf{e}_\mathbf{u}\|_{a_h,T_\nu}+\eta_{T_\nu}^{(1)}+\mathrm{osc}_{T_\nu})\ ,$$

which proves (6.42).

For the proof of (6.43) we follow along the same lines. We set $g_h:=[\mathbf{n}\cdot\beta_T\ \mathbf{u}_h]|_F$ and extend it continuously to a polynomial function $\tilde{g}_h$ on $T_1\cup T_2$ such that

$$\|\tilde{g}_h\|_{0,T_\nu}\le Ch_{T_\nu}^{1/2}\|g_h\|_{0,F}\ ,\ 1\le\nu\le 2\ . \tag{6.45}$$

Applying Green's theorem and (6.31) to the face residual $\eta_F^{(2)}$ yields

$$\begin{aligned}\frac{\beta_a}{h_F}(\eta_F^{(2)})^2=\|[\mathbf{n}\cdot\beta_T\ \mathbf{u}_h]|_F\|_{0,F}^2&\le C\int\limits_F[\mathbf{n}\cdot\beta_T\,\mathbf{u}_h]|_F\,\kappa_F g_h\,d\sigma=\\&=C\sum_{\nu=1}^{2}\int\limits_{T_\nu}\Big(\,\mathrm{div}(\beta_T\mathbf{u}_h)(\kappa_F g_h)+\beta_T\mathbf{u}_h\cdot\mathbf{grad}(\kappa_F g_h)\Big)\,dV\ .\end{aligned}$$

Since $\mathrm{div}\,\mathbf{f}=0$ the solution $\mathbf{u}$ satisfies

$$\sum_{\nu=1}^{2}\int\limits_{T_\nu}\beta_T\mathbf{u}\cdot\mathbf{grad}(\kappa_F g_h)\,dV=0\ .$$

If we observe (6.31), (6.32), and (6.45), we end up with

$$\|[\mathbf{n}\cdot\beta_T\ \mathbf{u}_h]\|_{0,F}^2 \le C\sum_{\nu=1}^{2}\int_{T_\nu}\Big(\operatorname{div}(\beta_T\mathbf{u}_h)(\kappa_F g_h)-\beta_T\mathbf{e_u}\cdot\mathbf{grad}(\kappa_F g_h)\Big)\,dV \le$$

$$\le C\|\sqrt{\beta_a}g_h\|_{0,F}\sum_{\nu=1}^{2}\Big(h_{T_\nu}^{1/2}\|\operatorname{div}\sqrt{\beta_T}\mathbf{u}_h\|_{0,T_\nu}+h_{T_\nu}^{-1/2}\|\sqrt{\beta_T}\mathbf{e_u}\|_{0,T_\nu}\Big)\ ,$$

which gives

$$\eta_F^{(5)} \le C\ \sum_{\nu=1}^{2}\Big(\|\mathbf{e_u}\|_{a_h,T_\nu}+\eta_{T_\nu}^{(2)}\Big)\ .$$

•

An upper bound for $\eta_F^{(4)}$ is given by the following lemma.

Lemma 6.6 (Upper bound for $\eta_F^{(4)}$)
For $F\in\mathcal{F}_h(\delta_k)$, $1\le k\le M$, let the face residual $\eta_F^{(4)}$ be given by (6.11). *Then the sum of these face residuals is bounded from above by*

$$\sum_{k=1}^{M}\sum_{F\in\mathcal{F}_h(\delta_k)}\frac{\chi_T}{h_F}\|[\mathbf{u}_h\wedge\mathbf{n}]|_F\|_{0,F}^2 \le C\,\|\mathbf{e_u}\|_{a_h}^2\ . \tag{6.46}$$

Proof:
Let $Q_h^{\delta_k}:(L^2(\gamma_k))^2\to\mathbf{M}_h(\delta_k)$ be the L^2-projection operator of Lemma 5.1. Then there exists a constant $C_\Gamma>0$ such that

$$\sum_{T\in\gamma_k}\frac{1}{h_F}\|\mathbf{q}-Q_h^{\delta_k}\mathbf{q}\|_{0,\gamma_k}^2 \le C_\Gamma\,|\mathbf{q}|_{\frac12,\gamma_k}^2\ ,\ \forall\mathbf{q}\in(H^{\frac12}(\gamma_k))^2\ . \tag{6.47}$$

Moreover, since both $[Q_h^{\delta_k}(\mathbf{u}_h\wedge\mathbf{n})]|_F=0$ and $[Q_h^{\delta_k}(\mathbf{u}\wedge\mathbf{n})]|_F=0$, we get by means of (6.47) and Assumption 1

$$\begin{aligned}
&\sum_{k=1}^{M}\sum_{F\in\gamma_k}\frac{\chi_F}{h_F}\|[\mathbf{u}_h\wedge\mathbf{n}]|_F\|_{0,F}^2 =\\
&\quad=\sum_{k=1}^{M}\sum_{T\in\gamma_k}\frac{\chi_F}{h_F}\|[(\mathbf{u}\wedge\mathbf{n}-\mathbf{u}_h\wedge\mathbf{n})-Q_h^{\delta_k}(\mathbf{u}\wedge\mathbf{n}-\mathbf{u}_h\wedge\mathbf{n})]|_F\|_{0,F}^2\\
&\quad\le\sum_{k=1}^{M}\Big(\chi_{\Omega_{s(k)}}|(\mathbf{u}|_{\Omega_{s(k)}}-\mathbf{u}_h|_{\Omega_{s(m)}})\wedge\mathbf{n}|_{\frac12,\gamma_k}+\\
&\qquad+\chi_{\Omega_{m(k)}}|(\mathbf{u}|_{\Omega_{m(k)}}-\mathbf{u}_h|_{\Omega_{m(k)}})\wedge\mathbf{n}|_{\frac12,\gamma_k}\Big)\le\hat{C}_\Gamma\|\mathbf{e_u}\|_{a_h}^2\ ,
\end{aligned}$$

where χ_{Ω_i} is the maximum of χ restricted to Ω_i and the constant $\hat{C}_\Gamma$ depends on the variation of χ on the subdomains.

•

In order to finish the proof of Theorem 6.1, we have to deal with the face residuals $\eta_F^{(3)}$ and $\eta_F^{(5)}$. An upper bound for $\eta_F^{(3)}$ can be established quite easily and is given by the following lemma.

Lemma 6.7 (Upper bound for $\eta_F^{(3)}$)
Assume $F \in \mathcal{F}_h(\delta_k)$ such that $F = \bar{T} \cap \delta_k$ for some $T \in \mathcal{T}_{s(k)}$ and let $\eta_F^{(3)}$ be given by (6.10)*. Then the face residual $\eta_F^{(3)}$ satisfies*

$$\eta_F^{(3)} \leq C(\|\mathbf{e_u}\|_{a_h,T} + \eta_T^{(1)} + \sqrt{\frac{h_F}{\chi_T}}\|\boldsymbol{\lambda} - \boldsymbol{\lambda}_h\|_{0,F} + osc_T) \ . \tag{6.48}$$

Proof:
For the proof of (6.48), we set $\mathbf{g}_h := \mathbf{n} \wedge (\chi_T \, \mathbf{curl}\, \mathbf{u}_h \wedge \mathbf{n}) - \boldsymbol{\lambda}_h$ and define a continuous piecewise polynomial function $\tilde{\mathbf{g}}_h$ on T such that

$$\|\tilde{\mathbf{g}}_h\|_{0,T} \leq C h_T^{1/2} \|\mathbf{g}_h\|_{0,F} \quad \text{and} \quad (\tilde{\mathbf{g}}_h \wedge \mathbf{n})|_F = \mathbf{g}_h \ . \tag{6.49}$$

Then we have

$$\begin{aligned} \frac{\chi_T}{h_F}(\eta_F^{(1)})^2 = \|\mathbf{n} \wedge (\chi_T \, \mathbf{curl}\, \mathbf{u}_h \wedge \mathbf{n}) - \boldsymbol{\lambda}_h\|_{0,F}^2 \leq \\ \leq C \int_F (\mathbf{n} \wedge (\chi_T \ \ \mathbf{curl} \ \ \mathbf{u}_h \wedge \mathbf{n}) - \boldsymbol{\lambda}_h) \cdot (\kappa_F \tilde{\mathbf{g}}_h \wedge \mathbf{n}) \, d\sigma \ . \end{aligned} \tag{6.50}$$

Applying Stokes' theorem gives

$$\begin{aligned} \int_F (\mathbf{n} \wedge (\chi_T \, \mathbf{curl}\, \mathbf{u}_h \wedge \mathbf{n})) \cdot (\kappa_F \tilde{\mathbf{g}}_h \wedge \mathbf{n}) \, d\sigma = \\ \int_T \chi_T \, \mathbf{curl}\, \mathbf{u}_h \cdot \mathbf{curl}(\kappa_F \tilde{\mathbf{g}}_h) \, dV - \int_T \mathbf{curl}\, \chi_T \, \mathbf{curl}\, \mathbf{u}_h \cdot (\kappa_F \tilde{\mathbf{g}}_h) \, dV \ . \end{aligned} \tag{6.51}$$

According to Assumption 2, the solution $\mathbf{u}$ satisfies

$$\begin{aligned} \int_T \mathbf{f} \cdot (\kappa_F \tilde{\mathbf{g}}_h) \, dV = \\ \int_T \left[\chi_T \, \mathbf{curl}\, \mathbf{u} \cdot \mathbf{curl}(\kappa_F \tilde{\mathbf{g}}_h) + \beta_T \mathbf{u} \cdot (\kappa_F \tilde{\mathbf{g}}_h)\right] dV - \int_F \boldsymbol{\lambda} \cdot (\kappa_F \tilde{\mathbf{g}}_h \wedge \mathbf{n}) \, d\sigma \ . \end{aligned} \tag{6.52}$$

Using (6.51), (6.52) in (6.50) and observing (6.33), (6.49), we get

$$\begin{aligned}
&\|\boldsymbol{\lambda}_h - \mathbf{n}\wedge(\chi_T\,\mathbf{curl}\,\mathbf{u}_h\wedge\mathbf{n})\|_{0,F}^2 \le \\
&\quad\le C\Big[\int_T (\mathbf{f}-\mathbf{f}_h)\cdot(\kappa_F\tilde{\mathbf{g}}_h)\,dV + \int_T \Big(\mathbf{f}_h - \mathbf{curl}(\chi_T\,\mathbf{curl}\,\mathbf{u}_h) - \beta_T\mathbf{u}_h\Big)\cdot(\kappa_F\tilde{\mathbf{g}}_h)\,dV \\
&\qquad - \int_T \Big(\chi_T\,\mathbf{curl}\,\mathbf{e_u}\cdot\mathbf{curl}(\kappa_F\tilde{\mathbf{g}}_h) + \beta_T\mathbf{e_u}\cdot(\kappa_F\tilde{\mathbf{g}}_h)\Big)\,dV + \\
&\qquad + \int_F (\boldsymbol{\lambda}-\boldsymbol{\lambda}_h)\cdot(\kappa_F\tilde{\mathbf{g}}_h\wedge\mathbf{n})\Big] \\
&\quad\le C\|\sqrt{\chi_T}\mathbf{g}_h\|_{0,F}\Big[\sqrt{\frac{h_T}{\chi_T}}\Big(\|\mathbf{f}-\mathbf{f}_h\|_{0,T} + \|\mathbf{f}_h - \mathbf{curl}(\chi_T\,\mathbf{curl}\,\mathbf{u}_h) - \beta_T\mathbf{u}_h\|_{0,T}\Big) \\
&\qquad + \frac{1}{\sqrt{\chi_T}}\|\boldsymbol{\lambda}-\boldsymbol{\lambda}_h\|_{0,F} + h_{T_\nu}^{-1/2}\,\|\mathbf{e_u}\|_{a_h,T}\Big]\,.
\end{aligned}$$

Finally, in view of the shape regularity of the triangulations $\mathcal{T}_i$, $1\le i\le N$, we arrive at

$$\eta_F^{(3)} \le C\Big(\|\mathbf{e_u}\|_{a_h,T} + \eta_T^{(1)} + \sqrt{\frac{h_F}{\chi_T}}\|\boldsymbol{\lambda}-\boldsymbol{\lambda}_h\|_{0,F} + osc_T\Big)\,,$$

which is (6.48).

•

In contrast to the previous lemma, the restriction of $(\boldsymbol{\lambda}_h - \mathbf{n}\wedge(\chi_T\ \mathbf{curl}\ \mathbf{u}_h\wedge\mathbf{n}))|_F$ to faces of the master interface is not a polynomial on F. Thus an upper bound for $\eta_F^{(5)}$ cannot be established as easily as for $\eta_F^{(3)}$.

Lemma 6.8 (Upper bound for $\eta_F^{(5)}$)
For $F\in\mathcal{F}_h(\varrho_k)$, $1\le k\le M$, let the face residuals $\eta_F^{(5)}$ be given by (6.12)*. Then an upper bound for the sum of these face residuals is given by*

$$\sum_{k=1}^{M}\sum_{F\in\mathcal{F}_h(\delta_k)}\frac{h_F}{\chi_T}\|\boldsymbol{\lambda}_h - \mathbf{n}\wedge(\chi_T\ \mathbf{curl}\,\mathbf{u}_h\wedge\mathbf{n})\|_{0,F}^2 \le C(\|\mathbf{e_u}\|_{a_h}^2 + osc^2)\,. \qquad (6.53)$$

Proof:
Let $\Pi_F : (L^2(F))^2 \to \mathbf{P}_0(F)$, $F\in\mathcal{F}_h(\varrho_k)$, be the weighted L^2-projection given by

$$\int_F \kappa_F\Pi_F(\mathbf{v})\,\mathbf{p}\,d\sigma = \int_F \kappa_F\mathbf{v}\,\mathbf{p}\,d\sigma \quad \forall\mathbf{p}\in\mathbf{P}_0(F)\,.$$

Then we have

$$\begin{aligned}
&\|\boldsymbol{\lambda}_h - \mathbf{n}\wedge(\chi_T\ \mathbf{curl}\,\mathbf{u}_h\wedge\mathbf{n})\|_{0,F} \le \\
&\qquad\le \|\Pi_F(\boldsymbol{\lambda}_h) - \mathbf{n}\wedge(\chi_T\ \mathbf{curl}\,\mathbf{u}_h\wedge\mathbf{n})\|_{0,F}^2 + \|\boldsymbol{\lambda}_h - \Pi_F(\boldsymbol{\lambda}_h)\|_{0,F}\,.
\end{aligned}$$

Using the same techniques as in the proof of Lemma 6.7, we get

$$\begin{aligned}
&\sqrt{\frac{h_F}{\chi_T}}\|\Pi_F(\boldsymbol{\lambda}_h) - \{\mathbf{n}\wedge(\chi_T\,\mathbf{curl}\,\mathbf{u}_h\wedge\mathbf{n})\}\|_{0,F} \leq \\
&\qquad \leq C\Big(\|\mathbf{e_u}\|_{a_h,T} + \eta_T^{(1)} + \sqrt{\frac{h_F}{\chi_T}}\|\boldsymbol{\lambda} - \Pi_F(\boldsymbol{\lambda}_h)\|_{0,F} + osc_T\Big) \\
&\qquad \leq C\Big(\|\mathbf{e_u}\|_{a_h,T} + \eta_T^{(1)} + \sqrt{\frac{h_F}{\chi_T}}\|\boldsymbol{\lambda} - \boldsymbol{\lambda}_h\|_{0,F} + \\
&\qquad\quad + \sqrt{\frac{h_F}{\chi_T}}\|\boldsymbol{\lambda}_h - \Pi_F(\boldsymbol{\lambda}_h)\|_{0,F} + osc_T\Big)\ ,
\end{aligned}$$

where $F \in \partial T$. To finish the proof, we have to estimate $\|\boldsymbol{\lambda}_h - \Pi_F(\boldsymbol{\lambda}_h)\|_{0,F}$. Since the projection Π_F preserves constant vectors, we surely have

$$\|\boldsymbol{\lambda}_h - \Pi_F(\boldsymbol{\lambda}_h)\|_{0,F} \leq Ch_F\|\operatorname{div}_\Gamma \boldsymbol{\lambda}_h\|_{0,F}\ .$$

Observing the shape regularity of the triangulations and that $\boldsymbol{\lambda}_h|_{\gamma_k} \in \mathbf{H}(\operatorname{div},\gamma_k)$, we get

$$\sum_{F\in\mathcal{F}_h(\varrho_k)} h_F\|\operatorname{div}_\Gamma \boldsymbol{\lambda}_h\|_{0,F} \leq C \sum_{F\in\mathcal{F}_h(\delta_k)} h_F\|\operatorname{div}_\Gamma \boldsymbol{\lambda}_h\|_{0,F}\ .$$

Moreover, using (6.34) gives

$$h_F\|\operatorname{div}_\Gamma \boldsymbol{\lambda}_h\|_{0,F} \leq \|\boldsymbol{\lambda}_h - \{\mathbf{n}\wedge(\chi_T\,\mathbf{curl}\,\mathbf{u}_h\wedge\mathbf{n})\}\|_{0,F}\ ,$$

for $F \in \mathcal{F}_h(\delta_k)$. Summing over all faces F and using the shape regularity of the triangulations together with the results of the previous lemmas, we obtain (6.53).

•

Finally, combining the results of Lemmas 6.4 - 6.8 proves the first inequality in (6.14).

Chapter 7

Multilevel Based Iterative Solution

In realistic three-dimensional problems the edge element discretization of the saddle point problem (4.28) can result in a high dimensional system of linear equations where the number of unknowns can range from 10^5 to 10^8. If we want to solve these equations, we cannot rely on direct solvers, but have to use iterative methods. However, in the setting of Maxwell's equations standard iterative solvers like the Jacobi or Gauss-Seidel method fail [AFW00, Hip98]. Especially, if $\beta \ll \chi$, the convergence rates can be worse than 0.9999, which indicates the poor behaviour of standard solvers for these problems.

The reason for this failure is the fact that the bilinear form $a(\cdot,\cdot)$ behaves in an utterly different way on the large kernel of the **curl**-operator and its orthogonal complement. Thus an essential feature of an efficient iterative solver will be the appropriate treatment of the nontrivial kernel of the discrete **curl**-operator. In [AFW00, Hip98] two different approaches have been proposed in order to come to terms with this problem. In [Ste03] the multigrid method described in [Hip98, Hip02a] has been successfully applied for time harmonic eddy current equations. Mortar edge element methods based on Nédélec's edge elements of the second family have been treated in [BBM02]. For the solution of the resulting linear equation the conjugate gradient method has been used with an additive multigrid as preconditioner. However, no special treatment of the kernel has been done. So far the author is not aware of any attempt to apply adaptive multigrid ideas to mortar edge element methods that take care of the kernel of the **curl**-operator in an appropriate way.

In order to address the problems arising for the construction of a good iterative solver for mortar edge element methods, we will first discuss this issue for an edge element discretization with respect to a shape regular and conforming simplicial triangulation $\mathcal{T}_h$ of the computational domain Ω before we extend the results to the mortar setting.

7.1 Iterative Solver for the Conforming Setting

In case of a single grid approximation, we have to compute $\mathbf{u}_h \in \mathbf{Nd}_{1,0}(\Omega;\mathcal{T}_h)$ such that

$$\int_\Omega \Big(\chi\,\mathbf{curl}\,\mathbf{u}_h\cdot\mathbf{curl}\,\mathbf{q}_h+\beta\mathbf{u}_h\cdot\mathbf{q}_h\Big)\,dV=\int_\Omega \mathbf{f}\cdot\mathbf{q}_h\,dV \quad \forall\mathbf{q}_h\in\mathbf{Nd}_{1,0}(\Omega;\mathcal{T}_h)\ . \tag{7.1}$$

Following standard procedures, we define a finite element basis of $\mathbf{Nd}_{1,0}(\Omega;\mathcal{T}_h)$, i.e. we assume $\mathbf{Nd}_{1,0}(\Omega;\mathcal{T}_h)=\mathrm{span}\{\mathbf{q}_E^{(\nu)}\mid 1\le\nu\le n_h\}$. Identifying the edge element function $\mathbf{u}_h\in\mathbf{Nd}_{1,0}(\Omega;\mathcal{T}_h)$ with a vector $\mathbf{u}_h\in\mathbb{R}^{n_h}$, the algebraic form of (7.1) can be written as

$$\Big(\mathbf{A}_h^\chi+\mathbf{A}_h^\beta\Big)\,\mathbf{u}_h=\mathbf{b}_h\ , \tag{7.2}$$

where $\mathbf{A}_h^\chi=(a_{\nu\mu,\chi})_{\nu,\mu=1}^{n_h}$, $\mathbf{A}_h^\beta=(a_{\nu\mu,\beta})_{\nu,\mu=1}^{n_h}$, and $\mathbf{b}_h=(b_1,...,b_{n_h})^T$ are given by

$$\begin{aligned}
a_{\nu\mu,\chi}&:=\int_\Omega \chi\,\mathbf{curl}\,\mathbf{q}_E^{(\nu)}\cdot\mathbf{curl}\,\mathbf{q}_E^{(\mu)}\,dV\ ,\ 1\le\nu,\mu\le n_h\ ,\\
a_{\nu\mu,\beta}&:=\int_\Omega \beta\,\mathbf{q}_E^{(\nu)}\cdot\mathbf{q}_E^{(\mu)}\,dV\ ,\ 1\le\nu,\mu\le n_h\ ,\\
b_\nu&:=\int_\Omega \mathbf{f}\cdot\mathbf{q}_E^{(\nu)}\,dV\ ,\ 1\le\nu\le n_h\ .
\end{aligned}$$

The stiffness matrix $\mathbf{A}_h^\chi$ has a nontrivial kernel due to the kernel of the discrete **curl**-operator. The influence of this nontrivial kernel will be illustrated by the following example. For simplicity, we assume that the algebraic system (7.2) reduces to

$$\Big(\mathbf{A}_h^\chi+\beta\mathbf{A}_h^\beta\Big)\,\mathbf{x}_h=\mathbf{b}_h\ , \tag{7.3}$$

where

$$\mathbf{A}_h^\chi:=\begin{pmatrix}1&-1\\-1&1\end{pmatrix}\quad,\quad \mathbf{A}_h^\beta:=\begin{pmatrix}1&0\\0&1\end{pmatrix}\ ,$$

and $\beta>0$. The eigenvalues of $\mathbf{A}_h^\chi$ are $\lambda_h^{(1)}=0$ and $\lambda_h^{(2)}=2$ with the associated eigenvectors $\mathbf{v}_h^{(1)}=(1,1)^T$ and $\mathbf{v}_h^{(2)}=(1,-1)^T$, respectively. If we use the damped Jacobi iteration with damping parameter $\omega_1>0$ to solve equation (7.3), the error $\mathbf{e}_h^{(k)}:=\mathbf{x}_h-\mathbf{x}_h^{(k)}$ with respect to the k-th iterate $\mathbf{x}_h^{(k)}\in\mathbb{R}^2$ satisfies

$$\mathbf{e}_h^{(k+1)}=\mathbf{M}_h\mathbf{e}_h^{(k)}\ , \tag{7.4}$$

where

$$\mathbf{M}_h := \mathbf{I}_h - \frac{\omega_1}{1+\beta}\left(\mathbf{A}_h^{\chi} + \beta \mathbf{A}_h^{\beta}\right) . \tag{7.5}$$

If we split the error according to $\mathbf{e}_h^{(k)} = \alpha_k^{(1)}\mathbf{v}_h^{(1)} + \alpha_k^{(2)}\mathbf{v}_h^{(2)}$, we obtain for the individual components of the error

$$\begin{aligned}
\mathbf{M}_h\mathbf{v}_h^{(1)} &= (1 - \omega_1\frac{\beta}{1+\beta})\mathbf{v}_h^{(1)} , \\
\mathbf{M}_h\mathbf{v}_h^{(2)} &= (1 - \omega_1\frac{2+\beta}{1+\beta})\mathbf{v}_h^{(2)} .
\end{aligned}$$

If we use the optimal damping parameter $\omega_1 = 1$, we have

$$\begin{aligned}
\mathbf{M}_h\mathbf{v}_h^{(1)} &= +\frac{1}{1+\beta}\,\mathbf{v}_h^{(1)} , \\
\mathbf{M}_h\mathbf{v}_h^{(2)} &= -\frac{1}{1+\beta}\,\mathbf{v}_h^{(2)} .
\end{aligned}$$

In the case $\beta \ll 1$ the fraction $1/(1+\beta)$ tends to 1, which means that both components of the error are hardly reduced. However, if we choose the damping parameter according to $\omega_1 = (1+\beta)/(2+\beta)$, we obtain

$$\begin{aligned}
\mathbf{M}_h\mathbf{v}_h^{(1)} &= \frac{2}{2+\beta}\,\mathbf{v}_h^{(1)} , \\
\mathbf{M}_h\mathbf{v}_h^{(2)} &= 0
\end{aligned}$$

for the components of the error. This choice of the damping parameter is optimal with respect to $\alpha_k^{(2)}\mathbf{v}_h^{(2)}$. However, for $\beta \ll 1$ we observe a very bad damping for the component $\alpha_k^{(1)}\mathbf{v}_h^{(1)}$. The best available damping for $\alpha_k^{(1)}\mathbf{v}_h^{(1)}$ will be obtained if we choose the biggest possible damping parameter $\omega_1 = (2\beta+2)/(2+\beta)$. This choice yields

$$\begin{aligned}
\mathbf{M}_h\mathbf{v}_h^{(1)} &= \frac{2-\beta}{2+\beta}\,\mathbf{v}_h^{(1)} , \\
\mathbf{M}_h\mathbf{v}_h^{(2)} &= -\mathbf{v}_h^{(2)} .
\end{aligned}$$

We see that even in this case small values of β lead to a poor damping of the error. Taking this into account, we see that the component $\alpha_k^{(1)}\mathbf{v}_h^{(1)}$, living in the kernel of $\mathbf{A}_h^{\chi}$, experiences a very bad damping in case $\beta \ll 1$, whereas the other component $\alpha_k^{(2)}\mathbf{v}_h^{(2)}$, living in the orthogonal subspace, is satisfactorily damped if we choose the damping parameter appropriately.

A convenient remedy to improve the convergence of the iterative process, as proposed in [Hip99], is to perform a defect correction on the kernel of $\mathbf{A}_h^{\chi}$. Given the iterate $\mathbf{x}_h^{(k+1/2)}$ obtained by applying one step of the damped Jacobi iteration

to (7.3) with $\mathbf{x}_h^{(k)}$ as startiterate, the defect with respect to this iterate is given by

$$\begin{aligned}\mathbf{d}_h^{(k)} &= \mathbf{b}_h - (\mathbf{A}_h^\chi + \beta\mathbf{A}_h^\beta)\mathbf{x}_h^{(k+1/2)} \ , \\ \mathbf{x}_h^{(k+1/2)} &= \Big(\mathbf{I}_h - \frac{\omega_1}{1+\beta}\,(\mathbf{A}_h^\chi + \beta\mathbf{A}_h^\beta)\Big)\mathbf{x}_h^{(k)} + \frac{\omega_1}{1+\beta}\,\mathbf{b}_h \ .\end{aligned}$$

For the correction on the kernel of $\mathbf{A}_h^\chi$ we have to define the matrix $\mathbf{C}_h$ and the vector r_h^k which represent the restriction of $\mathbf{A}_h^\chi + \beta\mathbf{A}_h^\beta$ and of $\mathbf{d}_h^k$ onto this subspace, respectively. Setting

$$\begin{aligned}\mathbf{C}_h &:= (\mathbf{v}_h^{(1)})^T\Big(\mathbf{A}_h^\chi + \beta\mathbf{A}_h^\beta\Big)\mathbf{v}_h^{(1)} = (\mathbf{v}_h^{(1)})^T\beta\mathbf{A}_h^\beta\mathbf{v}_h^{(1)} = 2\beta \ , \\ r_h^{(k)} &:= (\mathbf{v}_h^{(1)})^T\mathbf{d}_h^{(k)} \ ,\end{aligned}$$

the scalar defect correction takes the form

$$\mathbf{C}_h c_h^k = r_h^{(k)}$$

and results in the new iterate

$$\mathbf{x}_h^{(k+1)} = \mathbf{x}_h^{(k+1/2)} + \omega_2 c_h^k \mathbf{v}_h^{(1)} = \mathbf{x}_h^{(k+1/2)} + \omega_2\left(\mathbf{C}_h^{-1} r_h^{(k)}\right)\mathbf{v}_h^{(1)} \ , \tag{7.6}$$

where the correction has been damped by the factor $\omega_2 > 0$. The iteration operator $\hat{\mathbf{M}}_h$ associated with (7.6) is given by

$$\hat{\mathbf{M}}_h = \Big(\mathbf{I}_h - \omega_2\mathbf{v}_h^{(1)}\mathbf{C}_h^{-1}(\mathbf{v}_h^{(1)})^T(\mathbf{A}_h^\chi + \beta\mathbf{A}_h^\beta)\Big)\Big(\mathbf{I}_h - \frac{\omega_1}{1+\beta}(\mathbf{A}_h^\chi + \beta\mathbf{A}_h^\beta)\Big) \ .$$

Taking into account that $\mathbf{C}_h = 2\beta$, we obtain for the two components of the error

$$\hat{\mathbf{M}}_h\mathbf{v}_h^{(1)} = (1-\omega_2)(1-\omega_1\frac{\beta}{1+\beta})\mathbf{v}_h^{(1)} \ , \tag{7.7}$$

$$\hat{\mathbf{M}}_h\mathbf{v}_h^{(2)} = (1-\omega_1\frac{2+\beta}{1+\beta})\mathbf{v}_h^{(2)} \ , \tag{7.8}$$

which shows that excellent damping properties for both components of the error can be achieved if we choose the damping parameters ω_1 and ω_2 appropriately.

This simple example already showed the main ingredients of the hybrid smoother introduced in [Hip99]. In the context of iterative solvers for the edge element discretization (7.1) the above mentioned defect correction will be performed on the nontrivial kernel of the discrete **curl**-operator. This kernel is given by the subspace of irrotational vector fields spanned by the gradients of the conforming P1 finite elements.

Then for the defect correction we have to compute $\varphi_h \in S_{1,0}(\Omega;\mathcal{T}_h)$ such that

$$\int_\Omega \beta\,\mathbf{grad}\,\varphi_h \cdot \mathbf{grad}\,v_h\,dV = r(v_h) \quad \forall v_h \in S_{1,0}(\Omega;\mathcal{T}_h) \tag{7.9}$$

where $r(\cdot)^{(k+1/2)}$ denotes the residual

$$r(v_h)^{(k+1/2)} := \ell(\mathbf{grad}\, v_h) - a_h(\mathbf{u}_h^{(k+1/2)}, \mathbf{grad}\, v_h) \ , \ v_h \in S_{1,0}(\Omega; \mathcal{T}_h) \ .$$

Assuming $S_{1,0}(\Omega; \mathcal{T}_h) = \mathrm{span}\{\varphi_h^{(\nu)} \mid 1 \leq \nu \leq m_h\}$, we define the stiffness matrix $\mathbf{C}_h = (c_{\nu\mu})_{\nu,\mu=1}^{m_h}$ and the residual vector $\mathbf{r}_h^{(k+1/2)} = (r_1^{(k+1/2)}, ..., r_{m_h}^{(k+1/2)})^T$ according to

$$c_{\nu\mu} := \int_\Omega \beta\, \mathbf{grad}\, \varphi_h^{(\nu)} \cdot \mathbf{grad}\, \varphi_h^{(\mu)}\, dV \ , \ 1 \leq \nu, \mu \leq m_h \ ,$$
$$r_\nu^{(k+1/2)} := r^{(k+1/2)}(\varphi_h^{(\nu)}) \ , \ 1 \leq \nu \leq m_h \ .$$

If we identify $\varphi_h \in S_{1,0}(\Omega; \mathcal{T}_h)$ with a vector $\boldsymbol{\varphi}_h \in \mathbb{R}^{m_h}$, we obtain for the defect equation (7.9) the algebraic form

$$\mathbf{C}_h \boldsymbol{\varphi}_h = \mathbf{r}_h^{(k+1/2)} \ . \tag{7.10}$$

Recalling the example, we obtain a hybrid iterative process, applying classical iterative methods to the fully edge element discretized problem and to the defect correction problem. In particular, if we use the symmetric SOR method as smoother, a cycle of the hybrid iterative solver is given by the following steps:

Step 1: SSOR step on the edge element discretized problem
Compute $\mathbf{u}_h^{(k+1/2)} \in \mathbb{R}^{n_h}$ by applying ν_1 steps of the symmetric SOR method to the algebraic system

$$\mathbf{A}_h \mathbf{u}_h = \mathbf{b}_h \ ,$$

using $\mathbf{u}_h^{(k)}$ as a startiterate.

Step 2: Correctional SSOR sweep on the defect correction problem
Compute $\boldsymbol{\varphi}_h^{(k+1/2)} \in \mathbb{R}^{m_h}$ by performing ν_2 steps of the symmetric SOR scheme on

$$\mathbf{C}_h \boldsymbol{\varphi}_h = \mathbf{r}_h^{(k+1/2)} \ ,$$

using $\mathbf{0}$ as a startiterate.

Step 3: Additive correction
Denoting by $\boldsymbol{\psi}_h^{(k+1/2)} \in \mathbb{R}^{n_h}$ the vector representing $\mathbf{grad}\, \varphi_h^{(k+1/2)} \in \mathbf{Nd}_{1,0}(\Omega; \mathcal{T}_h)$, $\varphi_h^{(k+1/2)} \in S_{1,0}(\Omega; \mathcal{T}_h)$, the new iterate $\mathbf{u}_h^{(k+1)} \in \mathbb{R}^{n_h}$ is given by

$$\mathbf{u}_h^{(k+1)} = \mathbf{u}_h^{(k+1/2)} + \boldsymbol{\psi}_h^{(k+1/2)} \ .$$

Although the hybrid smoother as defined above, has improved damping properties the performance of an iterative solver using this smoother in each step is still

poor for high-dimensional algebraic systems. This behavior, also observed for other standard smoothers, suggests to use multigrid methods applying the hybrid iterative process as a smoother on all levels j of the hierarchy $\mathcal{T}_j$, $0 \leq j \leq L$, of nested simplicial triangulations of the computational domain Ω as well as an iterative solver on the lowest level $j = 0$.

The convergence of multigrid V-cycles with the hybrid smoother and canonical intergrid transfers has been analyzed in [Hip98] (cf. also [Hip02b]) in the framework of multiplicative Schwarz iterations with respect to a multilevel decomposition of the edge element space $\mathbf{Nd}_{1,0}(\Omega; \mathcal{T}_L)$ with respect to the finest grid.

Considering the superior smoothing properties of the hybrid smoother, a natural idea is to apply this smoother to problems discretized by mortar edge elements. However, as will be shown in the following sections, transferring these concepts to linear equations arising from mortar methods shows severe problems. To illustrate this, we will first consider the iterative solution of algebraic equations that arise when using the constrained space.

7.2 Iterative Solver for the Constrained Formulation

To simplify the presentation, we will restrict ourselves to the case of two domains $\bar{\Omega} = \bar{\Omega}_s \cup \bar{\Omega}_m$, where Ω_s and Ω_m denote the slave and master domain, respectively. Of course we require $\Omega_s \cap \Omega_m = \emptyset$ and denote by $\bar{\Sigma} = \bar{\Omega}_s \cap \bar{\Omega}_m$ the common interface of the two domains. Following Section 5.1, we equip both domains with meshes $\mathcal{T}_s$ and $\mathcal{T}_m$. Using the L^2-projection $Q_h^{\Sigma_s}$, we introduce the constrained mortar edge element space $\tilde{\mathbf{V}}_h$:

$$\begin{aligned} \tilde{\mathbf{V}}_h &:= \{\mathbf{q}_h \in \mathbf{V}_h \mid \; Q_h^{\Sigma_s}(\mathbf{q}_h \wedge \mathbf{n}|_{\Sigma_m}) = Q_h^{\Sigma_s}(\mathbf{q}_h \wedge \mathbf{n}|_{\Sigma_s})\} \;, \\ \mathbf{V}_h &:= \{\mathbf{q}_h \in L^2(\Omega)^3 \mid \mathbf{q}_h|_{\Omega_i} \in \mathbf{Nd}_{1,\Gamma_i}(\Omega_i; \mathcal{T}_i) \;,\; i = s, m\} \;, \end{aligned}$$

where $\bar{\Sigma}_s = \bar{\Omega}_s \cap \bar{\Sigma}$ and $\bar{\Sigma}_m = \bar{\Omega}_m \cap \bar{\Sigma}$. Then we have to find $\mathbf{u}_h \in \tilde{\mathbf{V}}_h$ such that

$$a_h(\mathbf{u}_h, \mathbf{q}_h) = l(\mathbf{q}_h) \quad \forall \mathbf{q}_h \in \tilde{\mathbf{V}}_h \;, \tag{7.11}$$

where the bilinear form $a_h(\cdot, \cdot) : \tilde{\mathbf{V}}_h \times \tilde{\mathbf{V}}_h \to \mathbb{R}$ is given by

$$a_h(\mathbf{u}_h, \mathbf{q}_h) = \sum_{i=s,m} \int_{\Omega_i} (\chi \, \mathbf{curl}\, \mathbf{u}_h \cdot \mathbf{curl}\, \mathbf{q}_h + \beta \, \mathbf{u}_h \cdot \mathbf{q}_h) \, dV \;. \tag{7.12}$$

In order to apply the hybrid smoother, we have to consider the spaces $\tilde{\mathbf{V}}_h^0$ and $\tilde{\mathbf{V}}_h^\perp$ which are given by

$$\begin{aligned}
\tilde{\mathbf{V}}_h^0 &:= \{\mathbf{grad}\,\varphi_h \mid \varphi_h \in S_h, \text{ and for any } \Sigma_s = \Sigma_m = \Sigma, \\
&\qquad Q_h^{\Sigma_s}(\mathbf{grad}\,\varphi_h \wedge \mathbf{n}|_{\Sigma_m}) = Q_h^{\Sigma_s}(\mathbf{grad}\,\varphi_h \wedge \mathbf{n}|_{\Sigma_s})\} \ , \\
S_h &:= \{\varphi_h \in L^2(\Omega) \mid \varphi_h|_{\Omega_i} \in S_{1,\Gamma_i}(\Omega_i;\mathcal{T}_i) \ , \ i = s,m\} \ , \\
\tilde{\mathbf{V}}_h^\perp &:= \{\mathbf{q}_h \mid \mathbf{q}_h \in \mathbf{V}_h^\perp, \text{ and for any } \Sigma_s = \Sigma_m = \Sigma, \\
&\qquad Q_h^{\Sigma_s}(\mathbf{q}_h \wedge \mathbf{n}|_{\Sigma_m}) = Q_h^{\Sigma_s}(\mathbf{q}_h \wedge \mathbf{n}|_{\Sigma_s})\} \ , \\
\mathbf{V}_h^\perp &:= \{\mathbf{q}_h \in L^2(\Omega)^3 \mid \mathbf{q}_h|_{\Omega_i} \in (\mathbf{grad}\,S_{1,\Gamma_i}(\Omega_i;\mathcal{T}_i))^\perp \ , \ i = s,m\} \ .
\end{aligned}$$

If we follow the steps of the hybrid smoother, we first have to perform one smoothing step on the full problem (7.12) discretized by the space $\tilde{\mathbf{V}}_h$ followed by a correction step of (7.12) restricted to the space $\tilde{\mathbf{V}}_h^0$. Although this approach was quite successful in the conforming setting, it fails in this case. This failure is due to the fact that the space $\tilde{\mathbf{V}}_h$ is not a direct sum of the spaces $\tilde{\mathbf{V}}_h^\perp$ and $\tilde{\mathbf{V}}_h^0$, but we have

$$\tilde{\mathbf{V}}_h = \tilde{\mathbf{V}}_h^0 \oplus \tilde{\mathbf{V}}_h^\perp \oplus \tilde{\mathbf{Y}}_h \ . \tag{7.13}$$

To give a characterization of the space $\tilde{\mathbf{Y}}_h$, we have to take a closer look at the mortar constraint. Considering the spaces $S_{1,\Gamma_m}(\Omega_m;\mathcal{T}_m)$ and $S_{1,\Gamma_s}(\Omega_s;\mathcal{T}_s)$, we cannot expect that

$$Q_h^{\Sigma_s}\big(\mathbf{grad}\,S_{1,\Gamma_m}(\Omega_m;\mathcal{T}_m)\big) \subset Q_h^{\Sigma_s}\big(\mathbf{grad}\,S_{1,\Gamma_s}(\Omega_s;\mathcal{T}_s)\big)$$

or

$$Q_h^{\Sigma_s}\,\mathbf{grad}\,\big(S_{1,\Gamma_s}(\Omega_s;\mathcal{T}_s)\big) \subset Q_h^{\Sigma_s}\big(\mathbf{grad}\,S_{1,\Gamma_m}(\Omega_m;\mathcal{T}_m)\big)$$

in the general case of nonmatching triangulations at the interface Σ. Therefore, it is possible that there exists $\varphi_{m,h} \in S_{1,\Gamma_m}(\Omega_m;\mathcal{T}_m)$ with no matching function $\varphi_{s,h} \in S_{1,\Gamma_s}(\Omega_s;\mathcal{T}_s)$ such that

$$Q_h^{\Sigma_s}(\mathbf{grad}\,\varphi_{m,h} \wedge \mathbf{n}|_{\Sigma_m}) = Q_h^{\Sigma_s}(\mathbf{grad}\,\varphi_{s,h} \wedge \mathbf{n}|_{\Sigma_s}) \ . \tag{7.14}$$

However, due to the fact that $Q_h^{\Sigma_s}$ is a surjective mapping of $\mathbf{Nd}_{1,\Gamma_s}(\Omega_s;\mathcal{T}_s)$ onto $\mathbf{M}_h(S)$, it is possible to find $\mathbf{q}_{s,h} \in \mathbf{Nd}_{1,\Gamma_s}(\Omega_s;\mathcal{T}_s)$ such that

$$Q_h^{\Sigma_s}(\mathbf{grad}\,\varphi_{m,h} \wedge \mathbf{n}|_{\Sigma_m}) = Q_h^{\Sigma_s}(\mathbf{q}_{s,h} \wedge \mathbf{n}|_{\Sigma_s}) \ . \tag{7.15}$$

This means that the function $\tilde{\mathbf{q}}_h$ which is defined according to

$$\begin{aligned}
\tilde{\mathbf{q}}_h|_{\Omega_s} &:= \mathbf{q}_{s,h} \ , \\
\tilde{\mathbf{q}}_h|_{\Omega_m} &:= \mathbf{grad}\,\varphi_{m,h}
\end{aligned}$$

is an element of $\tilde{\mathbf{V}}_h$ but neither an element of $\tilde{\mathbf{V}}_h^{\perp}$ nor of $\tilde{\mathbf{V}}_h^0$. Moreover, $\tilde{\mathbf{q}}_h$ cannot be written as a linear combination of elements of these two spaces. Of course it might also be possible that there exist functions $\tilde{\mathbf{v}}_h \in \tilde{\mathbf{V}}_h$ such that

$$\begin{aligned} \tilde{\mathbf{v}}_h|_{\Omega_m} &= \mathbf{q}_{m,h} \qquad , \ \mathbf{q}_{m,h} \in \mathbf{Nd}_{1,\Gamma_m}(\Omega_m; \mathcal{T}_m) \ , \\ \tilde{\mathbf{v}}_h|_{\Omega_s} &= \mathbf{grad}\, \varphi_{s,h} \ , \ \varphi_{s,h} \in S_{1,\Gamma_s}(\Omega_s; \mathcal{T}_s) \ . \end{aligned}$$

From the definition of these functions it is clear that they are neither pure gradients nor are they pure elements of the orthogonal complement. Therefore, $\tilde{\mathbf{Y}}_h$ might be called the space of "mixed gradients". If we compare the eigenvalues of $\mathbf{A}_h$, the matrix representation of $a_h(\cdot,\cdot)$, we notice that the eigenvalues related to $\tilde{\mathbf{Y}}_h$ are greater than the ones related to $\tilde{\mathbf{V}}_h^0$, but smaller than those related to $\tilde{\mathbf{V}}_h^{\perp}$. Thus the spectrum of $\mathbf{A}_h$ consists of three nonintersecting blocks, while in the conforming case we have only two blocks. The new block of eigenvalues associated with $\tilde{\mathbf{Y}}_h$ causes great problems for an iterative solver as will be shown by the following two-dimensional example. Although the example is very simple — two subdomains, eight triangles — it incorporates all important aspects that are encountered in more complicated problems.

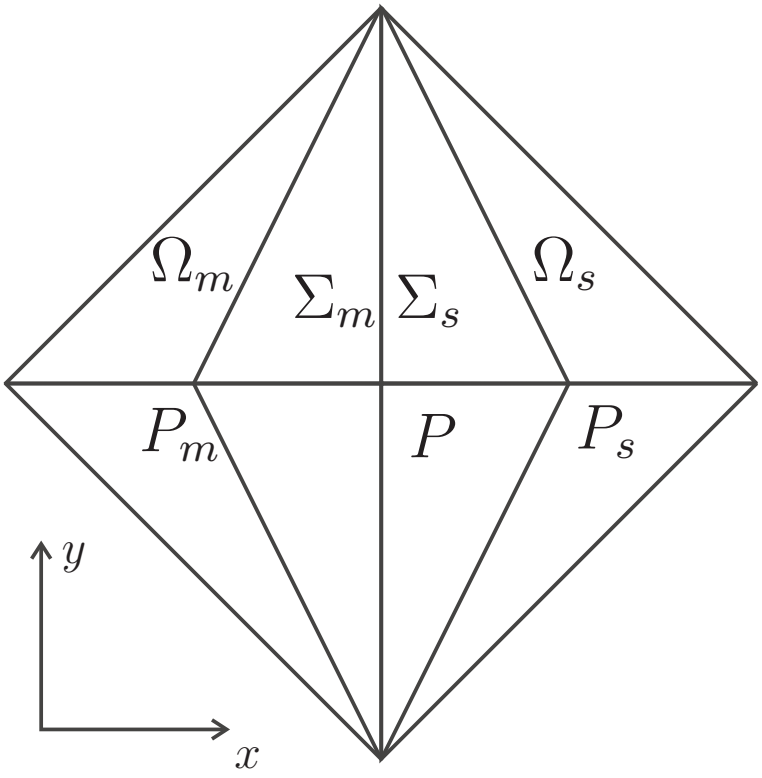

Figure 7.1: 2D computational domain of the example.

For this example we use the computational domain depicted in Figure 7.1 and set $\chi = 1$ and $\beta = 10^{-2}$. Moreover, we assume zero Dirichlet boundary conditions

and choose the left subdomain as master side and accordingly the right subdomain as slave side.

As in the conforming case, we assume $\mathbf{Nd}_{1,\Gamma_i}(\Omega_i;\mathcal{T}_i) = \text{span}\{\mathbf{q}_{E,i}^{(\nu)} \mid 1 \le \nu \le n_i\}$, $i = s, m$, $n_s = n_m = 6$, and identify the edge element function $\mathbf{u}^i \in \mathbf{Nd}_{1,\Gamma_i}(\Omega;\mathcal{T}_i)$ with a vector $\mathbf{u}^i \in \mathbb{R}^{n_i}$. We divide the unknowns in each subdomain into two blocks: the first block $\mathbf{u}_{Int}^i$ contains the unknowns associated with edges in the interior of Ω_i, while the second block $\mathbf{u}_{\Sigma_i\setminus\partial\Sigma_i}^i$ contains the unknowns associated with edges in the interior of Σ_i. So far we have $n_s + n_m = 12$ variables. However, the actual number of unknowns is smaller, since $\mathbf{u}_{\Sigma_s\setminus\partial\Sigma_s}^s$ is connected to $\mathbf{u}_{\Sigma_m\setminus\partial\Sigma_m}^m$ via the mortar matching conditions. We have

$$\mathbf{u}_{\Sigma_s\setminus\partial\Sigma_s}^s = \mathbf{Q}\mathbf{u}_{\Sigma_m\setminus\partial\Sigma_m}^m \ ,$$

where $\mathbf{Q}$ is a rectangular full rank matrix obtained from the discretization of the matching condition. Introducing the following matrices

$$\mathbf{A} := \begin{pmatrix} \mathbf{A}^m & 0 \\ 0 & \mathbf{A}^s \end{pmatrix} \quad , \quad \tilde{\mathbf{Q}} := \begin{pmatrix} \mathbf{Id} & 0 & 0 \\ 0 & \mathbf{Id} & 0 \\ \mathbf{Q} & 0 & 0 \\ 0 & 0 & \mathbf{Id} \end{pmatrix} \ ,$$

where $\mathbf{A}^i := \mathbf{A}_\chi^i + \mathbf{A}_\beta^i$, $i = s, m$, is given by

$$a_{\nu\mu,\chi}^i := \int_{\Omega_i} \chi\, \mathbf{curl}\, \mathbf{q}_{E,i}^{(\nu)} \cdot \mathbf{curl}\, \mathbf{q}_{E,i}^{(\mu)}\, dV \ , \ 1 \le \nu, \mu \le n_i \ ,$$

$$a_{\nu\mu,\beta}^i := \int_{\Omega_i} \beta\, \mathbf{q}_{E,i}^{(\nu)} \cdot \mathbf{q}_{E,i}^{(\mu)}\, dV \ , \ 1 \le \nu, \mu \le n_i \ ,$$

and setting $\mathbf{y} := (\mathbf{u}_{\Sigma_m\setminus\partial\Sigma_m}^m, \mathbf{u}_{Int}^m, \mathbf{u}_{Int}^s)^T$ and $\mathbf{b} := (b_1^m, ..., b_{n_m}^m, b_1^s, ..., b_{n_s}^s)^T$, with $b_\nu^i := \int_{\Omega_i} \mathbf{f} \cdot \mathbf{q}_{E,i}^{(\nu)}\, dV \ , \ 1 \le \nu \le n_i$, the solution of (7.11) is computed by solving the symmetric positive definite system

$$\tilde{\mathbf{A}}\,\mathbf{y} = \tilde{\mathbf{Q}}^T\mathbf{A}\tilde{\mathbf{Q}}\,\mathbf{y} = \tilde{\mathbf{Q}}^T\mathbf{b} \ . \tag{7.16}$$

Before applying the hybrid smoother to this problem, it is advisable to first have a look at the spectrum of $\tilde{\mathbf{A}}$. As mentioned before, the elements of $\tilde{\mathbf{Y}}_h$ depend strongly on the relationship between the triangulations $\mathcal{T}_s$ and $\mathcal{T}_m$ on Σ_m and Σ_s. To show the influence of this relationship, we start with a matching triangulation at the interface and increase the y-coordinate of the point P on the master side gradually to obtain nonmatching triangulations. The scaling of the four smallest eigenvalues of the matrix $\tilde{\mathbf{A}}$ are shown in Figure 7.2.

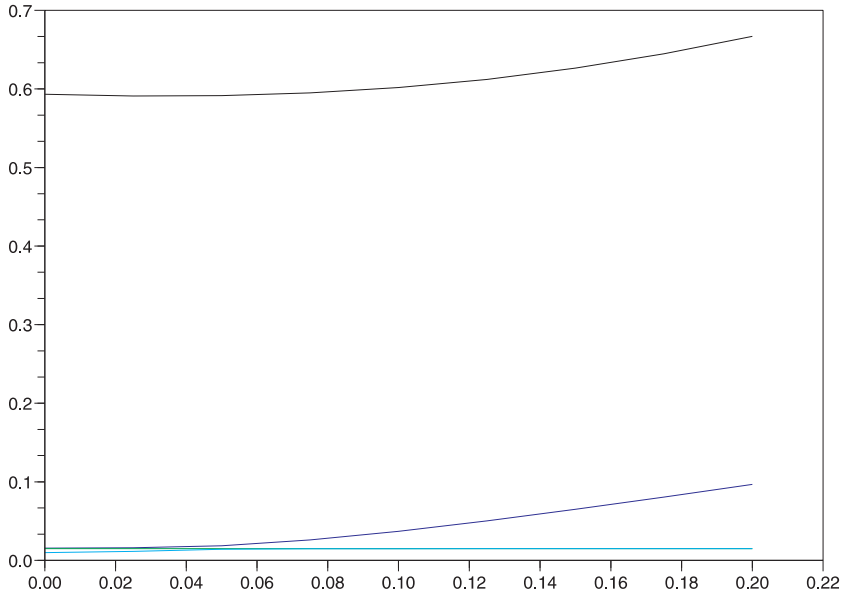

Figure 7.2: Scaling of the four smallest eigenvalues of $\tilde{\mathbf{A}}$.

In the case of matching triangulations on Σ_m and Σ_s, we have $\tilde{\mathbf{Y}}_h = \emptyset$, which gives a similar situation as in the conforming case. The three smallest eigenvalues are connected with the subspace $\tilde{\mathbf{V}}_h^0$, while the other eigenvalues are associated with $\tilde{\mathbf{V}}_h^\perp$. If we increase the y-coordinate of point P, one of the three smallest eigenvalues is increasing drastically compared with the others. This increase is due to the fact that in this case the space $\tilde{\mathbf{Y}}_h$ is no longer empty. Now, we have the following situation:

- The two smallest eigenvalues, which do not change their value much, are connected with the space $\tilde{\mathbf{V}}_h^0$.
- The third smallest eigenvalue, which is increasing by a great amount, is related to the space $\tilde{\mathbf{Y}}_h$, which is one-dimensional in this example.
- The remaining eigenvalues are related to the space $\tilde{\mathbf{V}}_h^\perp$. Their values do not change much with increasing values of the y-coordinate.

Applying standard iterative solvers to (7.16) gives a similar result as in the conforming case. If $\beta \ll \chi$, error components related to both the spaces $\tilde{\mathbf{V}}_h^0$ and $\tilde{\mathbf{Y}}_h$ are hardly reduced, while we get a good reduction of the error on $\tilde{\mathbf{V}}_h^\perp$. If we apply a correction step on $\tilde{\mathbf{V}}_h^0$, we can achieve that the error components related to $\tilde{\mathbf{V}}_h^0$ and $\tilde{\mathbf{V}}_h^\perp$ are reduced quite well but we still have almost no reduction of the error on $\tilde{\mathbf{Y}}_h$.

A natural consequence would be to perform a second correction step on $\tilde{\mathbf{Y}}_h$. However, this idea is connected with the problem that we have to compute a basis for

$\tilde{\mathbf{Y}}_h$. Since the elements of $\tilde{\mathbf{Y}}_h$ depend on the relationship of the triangulations at the interface and on the operator $Q_h^{\Sigma_s}$, this task can be extremely complicated for arbitrary independent meshes on the subdomains. Not to mention how difficult it would be to give a finite element basis for $\tilde{\mathbf{Y}}_h$.

Moreover, in order to perform the correction on $\tilde{\mathbf{V}}_h^0$, we have to compute a basis for this space. Again this is quite a difficult task, since it involves the operator $Q_h^{\Sigma_s}$, which is defined via surface integrals. Thus for general problems we will not be able to find a finite element basis for these two spaces without increasing the computational cost considerably.

Summarizing the results of this section, we can expect the hybrid smoother, extended by a second correction step on $\tilde{\mathbf{Y}}_h$, to be a good choice to solve (7.11) from the theoretical point of view. However, this method is connected with great problems for practical implementation, which makes it impossible to use unless a relative easy way is found to compute basis functions for $\tilde{\mathbf{V}}_h^0$ and $\tilde{\mathbf{Y}}_h$.

7.3 Iterative Solver for the Unconstrained Formulation

As seen in the last section, one major problem for the iterative solution of (7.11) is that we have to compute basis functions for the constrained space $\tilde{\mathbf{V}}_h^0$, which involves the operator $Q_h^{\Sigma_s}$. However, we can avoid these computationally expensive calculations if we use unconstrained spaces. Of course, this change is not for free, since in this case we have to solve an indefinite saddle point problem. Recalling Section 4.4, this saddle point problem is given by:

Find $(\mathbf{u}_h, \boldsymbol{\lambda}_h) \in \mathbf{V}_h \times \mathbf{M}_h(S)$ such that

$$\begin{aligned} a_h(\mathbf{u}_h, \mathbf{q}_h) + b_h(\mathbf{q}_h, \boldsymbol{\lambda}_h) &= \ell(\mathbf{q}_h) \quad \forall \mathbf{q}_h \in \mathbf{V}_h \quad , \\ b_h(\mathbf{u}_h, \boldsymbol{\mu}_h) &= 0 \quad \forall \boldsymbol{\mu}_h \in \mathbf{M_h}(S) \ . \end{aligned} \tag{7.17}$$

Introducing finite element bases for the spaces $\mathbf{V}_h(\Omega)$ and $\mathbf{M}_h(S)$, the mortar edge element approximation (7.17) can be written as the algebraic saddle point problem

$$\begin{pmatrix} \mathbf{A}_h & \mathbf{B}_{e,h}^T \\ \mathbf{B}_{e,h} & 0 \end{pmatrix} \begin{pmatrix} \mathbf{u}_h \\ \boldsymbol{\lambda}_h \end{pmatrix} = \begin{pmatrix} \mathbf{b}_h \\ 0 \end{pmatrix} \ , \tag{7.18}$$

where $\mathbf{B}_{e,h}$ denotes the matrix associated with the bilinear form $b_h(\cdot,\cdot)$ and the block matrix $\mathbf{A}_h$ is given by

$$\mathbf{A}_h := \begin{pmatrix} \mathbf{A}_h^{(1)} & & 0 \\ & \ddots & \\ 0 & & \mathbf{A}_h^N \end{pmatrix} \ ,$$

where the $\mathbf{A}_h^{(i)}$, $1 \leq i \leq N$, are the matrix representations of the edge element discretized subdomain problems. The right hand side vector $\mathbf{b}_h = (\mathbf{b}_h^{(1)}, ..., \mathbf{b}_h^{(N)})^T$ results from the representation of $\ell_h(\cdot)$ restricted to $\mathbf{Nd}_{1,\Gamma_i}(\Omega_i; \mathcal{T}_i)$, $1 \leq i \leq N$.

In order to solve the symmetric but indefinite linear system (7.18), we use iterative schemes based on the iterative solver proposed in [BD98, BDW00]. This solver is based on the following concept. Suppose that $\mathbf{P}_h$ is a preconditioner for $\mathbf{A}_h$ which satisfies

$$\mathbf{v}_h^T \mathbf{A}_h \mathbf{v}_h \leq \mathbf{v}_h^T \mathbf{P}_h \mathbf{v}_h \ , \ \mathbf{v}_h \in \mathbf{V}_h \ ,$$

and has the property that the linear system

$$\begin{pmatrix} \mathbf{P}_h & \mathbf{B}_{e,h}^T \\ \mathbf{B}_{e,h} & 0 \end{pmatrix} \begin{pmatrix} \mathbf{v}_h \\ \boldsymbol{\mu}_h \end{pmatrix} = \begin{pmatrix} \mathbf{d}_h \\ \mathbf{e}_h \end{pmatrix} \tag{7.19}$$

can be solved more easily. Then the iterative solver has the form:
Given $\left(\mathbf{u}_h^{(0)}, \boldsymbol{\lambda}_h^{(0)}\right)$, compute $\left(\mathbf{u}_h^{(k+1)}, \boldsymbol{\lambda}_h^{(k+1)}\right)$ by

$$\begin{aligned} \begin{pmatrix} \mathbf{u}_h^{(k+1)} \\ \boldsymbol{\lambda}_h^{(k+1)} \end{pmatrix} &= \begin{pmatrix} \mathbf{u}_h^{(k)} \\ \boldsymbol{\lambda}_h^{(k)} \end{pmatrix} + \\ &+ \begin{pmatrix} \mathbf{P}_h & \mathbf{B}_{e,h}^T \\ \mathbf{B}_{e,h} & 0 \end{pmatrix}^{-1} \left[\begin{pmatrix} \mathbf{b}_h \\ 0 \end{pmatrix} - \begin{pmatrix} \mathbf{A}_h & \mathbf{B}_{e,h}^T \\ \mathbf{B}_{e,h} & 0 \end{pmatrix} \begin{pmatrix} \mathbf{u}_h^{(k)} \\ \boldsymbol{\lambda}_h^{(k)} \end{pmatrix} \right], \end{aligned} \tag{7.20}$$

where the superscripts denote the iteration indices of the smoothing steps. According to the construction of the smoother, the iterates $\mathbf{u}_h^{(k)}$ always satisfy the mortar constraint, i.e.

$$\mathbf{B}_{e,h} \mathbf{u}_h^{(k)} = 0 \ , \ k > 0 \ .$$

As mentioned in Section 7.1, the successful application of iterative schemes to Maxwell's equations crucially depends on treating the kernel of the **curl**-operator and its orthogonal complement in an appropriate way. If we consider the iterative error of (7.20), which is given by

$$\begin{pmatrix} \mathbf{e}_u^{(k+1)} \\ \mathbf{e}_\lambda^{(k+1)} \end{pmatrix} = \begin{pmatrix} \left(\mathbf{Id}_h - \mathbf{P}_h^{-1} \mathbf{B}_{e,h}^T \left(\mathbf{B}_{e,h} \mathbf{P}_h^{-1} \mathbf{B}_{e,h}^T \right)^{-1} \mathbf{B}_{e,h} \right) \left(\mathbf{Id}_h - \mathbf{P}_h^{-1} \mathbf{A}_h \right) \mathbf{e}_u^{(k)} \\ \left(\mathbf{B}_{e,h} \mathbf{P}_h^{-1} \mathbf{B}_{e,h}^T \right)^{-1} \mathbf{B}_{e,h} \left(\mathbf{Id}_h - \mathbf{P}_h^{-1} \mathbf{A}_h \right) \mathbf{e}_u^{(k)} \end{pmatrix} \ ,$$

where $\mathbf{e}_u^{(k)} = \mathbf{u}_h^* - \mathbf{u}_h^{(k)}$, $\mathbf{e}_{\boldsymbol{\lambda}}^{(k)} = \boldsymbol{\lambda}_h^* - \boldsymbol{\lambda}_h^{(k)}$, and $(\mathbf{u}_h^*, \boldsymbol{\lambda}_h^*)$ is the solution of (7.18), we observe that the Lagrangian error $\mathbf{e}_{\boldsymbol{\lambda}}^{(k+1)}$ does not depend on $\mathbf{e}_{\boldsymbol{\lambda}}^{(k)}$ but is only dependent on $\mathbf{e}_u^{(k)}$. Additionally, $\mathbf{e}_u^{(k)}$ strongly depends on $\mathbf{Id}_h - \mathbf{P}_h^{-1} \mathbf{A}_h$, which indicates that we have to use a preconditioner that performs well on both spaces $\mathbf{V}_h^0$ and $\mathbf{V}_h^\perp$.

The natural consequence of these properties is to use the hybrid smoother as preconditioner $\mathbf{P}_h$. This choice has the benefit of guaranteeing good smoothing on both the kernel and its complement on each subdomain independent of the triangulations at the interfaces. Especially we have no counterpart of the space $\tilde{\mathbf{Y}}_h$ in this case. However, this choice is not advisable from the algorithmic point of view as will be described in the following section.

7.3.1 Hybrid Smoother as Preconditioner $\mathbf{P}_h$

One condition for the choice of the preconditioner $\mathbf{P}_h$ was the requirement that the linear system (7.19) is relatively easy to solve. In actual computations the solution of this system is given by

$$\mathbf{S}_h \boldsymbol{\mu}_h = \mathbf{B}_{e,h}\mathbf{P}_h^{-1}\mathbf{d}_h - \mathbf{e}_h \ , \tag{7.21}$$

$$\mathbf{v}_h = \mathbf{P}_h^{-1}(\mathbf{d}_h - \mathbf{B}_{e,h}^T \boldsymbol{\mu}_h) \ , \tag{7.22}$$

where

$$\mathbf{S}_h := \mathbf{B}_{e,h}\mathbf{P}_h^{-1}\mathbf{B}_{e,h}^T \tag{7.23}$$

is the Schur complement of (7.19). According to the definition of the hybrid smoother, the inverse of $\mathbf{P}_h$ is given by

$$\mathbf{P}_h^{-1} = \mathbf{P}_{e,h}^{-1} + \mathbf{T}_h\mathbf{P}_{n,h}^{-1}\mathbf{T}_h^T(\mathbf{Id}_h - \mathbf{A}_h\mathbf{P}_{e,h}^{-1}) \ ,$$

where $\mathbf{P}_{e,h}^{-1}$ and $\mathbf{P}_{n,h}^{-1}$ denote an iterative step, like a Jacobi or Gauss-Seidel step, on $\mathbf{A}_h$ and $\mathbf{C}_h$, respectively. $\mathbf{T}_h$ denotes the matrix associated with the embedding of $\mathbf{V}_h^0$ into $\mathbf{V}_h$. Then the Schur complement has the form

$$\begin{aligned}\mathbf{S}_h &= \mathbf{B}_{e,h}(\mathbf{P}_{e,h}^{-1} + \mathbf{T}_h\mathbf{P}_{n,h}^{-1}\mathbf{T}_h^T(\mathbf{Id}_h - \mathbf{A}_h\mathbf{P}_{e,h}^{-1}))\mathbf{B}_{e,h}^T = \\ &= \mathbf{B}_{e,h}\mathbf{P}_{e,h}^{-1}\mathbf{B}_{e,h}^T + \mathbf{B}_{e,h}\mathbf{T}_h\mathbf{P}_{n,h}^{-1}\mathbf{T}_h^T(\mathbf{Id}_h - \mathbf{A}_h\mathbf{P}_{e,h}^{-1})\mathbf{B}_{e,h}^T =: \mathbf{S}_{e,h} + \mathbf{S}_{n,h} \ .\end{aligned}$$

For the further analysis it is important to consider $\mathbf{S}_{e,h}$ and $\mathbf{S}_{n,h}$ separately. Since $\mathbf{B}_{e,h}$ satisfies an inf-sup condition, the matrix $\mathbf{S}_{e,h}$ is regular and well-conditioned if $\mathbf{P}_{e,h}$ is chosen appropriately. However, for $\mathbf{S}_{n,h}$ the situation is less encouraging. According to the properties of $\mathbf{T}_h$, $\mathbf{A}_h$, and $\mathbf{P}_{e,h}$, we can neglect $\mathbf{B}_{e,h}\mathbf{T}_h\mathbf{P}_{n,h}^{-1}\mathbf{T}_h^T\mathbf{A}_h\mathbf{P}_{e,h}^{-1}\mathbf{B}_{e,h}^T$ and can assume that

$$\mathbf{S}_{n,h} \approx \mathbf{B}_{e,h}\mathbf{T}_h\mathbf{P}_{n,h}^{-1}\mathbf{T}_h^T\mathbf{B}_{e,h}^T \ .$$

Since $\mathbf{T}_h^T$ is a rectangular matrix that has a large kernel, the square matrix $\mathbf{S}_{n,h}$ is not regular. If we compare the spectrum of $\mathbf{S}_{e,h}$ and $\mathbf{S}_{n,h}$, we observe that for $\beta \ll \chi$ the positive eigenvalues of $\mathbf{S}_{n,h}$ are much bigger than the eigenvalues of $\mathbf{S}_{e,h}$. In some sense this situation is similar to the situation in Section 7.1. Recalling the example given in that section, standard iterative solvers or even the

conjugate gradient method would fail for the solution of the Schur complement equation (7.21), since error components related to the kernel of $\mathbf{S}_{n,h}$ will not be damped effectively.

To solve (7.21) an new hybrid smoother would be needed that performs a correctional step on the kernel of $\mathbf{S}_{n,h}$. Since the kernel of $\mathbf{S}_{n,h}$ is caused by the interaction of the matrices $\mathbf{T}_h$ and $\mathbf{B}_{e,h}^T$, the kernel has to be calculated and cannot be stated a priori as in the case of the kernel of the **curl**-operator. Moreover, the structure of this kernel crucially depends on the relationship between the triangulations on the master and on the slave interface. Thus finding a basis for the kernel can result in an extremely ill-conditioned problem, which means that the hybrid smoother would be an excellent choice for the preconditioner if we were be able to solve the Schur complement system, which is not possible at the moment.

7.3.2 Split Preconditioners

In the last section we used the hybrid smoother as preconditioner for the iterative solver. However, this method is not a direct implementation of the ideas of the hybrid smoother. In Section 7.2 we observed that the application of the hybrid smoother to the constrained algebraic system would be successful if we could avoid the occurrence of the space $\tilde{\mathbf{Y}}_h$. As mentioned in that section, the space $\tilde{\mathbf{Y}}_h$ would be empty if for given $\varphi_{m(k),h} \in S_{1,\Gamma_{m(k)}}(\Omega_{m(k)}; \mathcal{T}_{m(k)})$, $1 \leq k \leq M$, there existed at least one $\varphi_{s(k),h} \in S_{1,\Gamma_{s(k)}}(\Omega_{s(k)}; \mathcal{T}_{s(k)})$ such that

$$Q_h^{\Sigma_{s(k)}}(\mathbf{grad}\,\varphi_{m(k),h} \wedge \mathbf{n}|_{\Sigma_{m(k)}}) = Q_h^{\Sigma_{s(k)}}(\mathbf{grad}\,\varphi_{s(k),h} \wedge \mathbf{n}|_{\Sigma_{s(k)}}) \ .$$

Recalling the simple example in Section 7.2, this condition will not be fulfilled for independent triangulations on the interfaces γ_k. Therefore, we have to require that the triangulations $\mathcal{T}_{\delta_k}$ and $\mathcal{T}_{\varrho_k}$ obey certain compatibility conditions. At the moment we are only able to show that the space $\tilde{\mathbf{Y}}_h$ is empty if the triangulation $\mathcal{T}_{\varrho_k}$ is contained in $\mathcal{T}_{\delta_k}$, i.e. $\mathcal{T}_{\delta_k}$ is an arbitrary refinement of $\mathcal{T}_{\varrho_k}$. Although this does not allow for independent triangulations on the interfaces, we are still able to use different mesh sizes on the subdomains.

Then, defining the space of discrete potentials by

$$S_h := \{\varphi_h \in L^2(\Omega) \mid \varphi_h|_{\Omega_i} \in S_{1,\Gamma_i}(\Omega_i; \mathcal{T}_i) \ , \ 1 \leq i \leq N\} \ ,$$

we have to compute a correction $(\varphi_h, \boldsymbol{\nu}_h) \in S_h \times \mathbf{M}_h(S)$ such that

$$c_h(\varphi_h, \psi_h) + b_h(\mathbf{grad}\,\psi_h, \boldsymbol{\nu}_h) = r(\mathbf{grad}\,\psi_h) \quad \forall \psi_h \in S_h \ , \tag{7.24}$$

$$b_h(\mathbf{grad}\,\varphi_h, \boldsymbol{\mu}_h) = 0 \quad \forall \boldsymbol{\mu}_h \in \mathbf{M}_h(S) \ , \tag{7.25}$$

where the bilinear form $c(\cdot,\cdot)$ is given by

$$c_h(\varphi_h,\psi_h) := \sum_{i=1}^{N} \int_{\Omega_i} \beta\, \mathbf{grad}\, \varphi_h|_{\Omega_i} \cdot \mathbf{grad}\, \psi_h|_{\Omega_i}\, dV \ . \tag{7.26}$$

Introducing a nodal basis for $S_{1,\Gamma}(\Omega_i;\mathcal{T}_i)$, $1 \le i \le N$, the defect correction (7.24) can be written as the algebraic saddle point problem

$$\begin{pmatrix} \mathbf{C}_h & \mathbf{D}_h^T \\ \mathbf{D}_h & 0 \end{pmatrix} \begin{pmatrix} \mathbf{u}_h \\ \boldsymbol{\nu}_h \end{pmatrix} = \begin{pmatrix} \mathbf{r}_h \\ 0 \end{pmatrix} \ , \tag{7.27}$$

where by $\mathbf{C}_h$ denotes the block matrix

$$\mathbf{C}_h \ := \ \begin{pmatrix} \mathbf{C}_h^{(1)} & & 0 \\ & \ddots & \\ 0 & & \mathbf{C}_h^{(N)} \end{pmatrix} \ ,$$

where the $\mathbf{C}_h^{(\mathbf{i})}$, $1 \le i \le N$, and $\mathbf{D}_h$ are the matrix representations of $c_h(\cdot,\cdot)$ and $b_h(\cdot,\cdot)$ restricted to $S_{1,\Gamma}(\Omega_i;\mathcal{T}_i) \times S_{1,\Gamma}(\Omega_i;\mathcal{T}_i)$ and $\mathbf{grad}\, S_h \times \mathbf{M}_h(S)$, respectively. Moreover, $\mathbf{r}_h = (\mathbf{r}_h^{(1)},...,\mathbf{r}_h^{(N)})^T$ denotes the vector associated with $r_h(\cdot)$ restricted to $\mathbf{grad}\, S_{1,\Gamma}(\Omega_i;\mathcal{T}_i)$.

However, equation (7.27) does not have a unique solution for $\boldsymbol{\nu}_h$, since $\mathbf{D}_h$ does not fulfill an inf-sup condition for the whole space $\mathbf{M}_h(S)$. In order to guarantee the existence and uniqueness of a solution to (7.27), we have to use a subspace of $\mathbf{M}_h(S)$ for the correction equation. To determine this subspace, we have to look at the mortar matching condition

$$b_h(\mathbf{grad}\, \varphi_h, \boldsymbol{\mu}_h) := \sum_{\gamma_k \in S} \int_{\gamma_k} [\mathbf{n} \wedge \mathbf{grad}\, \varphi_h]\,|_{\gamma_k} \boldsymbol{\mu}_h\, d\sigma = 0 \quad \forall \boldsymbol{\mu}_h \in \mathbf{M}_h(S) \ , \tag{7.28}$$

more closely. Using (7.28), we can write the Lagrange multiplier space $\mathbf{M}_h(S)$ as the direct sum of two spaces, i.e.

$$\begin{aligned} \mathbf{M}_h(S) &= \mathbf{M}_h^1(S) \oplus \mathbf{M}_h^2(S) \ , \\ \mathbf{M}_h^1(S) &:= \ \{\boldsymbol{\mu}_h \in \mathbf{M}_h(S) \mid b_h(\mathbf{grad}\, \varphi_h, \boldsymbol{\mu}_h) = 0 \quad \forall \varphi_h \in S_h\} \ , \\ \mathbf{M}_h^2(S) &:= \ \{\boldsymbol{\mu}_h \in \mathbf{M}_h(S) \mid \exists \varphi_h \in S_h \ : \ \boldsymbol{\mu}_h = \mathbf{n} \wedge \mathbf{grad}\, \varphi_h|_S\} \ . \end{aligned}$$

Note that according to the construction of $\mathbf{M}_h(S)$ the space of $\mathbf{M}_h^2(S)$ is well-defined and is the orthogonal complement of $\mathbf{M}_h^1(S)$ with respect to the $\mathbf{L}^2$ inner product on S. Since equation (7.28) is automatically fulfilled if we take Lagrange multipliers from $\mathbf{M}_h^1(S)$, it is sufficient to consider $\mathbf{M}_h^2(S)$ as Lagrange multiplier space for the defect correction. Then the correction problem is given by

$$\begin{pmatrix} \mathbf{C}_h & \mathbf{B}_{n,h}^T \\ \mathbf{B}_{n,h} & 0 \end{pmatrix} \begin{pmatrix} \mathbf{u}_h \\ \boldsymbol{\nu}_h \end{pmatrix} = \begin{pmatrix} \mathbf{r}_h \\ 0 \end{pmatrix} \ , \tag{7.29}$$

where $\mathbf{B}_{n,h}$ denotes the matrix associated with the bilinear form $b_h(\cdot,\cdot)$ restricted to $\mathbf{grad}\, S_h \times \mathbf{M}_h^2(S)$. Resulting from the definition of $\mathbf{M}_h^2(S)$, the bilinear form $b_h(\cdot,\cdot)$ restricted to $S_h \times \mathbf{M}_h^2(S)$ fulfills an inf-sup condition, which guarantees the existence and uniqueness of a solution of (7.29).

We are now in a position to state the hybrid iterative process with respect to the mortar edge element approximation of the eddy current equations:

Step 1: Iterative sweeps on the mortar edge element discretized problem

Compute $(\mathbf{q}_h^{(\mu_1)}, \boldsymbol{\mu}_h^{(\mu_1)})$ by applying $\mu_1 > 0$ preconditioned Richardson iterations to the saddle point problem (7.18):

$$\begin{pmatrix} \mathbf{q}_h^{(k+1)} \\ \boldsymbol{\mu}_h^{(k+1)} \end{pmatrix} = \begin{pmatrix} \mathbf{q}_h^{(k)} \\ \boldsymbol{\mu}_h^{(k)} \end{pmatrix} - \tag{7.30}$$
$$- \begin{pmatrix} \mathbf{P}_{e,h} & \mathbf{B}_{e,h}^T \\ \mathbf{B}_{e,h} & 0 \end{pmatrix}^{-1} \left\{ \begin{pmatrix} \mathbf{A}_h & \mathbf{B}_{e,h}^T \\ \mathbf{B}_{e,h} & 0 \end{pmatrix} \begin{pmatrix} \mathbf{q}_h^{(k)} \\ \boldsymbol{\lambda}_h^{(k)} \end{pmatrix} - \begin{pmatrix} \mathbf{b}_h \\ 0 \end{pmatrix} \right\} ,$$

where $\mathbf{P}_{e,h} := \mathrm{diag}\,(\mathbf{P}_{e,h}^{(1)}, ..., \mathbf{P}_{e,h}^{(N)})$ with $\mathbf{P}_{e,h}^{(i)}$, $1 \le i \le N$, represent damped Jacobi or Gauss-Seidel sweeps on the subdomain problems. As startiterates we choose $(\mathbf{q}_h^{(0)}, \boldsymbol{\mu}_h^{(0)}) = (\mathbf{u}_h^{(j)}, \boldsymbol{\lambda}_h^{(j)})$ and set $(\mathbf{u}_h^{(j+1/2)}, \boldsymbol{\lambda}_h^{(j+1/2)}) := (\mathbf{q}_h^{(\mu_1)}, \boldsymbol{\mu}_h^{(\mu_2)})$.

Step 2: Defect correction on the irrotational part

Compute $(\boldsymbol{\varphi}_h^{(\mu_2)}, \boldsymbol{\eta}_h^{(\mu_2)})$ by the application of $\mu_2 > 0$ preconditioned Richardson iterations to the defect correction problem (7.27):

$$\begin{pmatrix} \boldsymbol{\varphi}_h^{(k+1)} \\ \boldsymbol{\nu}_h^{(k+1)} \end{pmatrix} = \begin{pmatrix} \boldsymbol{\varphi}_h^{(k)} \\ \boldsymbol{\nu}_h^{(k)} \end{pmatrix} - \tag{7.31}$$
$$- \begin{pmatrix} \mathbf{P}_{n,h} & \mathbf{B}_{n,h}^T \\ \mathbf{B}_{n,h} & 0 \end{pmatrix}^{-1} \left\{ \begin{pmatrix} \mathbf{C}_h & \mathbf{B}_{n,h}^T \\ \mathbf{B}_{n,h} & 0 \end{pmatrix} \begin{pmatrix} \boldsymbol{\varphi}_h^{(k)} \\ \boldsymbol{\nu}_h^{(k)} \end{pmatrix} - \begin{pmatrix} \mathbf{r}_h^{(j+1/2)} \\ 0 \end{pmatrix} \right\} ,$$

where $\mathbf{P}_{n,h} := \mathrm{diag}\,(\mathbf{P}_{n,h}^{(1)}, ..., \mathbf{P}_{n,h}^{(N)})$ with $\mathbf{P}_{n,h}^{(i)}$, $1 \le i \le N$, are damped Jacobi or Gauss-Seidel sweeps on the defect correction problems associated with the individual subdomains and $\mathbf{r}_h^{(k+1/2)}$ is the vector representing $r_h(\cdot)$ with $\mathbf{u}_h$ replaced by $\mathbf{u}_h^{(j+1/2)}$. Moreover, we choose $(\boldsymbol{\varphi}_h^{(0)}, \boldsymbol{\nu}_h^{(0)}) = (0, 0)$ as startiterates.

Step 3: Additive correction

Denoting by $\mathbf{v}_h$ the vector representing the embedding of $\mathbf{grad}\, \varphi_h^{(\mu_2)}$, $\varphi_h^{(\mu_2)} \in S_h$, into the space $\mathbf{V}_h$, set

$$\mathbf{u}_h^{(j+1)} := \mathbf{u}_h^{(j+1/2)} + \mathbf{v}_h \ ,$$
$$\boldsymbol{\lambda}_h^{(j+1)} := \boldsymbol{\lambda}_h^{(j+1/2)} + \boldsymbol{\nu}_h^{(\mu_2)} \ .$$

Since the Schur complements of (7.30) and (7.31) are given by

$$\begin{aligned} \mathbf{S}_{e,h} &= \mathbf{B}_{e,h}\mathbf{P}_{e,h}^{-1}\mathbf{B}_{e,h}^{T} \\ \text{and} \quad \mathbf{S}_{n,h} &= \mathbf{B}_{n,h}\mathbf{P}_{n,h}^{-1}\mathbf{B}_{n,h}^{T} \ , \end{aligned}$$

we have to compute $\mathbf{P}_{e,h}^{-1}$ and $\mathbf{P}_{n,h}^{-1}$ for the solution of the corresponding Schur complement systems, which can be very costly. From a computational point of view, a significant simplification of the Schur complement can be achieved if we use a nondiagonal preconditioner only for the unknowns associated with edges (Step 1) and grid points (Step 2) in the interior of the subdomains, whereas we apply a diagonal preconditioner on the skeleton of the decomposition.

Splitting the unknowns $\mathbf{u}_h$ and $\boldsymbol{\varphi}_h$ into blocks associated with the unknowns in the interior of the subdomains and those situated on the skeleton, this simplification results in the solution of block systems of the form

$$\begin{pmatrix} \tilde{\mathbf{P}}_{e,h} & 0 & 0 \\ 0 & \alpha_1 \mathbf{Id}_h & \tilde{\mathbf{B}}_{e,h}^{T} \\ 0 & \tilde{\mathbf{B}}_{e,h} & 0 \end{pmatrix} \begin{pmatrix} \mathbf{u}_h^{(\mathbf{I})} \\ \mathbf{u}_h^{(\mathbf{S})} \\ \boldsymbol{\lambda}_h \end{pmatrix} = \begin{pmatrix} \mathbf{b}_h^{(\mathbf{I})} \\ \mathbf{b}_h^{(\mathbf{S})} \\ 0 \end{pmatrix} \tag{7.32}$$

and

$$\begin{pmatrix} \tilde{\mathbf{P}}_{n,h} & 0 & 0 \\ 0 & \alpha_2 \mathbf{Id}_h & \tilde{\mathbf{B}}_{n,h}^{T} \\ 0 & \tilde{\mathbf{B}}_{n,h} & 0 \end{pmatrix} \begin{pmatrix} \boldsymbol{\varphi}_h^{(\mathbf{I})} \\ \boldsymbol{\varphi}_h^{(\mathbf{S})} \\ \boldsymbol{\eta}_h \end{pmatrix} = \begin{pmatrix} \mathbf{r}_h^{(\mathbf{I})} \\ \mathbf{r}_h^{(\mathbf{S})} \\ 0 \end{pmatrix} \ . \tag{7.33}$$

When solving (7.32) and (7.33), we are faced with the solution of Schur complement systems with the Schur complements

$$\tilde{\mathbf{S}}_{e,h} := \boldsymbol{\alpha}_1^{-1}\tilde{\mathbf{B}}_{e,h}\,\tilde{\mathbf{B}}_{e,h}^{T} \ , \tag{7.34}$$

$$\tilde{\mathbf{S}}_{n,h} := \boldsymbol{\alpha}_2^{-1}\tilde{\mathbf{B}}_{n,h}\,\tilde{\mathbf{B}}_{n,h}^{T} \ . \tag{7.35}$$

As shown in [BD98], the fact that both $\tilde{\mathbf{B}}_{e,h}$ and $\tilde{\mathbf{B}}_{n,h}$ fulfill inf-sup conditions imply the existence of constants $C_i > 0$, $1 \le i \le 2$, independent of the subdomain triangulations and the number of subdomains such that the spectral condition numbers $\kappa(\tilde{\mathbf{B}}_{e,h}\,\tilde{\mathbf{B}}_{e,h}^{T})$ and $\kappa(\tilde{\mathbf{B}}_{n,h}\,\tilde{\mathbf{B}}_{n,h}^{T})$ are bounded by

$$\kappa(\tilde{\mathbf{B}}_{e,h}\,\tilde{\mathbf{B}}_{e,h}^{T}) \le C_1 \ , \tag{7.36}$$

$$\kappa(\tilde{\mathbf{B}}_{n,h}\,\tilde{\mathbf{B}}_{n,h}^{T}) \le C_2 \ . \tag{7.37}$$

Therefore, the Schur complement systems encountered in the smoothing steps can be efficiently solved by a conjugate gradient iteration.

Assuming that the problem is $\mathbf{H}^2$-regular in the sense that for given $\mathbf{f} \in \mathbf{L}^2(\Omega)$ the solution $\mathbf{u}$ is an element of $\mathbf{H}^2(\Omega) \cap \mathbf{H}_0(\mathbf{curl}; \Omega)$, a smoothing and an approximation property can be established by following the steps described in [BDW00]

and applying classical multigrid convergence theory combined with duality arguments for nonconforming finite element approximations.

These properties assure the multigrid convergence of W-cycles with a convergence rate that is independent of the number of subdomains, the number of levels in the hierarchies of triangulations, and the granularities of the triangulations [Hac85] if sufficiently many smoothing steps are chosen. However, in most practical realizations multigrid iterations with V-cycles and only a few smoothing steps show a better performance [BDW00].

Chapter 8

Numerical Results

In Chapter 6 we showed that the error estimator provides a norm equivalence for the true error with constants that depend on the domain Ω, the physical coefficients β and χ, and the shape regularity of the triangulations. Moreover, in Chapter 7 we developed a multigrid iterative scheme with a convergence rate which is independent of the number of levels. However, there is no information about the actual size of these constants or about the convergence rate. Additionally, we had to make assumptions on the solution and the domain that are not met in many cases relevant for practical applications.

Since the performance of the error estimator and the multigrid scheme is determined by these constants, it is desirable to know more about them. In many cases we will not be able to find values for these constants or for the convergence rate theoretically. To offset these shortcomings, we have to demonstrate the performance of the error estimator and the multigrid scheme by actual computations. Of course we are not able to cover the whole range of electromagnetic problems with our test problems. Therefore, we will present a variety of typical settings, confirm the validity of the methods, and give information about the constants for these problems.

8.1 Multigrid Convergence

We first study the convergence of V(1,1)-cycles applied to (4.28). For simplicity, we start with experiments carried out on the domain Ω with $\bar{\Omega} = \bar{\Omega}_m \cup \bar{\Omega}_s$, where $\Omega_m = (0,1)^3$ is the master and $\Omega_s = (1,2) \times (0,1)^2$ the slave domain (cf. Figure 8.1). Each domain is equipped with a uniform tetrahedral mesh. Moreover, in order to comply with the compatibility condition on the triangulations at the interface, we choose the initial triangulations such that the triangulation of the slave interface is a regular refinement of the master triangulation, i.e. we have $h_m = 2h_s$.

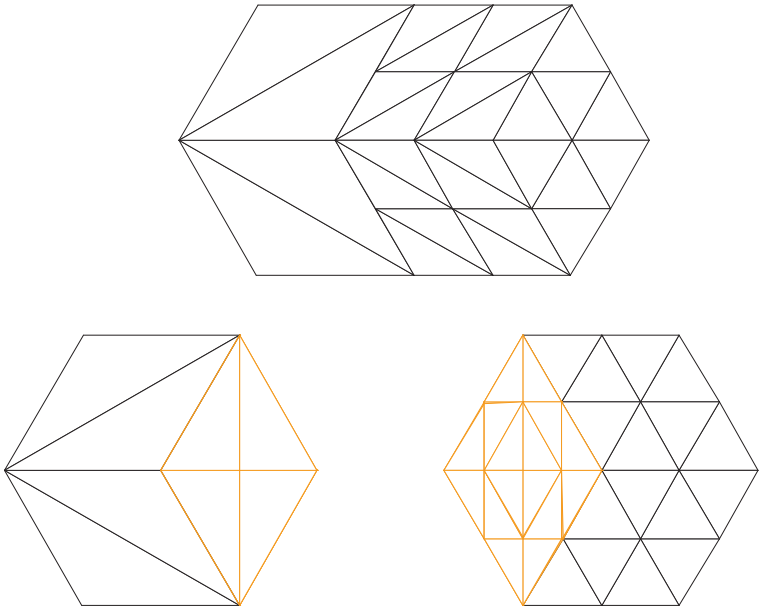

Figure 8.1: Initial triangulation of the computational domain for Experiments 1 to 5. The triangulation of the slave interface (right) is a regular refinement of the triangulation of the master interface (left).

The coarsest grid $\mathcal{T}_0$ consists of 26 tetrahedra, which are successively regularly refined to create the hierarchy of triangulations $\mathcal{T}_1$, ... , $\mathcal{T}_L$. Since we use linear finite elements for the discretization of the problem, it is sufficient to use Gaussian quadrature of order 2 for the computation of the stiffness matrix.

We set the right hand side $\mathbf{f} = 0$ and impose homogenous Dirichlet boundary conditions on $\partial\Omega$. The rate of convergence is determined from the reduction of the Euclidian norm of the residual in the last of 30 multigrid iterations, i.e. we set

$$\rho_L := \frac{\|r_L^{30}\|}{\|r_L^{29}\|} .$$

To prevent results depending on the startiterate we use a random guess for the startiterate and present the average rate of two runs in each experiment.

Experiment 1 (V(1,1)-Multigrid with full split preconditioner)
As mentioned in Chapter 3, the values of β are determined by the conductivity σ and the timestep τ. In computations we have to face problems with both small and big values for σ and τ. To address this we investigate the influence of the relative scaling of different parts of the bilinear form and set the coefficients $\chi \equiv 1$ and $\beta = const$, but vary the ratio χ/β.

For the solution of (4.28) we apply multigrid V(1,1)-cycles using the full split preconditioner, given by (7.30) and (7.31), for pre- and postsmoothing and as

iterative solver on the lowest level. In both steps of the smoother symmetric Gauss-Seidel sweeps are used for $\mathbf{P}_h^{(1)}$ and $\mathbf{P}_h^{(2)}$. In each smoothing iteration the computationally most costly process is the solution of the Schur complement system. The best way to minimize this hidden cost is to solve the Schur complement system by preconditioned conjugate gradient iterations. Since it would be to expensive to assemble the Schur complement matrices $\mathbf{S}_{e,h}$ and $\mathbf{S}_{n,h}$, we have to use a simplification of $\mathbf{S}_{e,h}$ and $\mathbf{S}_{n,h}$ for preconditioning. Setting

$$\mathbf{D}_{e,h} := \mathrm{diag}(\mathbf{A}_h) \ ,$$
$$\mathbf{D}_{n,h} := \mathrm{diag}(\mathbf{C}_h) \ ,$$

we approximate $\mathbf{S}_{e,h}$ and $\mathbf{S}_{n,h}$ by

$$\tilde{\mathbf{D}}_{e,h}^{(1)} := \mathbf{B}_{e,h}\mathbf{D}_{e,h}^{-1}\mathbf{B}_{e,h}^T \ , \tag{8.1}$$
$$\tilde{\mathbf{D}}_{n,h}^{(1)} := \mathbf{B}_{n,h}\mathbf{D}_{n,h}^{-1}\mathbf{B}_{n,h}^T \ , \tag{8.2}$$

and use a symmetric Gauss-Seidel step on $\tilde{\mathbf{D}}_{e,h}^{(1)}$ and $\tilde{\mathbf{D}}_{n,h}^{(1)}$ as preconditioner. The convergence rates of the multigrid V(1,1)-cycle are given in Table 8.1.

Level	2	3	4	5
$\beta = 10^{-4}$	0.505	0.606	0.657	0.678
$\beta = 10^{-2}$	0.504	0.606	0.657	0.678
$\beta = 1$	0.492	0.601	0.656	0.677
$\beta = 10^{2}$	0.224	0.446	0.578	0.678
$\beta = 10^{4}$	0.212	0.220	0.257	0.310

Table 8.1: Multigrid convergence rates for Experiment 1.

For small values of β the convergence rates quickly saturate for increasing number of levels. For $\beta = 10^2$ and $\beta = 10^4$ this saturation cannot be seen for the considered number of levels. If the number of levels is small, equation (4.28) is dominated by the properties of the matrix $\mathbf{A}_h^\beta$. Since $\beta \gg \chi$ the eigenvalues of $\mathbf{A}_h^\chi$ are relatively small on coarse grids. However, if we increase the number of levels, the eigenvalues of the matrix $\mathbf{A}_h^\chi$ will tend to infinity, while the eigenvalues of $\mathbf{A}_h^\beta$ stay bounded. Thus on coarse grids the convergence rate will be determined by the properties of the matrix $\mathbf{A}_h^\beta$, while on finer grids $\mathbf{A}_h^\chi$ is dominant as in the case of small values of β. Therefore, a saturation of the convergence rates will be observed if we further increase the number of levels. Considering this behaviour, the computations show that the convergence rates are uniformly bounded as predicted in Chapter 7. Moreover, the convergence of the multigrid method is robust with respect to the values of χ/β.

Experiment 2 (V(1,1)-Multigrid without node correction)
To investigate the influence of the additional smoothing in potential space, we use the same setting as in Experiment 1, but apply multigrid V(1,1)-cycles omitting the defect correction on the subspace of irrotational vector fields. The convergence rates of this multigrid method are given in Table 8.2.

Level	2	3	4	5
$\beta = 10^{-4}$	-	-	-	-
$\beta = 10^{-2}$	0.998	0.999	0.999	0.999
$\beta = 1$	0.949	0.979	0.981	0.985
$\beta = 10^{2}$	0.354	0.623	0.872	0.943
$\beta = 10^{4}$	0.257	0.291	0.297	0.394

Table 8.2: Multigrid convergence rates for Experiment 2. "-" indicates that the convergence rate is worse than 0.9999.

As expected from the analysis in Chapter 7, the standard multigrid methods fails for small values of β. However, if β is considerably big and the mesh is not too fine, this multigrid method might still be able to produce satisfactory results. As mentioned in Experiment 1, this is due to the fact that in this case equation (4.28) is dominated by the properties of $\mathbf{A}_h^\beta$. Since $\mathbf{A}_h^\beta$ does not contain a differential operator, multigrid methods which do not take care of the kernel of the **curl**-operator can cope with the problem. However, if we proceed to finer grids, this multigrid method will fail as well.

Experiment 3 (V(1,1)-Multigrid without compatibility condition)
In Chapter 7 we had to introduce a compatibility condition to obtain an efficient smoother for our problem. It is natural to ask if this condition is really necessary. To address this question, we repeat Experiment 1, however, this time we choose the initial triangulation at the interface such that the compatibility condition is not fulfilled. As indicated by Tables 8.1 and 8.2, the performance of the smoother is determined by small values of β. Therefore, we only consider $\beta = 1$ in this experiment. Note that for smaller values of β the results will be even worse. The convergence rates for this experiment are given in Table 8.3. The results show that the compatibility condition is really essential for the smoother.

Although in Experiments 1 and 2 an approximation of the Schur complement is used for preconditioning, it can be extremely time consuming to assemble these matrices. Without parallelization of the assembling routines, a successful application of this multigrid method is limited by the high computational cost needed

Level	2	3	4	5
$\beta = 1$	0.531	0.733	0.877	0.949

Table 8.3: Multigrid convergence rates for Experiment 3.

for the preconditioner. Of course we could use a more simplified Schur complement matrix as preconditioner for the conjugate gradient method. However, this results in an increase of the number of iterative steps needed to solve the Schur complement system. A remedy of this problem is given by replacing the full split preconditioner by its simplified version.

Experiment 4 (V(1,1)-Multigrid with simplified split preconditioner) In order to compare the performance of multigrid cycles based on the simplified split preconditioner with previous results, we repeat Experiment 1, but use the simplified split preconditioner, given by (7.32) and (7.33), for pre- and postsmoothing and as iterative solver on the lowest level. We use symmetric Gauss-Seidel sweeps for $\tilde{\mathbf{P}}_h^{(1)}$ and $\tilde{\mathbf{P}}_h^{(2)}$, whereas we apply a damped Jacobi sweep for the unknowns on the skeleton of the decomposition.

For the solution of the Schur complement systems we use the conjugate gradient method preconditioned by

$$\tilde{\mathbf{D}}_{e,h}^{(2)} := \operatorname{diag}(\tilde{\mathbf{D}}_{e,h}^{(1)}) \quad \text{and} \quad \tilde{\mathbf{D}}_{n,h}^{(2)} := \operatorname{diag}(\tilde{\mathbf{D}}_{n,h}^{(1)}) \ ,$$

respectively. The convergence rates obtained by this multigrid method are given in Table 8.4.

Level	2	3	4	5
$\beta = 10^{-4}$	0.540	0.650	0.729	0.744
$\beta = 10^{-2}$	0.540	0.648	0.720	0.744
$\beta = 1$	0.527	0.626	0.678	0.726
$\beta = 10^{2}$	0.351	0.521	0.613	0.723
$\beta = 10^{4}$	0.320	0.369	0.402	0.463

Table 8.4: Multigrid convergence rates for Experiment 4.

As in Experiment 1, the convergence rates saturate for small values of β, while for bigger values a saturation is not observed for the considered number of levels. However, applying the same arguments as in Experiment 1, the convergence rates will saturate on higher levels as well. Comparing Tables 8.1 and 8.4, we

see that the convergence of the full split preconditioner is not significantly better than the convergence of the simplified split preconditioner. However, if we take into account that the simplified split preconditioner offers more possibilities for parallelization and that solving the Schur complement system is cheaper in this case, it is more efficient to use the simplified split preconditioner.

So far we considered examples with constant coefficients. As mentioned in Section 3.2, problems with discontinuous coefficients β or χ can benefit from the application of mortar methods. Therefore, we will investigate the behaviour of the multigrid method for problems with strongly varying coefficients.

Experiment 5 (Discontinuous coefficient β and χ)
In this experiment we use the same geometric setting as in Experiment 1, but now the coefficients depend on space. We set

$$\beta(\mathbf{x}) := \begin{cases} \beta_0 & , \ \mathbf{x} \in \Omega_s \\ 1 & , \ \mathbf{x} \in \Omega_m \end{cases} , \ \chi(\mathbf{x}) := \begin{cases} \chi_0 & , \ \mathbf{x} \in \Omega_s \\ 1 & , \ \mathbf{x} \in \Omega_m \end{cases} ,$$

and vary χ_0 and β_0. Moreover, in order to compare the full and simplified split preconditioner, we use both preconditioners for the solution of the algebraic equations. The convergence rates for this experiment are given in Table 8.5. The values in parentheses are the convergence rates obtained by the simplified split preconditioner whereas the others are the convergence rates of the full split preconditioner. If we set $\chi|_{\Omega_s} \equiv 1$, $\beta|_{\Omega_s} \equiv 1$, and vary χ and β on Ω_m, we get similar results. Comparing the results of Tables 8.1, 8.4, and 8.5, we see that the convergence rates are almost the same, which shows the robustness of the method with respect to large jumps in the coefficient functions χ and β.

Level		2	3	4	5
$\chi_0 = 1$	$\beta_0 = 10^{-4}$	0.50 (0.53)	0.61 (0.64)	0.66 (0.69)	0.68 (0.74)
$\chi_0 = 1$	$\beta_0 = 10^{-2}$	0.51 (0.53)	0.61 (0.64)	0.66 (0.69)	0.68 (0.74)
$\chi_0 = 1$	$\beta_0 = 10^{2}$	0.23 (0.49)	0.45 (0.59)	0.58 (0.68)	0.68 (0.75)
$\chi_0 = 1$	$\beta_0 = 10^{4}$	0.21 (0.43)	0.34 (0.59)	0.46 (0.68)	0.60 (0.75)
$\chi_0 = 10^{-4}$	$\beta_0 = 1$	0.53 (0.62)	0.63 (0.70)	0.66 (0.72)	0.71 (0.76)
$\chi_0 = 10^{-2}$	$\beta_0 = 1$	0.53 (0.62)	0.63 (0.70)	0.66 (0.71)	0.71 (0.76)
$\chi_0 = 10^{2}$	$\beta_0 = 1$	0.21 (0.48)	0.39 (0.55)	0.52 (0.66)	0.60 (0.70)
$\chi_0 = 10^{4}$	$\beta_0 = 1$	0.28 (0.33)	0.35 (0.53)	0.52 (0.66)	0.60 (0.71)

Table 8.5: Multigrid convergence rates for Experiment 5.

The previous experiments were carried out on a domain with only two subdomains. However, from the practical point of view, it is important to know if the previous results are still obtained for several subdomains. Since the results of the previous experiments indicate that the simplified split preconditioner is the method of choice, we will in the following only consider multigrid V(1,1)-cycles based on this smoother.

Experiment 6 (Continuously varying χ)
In this experiment we consider the domain

$$\bar{\Omega} = \bar{\Omega}_{s_1} \cup \bar{\Omega}_{s_2} \cup \bar{\Omega}_{m_1} \cup \bar{\Omega}_{m_2} \ , \tag{8.3}$$

where the slave subdomains are $\Omega_{s_1} = (0,1)^3$ and $\Omega_{s_2} = (1,2)^2 \times (0,1)$ and the master subdomains are $\Omega_{m_1} = (1,2) \times (0,1)^2$ and $\Omega_{m_2} = (0,1) \times (1,2) \times (0,1)$ (cf. Figure 8.2). For the initial triangulation we choose $h_s := h_{s_1} = h_{s_2}$ and $h_m := h_{m_1} = h_{m_2}$ and require that $h_m = 2h_s$. Moreover, the triangulations of the slave interfaces are a refinement of the corresponding triangulations of the master interface. The initial triangulation consists of 108 tetrahedra.
We set $\beta \equiv 1$, whereas the other coefficient χ is given by

$$\chi(\mathbf{x}) = 1.5 + \sin(2\pi x_1)\sin(2\pi x_2)\sin(2\pi x_3) \ .$$

Again we choose a zero right hand side and use random guesses for the startiterate. The results of this experiment are documented in Table 8.6.

Experiment 7 (Continuously varying β)
We repeat the last experiment, however, this time we set $\chi \equiv 1$ and

$$\beta(\mathbf{x}) = 1.5 + \sin(2\pi x_1)\sin(2\pi x_2)\sin(2\pi x_3) \ .$$

The convergence rates are given in Table 8.6.

Comparing the convergence rates of Table 8.6 with the previous results, we see that the performance of the smoother does not depend much on the number of subdomains.

Level	2	3	4	5
Experiment 6	0.74	0.76	0.77	0.77
Experiment 7	0.71	0.73	0.74	0.74

Table 8.6: Multigrid convergence rates for Experiments 6 and 7.

To finish the experiments for the multigrid convergence, we consider irregularly shaped domains and locally refined unstructured meshes.

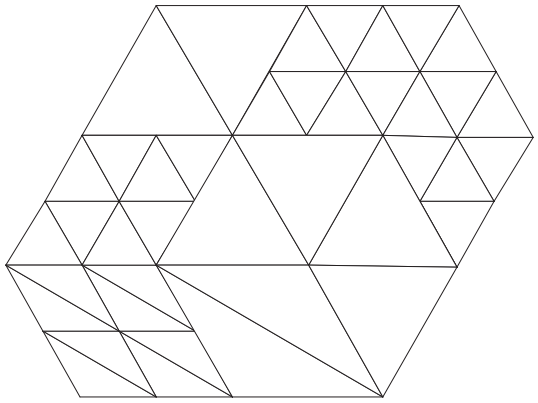

Figure 8.2: Initial triangulation of the computational domain for Experiments 6 and 7.

Experiment 8 (Uniformly refined "L-shaped" domain)
In this experiment we consider the three-dimensional nonconvex "L-shaped" domain

$$\bar{\Omega} = \bar{\Omega}_s \cup \bar{\Omega}_{m_1} \cup \bar{\Omega}_{m_2} \ ,$$

where the slave domain is $\Omega_s = (0,1)^3$ and the master domains are $\Omega_{m_1} = (1,2) \times (0,1)^2$ and $\Omega_{m_2} = (0,1) \times (1,2) \times (0,1)$. For the initial triangulation we choose $h_m := h_{m_1} = h_{m_2}$ and require that $h_m = 2h_{s_1}$. As in the previous experiments, the triangulations of the slave interfaces are a refinement of the corresponding triangulations of the master interface. The initial triangulation consists of 60 tetrahedra. Figure 8.3 shows the computational domain together with the initial triangulation. We set $\chi \equiv 1$ and choose

$$\beta(\mathbf{x}) = 1.5 + \sin(2\pi x_1)\sin(2\pi x_2)\sin(2\pi x_3) \ .$$

The convergence rates of this experiment are presented in Table 8.7.

Level	2	3	4	5
Experiment 8	0.68	0.70	0.77	0.78
Experiment 9	0.68	0.68	0.73	0.73

Table 8.7: Multigrid convergence rates for Experiments 8 and 9.

Experiment 9 (Locally refined "L-shaped" domain)
This experiment deals with the performance of the multigrid V(1,1)-cycle on locally refined unstructured tetrahedral meshes. We use the same computational

domain and initial triangulation as in the last experiment. Throughout the domain we set χ and β to 1 and employ such boundary conditions and right hand side that the solution is given in cylindrical coordinates by

$$\mathbf{u} = \mathbf{grad}(r^{\frac{2}{3}} \sin(\frac{2}{3}\,\phi + \frac{\pi}{3})) \ .$$

Note that the gradient field $\mathbf{u}$ is both irrotational and divergence-free. Moreover, the solution $\mathbf{u}$ has a singularity along the edge $\{x_1 = 0, x_2 = 0\}$ and does not even belong to $\mathbf{H}^1(\Omega)$. The hierarchy of triangulations is obtained by adaptive mesh refinement based on the error estimator of Chapter 6. However, in order to prevent problems arising from a violation of the compatibility condition, only the slave domain Ω_s is refined. Due to this restriction, most of the refinement takes place near the singular edge and on the interface (see fig. 8.3). Comparing the results of this experiment (cf. Table 8.7) with the previous results, we see that the convergence is not severely affected by local refinement.

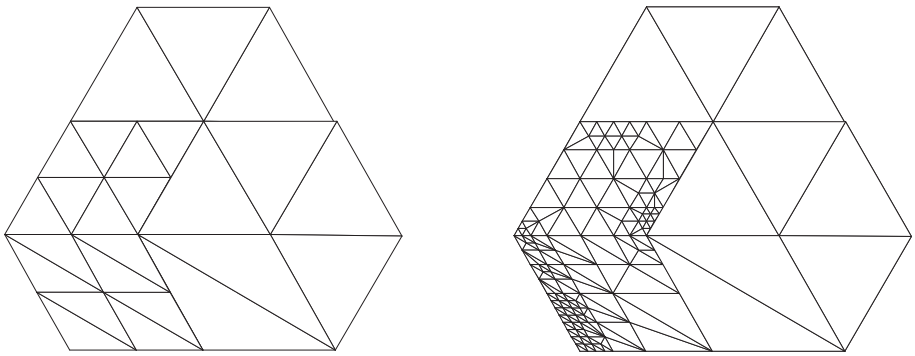

Figure 8.3: Triangulations of the computational domain for Experiments 8 and 9. On the left side the initial triangulation is shown, while the other side displays the grid after adaptive refinement.

8.2 Performance of the Error Estimator

In Chapter 6 we showed that the error estimator provides lower and upper bounds for the true error of the solution. Since we want to use this error estimator for adaptive grid refinement, we split the error estimator into local contributions in order to obtain an estimate for the local error. Following [Ver96, Woh99c] we define for an element T of the triangulation its local error estimate by

$$\hat{\eta}_T^2 := (\eta_T^{(1)})^2 + (\eta_T^{(2)})^2 + \sum_{F \in \mathcal{F}(T) \cap \mathcal{F}_h^{int}(\Omega)} \frac{1}{2} \left((\eta_F^{(1)})^2 + (\eta_F^{(2)})^2 \right) + \tag{8.4}$$
$$+ \sum_{F \in \mathcal{F}(T) \cap \mathcal{F}_h(\delta_k)} \left((\eta_F^{(3)})^2 + (\eta_F^{(4)})^2 \right) + \sum_{F \in \mathcal{F}(T) \cap \mathcal{F}_h(\varrho_k)} (\eta_F^{(5)})^2 \ .$$

Note that the error estimator is given by $\eta^2 = \sum_{i=1}^{N} \sum_{T \in \mathcal{T}_i} \hat{\eta}_T^2$. Based on this local estimate we mark an element T for refinement if

$$\hat{\eta}_T^2 > \sigma \frac{\eta^2}{n_T} \ , \tag{8.5}$$

where n_T denotes the number of elements of the triangulation and $\sigma = 0.95$ is a safety factor. To test the quality of the error estimator and of our adaptive refinement strategy, we introduce different quality measures.

The quality of the error estimate is measured by the effectivity index $\varepsilon := \frac{\eta}{\eta_{True}}$, which is the ratio between the estimated η and the true discretization error η_{True}. Good error estimators are characterized by an effectivity index which rapidly approaches a constant as refinement proceeds. Since the proposed error estimator provides only a norm equivalence of the true error, the effectivity index may be far off the ideal value of 1.

Since we want to use the error estimator for local refinement, we have to know how much our marking based on the local error estimators differs from the ideal marking based on the true error. To address this problem, we introduce the sets

$$\hat{A} := \left\{ T \in \mathcal{T}_h \mid \hat{\eta}_T^2 \geq \sigma \frac{\eta^2}{n_T} \right\} \ ,$$
$$A := \left\{ T \in \mathcal{T}_h \mid \eta_T^2 \geq \sigma \frac{\eta_{True}^2}{n_T} \right\} \ ,$$

where η_T denotes the true local error of the element T and $\mathcal{T}_h$ denotes the global triangulation of Ω. Since $\hat{A}$ is the set of elements that are marked by our refinement strategy and A the set of elements that should have been marked, we define the percentage of incorrect decisions $\mu^{(1)}$ by

$$\mu^{(1)} := \frac{1}{n_T} \# \left\{ (A \cap C\hat{A}) \cup (CA \cap \hat{A}) \right\} .$$

For a good error estimator we have to require that $\mu^{(1)}$ stays bounded well below 1 as refinement proceeds.

Although $\mu^{(1)}$ provides a good measure for the quality of the error estimator, it is important to know how much our refinement strategy is affected by incorrect

decisions. According to the theory presented in Chapter 5, we expect that the refinement of a single element reduces the local error by a factor of 2. Therefore, the total error on the adaptively refined mesh is approximately given by

$$\eta_{new}^2 = \frac{1}{4}\sum_{T\in\hat{A}} \eta_T^2 + \sum_{T\in C\hat{A}} \eta_T^2 \ ,$$

while the "optimal" new error can be expressed as

$$\eta_{opt}^2 = \frac{1}{4}\sum_{T\in A} \eta_T^2 + \sum_{T\in CA} \eta_T^2 \ .$$

Then a measure for the severity of incorrect decisions is given by

$$\mu^{(2)} := \frac{|\eta_{new}^2 - \eta_{opt}^2|}{\eta_{opt}^2} \ .$$

Of course, we have to require that $\mu^{(2)}$ stays bounded well below 1.

One aim of adaptive grid refinement is to obtain an error that is equally distributed on the elements of the triangulation. Therefore, the error estimator must be able to detect local errors and zero in on singularities. Introducing the quantity

$$\mu^{(3)} := \sqrt{\sum_{T\in\mathcal{T}_h} \left(|\Omega_T| \left(\frac{\hat{\eta}_T^2}{\|\hat{\eta}_T^2\|_{L^1}} - \frac{\eta_T^2}{\|\eta_T^2\|_{L^1}} \right) \right)^2} \ ,$$

where

$$\|\eta_T^2\|_{L^1} := \sum_{T\in\mathcal{T}_h} \eta_T^2 |\Omega_T| \quad , \quad \|\hat{\eta}_T^2\|_{L^1} := \sum_{T\in\mathcal{T}_h} \hat{\eta}_T^2 |\Omega_T| \ ,$$

an estimator fails to tell the approximate spatial distribution of the discretization error if $\mu^{(3)}$ is big.

To demonstrate the performance of the error estimator in actual computations, we choose several numerical experiments. In each experiment we use an unstructured tetrahedral grid. For the computation of the stiffness matrix and the right hand side we use Gaussian quadrature of order 5 and interpolate boundary values by the same order. The solution of the algebraic equations is obtained by multigrid V(1,1)-cycles using the simplified split preconditioner as pre- and postsmoother and as basesolver. The iterations are stopped when the Euclidian norm of the residual vector for the current iterate is less than 10^{-10} times the Euclidean norm of the algebraic right hand side.

Following the steps of the last section, we first consider test problems related to different relative scaling of the coefficients χ and β.

Experiment 10 (Performance for varying values of β)
We repeat Experiment 4 and set $\chi \equiv 1$ and keep β constant all over the domain, but vary the value of β. For our computations the boundary data and the right hand side are chosen such that we obtain the smooth solution

$$\mathbf{u}(\mathbf{x}) = (0, \sin(\pi x_1), 0)^T \ .$$

The results of this experiment are reported in Table 8.8.

As expected, the effectivity index does not obtain the ideal value of $\varepsilon = 1$. However, the index reaches a stable limit on finer grids, which indicates that the true error can be estimated by the error estimator. Concerning the quality measures $\mu^{(1)}$, $\mu^{(2)}$, and $\mu^{(3)}$, we see that the error estimates shows the properties of a good error estimator. Moreover, the performance is not severely affected by different values of β.

Experiment 11 (Performance for strongly discontinuous values of β)
This experiment considers a strongly discontinuous coefficient function β. Using the same setting as in the previous experiment, we set $\chi \equiv 1$ and

$$\beta(\mathbf{x}) := \begin{cases} \beta_0 & , \ \mathbf{x} \in \Omega_s \\ 1 & , \ \mathbf{x} \in \Omega_m \end{cases} \ .$$

The quality measures for this experiment are given in Table 8.9. Comparing Tables 8.8 and 8.9, we see that the proposed error estimator behaves equally well, which shows that the error estimator is hardly affected by strongly discontinuous values of β.

Experiment 12 (Performance for solenoidal solution)
In order to address problems with solenoidal solutions, we repeat Experiment 10. However, this time we employ boundary conditions and right hand side such that the smooth solenoidal solution

$$\mathbf{u} = \mathbf{curl}(\sin(\pi x_2 x_3), \sin(\pi x_1 x_3), \sin(\pi x_1 x_2))^T$$

is generated. The quality measures of this experiment (cf. Table 8.10) indicate that the error estimator is insensitive to solenoidal solutions.

Experiment 13 (Performance for irrotational solution)
For this experiment we consider the same geometric setting as in the last experiment but choose the boundary conditions and the right hand side such that we obtain the smooth irrotational solution

$$\mathbf{u} = \mathbf{grad}(x_1 x_2 x_3) \ .$$

The quality measures of this experiment are recorded in Table 8.11. Again, the measures reflect the behaviour of a good error estimator, which shows that the error estimator is able to cope with irrotational solutions.

Level	2	3	4	5
Effectivity index ε				
$\beta = 10^{-4}$	6.40	7.62	7.75	7.85
$\beta = 10^{-2}$	6.40	7.60	7.73	7.82
$\beta = 1$	5.07	7.43	7.52	7.60
$\beta = 10^{2}$	3.41	4.58	5.05	5.34
$\beta = 10^{4}$	8.13	5.44	4.99	5.05
Percentage of incorrect decisions $\mu^{(1)}$				
$\beta = 10^{-4}$	0.077	0.051	0.045	0.047
$\beta = 10^{-2}$	0.077	0.051	0.046	0.048
$\beta = 1$	0.137	0.042	0.047	0.049
$\beta = 10^{2}$	0.051	0.058	0.055	0.053
$\beta = 10^{4}$	0.239	0.112	0.063	0.051
Severity of incorrect decisions $\mu^{(2)}$				
$\beta = 10^{-4}$	0.035	0.0082	0.0116	0.0169
$\beta = 10^{-2}$	0.035	0.0082	0.0078	0.013
$\beta = 1$	0.13	0.016	0.00073	0.00039
$\beta = 10^{2}$	0.038	0.031	0.025	0.039
$\beta = 10^{4}$	0.68	0.17	0.024	0.015
Detection of local errors $\mu^{(3)}$				
$\beta = 10^{-4}$	0.11	0.076	0.023	0.0078
$\beta = 10^{-2}$	0.11	0.076	0.023	0.0077
$\beta = 1$	0.11	0.073	0.022	0.0076
$\beta = 10^{2}$	0.20	0.088	0.026	0.0082
$\beta = 10^{4}$	0.74	0.10	0.027	0.0079

Table 8.8: Quality measures for Experiment 10.

In the previous experiments we considered regularly shaped domains with only two subdomain and piecewise constant coefficients. However, it is important to know how the performance changes if the domain consists of several subdomains. Moreover, the case of less regularly shaped domains and coefficients which are not piecewise constant is not covered by the theoretical analysis.

Level	2	3	4	5
Effectivity index ε				
$\beta_0 = 10^{-4}$	5.07	7.47	7.57	7.65
$\beta_0 = 10^{-2}$	5.07	7.47	7.57	7.65
$\beta_0 = 10^{2}$	4.18	5.60	5.89	6.06
$\beta_0 = 10^{4}$	7.33	5.00	5.04	5.15
Percentage of incorrect decisions $\mu^{(1)}$				
$\beta_0 = 10^{-4}$	0.094	0.041	0.046	0.047
$\beta_0 = 10^{-2}$	0.094	0.041	0.046	0.047
$\beta_0 = 10^{2}$	0.14	0.094	0.080	0.061
$\beta_0 = 10^{4}$	0.30	0.12	0.07	0.056
Severity of incorrect decisions $\mu^{(2)}$				
$\beta_0 = 10^{-4}$	0.090	0.018	0.0049	0.0044
$\beta_0 = 10^{-2}$	0.090	0.018	0.0049	0.0043
$\beta_0 = 10^{2}$	0.095	0.18	0.11	0.076
$\beta_0 = 10^{4}$	0.65	0.15	0.054	0.034
Detection of local errors $\mu^{(3)}$				
$\beta_0 = 10^{-4}$	0.11	0.073	0.022	0.0076
$\beta_0 = 10^{-2}$	0.11	0.073	0.022	0.0076
$\beta_0 = 10^{2}$	0.082	0.072	0.022	0.0073
$\beta_0 = 10^{4}$	2.07	0.10	0.011	0.0034

Table 8.9: Quality measures for Experiment 11.

Experiment 14 (Continuously varying coefficient χ)
In order to study the performance of the error estimator on several subdomains, we repeat Experiment 6. Recall that for this experiment $\beta = 1$, whereas χ is given by

$$\chi(\mathbf{x}) = 1.5 + \sin(2\pi x_1)\sin(2\pi x_2)\sin(2\pi x_3) \ .$$

As in Experiment 10, we choose the boundary conditions and the right hand side such that we obtain the smooth solution

$$\mathbf{u}(\mathbf{x}) = (0, \sin(\pi x_1), 0)^T \ .$$

Level	2	3	4	5
Effectivity index ε				
$\beta = 10^{-4}$	5.24	6.86	7.55	7.65
$\beta = 10^{-2}$	7.59	7.47	7.57	7.65
$\beta = 1$	7.59	7.40	7.47	7.55
$\beta = 10^{2}$	3.56	4.39	4.99	5.51
$\beta = 10^{4}$	6.55	4.68	4.77	4.92
Percentage of incorrect decisions $\mu^{(1)}$				
$\beta = 10^{-4}$	0.11	0.13	0.12	0.10
$\beta = 10^{-2}$	0.23	0.13	0.12	0.10
$\beta = 1$	0.17	0.13	0.11	0.099
$\beta = 10^{2}$	0.25	0.12	0.084	0.078
$\beta = 10^{4}$	0.35	0.14	0.091	0.079
Severity of incorrect decisions $\mu^{(2)}$				
$\beta = 10^{-4}$	0.074	0.12	0.084	0.063
$\beta = 10^{-2}$	0.26	0.12	0.084	0.063
$\beta = 1$	0.17	0.11	0.076	0.057
$\beta = 10^{2}$	0.15	0.041	0.041	0.023
$\beta = 10^{4}$	1.12	0.14	0.052	0.038
Detection of local errors $\mu^{(3)}$				
$\beta = 10^{-4}$	0.14	0.050	0.023	0.010
$\beta = 10^{-2}$	0.14	0.057	0.023	0.010
$\beta = 1$	0.18	0.055	0.023	0.0097
$\beta = 10^{2}$	0.18	0.085	0.028	0.0082
$\beta = 10^{4}$	1.78	0.12	0.030	0.0084

Table 8.10: Quality measures for Experiment 12.

The quality measures, given in Table 8.12, show qualitatively the same behaviour as in the previous experiments. This shows that the error estimator performs equally well for this setting.

Level	2	3	4	5
Effectivity index ε				
$\beta = 10^{-4}$	4.67	5.19	5.26	4.85
$\beta = 10^{-2}$	4.67	5.19	5.29	5.26
$\beta = 1$	4.75	5.22	5.29	5.27
$\beta = 10^{2}$	4.63	5.04	5.25	5.31
$\beta = 10^{4}$	7.28	5.33	5.13	5.16
Percentage of incorrect decisions $\mu^{(1)}$				
$\beta = 10^{-4}$	0.12	0.089	0.089	0.10
$\beta = 10^{-2}$	0.12	0.089	0.089	0.086
$\beta = 1$	0.12	0.088	0.089	0.086
$\beta = 10^{2}$	0.094	0.090	0.088	0.084
$\beta = 10^{4}$	0.21	0.10	0.085	0.082
Severity of incorrect decisions $\mu^{(2)}$				
$\beta = 10^{-4}$	0.084	0.082	0.042	0.14
$\beta = 10^{-2}$	0.084	0.082	0.044	0.040
$\beta = 1$	0.086	0.080	0.043	0.041
$\beta = 10^{2}$	0.013	0.030	0.031	0.034
$\beta = 10^{4}$	0.33	0.061	0.037	0.035
Detection of local errors $\mu^{(3)}$				
$\beta = 10^{-4}$	0.27	0.063	0.034	0.012
$\beta = 10^{-2}$	0.27	0.063	0.035	0.013
$\beta = 1$	0.25	0.060	0.034	0.013
$\beta = 10^{2}$	0.20	0.051	0.031	0.012
$\beta = 10^{4}$	0.65	0.057	0.029	0.010

Table 8.11: Quality measures for Experiment 13.

Experiment 15 (Continuously varying coefficient β)
We repeat the last experiment, however, this time we exchange the roles of the coefficients. We set $\chi \equiv 1$,

$$\beta(\mathbf{x}) = 1.5 + \sin(2\pi x_1)\sin(2\pi x_2)\sin(2\pi x_3) \ ,$$

and choose the same solution as in the last experiment. The results of this experiment are given in Table 8.13. Again, the error estimator performs satisfactorily.

Level	2	3	4	5
ε	5.76	7.09	7.22	7.44
$\mu^{(1)}$	0.0	0.0	0.0032	0.0055
$\mu^{(2)}$	0.0	0.0	0.0065	0.011
$\mu^{(3)}$	0.051	0.047	0.015	0.0049

Table 8.12: Quality measures for Experiment 14.

Level	2	3	4	5
ε	4.54	6.86	7.34	7.41
$\mu^{(1)}$	0.0	0.0	0.0032	0.0024
$\mu^{(2)}$	0.0	0.0	0.0086	0.0065
$\mu^{(3)}$	0.085	0.052	0.016	0.0054

Table 8.13: Quality measures for Experiment 15.

In all previous experiments we used a rather smooth solution for our tests. Therefore, we cannot expect that adaptive refinement will show superior results compared to adaptive refinement. However, problems with singular solutions should greatly benefit from adaptive refinement, since only the singular regions should be refined in this case.

Experiment 16 (Singular solution on "L-shaped" domain)
In Experiment 9 we considered the three-dimensional nonconvex "L-shaped" domain

$$\bar{\Omega} = [0,1]^3 \cup [1,2] \times [0,1]^2 \cup [0,1] \times [1,2] \times [0,1] \ ,$$

together with the singular solution (in cylindrical coordinates)

$$\mathbf{u} = \mathbf{grad}(r^{\frac{2}{3}} \sin(\frac{2}{3}\,\phi + \frac{\pi}{3})) \ .$$

In [BHHW00] it was shown that in the conforming case adaptive grid refinement results in a great reduction of the computational cost. Therefore, we repeat this experiment in order to test the quality of the error estimator.

As mentioned in Experiment 9, adaptive grid refinement poses a severe problem on the convergence of the multigrid scheme, since we have to make sure that the

compatibility condition on the interface triangulation is fulfilled. At the moment it is not possible to obey this condition without reducing the performance of the error estimator considerably. However, in order to show the qualities of the error estimator, we modify the setting of Experiment 9. Since the solution is singular at the edge $\{x_1 = 0, x_2 = 0\}$, we consider in this experiment the domain

$$\bar{\Omega} = [0,2]^3 \cup [2,4] \times [0,2]^2 \cup [0,2] \times [2,4] \times [0,2] \ ,$$

and use an initial triangulation with matching interface triangulations. By increasing the computational domain we hope to reduce the refinement at the interfaces. Moreover, for the solution of the algebraic equations we use the conjugate gradient method preconditioned by the multigrid V(1,1)-cycle. Surprisingly, it turned out that an average of 16 iterations is enough to reduce the Euclidean norm of the initial residual by a factor of 10^{-10}, although the multigrid method itself performs poorly.

In the first part of the experiment we use an initial triangulation consisting of 294 triangles and refine the grid uniformly. The quality measures for this experiment are presented in Table 8.14 (top). For the second part of this experiment we use the same initial triangulation, however, this time the grid is adaptively refined by the error estimator. Figure 8.4 displays the initial triangulation and the triangulation after 5 refinement steps. Note that most of the refinement takes place in the slave domain. Table 8.14 (bottom) shows the quality measures in this case. The results of this experiment indicate that we can rely on the error estimator in both cases.

Level	2	3	4	5
Uniform refinement				
ε	4.24	4.06	4.05	4.25
$\mu^{(1)}$	0.25	0.094	0.022	0.0050
$\mu^{(2)}$	0.016	0.0060	0.016	0.0034
$\mu^{(3)}$	0.16	0.13	0.070	0.034
Adaptive refinement				
ε	4.24	4.00	4.19	4.17
$\mu^{(1)}$	0.25	0.13	0.094	0.050
$\mu^{(2)}$	0.016	0.023	0.0050	0.011
$\mu^{(3)}$	0.16	0.053	0.14	0.055

Table 8.14: Quality measures for Experiment 16.

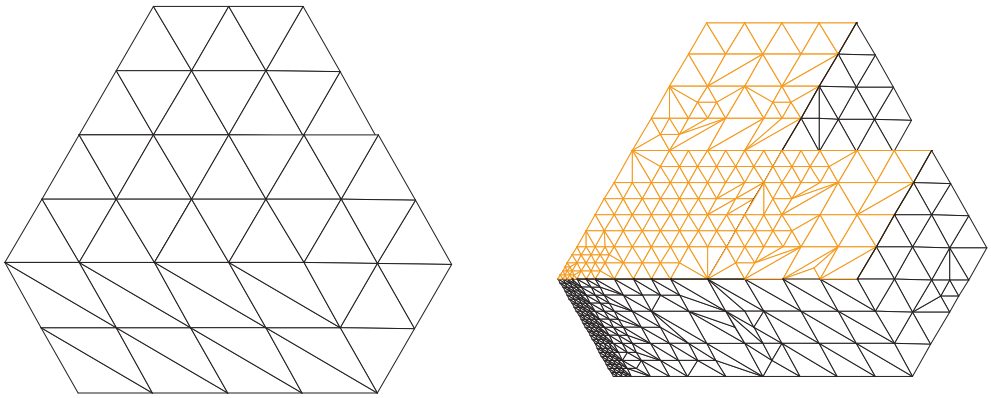

Figure 8.4: Triangulations of the computational domain for Experiment 16. On the left side the initial triangulation is shown, while the other side displays the grid after adaptive refinement.

As mentioned above, the vector field is singular at the edge $\{x_1 = 0, x_2 = 0\}$. Therefore, the error estimator should provide favourable grids and reduce the computational cost considerably. Indeed, Figure 8.5 clearly shows a superior performance if we use adaptive mesh refinement.

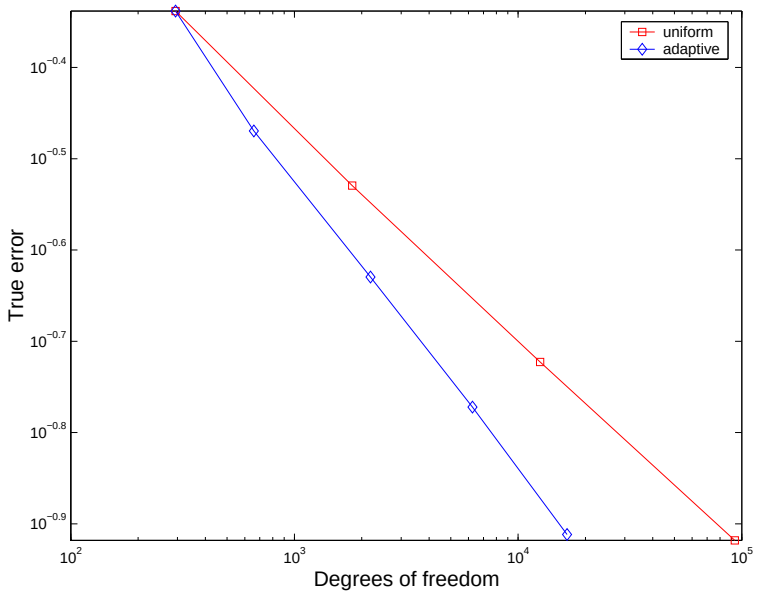

Figure 8.5: True error of the edge element discretization for uniform and adaptive mesh refinement (Exp. 16) measured in the L^2-norm.

8.3 Optimal Convergence of the Discretization

In the last two sections we considered the convergence of the multigrid scheme and the performance of the error estimator by solving several test problems. However, it still remains to be shown that the optimal error estimates for the mortar finite element method (cf. Chapter 5 and [XH05]) can be observed in numerical computations. This is particularly important, since in [BBM02] it is doubted that approximations based on the first family of Nédélec's edge elements show an optimal error estimate.

As in the previous sections, it is not possible to validate this estimate by numerical computations for all problems that fulfill the conditions of Theorem 5.7. Therefore, we resort to the test problems of the last sections, since they address typical situations encountered in eddy current computations. The asymptotic behaviour of the error for Experiments 12, 13, 14, and 15 is presented in Figures 8.6, 8.7, and 8.8, respectively. Note that the other experiments of the last section show similar results. Comparing the error of the numerical experiments with the optimal error estimate ($O(h)$), we see that the error agrees with the optimal error estimate stated in Theorem 5.7.

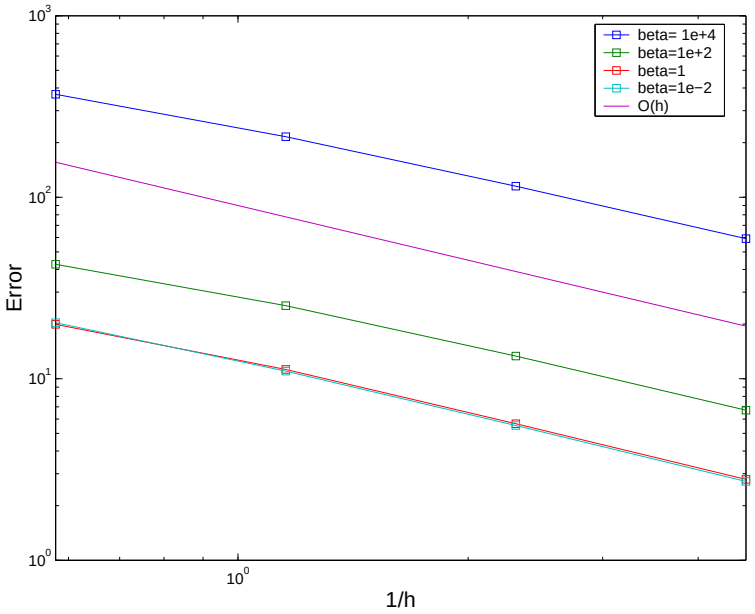

Figure 8.6: Error (in logarithmic scale) of the edge element discretization for Experiment 12. For comparison a line with optimal error $O(h)$ is drawn in the figure.

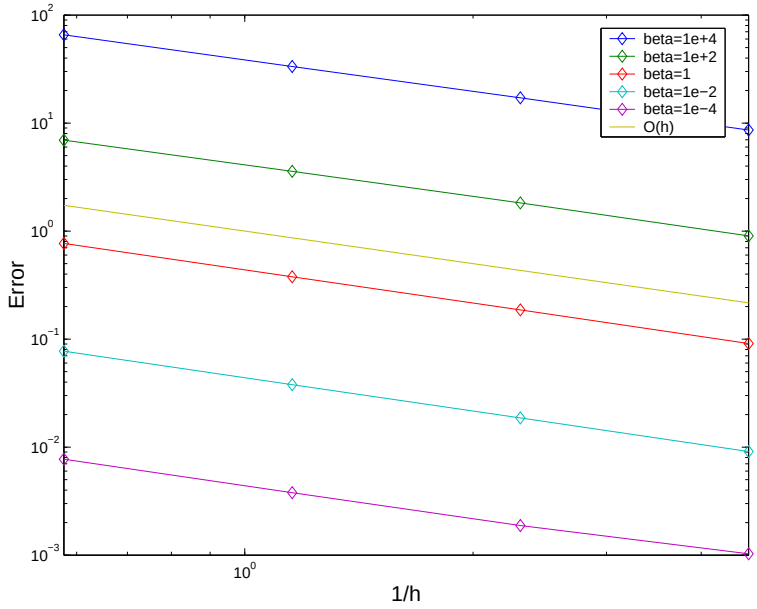

Figure 8.7: Error (in logarithmic scale) of the edge element discretization for Experiment 13. For comparison a line with optimal error $O(h)$ is drawn in the figure.

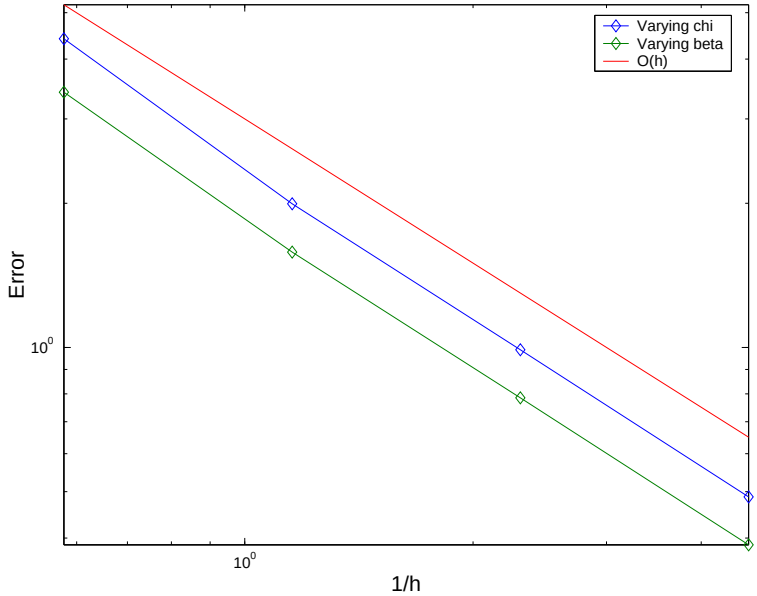

Figure 8.8: Error (in logarithmic scale) of the edge element discretization for Experiments 14 and 15. For comparison a line with optimal error $O(h)$ is drawn in the figure.

Chapter 9

Conclusions

In the first part of this work we presented and analyzed a mortar edge element method for the computation of three-dimensional eddy current problems. We showed that the resulting discrete saddle point problem fulfills an inf-sup condition and therefore has an unique solution. Moreover, we proved that the discrete solution converges to the solution of the continuous problem by establishing an optimal error estimate.

The second part dealt with adaptive multilevel methods for the numerical solution of the mortar edge element discretized eddy current problem. We designed a local a posteriori error estimator and could show that this estimator is both efficient and reliable if several assumptions hold true. However, we point out that these assumptions are not fulfilled in many realistic settings. Although numerical experiments indicate that the error estimator performs satisfactorily beyond the scope of the theoretical analysis, it is desirable to extend the theory to problems with nonconstant coefficients and arbitrarily shaped domains.

For the development of an efficient iterative solver for the solution of the algebraic equations arising from the mortar edge element discretization, we analyzed several approaches. From the theoretical point of view most of these approaches could provide an excellent smoother for a multilevel iterative solver. However, their practical implementation is connected with severe problems which prohibits their realization at the moment. In the end we decided to use a multilevel iterative scheme which is based on a hybrid smoother that takes care of the nontrivial kernel of the discrete **curl**-operator by performing a defect correction on the subspace of irrotational vector fields.

In order to guarantee the efficiency of the solver, we had to impose compatibility conditions on the triangulations of the master and slave interfaces. This poses a serious limitation on the application of the method, since for realistic problems we have to use grid generators which, in general, do not take care of these conditions. A possible remedy for this problem could be given by the construction of new Lagrange multiplier spaces or by considering different matching conditions at

the interfaces. Considering the latter, an interesting approach was proposed in [LVL05]. Its main characteristic is the introduction of an additional set of variables on each subdomain interface together with impedance like transmission conditions. The resulting matrix equation does not have a zero block, which avoids the solution of a Schur complement system.

In order to be able to treat more complex problems, it is advisable to parallelize the iterative method. Especially the computation of a preconditioner for the Schur complement could benefit from parallel routines. Since $\mathcal{UG}$ was designed for parallel computations, it should be possible to parallelize the implemented code without encountering severe problems.

Notation

Domains

Ω	Domain (open and connected) in $\mathbb{R}^d$
$\bar{\Omega}$	Closure of Ω
Ω_e	$:= \mathbb{R}^d \setminus \bar{\Omega}$
Ω_i	subset of Ω
Γ	Boundary of Ω
Γ_i	$:= \partial\Omega_i \cap \partial\Omega$
$\mathbf{n}$	Unit outer normal
S	Skeleton of the decomposition of Ω

General Notation

c, C	Positive constants
$\cdot$	dot product for $\mathbb{R}^d$ and $\mathbb{C}^d$
$\wedge$	vector product for $\mathbb{R}^d$ and $\mathbb{C}^d$
$[\cdot]_\Gamma$	Jump of a vector field along Γ
Re(a)	Real part of the complex number a
Im(a)	Imaginary part of the complex number a
$\forall$	For all
$\ker(L)$	Kernel of the linear mapping L
e_{ij}	Common edge of two adjacent faces Γ_i and Γ_j of an polyhedron
$\varphi_i =_{e_{ij}} \varphi_j$	$\Leftrightarrow \int_{\Gamma_i}\int_{\Gamma_j} \frac{\lvert\varphi(\mathbf{x})-\varphi(\mathbf{y})\rvert^2}{\lVert\mathbf{x}-\mathbf{y}\rVert^3}\, d\sigma(\mathbf{x})\, d\sigma(\mathbf{y}) < \infty$
$\mathcal{I}_i$	$:= \left\{ j \in 1, ..., K \mid \bar{\Gamma}_i \cap \bar{\Gamma}_j = e_{ij} \neq \emptyset \right\}$

Differential Operators

grad	Gradient of a scalar function
div	Divergence of a vector-valued function
curl	Curl of a three-dimensional vector-valued function
$\mathbf{grad}_\Gamma$	Tangential gradient

$\mathbf{curl}_\Gamma$	Tangential curl of a scalar function
div_Γ	Tangential divergence
curl_Γ	Tangential curl of a two-dimensional vector-valued function
$\dot{u}$	Weak time derivative of u

Electromagnetic Quantities

$\mathbf{E}$	Electric field intensity
$\mathbf{H}$	Magnetic field intensity
$\mathbf{D}$	Electric displacement
$\mathbf{B}$	Magnetic induction
$\mathbf{J}$	Current density
ρ	Electric charge density
$\boldsymbol{\epsilon}$	Electric permittivity
$\boldsymbol{\mu}$	Magnetic permeability
$\boldsymbol{\chi}$	$:= \boldsymbol{\mu}^{-1}$
ϵ_0	$= 4\pi \cdot 10^{-7}\ Hm^{-1}$
μ_0	$\approx 8.854 \cdot 10^{-12}\ Fm^{-1}$
$\boldsymbol{\sigma}$	Electric conductivity
ω	Frequency

Trace Operators

$\gamma_0(u)$	$:= u\|_\Gamma$, $u \in H^1(\Omega)$
$\gamma_n(\mathbf{u})$	$:= \mathbf{u}\|_\Gamma \cdot \mathbf{n}$, $\mathbf{u} \in \mathbf{H}(\mathrm{div};\Omega)$
$\gamma_t(\mathbf{u})$	$:= \mathbf{n} \wedge \mathbf{u}\|_\Gamma$, tangential trace
$\gamma_T(\mathbf{u})$	$:= \mathbf{n} \wedge (\mathbf{u} \wedge \mathbf{n})\,\|_\Gamma$, tangential components trace

Function Spaces

$C^m(\Omega)$	Space of m times continuously differentiable functions
$C(\Omega)$	$\equiv C^0(\Omega)$
$C_0^m(\Omega)$	Space of m times continuously differentiable functions with compact support in Ω
$C^\infty(\Omega)$	$:= \bigcap_{m=0}^{\infty} C^m(\Omega)$
$C_0^\infty(\Omega)$	Space of functions $\mathbf{u} \in C^\infty(\Omega)$ with compact support
$C^m(\bar{\Omega})$	$:= \left\{u\|_\Omega \mid u \in C_0^m(\mathbb{R}^d)\right\}$
$L^2(\Omega)$	Space of square Lebesgue-integrable functions on Ω
$\mathbf{L}^2(\Omega)$	$:= (L^2(\Omega))^d$, $d = 2, 3$
X'	Dual space of X

$H^m(\Omega)$	Standard Sobolev space of order m
$\mathbf{H}^m(\Omega)$	$:= (H^m(\Omega))^d$, $d = 2, 3$
$H_0^1(\Omega)$	$:= \{u \in H^1(\Omega) \mid \gamma_0(u) = 0\}$
$H^{1/2}(\Gamma)$	Trace space of $H_0^1(\Omega)$
$H^{-1/2}(\Gamma)$	Dual space of $H^{1/2}(\Gamma)$
$\tilde{u}$	Extension of u defined on $\Sigma \subset \Omega$ to Ω by zero outside Σ
$H_{00}^m(\Sigma)$	$:= \{u \in H^m(\Sigma) \mid \tilde{u} \in H^m(\Omega)\}$, $\Sigma \subset \Omega$
$\mathbf{H}(\mathrm{div};\Omega)$	$:= \{\mathbf{u} \in \mathbf{L}^2(\Omega) \mid \mathrm{div}\,\mathbf{u} \in L^2(\Omega)\}$
$\mathbf{H}_0(\mathrm{div};\Omega)$	$:= \{\mathbf{u} \in \mathbf{H}(\mathrm{div};\Omega) \mid \gamma_n(\mathbf{u}) = 0\}$
$\mathbf{H}(\mathbf{curl};\Omega)$	$:= \{\mathbf{u} \in \mathbf{L}^2(\Omega) \mid \mathbf{curl}\,\mathbf{u} \in \mathbf{L}^2(\Omega)\}$
$\mathbf{H}_0(\mathbf{curl};\Omega)$	$:= \{\mathbf{u} \in \mathbf{H}(\mathbf{curl};\Omega) \mid \gamma_t(\mathbf{u}) = 0\}$
$\mathbf{H}_{\Gamma_0}(\mathbf{curl},\Omega)$	$:= \{\mathbf{u} \in \mathbf{H}(\mathbf{curl};\Omega) \mid \gamma_t(\mathbf{u})\vert_{\Gamma_0} = 0\}$, $\Gamma_0 \subset \Gamma$
$\mathbf{H}^s(\mathbf{curl},\Omega)$	$:= \{\mathbf{u} \in \mathbf{H}^s(\Omega) \mid \mathbf{curl}\,\mathbf{u} \in \mathbf{H}^s(\Omega)\}$
$\mathbf{TH}^{1/2}(\Gamma)$	$:= \{\mathbf{q} : \Gamma \to \mathbb{R}^3 \mid \mathbf{q} = (q_1, q_2, q_3)^T \in \mathbf{H}^{1/2}(\Gamma)\ ,\ \mathbf{n} \cdot \mathbf{q} = 0\}$
$\mathbf{TH}^{-1/2}(\Gamma)$	Dual space of $\mathbf{TH}^{1/2}(\Gamma)$
$\mathbf{TH}_{00}^{1/2}(\Gamma_0)$	$:= \left\{\mathbf{q} \in \mathbf{TH}^{1/2}(\Gamma_0) \mid \tilde{\mathbf{q}} \in \mathbf{TH}^{1/2}(\Gamma)\right\}$, $\Gamma_0 \subset \Gamma$
$\mathbf{TH}^{-1/2}(\Gamma_0)$	Dual space of $\mathbf{TH}_{00}^{1/2}(\Gamma_0)$
$\mathbf{L}_t^2(\Gamma)$	$:= \{\mathbf{u} \in \mathbf{L}^2(\Gamma) \mid \mathbf{u} \cdot \mathbf{n}\vert_\Gamma = 0\}$
$\mathbf{H}_=^{1/2}(\Gamma)$	$:= \left\{\boldsymbol{\lambda} \in \mathbf{L}_t^2(\Gamma) \mid \boldsymbol{\lambda}_j \in \mathbf{H}^{1/2}(\Gamma_j)\ ,\ 1 \le j \le K\right\}$
$\mathbf{H}_\parallel^{1/2}(\Gamma)$	$:= \left\{\mathbf{u} \in \mathbf{H}_=^{1/2}(\Gamma) \mid \mathbf{u}_i \cdot \boldsymbol{\tau}_{ij} =_{e_{ij}} \mathbf{u}_j \cdot \tau_{ij}\ ,\ 1 \le i \le K\ ,\ j \in \mathcal{I}_j\right\}$
$\mathbf{H}_\parallel^{-1/2}(\Gamma)$	Dual space of $\mathbf{H}_\parallel^{1/2}(\Gamma)$
$\mathbf{H}_\perp^{1/2}(\Gamma)$	$:= \left\{\mathbf{u} \in \mathbf{H}_=^{1/2}(\Gamma) \mid \mathbf{u}_i \cdot \boldsymbol{\tau}_i =_{e_{ij}} \mathbf{u}_j \cdot \tau_j\ ,\ 1 \le i \le K\ ,\ j \in \mathcal{I}_j\right\}$
$\mathbf{H}_\perp^{-1/2}(\Gamma)$	Dual space of $\mathbf{H}_\perp^{1/2}(\Gamma)$
$\mathbf{H}_\parallel^{-1/2}(\mathrm{div}_\Gamma,\Gamma)$	$:= \left\{\boldsymbol{\lambda} \in \mathbf{H}_\parallel^{-1/2}(\Gamma) \mid \mathrm{div}_\Gamma\,\boldsymbol{\lambda} \in H^{-1/2}(\Gamma)\right\}$
$\mathbf{H}_\perp^{-1/2}(\mathrm{curl}_\Gamma,\Gamma)$	$:= \left\{\boldsymbol{\lambda} \in \mathbf{H}_\perp^{-1/2}(\Gamma) \mid \mathrm{curl}_\Gamma\,\boldsymbol{\lambda} \in H^{-1/2}(\Gamma)\right\}$
$\mathbf{X}_0$	$:= \{\mathbf{w} \in \mathbf{H}_0(\mathbf{curl};\Omega) \mid (\mathbf{w}, \mathbf{grad}\,p)_{0,\Omega} = 0 \quad \forall p \in H_0^1(\Omega)\}$
$L^p(a,b;\mathbf{B})$	$:= \left\{u : [a,b] \to \mathbf{B} \mid \text{ u is Bochner measurable, } \int_a^b \|u\|^p\,dt < \infty\right\}$
$W(0,T;\mathbf{X})$	$:= \{u \in L^2(0,T;\mathbf{X}) \mid \dot{u} \in L^2(0,T;\mathbf{X}')\}$
$\mathbf{X}$	$:= \{\mathbf{q} \in \mathbf{L}^2(\Omega) \mid \mathbf{q}\vert_{\Omega_i} \in \mathbf{H}_{\Gamma_i}(\mathbf{curl},\Omega_i)\}$
$\mathbf{V}$	$:= \left\{\mathbf{q} \in \mathbf{X} \mid [\mathbf{n} \wedge \mathbf{q}]\vert_{\Gamma_{ij}} \in \mathbf{TH}_{00}^{1/2}(\Gamma_{ij}) \quad \forall\,\Gamma_{ij} \subset S\right\}$
$\mathbf{M}(S)$	$:= \prod_{\Gamma_{ij} \subset S} \mathbf{TH}^{-1/2}(\Gamma_{ij})$

Norms and Products

$\|\cdot\|_{0,p,\Omega}$	$:= \left(\int_\Omega \vert\cdot\vert^p\,dV\right)^{1/p}$

$\|\cdot\|_{m,\Omega}$	$:= \left(\sum_{\|\alpha\|\le m}\int_\Omega \|D_w^\alpha \cdot\|^2\, dV\right)^{1/2}$
$\|\cdot\|_{m,\Omega}$	$:= \left(\sum_{\|\alpha\|= m}\int_\Omega \|D_w^\alpha \cdot\|^2\, dV\right)^{1/2}$
$\|\cdot\|_{H^s_{00}(\Sigma)}$	$:= \|\tilde{\cdot}\|_{s,\Omega}$, $\Sigma \subset \Omega$
$\|\cdot\|_{\mathrm{div},\Omega}$	$:= \left(\|\cdot\|^2_{2,\Omega} + \|\operatorname{div}\cdot\|^2_{2,\Omega}\right)^{1/2}$
$\|\cdot\|_{\mathbf{curl},\Omega}$	$:= \left(\|\cdot\|^2_{2,\Omega} + \|\mathbf{curl}\,\cdot\|^2_{2,\Omega}\right)^{1/2}$
$\|\cdot\|_{s,\mathbf{curl},\Omega}$	$:= \left(\|\cdot\|^2_{s,\Omega} + \|\mathbf{curl}\,\cdot\|^2_{s,\Omega}\right)^{1/2}$
$\|\cdot\|_{\|,1/2,\Gamma}$	Hilbert norm for $\mathbf{H}^{1/2}_{\|}(\Gamma)$
$\|\cdot\|_{\perp,1/2,\Gamma}$	Hilbert norm for $\mathbf{H}^{1/2}_{\perp}(\Gamma)$
$\|\cdot\|_{\|,-1/2,\Gamma}$	Dual norm for $\mathbf{H}^{-1/2}_{\|}(\Gamma)$
$\|\cdot\|_{\perp,-1/2,\Gamma}$	Dual norm for $\mathbf{H}^{-1/2}_{\perp}(\Gamma)$
$\|\cdot\|_{\mathbf{X}}$	$:= \left(\sum_{i=1}^N \|\cdot\|^2_{\mathbf{H}(\mathbf{curl},\Omega_i)}\right)^{1/2}$
$\|\cdot\|_{\mathbf{V}}$	$:= \left(\|\cdot\|^2_{\mathbf{X}} + \|[\mathbf{n}\wedge\cdot]\|^2_{1/2,S}\right)^{1/2}$
$\|\cdot\|_{\mathbf{M}(S)}$	$:= \left(\sum_{\Gamma_{ij}\subset S}\|\cdot\|_{\Gamma_{ij}}\|^2_{-1/2,\Gamma_{ij}}\right)^{1/2}$
$\|\cdot\|_{+\frac{1}{2},h,\gamma_k}$	$:= h^{-1/2}\|\cdot\|_{\gamma_k}\|_{0,\gamma_k}$
$\|\cdot\|_{+\frac{1}{2},h,S}$	$:= (\sum_{\gamma_k\subset S}\|\cdot\|_{\gamma_k}\|^2_{+\frac{1}{2},h,\gamma_k})^{1/2}$
$\|\cdot\|_{\mathbf{V}_h}$	$:= (\|\cdot\|^2_{\mathbf{X}} + \|[\mathbf{n}\wedge\cdot]\|_S\|^2_{+\frac{1}{2},h,S})^{1/2}$
$\|\cdot\|_{-1/2,h,\delta_k}$	$:= h^{1/2}\|\cdot\|_{\delta_k}\|_{0,\delta_k}$
$\|\cdot\|_{\mathbf{M}_h(S)}$	$:= (\sum_{k=1}^M \|\cdot\|^2_{-1/2,h,\delta_k})^{1/2}$
$\|\cdot\|_{a_h}$	$:= a_h(\cdot,\cdot)^{1/2}$
$\|\cdot\|_{L^{-1}}$	$:= (\sum_{k=1}^M \sum_{F\in\mathcal{F}_h(\delta_k)} \frac{\chi_T}{h_F}\|\cdot\|^2_{0,F})^{1/2}$
$(\cdot,\cdot)_{0,\Omega}$	Inner product of $L^2(\Omega)$ and $\mathbf{L}^2(\Omega)$
$(\cdot,\cdot)_{m,\Omega}$	Inner product of $H^m(\Omega)$ and $\mathbf{H}^m(\Omega)$
$(\cdot,\cdot)_{\mathrm{div},\Omega}$	$:= (\cdot,\cdot)_{0,\Omega} + (\operatorname{div}\cdot,\operatorname{div}\cdot)_{0,\Omega}$
$(\cdot,\cdot)_{\mathbf{curl},\Omega}$	$:= (\cdot,\cdot)_{0,\Omega} + (\mathbf{curl}\,\cdot,\mathbf{curl}\,\cdot)_{0,\Omega}$
$<\cdot,\cdot>_X$	Dual pairing between X' and X
$<\cdot,\cdot>_{1/2,\Gamma}$	Dual pairing between $\mathbf{H}^{-1/2}(\Gamma)$ and $\mathbf{H}^{1/2}(\Gamma)$
$<\cdot,\cdot>_{\|,1/2,\Gamma}$	Dual pairing between $\mathbf{H}^{-1/2}_{\|}(\Gamma)$ and $\mathbf{H}^{1/2}_{\|}(\Gamma)$
$<\cdot,\cdot>_{\perp,1/2,\Gamma}$	Dual pairing between $\mathbf{H}^{-1/2}_{\perp}(\Gamma)$ and $\mathbf{H}^{1/2}_{\perp}(\Gamma)$
$<\cdot,\cdot>_{\frac{1}{2},h,\delta_k}$	Dual pairing between $\mathbf{M}_h(\delta_k)'$ and $\mathbf{M}_h(\delta_k)$

Finite Element Discretization

$\mathcal{T}_i$	Triangulation of subdomain Ω_i
$\mathcal{T}_{\delta_k}$	Triangulation of the slave interface
$\mathcal{T}_{\varrho k}$	Triangulation of the master interface
h_i	$:= \max\{\text{diam } T \mid T \in \mathcal{T}_i\}$
h_{δ_k}	$:= \max\{\text{diam } T \mid T \in \mathcal{T}_{\delta_k}\}$
$h_{\varrho k}$	$:= \max\{\text{diam } T \mid T \in \mathcal{T}_{\varrho k}\}$
N	Number of subdomains
M	Number of interfaces
$\mathcal{F}_h(\Sigma)$	Set of faces in Σ
$\mathcal{E}_h(\Sigma)$	Set of edges in Σ
$\mathbf{Nd}_1(T)$	$:= \{\mathbf{q} := \mathbf{a} + \mathbf{b} \wedge \mathbf{x} \mid \mathbf{a}, \mathbf{b} \in \mathbb{R}^3, \mathbf{x} \in T\}$, lowest order edge element of Nédélec's first family
$\mathbf{Nd}_1(\Omega_i; \mathcal{T}_i)$	$:= \{\mathbf{q}_h \in \mathbf{H}(\mathbf{curl}; \Omega_i) \mid \mathbf{q}_h\|_T \in \mathbf{Nd}_1(T),\ T \in \mathcal{T}_i\}$
$\mathbf{Nd}_{1,\Gamma_i}(\Omega_i; \mathcal{T}_i)$	$:= \{\mathbf{q}_h \in \mathbf{Nd}_1(\Omega_i; \mathcal{T}_i) \mid \gamma_t(\mathbf{q}_h)\|_{\Gamma_i} = 0\}$
$S_1(\mathcal{T}_\Omega)$	Space of continuous, piecewise linear functions
$S_{1,0}(\mathcal{T}_\Omega)$	$:= \{q_h \in S_1(\mathcal{T}_\Omega) \mid \gamma_0(q_h)\|_{\Gamma_0} = 0\}$, $\Gamma_0 \subset \partial\Omega$
$S_{1,\Gamma_0}(\mathcal{T}_\Omega)$	$:= \{q_h \in S_1(\mathcal{T}_\Omega) \mid \gamma_0(q_h)\|_{\partial\Omega} = 0\}$
S_h	$:= \{\varphi_h \in L^2(\Omega) \mid \varphi_h\|_{\Omega_i} \in S_{1,\Gamma_i}(\Omega_i; \mathcal{T}_i)\ ,\ 1 \le i \le N\}$
$\mathbf{V}_h$	$:= \{\mathbf{q}_h \in \mathbf{L}^2(\Omega) \mid \mathbf{q}_h\|_{\Omega_i} \in \mathbf{Nd}_{1,\Gamma_i}(\Omega_i; \mathcal{T}_i)\ ,\ 1 \le i \le N\}$
V_h	$:= \{\ v_h \in L^2(\Omega) \mid v_h\|_{\Omega_i} \in S_{1,\Gamma_i}(\Omega_i; \mathcal{T}_i)\ ,\ 1 \le i \le N\}$
$\mathbf{RT}_0(T)$	$:= \{\mathbf{q} = \mathbf{a} + b\mathbf{x} \mid \mathbf{a} \in \mathbb{R}^2,\ b \in \mathbb{R}\ ,\ \mathbf{x} \in T\}$, lowest order Raviart-Thomas finite element
$\mathbf{RT}_0(\delta_k; \mathcal{T}_{\delta_k})$	$:= \{\mathbf{q}_h \in \mathbf{H}(\text{div}; \delta_k) \mid \mathbf{q}_h\|_T \in \mathbf{RT}_0(T)\ ,\ T \in \mathcal{T}_{\delta_k}\}$
$\mathbf{RT}_{0,0}(\delta_k; \mathcal{T}_{\delta_k})$	$:= \{\mathbf{q}_h \in \mathbf{RT}_0(\delta_k; \mathcal{T}_{\delta_k}) \mid \gamma_n(\mathbf{q}_h)\|_{\partial\delta_k} = 0\}$
$\mathbf{M}_h(S)$	Discrete Lagrange multiplier space
$\mathbf{M_h}(\delta_k)$	Local discrete Lagrange multiplier space on δ_k
$Q_h^{\delta_k}$	L^2-projection $Q_h^{\delta_k} : L^2(\gamma_k)^2 \to \mathbf{M}_h(\delta_k)$
$\tilde{\mathbf{V}}_h$	$:= \{\mathbf{q}_h \in \mathbf{V}_h \mid Q_h^{\delta_k}(\mathbf{q}_h \wedge \mathbf{n}\|_{\varrho_k}) = Q_h^{\delta_k}(\mathbf{q}_h \wedge \mathbf{n}\|_{\delta_k})\ ,\ 1 \le k \le M\}$
$\tilde{\mathbf{Y}}_h$	Space of "mixed gradients"

Bibliography

[ABDG98] C. Amrouche, C. Bernardi, M. Dauge, and V. Girault. Vector potentials in three dimensional nonsmooth domains. *Math. Meth. Appl. Sci.*, 21:823–864, 1998.

[ABN00] H. Ammari, Annalisa Buffa, and Jean-Claude Nédélec. A justification of eddy currents model for Maxwell equations. *SIAM J. Appl. Math.*, 60(5):1805–1823, 2000.

[Ada78] Robert A. Adams. *Sobolev Spaces*. Accademic Press, New York, 1978.

[AFW00] D. Arnold, R. Falk, and R. Winther. Multigrid in h(div) and h(curl). *Numer. Math.*, 85:197–218, 2000.

[AO00] M. Ainsworth and A Oden. *Posteriori Error Estimation in Finite Element Analysis*. Wiley, Chichester, 2000.

[BBL+97] P. Bastian, K. Birken, S. Lang, K. Johannsen, N. Neuß, H. Rentz-Reichert, and C. Wieners. UG: A flexible software toolbox for solving partial differential equations. *Computing and Visualization in Science*, 1:27–40, 1997.

[BBM01] F. Ben Belgacem, A. Buffa, and Y. Maday. The mortar finite element method for 3D Maxwell equations: first results. *SIAM J. Numer. Anal.*, 39(3):880–901, 2001.

[BBM02] F. Bouillault, A. Buffa, and F. Maday, Y.andRapetti. The mortar edge element method in three dimensions: application to magnetostatics. *SIAM J. on Scient. Comp.*, 24(4):1303–1327, 2002.

[BC01a] A. Buffa and Jr., P. Ciarlet. On traces for functional spaces related to Maxwell's equations. Part I: An integration by parts formula in Lipschitz polyhedra. *Math. Methods Appl. Sci.*, 24(1):9–30, 2001.

[BC01b] A. Buffa and Jr., P. Ciarlet. On traces for functional spaces related to Maxwell's equations. Part II: Hodge decompositions on the boundary

of Lipschitz polyhedra and applications. *Math. Methods Appl. Sci.*, 24(1):31–48, 2001.

[BCS02] A. Buffa, M. Costabel, and D. Shee. On traces for $\mathbf{H}(\mathbf{curl}, \Omega)$ in Lipschitz domains. *J. Math. Anal.Appl.*, 276/2:845–876, 2002.

[BD98] D. Braess and W. Dahmen. Stability estimates of the mortar finite element method for 3-dimensional problems. *East-West J. Numer. Math.*, 6(4):249–264, 1998.

[BDH+99] R. Beck, P. Deuflhard, R. Hiptmair, R. H.W. Hoppe, and B. Wohlmuth. Adaptive multilevel methods for edge element discretizations of Maxwell's equations. *Surveys of Math. in Industry*, 8:271–312, 1999.

[BDW00] D. Braess, W. Dahmen, and C. Wieners. A multigrid algorithm for the mortar finite element method. *SIAM J. Numer. Anal.*, 37:48–69, 2000.

[BF91] F. Brezzi and M. Fortin. *Mixed and hybrid finite element methods.* Springer, Berlin-Heidelberg-New York, 1991.

[BHHW00] R. Beck, R. Hiptmair, R. H.W. Hoppe, and B. Wohlmuth. Residual based a posteriori error estimator for eddy current computation. *M^2AN Math. Modeling and Numer. Anal.*, 34:159–182, 2000.

[BHW00] R. Beck, R. Hiptmair, and B.I. Wohlmuth. Hierarchical error estimator for Eddy current computation. In P. et al. Neittaanmäki, editor, *Proc. 2nd European Conference on Numerical Methods and Advanced Applications*. World Scientific, Singapore, 2000. ENUMATH 99, Jyväskylä, July 26 - 30, 1999.

[BLS04] F. Bachinger, U. Langer, and J. Schöberl. Numerical analysis of nonlinear multiharmonic eddy current problems. SFB "Numerical and Symbolic Scientific Computing" SFB Report Nr. 2004-01, Johannes Kepler University of Linz, Linz, 2004.

[BMP93] Christine Bernardi, Yvon Maday, and Anthony T. Patera. Domain decomposition by the mortar element method. In H.G. Kaper ans M. Garbey, editor, *Asymptotic and Numerical Methods for Partial Differential Equations with Critical Parameters*, pages 269–286. N.A.T.O. ASI, Kluwer Academic Publishers, 1993.

[BMP94] Christine Bernardi, Yvon Maday, and Anthony T. Patera. A new nonconforming approach to domain decomposition: the mortar element method. In H. Brezis and J.L. Lions, editors, *Nonlinear Partial*

Differential Equations and their Applications, pages 13–51. Pitman, 1994.

[BMR99] A. Buffa, Y. Maday, and F. Rapetti. The mortar element method for 3D Maxwell's equations: analysis and applications to magnetodynamics. In *12th Int. Conf. on Domain Decomposition Methods, Chiba, Japon*, pages 259–270, 1999.

[BR78a] I. Babuska and W. Rheinboldt. Error estimates for adaptive finite element computations. *SIAM J. Numer. Anal.*, 15:736–754, 1978.

[BR78b] I. Babuska and W. Rheinboldt. A posteriori error estimates for the finite element method. *Int. J. Numer. Methods Eng.*, 12:1597–1615, 1978.

[Bra92] Dietrich Braess. *Finite Elemente*. Springer, Berlin Heidelberg, 1992.

[BW85] R. Bank and A. Weiser. Some a posteriori error estimators for elliptic partial differential equations. *Math. Comput.*, 44:283–301, 1985.

[CD00] M. Costabel and M. Dauge. Singularities of electromagnetic fields in polyhedral domains. *Arch. Ration. Mech. Anal.*, 151:221–276, 2000.

[Cia78] Ph.G. Ciarlet. *The Finite Element Method for Elliptic Problem*. North-Holland, Amsterdam, 1978.

[Cos90] M. Costabel. A remark on the regularity of solutions of Maxwell's equations on Lipschitz domains. *Math. Meth. in the Appl. Sci.*, 12:365–368, 1990.

[DB94] Peter Deuflhard and Folkmar Bornemann. *Numerische Mathematik 2, Integration gewöhnlicher Differentialgleichungen*. de Gruyter, 1994.

[EJ88] K. Eriksson and C. Johnson. An adaptive finite element method for linear elliptic problems. *Math. Comput.*, 50:361–383, 1988.

[FMRW04] B. Flemisch, Y. Maday, F. Rapetti, and B. I. Wohlmuth. Coupling scalar and vector potentials on nonmatching grids for eddy currents in a moving conductor. *J. Comput. Appl. Math.*, 168(1-2):191–205, 2004.

[GR79] Vivette Girault and Pierre-Arnaud Raviart. *Finite Element Approximation of the Navier-Stokes Equations*. Springer-Verlag, Berlin Heidelberg New York, 1979.

[Gre91] Walter Greiner. *Klassische Elektrodynamik*. Harri Deusch, Frankfurt am Main, 1991.

[Gri85] P. Grisvard. *Elliptic Problems in Nonsmooth Domains*. Pitman, London, 1985.

[Hac85] W. Hackbusch. *Multi-grid methods and applications*. Springer, 1985.

[HIM00] R.H.W. Hoppe, Y. Iliash, and G. Mazurkevitch. Domain decomposition methods in the design of high power electronic devices. In M. Sändig and W. Wendland, editors, *Proc. Int. Conf. on Multifield Problems, Stuttgart, October 6-8, 1999*. Springer, Berlin-Heidelberg-New York, 2000. to appear.

[Hip98] R. Hiptmair. Multigrid method for Maxwell's equations. *SIAM J. Numer. Anal.*, 36 No. 1:204–225, 1998.

[Hip99] R. Hiptmair. Canonical construction of finite elements. *Math. of Computation*, 68, Nor. 228:1325–1346, 1999.

[Hip02a] R. Hiptmair. Analysis of multilevel methods for eddy current problems. *Mathematics of Computation*, 72(243):1281–1303, October 2002.

[Hip02b] R. Hiptmair. Finite elements in computational electromagnetism. *Acta Numerica*, 11:237–339, January 2002.

[Hop99] R.H.W. Hoppe. Mortar edge elements in $\mathbb{R}^3$. *East-West J. Numer. Anal.*, 7:159–173, 1999.

[Hop02] R.H.W. Hoppe. Adaptive domain decomposition techniques in electromagnetic field computation and electrothermomechanical coupling problems. In F. et al. Brezzi, editor, *Proc. 4th European Conference on Numerical Mathematics and Advanced Applications, Ischia, Italy, July 23-27, 2001*. Springer, Berlin-Heidelberg-New York, 2002.

[LVL05] Seung-Cheol Lee, Marinos N. Vouvakis, and Jin-Fa Lee. A non-overlapping domain decomposition method with non-matching grids for modeling large finite antenna arrays. *J. Comput. Phys.*, 203(1):1–21, 2005.

[Mon98] Peter Monk. A posteriori error indicators for maxwell's equations. *J. Comput. Appl. Math.*, 100(2):173–190, 1998.

[Mon03] P. Monk. *Finite Element Methods for Maxwell's equations*. Clarendon Press, Oxford, 2003.

[MS64] N. Meyers and J. Serrin. H = w. *Proc. Nat. Acad. Sci.*, 51:1055–1056, 1964.

[Néd83] J.-C. Nédélec. Mixed finite elements in $\mathbb{R}^3$. *Numer. Math.*, 35:315–341, 1983.

[Nol90] Wolfgang Nolting. *Grundkurs theoretische Physik: Elektrodynamik*, volume 3. Zimmermann-Neufang, Ulmen, 1990.

[QV99] Alfio Quarteroni and Alberto Valli. *Domain Decomposition Methods for Partial Differential Equations*. Clarendon Press, Oxford, 1999.

[SBG96] Barry Smith, Petter Bjørstad, and William Gropp. *Domain Decomposition Parallel Multilevel Methods for Elliptic Partial Differential Equations*. Cambridge University Press, 1996.

[Sch] J. Schöberl. A posteriori error estimates for maxwell equations. (submitted to Math Comp).

[Sch01] J. Schöberl. Commuting quasi-interpolation operators for mixed finite elements. Technical Report Technical Report ISC-01-10-MATH, Institute for Scientific Computation, College Station, Texas, 2001.

[Ste03] Oliver Sterz. *Modellierung und Numerik zeitharmonischer Wirbelstromprobleme in 3D Modelling and Numerics of 3D Time Harmonic Eddy Current Problems*. PhD thesis, Ruprecht-Karls-Universität Heidelberg, 2003.

[SZ90] L.R. Scott and Z. Zhang. Finite element interpolation of nonsmooth functions satisfying boundary conditions. *Math. Comp.*, 54:483–493, 1990.

[Ver96] R. Verfuehrt. *A Review of A Posteriori Error Estimation and Adaptive Mesh-Refinement Techniques*. Wiley and Teubner, 1996.

[Whi57] H. Whitney. *Geometric Integration Theory*. Princeton University Press, Princeton, 1957.

[Wlo82] J. Wloka. *Partielle Differentialgleichungen*. B.G. Teubner, Stuttgart, 1982.

[Woh99a] B. Wohlmuth. Error estimators for mortar finite element discretizations. *ZAMM*, 78:1133–1134, 1999.

[Woh99b] B. Wohlmuth. Hierarchical a posteriori error estimators for mortar finite element methods with lagrange multipliers. *SIAM J. Numer. Anal.*, 36:2639–1658, 1999.

[Woh99c] B. I. Wohlmuth. A residual based error estimator for mortar finite element discretizations. *Numer. Math.*, 84:143–171, 1999.

[WY05] M. F. Wheeler and I. Yotov. A posteriori error estimates for the mortar mixed finite element method. *SIAM J. Num. Anal.*, 43(3):1021–1024, 2005.

[XH05] Xuejun Xu and R.H.W. Hoppe. On the convergence of mortar edge element methods in $\mathbb{R}^3$. *SIAM J. Numer. Anal.*, 43:1276–1294, 2005.

[Zei90] Eberhard Zeidler. *Nonlinear Functional Analysis and its Applications II/A*. Springer, New York, 1990.

[ZZ87] O. Zienkiewicz and J. Zhu. A simple error estimator and adaptive procedure for practical engineering analysis. *J. Numer. Meth. Eng.*, 28:28–39, 1987.

Index